Alternative Androgen Metabolism in Resistance to Aromatase Inhibitors

by

Matthew Joseph Sikora

A dissertation submitted in partial fulfillment
of the requirements for the degree of
Doctor of Philosophy
(Pharmacology)
in The University of Michigan
2011

Doctoral Committee:

Assistant Professor James M. Rae, Chair
Emeritus Professor William B. Pratt
Emeritus Professor Raymond W. Ruddon
Professor Thomas E. Carey
Professor Paul F. Hollenberg
Assistant Professor Michael D. Johnson, Georgetown University

Dedication

This dissertation is dedicated to breast cancer patients and their families and friends who have been touched by this disease. I hope that this work is but the first step in a long career dedicated to ending suffering caused by breast cancer.

"I cannot do all the good that the World needs,
but the World needs all the good that I can do."
- Jana Stanfield

Acknowledgements

First and foremost, I would like to acknowledge my mentor, Dr. James Rae, who created an ideal environment for my graduate training. His guidance allowed me not only to be happy and productive, but allowed me to thrive as a bench scientist, a writer, and ultimately as a member of the breast cancer research community. I am immensely grateful for his time and efforts, and look forward to continuing our relationship as colleagues and friends.

I am indebted to Dr. Tom Carey, along with Dr. Carol Bradford and Dr. Josh Bauer, for allowing me to cut my teeth in cancer research under their mentorship. I appreciate now as a graduate student with undergraduates of my own how much energy Josh devoted to my training, and cannot thank him enough. Dr. Carey has continued to be an integral part of my training since my time in his lab. "As the sapling is bent, the tree grows", and I hope that my passion for translational cancer research can be a reflection of his. I also thank Jim Zabawski and Henry Ford Cytogenetics, who gave me my first lab experience and first research project. They planted the seeds that grew to a career in research.

Thank you to my committee members Dr. Michael Johnson, Dr. Paul Hollenberg, Dr. Bill Pratt and Dr. Ray Ruddon for their invaluable assistance in the development and execution of my research. I would like to acknowledge and thank the members of the Rae laboratory, as well as my support from PIBS, the Pharmacology department and the PSTP training program. I am thankful for the fruitful interactions over the years with our collaborators, especially Dr. Lynn Henry, Dr. Dan Hayes and Dr. Zerusenay Desta.

I thank my friends and family, especially my parents Ken and Emily for their love and support. Above all, I thank my wife Kristine for helping me to be more than I ever thought I could be, both as a scientist and as her husband.

This work is supported by the Breast Cancer Research Foundation and the Pharmacological Sciences Training Program.

Table of Contents

List of Figures

List of Tables

List of Appendices

List of Abbreviations

16αOH-TS	16α-hydroxytestosterone
16βOH-TS	16β-hydroxytestosterone
3βAdiol	5α-androstane-3β,17β-diol
A	Androstenedione
AI	Aromatase inhibitor
AQ-DNA	Amplification-quality DNA
AR	Androgen receptor
B	Bicalutamide
CCS	Charcoal-stripped calf serum
CYP450	Cytochrome P450
DHEA	Dehydroepiandrosterone
DHEA-S	Dehydroepiandrosterone sulfate
DHT	5α-dihydrotestosterone
E1	Estrone
E1-S	Estrone sulfate
E2	Estradiol
E3	Estriol
ER	Estrogen receptor
FBS	Fetal bovine serum
FFPE	Formalin-fixed, paraffin-embedded
GREB1	Gene regulated by estrogen in breast cancer 1
GSEA	Gene set enrichment analysis
HSD	Hydroxysteroid dehydrogenase
ICI	ICI 182,780; fulvestrant
IMEM	Improved minimum essential medium
LTED	Long-term estrogen deprivation
LTLT	Long-term letrozole treated
LY	LY294002
MAPK	Mitogen activated protein kinase
MSigDB	Molecular signature database
NES	Normalized enrichment score
SD	Standard deviation
SEM	Standard error of the mean
SHC	Src homology domain containing protein
SNP	Single nucleotide polymorphism
STS	Steroid sulfatase
TMA	Tissue microarray
TS	Testosterone
U	U0126
UTR	Untranslated region

Chapter I.
Introduction

Breast cancer and endocrine therapy

Breast cancer is the most common non-cutaneous malignancy among women in the Western world. Roughly 207,090 women will be diagnosed with and 39,840 women will die of breast cancer in 2010 in the United States [1]. Estrogenic hormones play a significant role in the development and progression of breast cancer; increased lifetime exposure to estrogen accounts for the most significant risk factors for the disease [2]. Approximately 70% of newly diagnosed patients present with tumors that express estrogen receptor alpha (ERα); these tumors are considered ER-positive and patients are candidates for treatment with endocrine therapy [3]. Targeted endocrine therapies that block the action of estrogens can block the growth of estrogen-dependent tumors [4], and are effective in preventing breast cancer [5-7].

The foundations of targeted endocrine therapy for patients with ER-positive tumors began with studies using the failed contraceptive agent ICI 46,474, or tamoxifen (reviewed in [8]). V. Craig Jordan, Arthur Walpole and colleagues demonstrated that tamoxifen competitively bound the estrogen receptor [9]. Marc Lippman and colleagues demonstrated that tamoxifen could inhibit the proliferation of breast cancer cells in culture, and that high concentrations of tamoxifen could kill breast cancer cells [10]. These data led to findings by Jordan et al., wherein tamoxifen blocked estrogen-dependent tumor growth in rat tumor models [11-13]. The results of these studies led to the hypothesis that long-term adjuvant therapy with tamoxifen would be necessary to maintain tumor regression, as demonstrated by subsequent clinical trials [14]. For nearly 30 years, adjuvant tamoxifen therapy served as front-line therapy for all women with ER-positive breast cancer [14].

During this time, increased understanding of steroidogenesis led to new hypotheses for strategies to block the actions of estrogens in breast cancer. Studies conducted largely at the Worcester Foundation for Experimental Biology in the 1950s through the 1970s demonstrated that production of estrogens was the result of the metabolism of androgens via an "aromatization process" (steroid hormone biosynthesis is further discussed below). This process was eventually found to be catalyzed by a single cytochrome P450 enzyme, termed aromatase (reviewed in [15]). Aromatase activity was initially identified in the ovaries and adrenals; consistent with this, most hypotheses limited steroid hormone production to endocrine glands. Paul MacDonald and colleagues reported extra-glandular aromatase activity in peripheral tissues, including adipose and breast [16-19]. Further, they suggested that adipose tissue serves as the primary source of estrogens in post-menopausal women [20]. Later studies by Alan Lipton, Richard Santen and Angela Brodie demonstrated that both benign and malignant breast tissues contain aromatase protein and activity [21-23].

Throughout this period, several groups recognized the therapeutic potential of inhibiting aromatase activity in treating estrogen-dependent breast cancer. Two classes of aromatase inhibitors, steroidal and non-steroidal inhibitors, were developed concurrently by a number of different groups. The pan-cytochrome P450 inhibitor aminoglutethemide and the steroid testololactone were identified as aromatase inhibitors. These compounds are considered the 'first generation' non-steroidal and steroidal aromatase inhibitors, respectively [24, 25]. Work by Harry and Angela Brodie identified 4-hydroxy-androstenedione, renamed formestane, as the first selective aromatase inhibitor (and a 'second generation' steroidal aromatase inhibitor). In collaboration with Paul Goss, Charles Coombes and Mitch Dowsett, this group demonstrated that formestane was effective in reducing serum estrogen concentrations and tumor burden in post-menopausal women with advanced breast cancer [26, 27]. Work by Richard Santen, William McGuire and others demonstrated that aromatase inhibition using aminoglutethemide was equally efficacious to surgical adrenalectomy in clinical response and estrogen suppression in breast cancer patients, suggesting that aromatase inhibitor therapy may spare patients radical surgery [28]. It was also confirmed that aromatase

inhibition would only be successful in post-menopausal women (and oophorectomized women), due to ovarian feedback increases in luteinizing hormone and follicle-stimulating hormone [29]. Promising clinical results with formestane and aminoglutethemide [15] piqued the interest of pharmaceutical companies, leading to the search for more specific and more potent aromatase inhibitors. Two non-steroidal inhibitors (anastrozole (Arimidex®), letrozole (Femara®)) and one steroidal inhibitor (exemestane (Aromasin®)) were identified as 'third generation' inhibitors [30]. Third generation aromatase inhibitors (AIs) decrease serum estradiol concentrations by 97-99% in postmenopausal women [31, 32]. Recent clinical trials have demonstrated that third generation AIs have superior efficacy when compared to tamoxifen in increasing disease-free survival and overall survival in postmenopausal women with ER-positive breast cancer [33-35]. Based on these results, AIs are now considered front-line therapy for post-menopausal women with ER-positive breast cancer [36].

Steroid hormone biosynthesis

Steroid hormone biosynthesis (Figure 1.1) begins with the multi-step removal of the hydrocarbon side chain from the D-ring of cholesterol (a 27 carbon sterol molecule) to form 19 carbon dehydroepiandrosterone (DHEA). This process is catalyzed entirely by two cytochrome P450 enzymes, CYP11A1 (P450scc) and CYP17A1 (reviewed in [37]). Initial cleavage of cholesterol by CYP11A1 yields the steroid hormone pregnenolone (21 carbon) which can be oxidized to progesterone by 3β-hydroxysteroid dehydrogenase (3β-HSD) [38], leading to the production of both mineralocorticoids and glucocorticoids. Pregnenolone is metabolized in two steps by CYP17A1, first catalyzing 17α-hydroxylation, followed by 17,20-lyase activity to complete the removal of the side chain from the molecule to yield DHEA [39]. The conversion of cholesterol to DHEA (and subsequent export of DHEA) occurs entirely in the adult adrenal zona reticularis, which expresses the ideal cohort of steroidogenic enzymes and co-factors required for this series of reactions [37]. DHEA is taken up by target tissues (e.g. adipose and breast) where it can serve as the precursor for androgen and estrogen synthesis.

While adrenal cytochrome P450s are responsible for the synthesis of DHEA, local synthesis of androgens and estrogens is regulated by 3- and 17-hydroxysteroid dehydrogenases (HSDs) and 5α-reductases [40]. This family of steroidogenic enzymes consists of at least fifteen 17β-HSDs [40-42], two 3β-HSDs [43] and three 5α-reductases [44, 45]. Additionally, at least 4 enzymes of the aldo-keto reductase superfamily (AKR1C1-1C4) are capable of catalyzing both 3α- and 3β- keto-hydroxysteroid conversions [42]. Specific HSD isoforms vary in their tissue specific expression and directionality (hydroxysteroid oxidation versus ketosteroid reduction) [40, 42, 46], which will be discussed further below. For simplicity, enzymes in the pathways described will be referred to by function rather than specific isoforms unless otherwise noted.

Local synthesis of androgens and estrogens in target tissues (Figure 1.1) proceeds when DHEA is metabolized to androstenedione (A) by 3β-HSD; A is converted to testosterone (TS) by 17β-HSD. In the biosynthesis of estrogens, either A or TS can be metabolized by aromatase to estrone (E1) and estradiol (E2), respectively (aromatase preferentially binds and metabolizes A versus TS [47, 48]). E1 and E2 (lower and higher potency estrogens, respectively [49], discussed further below) are inter-converted by 17β-HSD [50]. TS can instead continue in androgen biosynthesis and be metabolized by 5α-reductase to the potent androgen dihydrotestosterone (DHT). DHT is metabolized by 3β-HSD to the steroid 5α-androstane-3β,17β-diol (3βAdiol) [43], and 3βAdiol is eliminated via CYP7B1-mediated generation of 6α- and 7α-triols [51, 52]. Additional pathways exist as alternative metabolic routes producing the steroids listed and are discussed in references contained herein; however, the mechanisms outlined represent canonical steroid biosynthesis pathways.

DHEA is sulfated prior to export from the adrenals to the circulation, forming DHEA sulfate (DHEA-S) [37]. In peripheral tissues (particularly adipose [18, 53]), DHEA-S can be taken up and eventually aromatized, primarily to E1, where it is sulfated and exported as E1 sulfate (E1-S). In target tissues, DHEA-S is hydrolyzed by steroid sulfatase (STS) to remove the sulfate group; DHEA can then act as a sex steroid precursor. Similarly, STS hydrolyzes E1-S to yield E1, which can then be converted to E2 (described above).

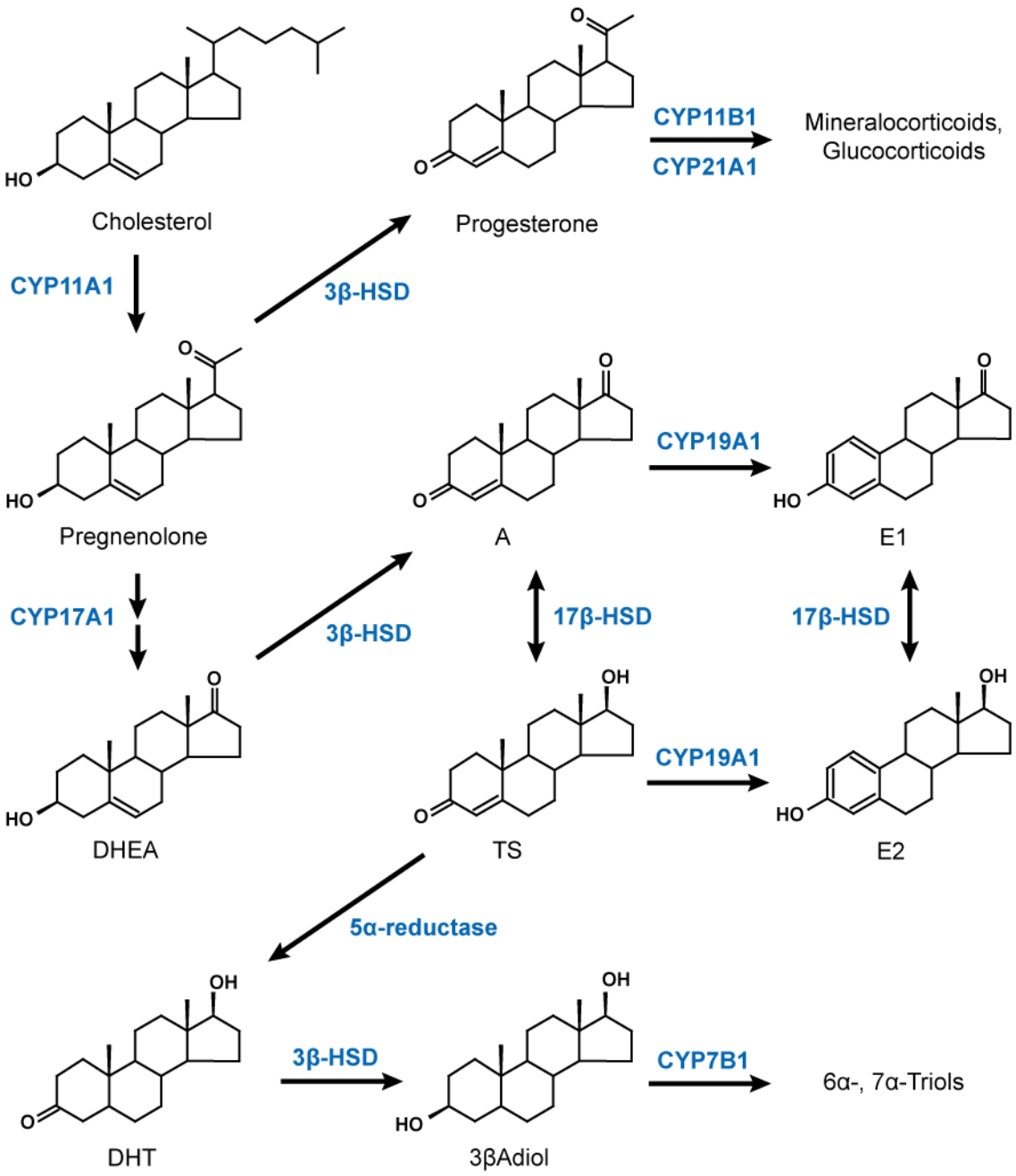

Figure 1.1. Steroid hormone biosynthesis. Details described further in text. A, androstenedione; TS, testosterone; E1, estrone; E2, estradiol; DHT, dihydrotestosterone; 3βAdiol, 5α-androstane-3β,17β-diol; HSD, hydroxysteroid dehydrogenase. The bi-directionality of 17β-HSDs is further discussed in text.

The uptake of circulating DHEA-S or E1-S for conversion into active estrogens is discussed below.

Steroid hormone biosynthesis in breast cancer

In post-menopausal women with breast cancer, concentrations of E2 have been demonstrated to be up to 10-fold higher in tumors than circulating in plasma [54-56]. Estrogens in breast tumor tissues are thought to be generated from three primary sources: metabolism and aromatization of circulating precursors (i.e. DHEA, DHEA-S), active uptake/conversion of circulating estrogens to more potent estrogens (i.e. E1-S), and direct uptake of circulating E2. Though the relative contributions of these mechanisms are under scrutiny and are an area of controversy [57, 58], breast tumors do express the necessary enzymes to generate E2 from circulating precursors [59].

As described above, aromatase expression and activity has been reported in both benign and malignant breast tissues by a number of groups [21-23]. Early studies of aromatase expression associated with breast tumors could not resolve whether the enzyme was expressed specifically in tumor epithelial cells or the surrounding stroma (reviewed by [15]). This was recently elucidated by Hironobu Sasano and colleagues with evidence that aromatase is localized to both the stromal and tumor epithelial cells [60]. Aromatase activity has also been demonstrated in breast cancer cells in culture [61, 62]. This dissertation demonstrates that the protein levels of aromatase increase in breast cancer cells following estrogen deprivation, potentially mimicking conditions in patients receiving AI therapy ([63], discussed in Chapter II). Based on these data, breast tumors express aromatase and can catalyze the key reaction in the formation of estrogens from androgen precursors (e.g. TS or A).

3β-HSD activity is required both to convert DHEA to A, and DHT to 3βAdiol. Two isoforms of specific 3β-HSD enzymes, HSD3B1 and HSD3B2, have been identified. While HSD3B2 is expressed primarily in the adrenals and gonads, HSD3B1 is expressed widely in peripheral tissues including the breast [64, 65]. Though 3β-HSD activity is critical in the synthesis of sex steroids from DHEA, minimal data exist regarding the

expression of either isoform in breast tumor tissue. Some studies of 3β-HSD in breast cancer cells suggest that over-expressing the enzyme is required [66]. However, this dissertation demonstrates that not only do MCF-7 cells in culture express 3β-HSD protein, but expression increases during estrogen deprivation. Furthermore, the enzyme is functional in metabolizing DHT to 3βAdiol ([63], as discussed in Chapter II). 3β-HSD activity has also been detected in breast carcinoma tissues [67], however, these studies used progesterone as a substrate, and it is unclear whether the level of activity observed is equivalent for DHEA or DHT metabolism. Though whether 3β-HSDs are expressed in breast tumors is unclear, a number of AKR1C family enzymes possess significant 3β-HSD activity, and have been demonstrated to be expressed in breast tumors (reviewed in [42]). These data suggest that breast tumors do possess 3β-HSD metabolic capacity, and can metabolize both DHEA and DHT to their downstream substrates. Importantly, though DHT is a potent androgen, it is available as a 3β-HSD substrate in breast tumors, due to metabolism of TS by 5α-reducatse in breast tumor cells [68].

Interconversion among androgen and estrogen pairs requires 17β-HSD enzymatic activity; both A and E1 require ketosteroid reduction at the 17-carbon to generate TS and E2, respectively. A number of 17β-HSD isoforms have been demonstrated to be expressed in breast tumors [57, 69-71]; HSD17B1, HSD17B5, HSD17B7 and HSD17B12 catalyze ketosteroid reduction (e.g. E1 → E2), while HSD17B2, HSD17B10 and HSD17B14 are primarily hydroxysteroid oxidases (e.g. E2 → E1). The balance of reductive and oxidative HSD17B isoforms has significant implications for the relative local concentrations of ketosteroids versus hydroxysteroids (discussed further below). However, whereas peripheral metabolism generally favors hydroxysteroid oxidation, breast tumor tissue has been shown to instead favor ketosteroid reduction [72], thus breast tumors will primarily convert A to TS, and E1 to E2.

The above observations strongly suggest that breast tumors contain the necessary enzymes to completely synthesize androgens and estrogens from DHEA. However, DHEA and E1 circulate primarily as DHEA-S and E1-S, respectively, and hydrolysis is necessary to remove the sulfate group prior to further metabolism; this reaction is

catalyzed by STS. STS activity has been observed in the majority of breast tumor tissues that have been evaluated, however, there appears to be broad intersubject variability in STS activity (reviewed by [73]). Though the clinical implications of STS expression and activity levels are unclear [74, 75], evidence of STS activity in breast tumors has warranted significant research into the development of STS inhibitors as a novel mode of endocrine therapy [73]. These observations strongly suggest that breast tumors are able to uptake circulating sulfated steroid hormones, and then metabolize them to active androgens and estrogens.

Steroidogenic enzymes as biomarkers and therapeutic targets in breast cancer

In addition to the pharmacological targeting of aromatase described above, steroidogenic enzymes have been evaluated as predictive and prognostic biomarkers in breast cancer, as well as drug targets. As described above, STS has recently been investigated as a therapeutic target in breast cancer, and a Phase I trial demonstrated that STS inhibition could decrease serum concentrations of E1, E2 and DHEA [76]. CYP17A1 has also recently been evaluated as a drug target displaying promising results in prostate cancer, with breast cancer trials currently underway (discussed in Chapter VI). Though a significant number of chemical inhibitors of 17β-HSDs have been developed [77], the inhibitors have yet to advance into clinical trials. However, due to the heterogeneity in the expression of reductive versus oxidative isoforms, a number of groups have investigated the implications of the expression of specific 17β-HSD isoforms in breast cancer prognosis and prediction of response to therapy (discussed below).

As described above, interconversion of E1 to E2 (and TS to A) is controlled by 17β-HSD isoforms, with individual isoforms favoring oxidation or reduction reactions. Increased expression of reductive isoforms that favor E2 production (e.g. HSD17B1, 5, 7 and 12) is hypothesized to negatively affect response to endocrine therapy by increasing local E2:E1 ratios. Conversely, increased expression of oxidative isoforms that favor E1 production (e.g. HSD17B2, 10 and 14) is hypothesized to decrease local E2:E1 ratios and improve response to endocrine therapy. A recent study by Haynes et al. examined expression of steroidogenic enzymes, including 17β-HSDs, and their correlation with

intratumoral E2 concentrations. HSD17B7 and HSD17B2 were shown to have significant positive and negative correlations, respectively, with intratumoral E2 concentrations, consistent with the above hypotheses [57]. The clinical implications of these observations have been examined by a number of groups [70]. Increased expression of reductive 17β-HSDs has been associated with poor prognosis and late relapse [69, 78, 79] as well as decreased benefit from tamoxifen therapy [80, 81]. Similarly, the absence of oxidative 17β-HSDs has also been associated with poor prognosis [69, 78, 82] and decreased benefit from tamoxifen therapy [80].

Mechanisms of resistance to aromatase inhibitor therapy

Though AI therapy has been clinically successful, resistance to AI therapy is common, and tumors recur in spite of drastically reduced concentrations of serum estrogens. Recent data from 10-year follow-up of the ATAC trial (Arimidex, Tamoxifen and Combination) demonstrate that nearly 20% of women receiving adjuvant AIs will experience disease relapse within 10 years of treatment initiation [83]. Importantly, there is no way to identify patients that will benefit from AI therapy, and mechanisms of resistance remain an active area of research. A number of potential mechanisms underlying resistance to AI therapy have been proposed, including patient non-adherence to therapy, pharmacogenomic mechanisms and altered signaling pathways involving growth factor receptor signaling and crosstalk with ER (discussed below).

Mechanisms including pharmacogenomics and tumor biology have been postulated to play a significant role in resistance to AI therapy. Additionally, recent studies have suggested that patient non-adherence to therapeutic regimens in oncology has potentially been under-estimated, and may be a significant factor contributing to lack of therapeutic efficacy [84]. Interestingly, though initial prospective clinical trials of tamoxifen reported discontinuation rates of ~15% [85, 86], more recent studies have estimated that up to 55% of women do not adhere to tamoxifen therapy [5, 87-90]. Similarly, Partridge et al. reported that nearly 40% of women receiving adjuvant AI therapy are non-adherent within only 3 years of treatment initiation [91]. We recently reported that pharmacogenomic factors may play a significant role in non-adherence to tamoxifen

therapy, potentially due to changes in the occurrence of side effects [92]. The aromatase gene is highly polymorphic, with 44 haplotypes currently described [93]. These polymorphisms may potentially play a role in either patient adherence or therapeutic efficacy by affecting enzyme activity or expression, drug and substrate binding or other enzyme characteristics. One polymorphism, rs4646, was found to be associated with improved time to progression in patients with metastatic breast cancer treated with letrozole [94]. Polymorphisms in drug metabolism enzymes, particularly phase II glucuronidation enzymes [95, 96], may also play a role in altering AI metabolism and therefore therapeutic efficacy. The role of aromatase pharmacogenomics in patient adherence to therapy is under investigation [97, 98].

Though patient adherence to therapy and pharmacokinetics have a potential effect on the efficacy of AI therapy, resistance often develops in the presence of AIs, suggesting that biological mechanisms play a role in resistance. Minimal data exist regarding mechanisms of acquired resistance to aromatase inhibitors. The development of cell culture models of AI resistance presents unique challenges versus selection for acquired resistance to more traditional cytotoxic agents where cells are maintained long term in a drug of choice. AI resistance models require that the estrogen environment in which the cells are maintained in mimic those of a patient on AI therapy, as it is estrogen deprivation, not the AI itself, which inhibits breast cancer cell growth. A number of groups have used long-term estrogen deprivation (LTED) to mimic tumor conditions in patients on AI therapy. ER-positive, estrogen-dependent breast cancer cells (e.g. MCF-7) are maintained long term (3-12 months) in the absence of steroid hormones, either in medium supplemented with charcoal stripped serum or in ovariectomized mice. Cells will often adapt to LTED and display an endocrine resistant phenotype, no longer requiring estrogen to maintain cell growth; these phenotypes may mimic those of recurrent tumors following AI therapy.

The key phenotype observed in LTED MCF-7 cells developed independently in the laboratories of Richard Santen and Mitch Dowsett (reviewed in [99] and [100], respectively) is an adaptive hypersensitivity to low concentrations of E2. In both models,

proliferation of LTED cells is maximally induced by 1,000 to 10,000-fold lower concentrations of E2 than the parental MCF-7 cells [101, 102]; the authors postulated for both models that LTED cells became hypersensitive to residual estrogens in the medium. This observation as a mechanism of resistance is supported by clinical data where premenopausal women who initially responded to ovarian suppression using gonadotropin-releasing hormone agonists relapsed and subsequently responded to the addition of an AI [103]. These data suggest that the tumors became hypersensitive to residual peripheral estrogens, which could be suppressed with AI therapy.

The proposed mechanism of adaptive hypersensitivity for the LTED cell models developed by the Santen and Dowsett laboratories requires the activity of ERα. However, the downstream ERα-mediated pathway is unique in each model. In the model presented by Dowsett and colleagues, hypersensitivity was accompanied by a 10-fold increase in ERα-mediated reporter output versus parental cells [104]. Martin et al. demonstrated that this increased transcription was associated with increased crosstalk with receptor tyrosine kinases (specifically ErbB2 and IGF1R) and subsequent MAPK signaling; kinase inhibitors including gefitinib and U0126 inhibited ERα-mediated transcription [104, 105]. Additionally, treatment with the anti-estrogen ICI 182,780 inhibited LTED cell growth and ERα-mediated basal transcription [105]. These data suggest that hypersensitivity was caused by an increase in ERα-mediated transcription induced by increased crosstalk with upstream kinase signaling cascades. Though these cells appear to signal via a classical 'genomic' ERα-mediated mechanism, the LTED model presented by Santen and colleagues suggests a primarily 'non-genomic' mechanism for ERα. In this model, E2 stimulation of LTED cells also resulted in activation of MAPK (mitogen activated protein kinase), however, maximal activation was observed following only 15 minutes of E2 treatment, suggesting that ERα-mediated transcription was not necessary to initiate this signaling pathway [106]. It was subsequently found that ERα associated with SHC (src homology domain containing protein), a receptor tyrosine kinase adaptor protein, facilitating activation of both the MAPK and PI_3K pathways [106, 107]. This was observed in the absence of ERα ligand, but was increased by the addition of estradiol. The association of ERα with SHC induced the localization of ERα to the plasma

membrane. Localization to the plasma membrane was later shown to be facilitated by interaction between SHC, ERα and IGF1R; knockdown of any of these components inhibited MAPK activation and LTED cell growth [108]. These data suggest that adaptive hypersensitivity in this model is mediated by the membrane-associated, non-genomic functions of ERα, rather than the increased ERα transcription observed by Dowsett and colleagues. The strength of these LTED models lie in their clinical correlate with estrogen hypersensitivity; however, the contributions of residual estrogens in these systems may be significant and may change the clinical scenario that is modeled (discussed in Chapter IV).

Early studies of aromatase inhibitors in cell culture models were technically challenging due to low levels of aromatase expression. To circumvent this, Shiuan Chen and colleagues stably transfected MCF-7 cells with an over-expression plasmid for aromatase, generating the MCF-7Ca cell line [109]. This cell line has been used extensively by the laboratory of Angela Brodie to study aromatase inhibitors and AI resistance mechanisms in *in vivo* xenograft models (reviewed in [110, 111]). To generate AI resistant cells, MCF-7Ca were grown in ovariectomized mice treated with androstenedione and letrozole. Tumors that outgrew letrozole treatment after ~1 year were then grown in culture as long term letrozole treated cells (LTLT cells)[112, 113]. LTLT cells were found to have increased expression of ErbB2, concurrent increases in downstream signaling via the MAPK pathway, and decreased expression of both ERα and aromatase. LTLT cells are not growth stimulated by E2; however, treatment of LTLT cells with the ErbB2 inhibitory antibody trastuzumab markedly inhibited cell growth, causing a concurrent increase in the expression of both ERα and aromatase. This increased ERα expression also enabled LTLT cells able to be growth-induced by E2. These data strongly suggested that trastuzumab treatment may re-sensitize LTLT cells to endocrine therapy [114]. To address this, MCF-7Ca cells were grown as xenografts in the presence of androstenedione and letrozole; upon tumor growth, treatment was switched to trastuzumab or trastuzumab plus letrozole. Both treatments caused regression of the recurrent tumor, consistent with the role of ErbB2 in resistance; however, the addition of letrozole caused prolonged recurrence regression. This is consistent with the hypothesis

that trastuzumab treatment re-sensitized AI-resistant cells to endocrine therapy [114]. These data suggest that adaptive changes in tumors as a response to AI therapy may be reversible and that endocrine-sensitivity may be restored with targeted agents. The LTLT model has clear advantages in not only being generated as xenograft models *in vivo*, but resistant cells are selected in a potentially therapeutically relevant background, i.e. AI plus an aromatase substrate. However, since the background used for this model is the MCF-7Ca aromatase over-expressing line, it is unclear whether this level of aromatase expression and changes in the regulation of expression is relevant to patient tumors.

A number of other groups have also recently reported on novel LTED phenotypes. Carlos Arteaga and colleagues selected 4 different ER-positive breast cancer cell lines using LTED, and performed proteomic profiling on LTED versus parental cells. These data demonstrated that hyperactivation of the PI_3K pathway, and subsequent activation of Akt and mTOR, is critical to the development and maintenance of the estrogen-independent phenotype [115]. Inhibitors targeting either PI_3K or mTOR induced apoptosis in LTED cells, and could prevent outgrowth of LTED cells from the parental cell lines. More recently, gene expression profiling of these cell lines revealed a critical role for the MYC oncogene in the LTED phenotype, implicating MYC activation in AI resistance [116]; these models are unique in that ERα does not appear to play a pivotal role in endocrine resistance. Aguilar et al. examined temporal changes in MCF-7 cells during LTED, combining genomic and transcriptomic data into a time course throughout LTED selection [117]. Results from this approach were consistent with previous observations suggesting that increased ERα crosstalk with receptor tyrosine kinases following LTED. Additional genomics-based approaches to studying LTED by Shiuan Chen and colleagues provide more evidence for enhanced ERα and kinase cascade crosstalk where ERα is activated in a ligand-independent manner [118].

Though LTED and AI resistance models have provided insight into numerous potential mechanisms of resistance, clinical advances based on these findings have been few and modest [119](discussed further in Chapter VI). Though a number of factors may account for the minimal success observed with targeted therapies in AI resistant breast cancer,

this may also suggest that current models are not accurately mimicking conditions in patient tumors. New hypotheses into mechanisms of AI resistance may yield novel targets for therapy, and may provide insight into which patients will benefit from targeted therapies.

Androgen metabolism in resistance to AI therapy

A significant body of work has been published in both breast and prostate cancer examining a role for enhanced growth factor and receptor tyrosine kinase signaling as mechanisms of resistance to estrogen/androgen deprivation. However, recent data in prostate cancer strongly suggests that hormone-refractory prostate cancer continues to require the activity of androgen receptor (AR) to maintain tumor growth. Further, it is likely that prostate tumors actively up-regulate the expression of steroidogenic enzymes to maintain high concentrations of potent androgens in the tumor, thus maintaining AR activation [120, 121]. However, in the case of AI therapy in breast cancer, a single enzyme is necessary for the generation of any of the potent estrogens (e.g. E1, E2), and this enzyme is strongly inhibited with targeted agents.

We hypothesize that despite inhibition of aromatase and depletion of estrogen, androgens may instead be metabolized by other, aromatase-independent, pathways. These alternative pathways of hormone metabolism produce estrogen-like compounds that may confer resistance to AIs and activate ERα in the absence of estrogen. The production of alternative estrogenic steroids may represent a novel mechanism of *de novo* resistance to AI therapy, while long-term adaptation to these ligands may induce novel mechanisms of acquired resistance.

Importantly, the potential role of androgen metabolites as ERα ligands in breast cancer has only recently become relevant as a mechanism of resistance to endocrine therapy, as front line treatment has shifted from tamoxifen to the AIs. In patients treated with tamoxifen, tamoxifen acts as an ER antagonist, directly competing with estrogens for binding to ERα thereby preventing ERα activation and subsequent growth induction. If these metabolites are produced in this treatment setting, ERα is saturated with an

antagonist (tamoxifen) and the high affinity ligands (estrogens) are still present. Therefore it is unlikely that the alternative androgen metabolites will be able to bind to ERα and exert any biological effects. However, AI-treated patients, not only is there no longer an antagonist present, but AI therapy depletes the high affinity ligands. In this setting, metabolites will be able to bind to and activate ERα, promoting tumor growth.

Cytochrome P450s in steroid hormone metabolism

The enzymes responsible for regulating alternative steroid metabolism represent key targets as biomarkers of resistance and potential therapeutic targets. We hypothesize that cytochrome P450 (CYP450) enzymes play a significant role in alternative pathways of androgen metabolism. CYP450s are a class of polymorphic, heme-containing mono-oxygenases, of which 57 isoforms have been identified in humans [122]. CYP450s are primarily considered as major components of hepatic detoxification and xenobiotic metabolism. Of the 50 CYP450s considered Class II enzymes (localized to the endoplasmic reticulum), 15 are thought to be largely involved in xenobiotic metabolism. 20 are involved primary in biosynthesis of molecules including sterols, fatty acids, eicosanoids and steroids; the remaining 15 enzymes are orphans with unknown substrates [122]. CYP450s are already known to play a major role in the etiology of breast cancer as steroidogenic enzymes; CYP19A1, CYP17A1 and CYP11A1 are necessary to metabolize cholesterol to estrogens, and CYP21A1 and CYP11B1 convert progestins to mineralocorticoids and glucocorticoids. A number of CYP450s are known to be involved in the oxidative metabolism of estrogens and androgens (discussed below).

The oxidative metabolism of estrogens, specifically E1 and E2, has been comprehensively examined for at least 15 P450 isoforms of the CYP1, CYP2, CYP3 and CYP4 isoform families by Anthony Lee and colleagues [123, 124]. Both E1 and E2 can be oxidized at the 2-, 4-, 6α-, 7α-, 15α- and 16α-carbon positions, with varying catalytic activity and regioselectivity between CYP450 isoforms. CYP1A2, CYP3A4 and CYP1A1 had the highest activities for 2- and 4-hydroxylation of both E1 and E2 among all isoforms tested, though the rate of E2 metabolism was ~10-fold greater than E1 metabolism in all cases. In general, CYP1 isoforms (1A1, 1A2, 1B1) and CYP3 isoforms

(3A4, 3A5, 3A7) were the most active in hydroxylating E1 and E2 at the specific sites listed above; minor contributions were observed for CYP2 isoforms (2B6, 2C8, 2C9, 2C19, 2D6). Notably, no oxidative metabolism at these sites on E1 or E2 was detected by CYP2A6, CYP2C18, CYP2E1 or CYP4A11. A novel pathway yielding 10β-ketosteroid derivatives of E1 and E2 has also been reported, with CYP1A1, CYP2B6 and CYP2E1 demonstrating this enzymatic activity [125]. Oxidative metabolites of E1 and E2 have varying unique activity compared to their precursor steroid. 16α-hydroxylation of E2 and E1 generates estriol (E3) and 16α-hydroxyestrone (an E3 precursor) respectively; E3 is the primary estrogen during pregnancy. However, 2- and 4-hydroxylated estrogens are postulated to be key intermediates of estrogen-mediated genomic toxicity via the formation of DNA adduct-forming quinones [126, 127]. Importantly, the role of CYP450-generated E1 and E2 metabolites as ER ligands is currently unclear.

No comprehensive evaluation of androgen metabolism by CYP450 enzymes has been published to date, but a number of groups have uncovered unique patterns of isoform activity versus those observed with estrogens. Early studies of testosterone metabolism using rat CYP450s demonstrated that testosterone could be hydroxylated at the 2α-, 2β-, 6β-, 7α-, 15α-, 15β-, 16α- and 16β-carbon positions; moreover, rat P450 enzymes demonstrate high catalytic activity for these reactions [128-130]. Human liver microsomes and recombinant human CYP450 enzymes appear to have greatly reduced capacities to metabolize testosterone versus rat homologs. Incubations of testosterone with human liver microsomes yield only a few major products, primarily 6β-hydroxytestosterone with <10% 2β- and 15β-hydroxytestosterone. 6β-hydroxytestosterone was shown to be primarily generated via CYP3A enzymes [131]. In 1991, David Waxman and colleagues tested the ability of 11 human microsomal P450s to metabolize testosterone [132]. Consistent with their previous report, CYP3A enzymes demonstrated the highest capacity for 6β-hydroxylation, while minor activity was observed with CYP4B1 and CYP2C8. However, P450s 2A6, 2B6, 2C9, 2D6, 2E1 and 1A2 were all reported to be inactive in the metabolism of testosterone and androstenedione. A later report by Imaoka et al. directly compared the catalytic activity of recombinant human CYP450s (1A2, 2A6, 2B6, 2C8, 2C9, 2C18, 2D6, 2E1 and 3A4)

to their rat homologs for their catalysis of various substrates, including testosterone [128]. Whereas testosterone hydroxylation was observed for all rat P450 homologs except CYP2E1, the only human P450s demonstrating testosterone hydroxylation were CYP3A4 (6β-, 2β-hydroxylation) and CYP2B6 (16α-, 16β-hydroxylation). CYP3A4 activity was consistent with previous reports and CYP2B6 activity was later confirmed by multiple groups [133, 134]. The role of these androgen metabolites as ligands for steroid hormone receptors, including AR, has not been explored.

While specific human CYP450 isoforms appear to metabolize estrogens extensively with limited regioselectivity and extensive redundancy among isoforms, androgen metabolism is limited to a few enzymes with marked regioselectivity and relatively low enzymatic capacity. Other CYP450s have demonstrated the ability to metabolize sterol molecules and steroid hormones, but these are generally 'unique' enzymes with limited homology to other P450s [122]. Of note, CYP7B1 exclusively metabolizes sterol molecules including DHEA, pregnenolone and 3βAdiol [135] (discussed further below).

Though CYP450s are considered primarily hepatic enzymes, isoforms are expressed in tissue-specific patterns in numerous extra-hepatic tissues, including the breast and breast tumors. A number of groups have examined CYP450 expression in breast and breast tumor tissue at the mRNA and protein level; CYP450s 1A1, 1B1, 2B6, 2E1, 2C, 2D6 and 3A (in addition to 19A1, aromatase) have been detected [136-138]. The expression of these P450s has also been observed in breast tumor samples using tumor gene expression microarray data at Oncomine (www.oncomine.org) (discussed further below). These data strongly suggest that hydroxylated metabolites of androgens and estrogens are generated in breast tumors, furthering the need for understanding of the role of these metabolites in breast cancer etiology.

The pharmacogenomics of cytochrome P450 enzymes

CYP450s are highly polymorphic in the human population, with over 350 functionally different alleles reported to date among the human isoforms [139]. The degree of polymorphisms is variable across isoforms, with the highest number of alleles reported

for CYP2D6 (63 alleles), CYP2B6 (28), CYP1B1 (26) and CYP2A6 (22), whereas few if any functional variants have been described for others including CYP2E1, CYP2R1 and CYP2S1 [139]. Variants consist primarily of single nucleotide polymorphisms (SNPs); SNPs may functionally cause missense mutations that alter substrate recognition or enzyme function (positively or negatively), nonsense mutations, or deletions that ablate enzyme function or expression. Promoter or intronic SNPs may alter gene expression or exon usage. Variant alleles range in frequency from extremely rare SNPs to those occurring in >50% of a population and allele frequencies often vary widely between ethnic groups [139]. As a result of polymorphisms, patient enzymatic activity also varies widely for particular CYP450s. For CYP2D6, 10% of Caucasians lack any enzymatic activity, while 4-5% of Caucasians have increased activity due to the presence of extra gene copies [139, 140]. Variability in CYP2D6 activity causes significant clinical differences in therapeutic efficacy for CYP2D6 substrates [139, 141, 142].

It is likely that CYP450s involved in the generation and elimination of androgen metabolites are polymorphic. Genetic polymorphisms in these CYP450s that affect their enzymatic activity may influence the production or elimination of these estrogen-like steroids and therefore patient genotypes may predict resistance to AIs. Of particular interest is CYP2B6; not only is CYP2B6 one of the few CYP450s capable of metabolizing testosterone, it is one of the most polymorphic CYP450s. The wild-type allele ranges in frequency from ~40-70% between ethnic groups. Four mutant alleles (CYP2B6*2, *4, *5, *6) account for the majority of variant alleles in Caucasians; the remainder are rare, but vary widely in frequency between ethnic groups [143]. Each allele variant causes unique changes in enzyme expression and substrate-specific catalytic activity. The most common variant in Caucasians, CYP2B6*6, displays decreased catalytic activity for biochemical assay probe substrates but increased activity for clinical agents including cyclophosphamide [143]. Domanski et al. mutated several residues mapped to substrate recognition sites in CYP2B1, the rat homolog of CYP2B6; all sites mutated were identical amino acids between rat CYP2B1 and human CYP2B6 [144]. These CYP2B1 mutant proteins were tested for their ability to 16-hydroxylate testosterone. Mutations at the majority of residues tested shifted the enzyme

regioselectivity for 16α- versus 16β-hydroxylation. While wild type enzyme produced these at a nearly 1:1 ratio, metabolite ratios were shifted as high as 81:1 and as low as 1:10 in mutant enzymes. Though none of the mutated residues map to known human SNPs, these observations suggest that single amino acid changes may drastically alter production of steroid metabolites. Allele-specific changes in the ability of CYP2B6 to metabolize testosterone have not been investigated, and may significantly alter the formation of 16α-/16β-hydroxytestosterone in target tissues, including the breast and breast tumors.

Implications for AI resistance

The studies described below will investigate the role of alternative pathways of androgen metabolism in generating estrogen-like steroids that may induce the growth of breast cancer cells in the absence of estrogen, therefore conferring resistance to AI therapy. The role of CYP450 enzymes in the generation and elimination of these metabolites will also be explored. The observations discussed above strongly suggest that an improved understanding of steroid hormone metabolism is necessary for better understanding of response to endocrine therapy. Understanding the role of alternative androgen metabolites and their associated enzymatic pathways in modulating the efficacy of AI therapy may provide biomarkers for determining the appropriate therapy for each patient, thereby preventing ineffective treatment and improving overall response to therapy. Elucidating the function of alternative steroidogenic pathways in regulating steroid metabolism in breast cancer will be the first step towards developing novel and improved interventions to regulate hormone levels at the site of action. Appropriate evaluation of the steroidogenic capacity and the potential contribution of alternative estrogens for individual tumors may allow the identification of patients who will and will not respond to specific endocrine therapies, allowing tailored approaches to anti-estrogen therapy.

Chapter II.

The androgen metabolite 5α-androstane-3β,17β-diol (3βAdiol) induces breast cancer growth via estrogen receptor

Introduction

Estrogens play a significant role in breast cancer development and progression and many of the most potent risk factors for the development of breast cancer can be explained in terms of increased lifetime exposure to estrogen. While the contributions of estrogens to breast cancer etiology are well established, the role of androgens in breast cancer development and progression is less well understood. Current dogma holds that androgens can inhibit the growth of breast cancer cells and that this effect is mediated through the androgen receptor [145]. However, many of the in vitro studies of androgen effects on breast cancer have been conducted in the presence of low concentrations of estrogen which complicates the interpretation of the results. In the current study we were interested in evaluating the effects of androgens on breast cancer cell growth under conditions of profound estrogen deprivation. Examining the effects of androgens under these conditions may be clinically relevant given the extremely low concentrations of estrogen in post-menopausal breast cancer patients undergoing therapy with aromatase inhibitors (AIs).

In post-menopausal women, estrogens are generated through peripheral conversion of adrenal androgens, including testosterone and androstenedione, to estrogens by CYP19 aromatase. These peripherally generated estrogens can stimulate estrogen receptor-positive, estrogen-dependent breast cancer growth in the absence of ovarian estrogens. The third-generation AIs (letrozole, exemestane, and anastrozole) inhibit the growth of such tumors by blocking the peripheral conversion of adrenal androgens to estrogens, suppressing circulating 17β-estradiol (E2) concentrations to below that detectable by current conventional methods (low pM range) [146, 147]. Although the AIs have proven

to be a highly effective therapy for post-menopausal estrogen receptor-positive (ER+) breast cancer, a significant number of patients receiving AIs will relapse within five years of treatment [148]. Thus, a better understanding of the mechanisms of AI resistance may lead to improved predictive markers of response and more effective treatment strategies. Treatment with AIs profoundly suppresses circulating estrogen concentrations; however, the concentrations of androgens are not significantly altered [149, 150]. We were therefore interested in the possibility that androgens and/or their downstream metabolites might play a role in resistance to AI therapy. A number of studies of the effects of androgens on breast cancer cells have been published, with the majority focusing on the effects of testosterone (TS) and 5α-dihydrotestosterone (DHT) on breast cancer growth [62, 145, 151-155]. Little is known, however, about the effects of these compounds on breast cancer cell growth under conditions of profound estrogen deprivation, similar to conditions found in women treated with AIs. Still less is known about the effects of downstream androgen metabolites, some of which have been shown to bind to estrogen receptors. TS is a relatively weak androgen and is metabolized by 5α-reductase to the potent androgen DHT, which in turn can be further metabolized by 3β-hydroxysteroid dehydrogenase (3β-HSD) to 5α-androstane-3β,17β-diol (3βAdiol) (Figure 1.1). 3βAdiol has been shown to bind both ERα and ERβ, although with approximately 30-fold and 14-fold lower affinity relative to that of 17β-estradiol (E2), respectively [156]. We therefore set out to evaluate the effects of androgens and their metabolites on the proliferation of estrogen responsive breast cancer cells grown under conditions of profound estrogen deprivation, with the goal of determining if these steroids might be playing a role in resistance to AI therapy.

Methods

Cell Lines, Culture Conditions, and Growth Assays

Testosterone (TS), 5α-dihydrotestosterone (DHT) and 17ß-estradiol (E2), were purchased from Sigma-Aldrich Inc. (St. Louis, MO). 5α-androstane-3β,17β-diol (3βAdiol) was purchased from Steraloids, Inc. (Newport, RI). Letrozole (Femara®) was purchased from Toronto Research Chemical (Toronto, Ontario, Canada). MCF-7, T47D and BT-474 cells were obtained from the Tissue Culture Shared Resource (TCSR) at the Lombardi

Comprehensive Cancer Center (Georgetown University, Washington, DC) and were routinely cultured in modified IMEM (Biosource International Inc., Camarillo, CA) supplemented with 10% fetal calf serum (Valley Biomedical Inc., Winchester, VA), at 37°C in a humidified 5% CO_2 atmosphere. For assays in defined hormone conditions, cells were repeatedly washed and grown in steroid depleted media (phenol red-free IMEM supplemented with 10% charcoal stripped calf bovine serum - CCS) as previously described [157]. For growth assays, cells were plated in steroid-depleted media at 2 X 10^3 cells / well in 96-well plates (Falcon, Lincoln Park, NJ) and allowed to attach overnight before being treating with vehicle control (ethanol 0.1%), E2, androgens, and the steroid antagonists. Relative cell number was determined using the crystal violet and WST assays as described previously [158].

RNA Extraction

Total RNA was isolated using TRIzol® Reagent (Invitrogen Corp., Carlsbad, CA) according to the manufacture's instructions. Yield and quality were determined by spectrophotometry (Beckman DU® 640, Beckman Coulter, Inc., Fullerton, CA) and using a Bioanalyzer RNA 6000 Nano chip (Agilent Technologies, Palo Alto, CA). All samples were stored at -80°C.

Western Blot

Western blot analysis was performed on whole cell lysates from breast cancer cell lines. Cell pellets were lysed using Gold Lysis Buffer [20 mmol/L Tris (pH 7.9), 137 mmol/L NaCl, 5 mmol/L EDTA, 10% glycerol, 1% Triton X-100, with protease inhibitor cocktail, Roche, Indianapolis, IN] and total protein from cell extracts was quantified using the Bradford assay (Bradford Reagent; Bio-Rad, Hercules, CA).

Thirty micrograms of protein per lane was resolved on 4-20% gradient polyacrylamide gels (Pierce, Rockford, IL), and transferred to PVDF membrane. CYP19 aromatase protein levels were evaluated by blotting with an anti-CYP19 antibody (ab18995, Abcam, Cambridge, MA), and 3β-HSD levels using an anti-3β-HSD antibody (P-18, Santa Cruz,

Santa Cruz, CA). Secondary antibodies were obtained from Jackson Laboratories (West Grove, PA). β-Actin was used as a loading control (I-19, Santa Cruz, Santa Cruz, CA).

Receptor binding assay

Fluorescence polarization based competitive binding assays were performed to measure the relative binding affinity of 3βAdiol for ERα using a commercially available kit (P2698, Invitrogen, Carlsbad, CA) according to the manufacturer's specifications. We have previously described the use of this assay to evaluate the relative affinity of ligands for ERα [159]. Reactions (100μL) were carried out in black-wall, low-volume 96-well plates (6006270, PerkinElmer, Waltham, MA). Following 2 hours of incubation at room temperature, fluorescence polarization values were obtained using a BMG PolarStar Omega plate reader (BMG Labtech, Durham, NC).

Real-time PCR

GREB1 mRNA expression was measured using a semi-quantitative real-time PCR assay as described previously [157]. Briefly, total RNA (1μg) was reverse transcribed using Reverse Transcription System (Promega, Madison, WI) and the resulting cDNA amplified in a 25μl reaction containing Platinum Supermix UDG (Invitrogen Corp., Carlsbad, CA), 250 nM of each primer (forward 5′-CAA AGA ATA ACC TGT TGG CCC TGC-3′ and reverse 5′-GAC ATG CCT GCG CTC TCA TAC TTA-3' - Integrated DNA Technologies, Inc., Coralville, IA), 10 nM fluorescein (BioRad Inc., Hercules, CA), and SYBR Green. Reactions were performed using an iCycler Thermal Cycler (Bio-Rad Laboratories, Inc., Hercules, CA). To control for RNA quality and quantity, GREB1 expression was normalized to the levels of the housekeeping genes 36B4 (forward 5′-GTG TTC GAC AAT GGC AGC AT-3′ and reverse 5′-GAC ACC CTC CAG GAA GCG A-3′) and GAPDH (forward 5′ - GAA GGT GAA GGT CGG AGT C - 3′ and reverse 5′ - GAA GAT GGT GAT GGG ATT TC - 3′) as described previously [157]. To evaluate the quality of product of real-time PCR assays, melt curve analyses were performed after each assay. Relative expression was determined using the $\Delta\Delta C_T$ method with either GAPDH or 36B4 as the reference genes [160].

Statistical Analyses and Curve Fitting

A two-tailed t test was used to compare treatments to respective controls (SigmaStat 3.5, Systat Software, Inc.). Curve fitting and effect concentration for half-maximal growth (EC_{50}) were determined using GraphPad Prism 4.03 (GraphPad Software, Inc.).

Results

Androgens induce estrogen-dependent breast cancer cell proliferation in estrogen-deprived conditions

To determine the effects of androgens on breast cancer cell proliferation in the absence of estrogen, we cultured MCF-7 cells under estrogen-free conditions and treated them with testosterone (TS) or 5α-dihydrotestosterone (DHT) at 10nM, and measured the increase in cell number over five days of treatment as described in Materials and Methods. Both TS and DHT induced the proliferation of MCF-7 cells under these conditions by approximately 30% and 56% over vehicle-treated controls, respectively (Figure 2.1). The stimulation of proliferation by both compounds was blocked by concomitant treatment with 500nM of the potent anti-estrogen ICI 182,780 (fulvestrant, checkered bars), whereas only the effects of TS were blocked by the aromatase inhibitor letrozole (500nM) (striped bars, Figure 2.1). The inability of the AI to block the stimulation by DHT suggests that this effect does not require aromatase activity. Similar data were generated using the estrogen dependent breast cancer cell lines T47D and BT474 (data not shown).

Steroid metabolizing enzymes are up-regulated under estrogen-deprived conditions

We observed that the androgens TS and DHT can stimulate the growth of estrogen dependent cells, and that this effect is apparently mediated through the estrogen receptor, since it is blocked by an estrogen receptor antagonist. These findings are surprising in light of the extremely low affinity of these androgens for ERα [156]. This led us to hypothesize that in estrogen-deprived culture conditions, the breast cancer cells are capable of metabolizing androgens into estrogens. This can be accomplished by CYP19 aromatase (TS to E2), 5α-reductase (TS to DHT) and 3β-HSD (DHT to 3βAdiol). To test this hypothesis we used Western blot analysis to examine the expression of the steroid

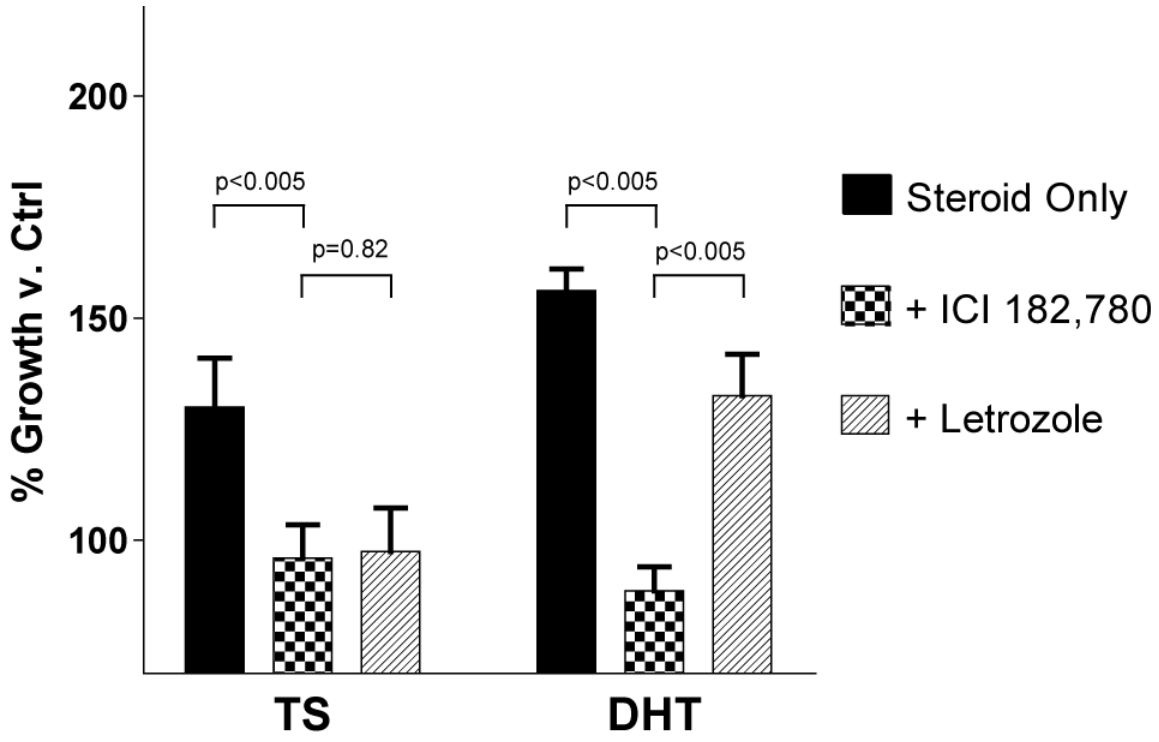

Figure 2.1. Androgens induce breast cancer cell growth. MCF-7 cells were grown in E2-free conditions as described in Materials and Methods. The indicated steroids were added to a final concentration of 10nM. ICI 182,780 (faslodex) and letrozole were added to a final concentration of 500nM. Bars represent 5-day growth vs. vehicle-treated control ± S.D.

metabolizing enzymes CYP19 aromatase and 3β-HSD in breast cancer cells. Cells grown in standard culture conditions (media supplemented with 10% fetal bovine serum) were compared to cells grown in estrogen-free conditions (media with 5% charcoal-stripped serum) for 1-4 days. Figure 2.2A shows that CYP19 aromatase and 3β-HSD levels were very low in MCF-7 cells grown under standard culture conditions. However, culture under conditions of profound estrogen deprivation resulted in a dramatic induction of CYP19 aromatase and 3β-HSD expression levels in a time-dependent manner. Densitometric analysis of the target/actin (loading control) ratio shows that levels of both CYP19 aromatase and 3β-HSD in MCF-7 cells increase more than 6-fold versus control (standard conditions) after 4 days in estrogen-free conditions (Figure 2.2B). Increases in CYP19 and 3β-HSD expression were also seen in T47D cells after incubation in estrogen-free conditions, though to lower levels, with approximately 2-fold increases in enzyme expression (data not shown). We observed that 5α-reductase is not expressed under estrogen-free conditions both functionally (Figure 2.1; TS-induced growth is completely blocked by aromatase inhibition, suggesting that it is not metabolized to DHT or 3βAdiol) and by cDNA microarray analysis (data not shown).

3βAdiol is a weak agonist of ERα growth induction

The potential for 3βAdiol to act as an ERα agonist and induce the growth of breast cancer cells has been largely ignored in the literature, despite previous work demonstrating its binding to ERα [156]. We therefore examined the ability of the androgen metabolite 3βAdiol to induce the growth of breast cancer cells under estrogen-free conditions as described in Materials and Methods. 3βAdiol induced the proliferation of MCF-7 cells approximately 82% over vehicle-treated controls, an effect inhibited by the anti-estrogen, but not by the aromatase inhibitor (Figure 2.3A), suggesting that this effect does not depend on metabolism by aromatase. Dose-response curves for growth induction were generated for TS, DHT and 3βAdiol, and compared to growth induction by E2 (Figure 2.3B). 3βAdiol appears to be approximately two logs less potent than E2 with respect to induction of the growth of MCF-7 cells (EC_{50} of approximately 0.2nM and 5.0pM, respectively). However, 3βAdiol is substantially more potent than DHT (EC_{50} ~0.8nM) and TS (EC_{50} ~2.4nM). Interestingly, 3βAdiol appears to act as a weak agonist of ERα

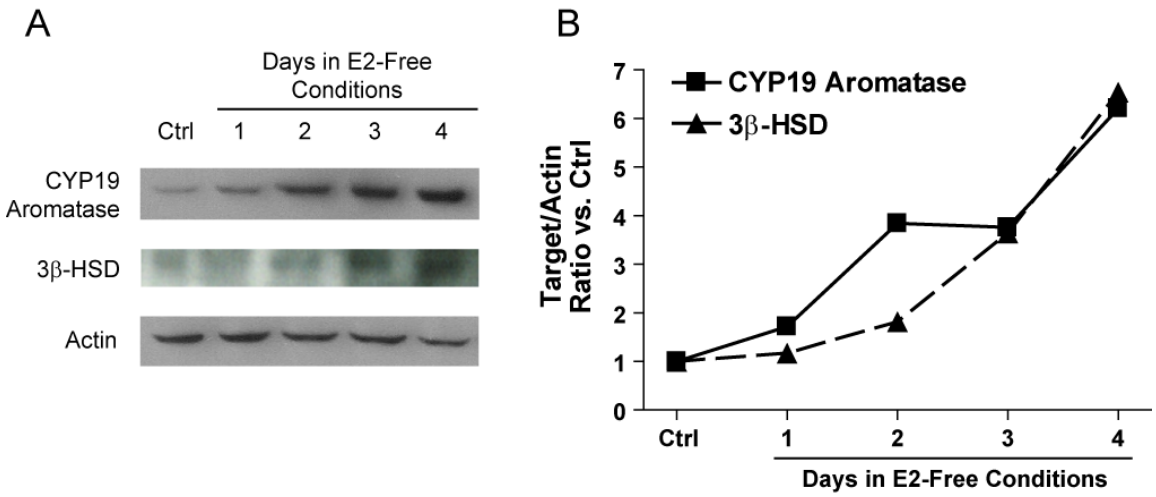

Figure 2.2. CYP19 Aromatase and 3β-HSD expression increases in breast cancer cells during growth in E2-free conditions. (A) Western blot of cells grown in normal media with 10% FBS (lane 1), and increased time after steroid hormone removal (described in Materials and Methods) and incubation in media with 5% CCS. (B) Densitometry analysis of target/actin ratio vs. the normal media control (loading control).

for growth induction, since the maximum stimulation of proliferation induction by 3βAdiol was roughly 75% of the maximal induction by E2. Similar results were observed in T47D cells (Figure 2.3C).

3βAdiol is a pharmacological partial agonist of growth induction in MCF-7 cells

The observation that 3βAdiol only induced ~75% maximal growth in MCF-7 cells versus E2 suggested that 3βAdiol may act as a partial agonist of ERα. We tested whether 3βAdiol as a partial agonist could antagonize E2-induced breast cancer cell growth. MCF-7 cells in estrogen-free conditions as described above were treated with 100pM E2 (~EC_{95}) and increasing concentrations of 3βAdiol. Increasing 3βAdiol suppressed growth induced by E2 to the maximal level induced by 3βAdiol alone (Figure 2.4).

3βAdiol growth induction is blocked by anti-estrogens

To confirm that growth stimulation by 3βAdiol is mediated through activation of ERα, we determined whether its effects could be blocked by the anti-estrogens tamoxifen, 4-hydroxytamoxifen (4-OHTam), and ICI 182,780 (fulvestrant). Cells were treated with either E2 or 3βAdiol (1nM) alone or in combination with increasing concentrations of the anti-estrogens. As shown in Figure 2.5, both E2- and 3βAdiol- induced MCF-7 cell proliferation was inhibited by the anti-estrogens in a dose-dependent manner (Figure 2.5 A and B respectively). ICI 182,780 and 4-OHTam inhibited the effects of 1nM E2 roughly equivalently (IC_{50} of 23nM and 47nM, respectively), and tamoxifen only partially inhibited growth at 1μM (IC_{50} >1μM), consistent with 2-fold lesser affinity for ERα versus ICI 182,780 and 4-OHTam. Significantly lower concentrations of the anti-estrogens were required to inhibit the effects of 1nM 3βAdiol on cell growth. ICI 182,780 and 4-OHTam were roughly equipotent (IC_{50} of 1.0nM and 2.0nM, respectively), and tamoxifen inhibited 3βAdiol-induced growth at sub-micromolar concentrations (IC_{50} ~0.2μM). The anti-androgen bicalutamide did not inhibit 3βAdiol-induced growth at similar concentrations (data not shown). Similar results were observed in T47D cells (data not shown).

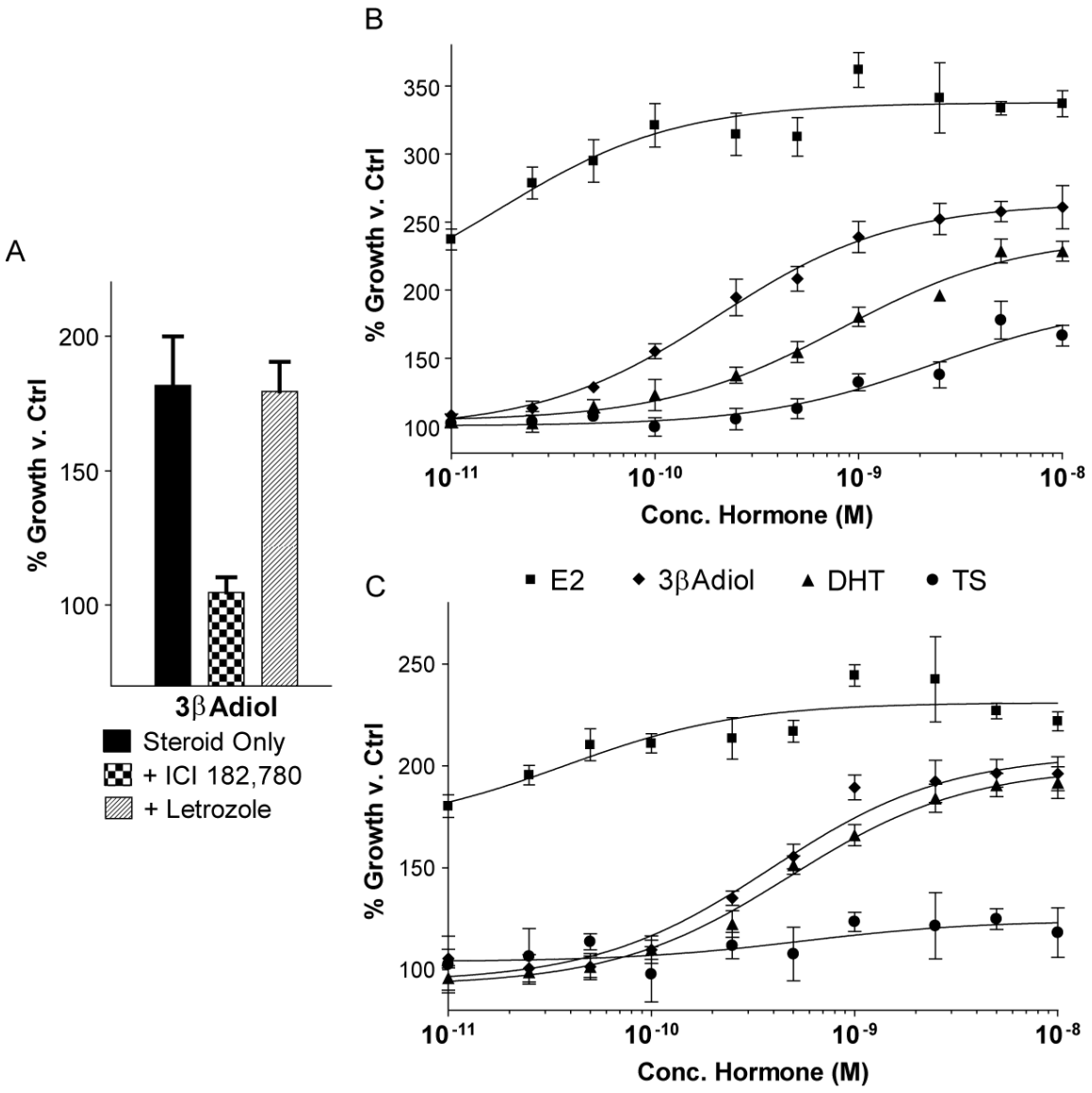

Figure 2.3. 3βAdiol induces the growth of breast cancer cells. Breast cancer cells were grown in E2-free conditions as described in Materials and Methods. (A) 3bAdiol was added to MCF-7 cells to a final concentration of 10nM. ICI 182,780 (faslodex) and letrozole were added to a final concentration of 500nM. Bars represent 5-day growth vs. vehicle-treated control ± S.D. MCF-7 (B) or T47D (C) cells were treated with the indicated steroid at concentrations from 10pM - 10nM at half-log intervals. Points represent 5-day growth vs. vehicle-treated control ± S.D.

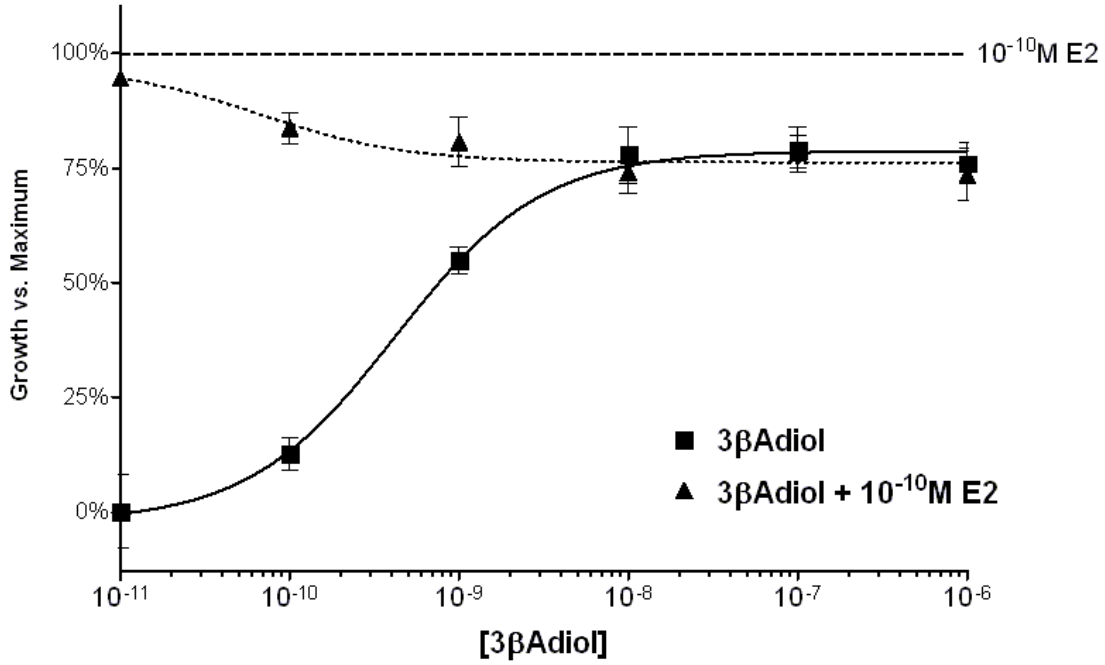

Figure 2.4. 3βAdiol is a partial agonist of ERα. MCF-7 cells were treated as described in Figure 1, with increasing 3βAdiol. Dashed line represents growth induced by 100pM E2 (data normalized to 100pM E2 growth as 100%). Points represent mean of six replicates ± SD.

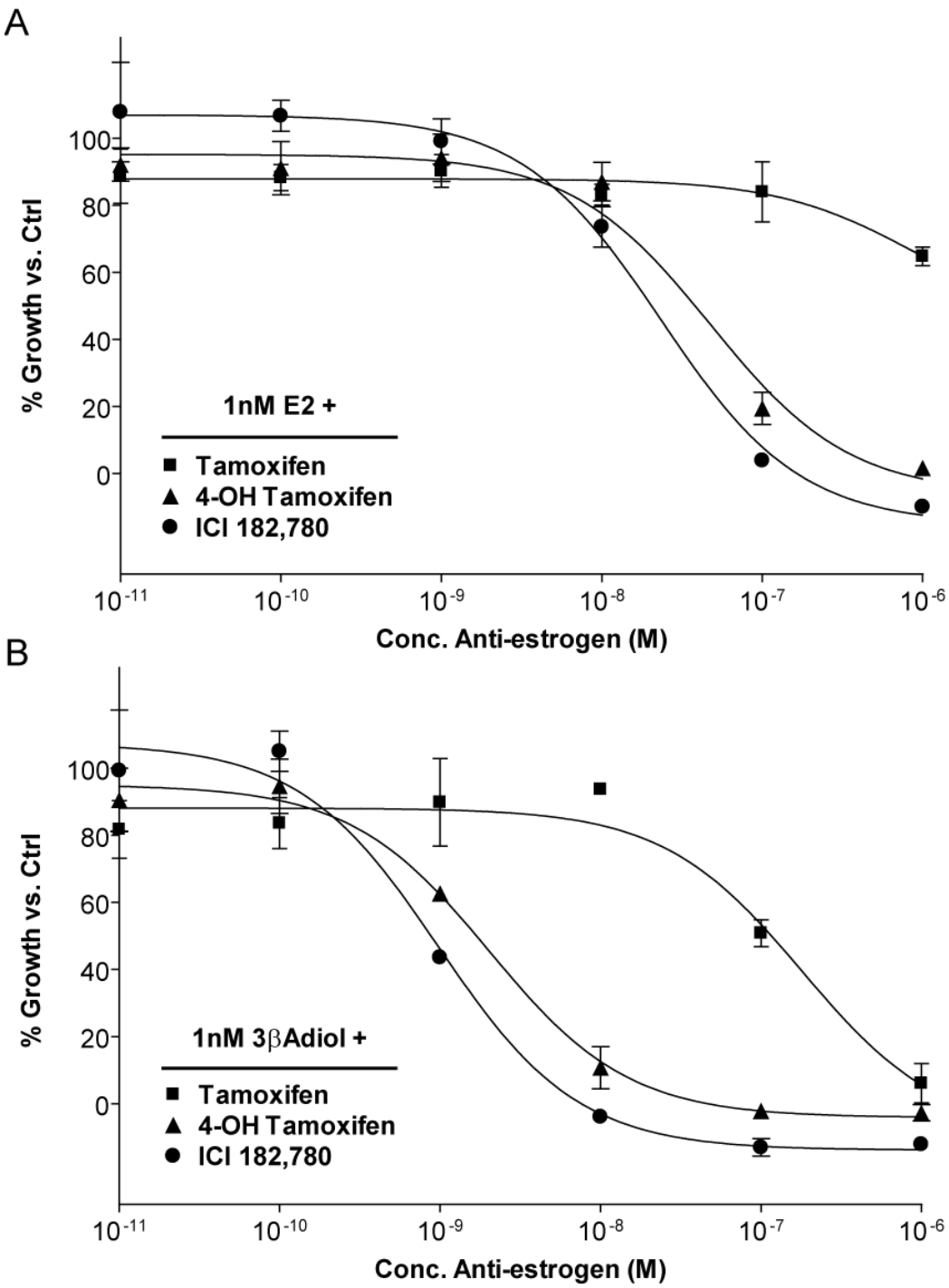

Figure 2.5. Anti-estrogens block 3βAdiol-induced growth. MCF-7 cells were grown in E2-free conditions as described in Materials and Methods. Growth induction by (A) 1nM E2 or (B) 1nM 3βAdiol was antagonized by the anti-estrogens tamoxifen, 4-hydroxy-tamoxifen (4-OH Tamoxifen), and ICI 182,780 (Faslodex). Anti-estrogens were added to final concentrations from 10pM - 1μM at log intervals. Points represent 5-day growth vs. vehicle-treated control ± S.D.

3βAdiol binds ERα with decreased affinity versus E2

We performed an in vitro, florescence polarization-based receptor binding assay to examine the relative affinities of 3βAdiol and E2 for ERα. Based on their ability to compete with a labeled ligand for binding to ERα, 3βAdiol bound ERα with an approximately 10-fold lower affinity than E2 (Figure 2.6). This decreased affinity of 3βAdiol for ERα is consistent with the reduced potency of 3βAdiol versus E2 observed in growth assays (Figure 2.3), and in previous reports [156].

3βAdiol induces expression of the ERα-responsive gene GREB1

To determine whether 3βAdiol activation of ERα induced ERα-mediated gene transcription, we examined the expression of GREB1 in breast cancer cells treated with 3βAdiol. We have previously demonstrated that GREB1 is an ERα-specific downstream target critically involved in the estrogen induced growth of breast cancer cells [157]. Cells were grown in estrogen-free conditions as described above, and GREB1 expression was measured 24 hours after the addition of 3βAdiol, alone or in combination with ICI 182,780 as described in Materials and Methods. Cells treated with 1nM 3βAdiol exhibited modest induction of GREB1 expression (~2.5-fold) over vehicle-treated controls (Figure 2.7), however, 10nM and 100nM 3βAdiol substantially induced GREB1 expression (17.5- and 56.4-fold vs. control, respectively). Treatment with 100nM 3βAdiol resulted in GREB1 expression levels comparable to those produced by treatment with 1nM E2, which caused a 49.0-fold induction in GREB1 expression (dashed line). Concomitant treatment with the anti-estrogen ICI 182,780 completely blocked the induction of GREB1 expression by both 3βAdiol and E2 (Inhibition of E2 stimulation not shown).

Discussion

The use of AI as first line endocrine therapy for post-menopausal, estrogen receptor positive breast cancer has increased dramatically over the last few years with the publication of clinical trials suggesting that these compounds may be more effective than the anti-estrogen tamoxifen [148]. Although the AIs are effective, well tolerated drugs, a significant percentage of patients experience disease relapse during AI therapy,

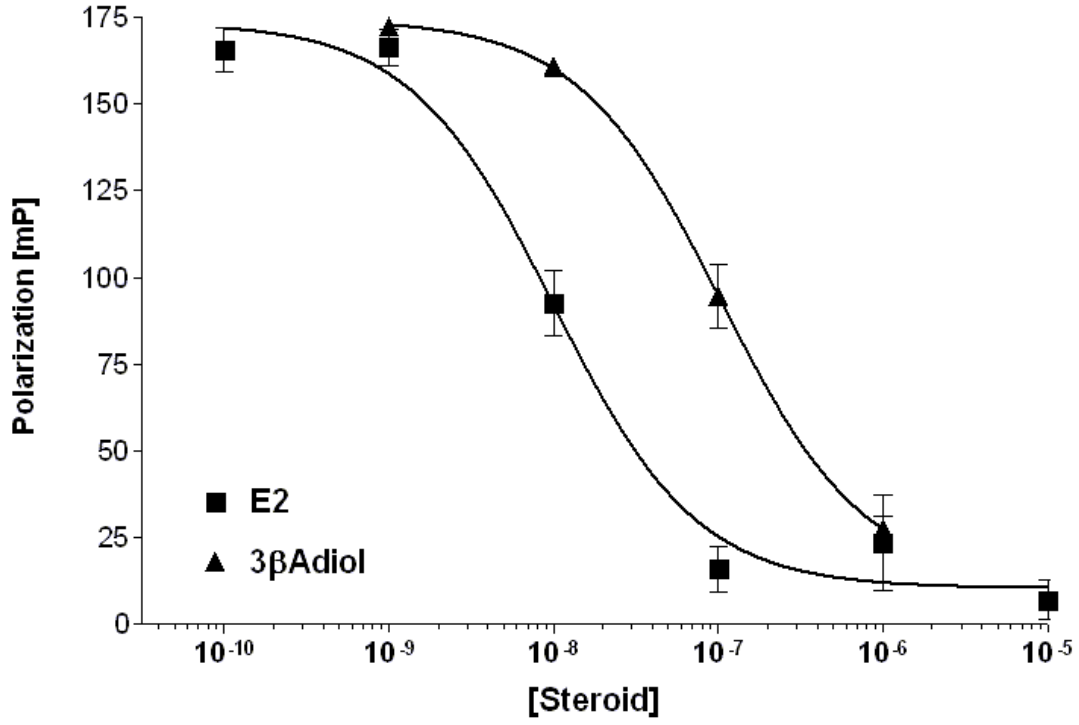

Figure 2.6. 3βAdiol binds recombinant ERα. Binding assays were performed with ERα competitive binding assays as described in Materials and Methods. Fluorescent ligand displacement decreases fluorophore polarization (mP), indicated increased test ligand binding. E2 IC_{50}: 10.0nM; 3βAdiol IC_{50}: 104nM.

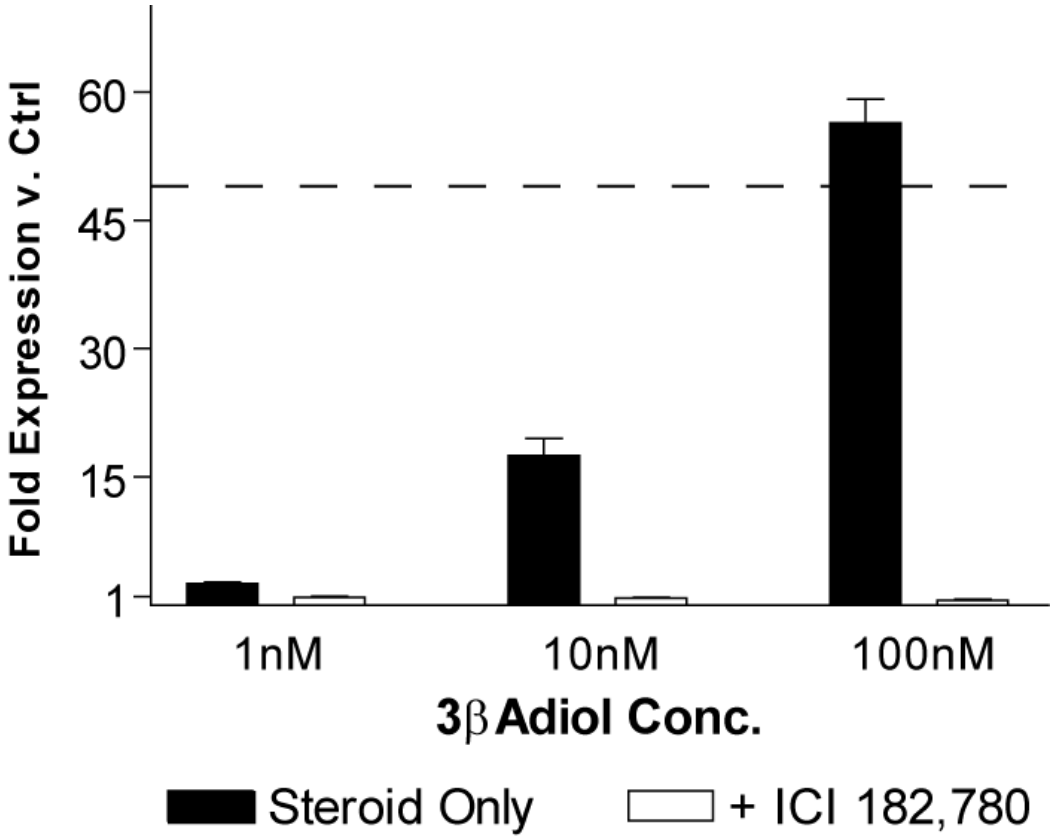

Figure 2.7. 3βAdiol induces the expression of GREB1 in breast cancer cells. MCF-7 cells were grown in E2-free conditions as described in Materials and Methods. Cells were treated with the indicated concentrations of 3βAdiol in the presence (light bars) or absence (dark bars) of 1mM ICI 182,780 for 24 hrs before harvest. Bars represent GREB1 expression vs. vehicle-treated control ± S.D. The dashed line represents GREB1 expression induced by 1nM E2.

suggesting that resistance to this class of compound is a significant problem. Anecdotal evidence suggests that some women that fail to respond to AIs may still respond to other modes of endocrine therapy, even though their serum estrogen concentrations have been successfully suppressed by AI therapy. This suggests that at least a proportion of these resistant tumors in these women are still estrogen dependent, and implies that non-classical estrogens may be playing a role in resistance to AI therapy.

Women on AI therapy have circulating concentrations of estrogen that are below the limit of detection (low pg/ml), however, the concentrations of androgens remain unchanged (low nM range) [149, 150]. We hypothesized that under conditions of profound estrogen deprivation, the weak estrogenic activity of other steroids might be sufficient to drive the proliferation of estrogen dependent breast cancer, thereby providing a mechanism for AI resistance. Specifically, we hypothesized that androgens and their metabolites, generated independent of aromatase activity, may contribute to breast cancer growth in the absence of estrogens.

A considerable amount of work has been done over the years studying the effects of androgens on the proliferation of breast cancer cells [62, 145, 151-155]. The literature is, however, somewhat confusing, with conflicting data coming from relatively similar experimental systems. For example, 30 years ago we demonstrated that under serum-free conditions, androgens stimulate thymidine incorporation in breast cancer cell lines apparently through the androgen receptor [152, 155]. Similarly, the testosterone metabolite DHT was shown by Birrell et al. to inhibit the growth of some breast cancer cell lines, but induce the growth of others [151]. Anti-androgens demonstrated mixed ability to inhibit the effects of DHT on growth, and this was attributed to the potential activity of un-indentified DHT metabolites [151]. Macedo et al. later showed that DHT is growth-inhibitory in MCF-7 cells under low-estrogen conditions, and that this effect was mediated by the androgen receptor [145]. One common thread of much of this work is that many of the studies use culture systems in which it is possible that low, but significant, amounts of residual estrogen remain, and so may not adequately model the conditions present in a woman on AI therapy. We have previously made use of a culture

system in which residual estrogen concentrations are extremely low (sub pM) [157, 159], and decided to make use of this system to revisit the effects of androgens and their metabolites on the proliferation of estrogen dependent breast cancer cells.

In this study we have demonstrated that profound estrogen depravation results in the up-regulated expression of two important steroid metabolizing enzymes, CYP19 aromatase and 3β-HSD. MCF-7 and T47D cells are generally considered to express very low levels of aromatase and the finding that estrogen withdrawal can substantially increase expression levels has important implications. The induced expression of aromatase may not be important in the context of AI therapy, since the newly expressed enzyme should be efficiently inhibited by the drug. However, the induction of 3β-HSD and potentially other enzymes raises the possibility of significant local metabolism of androgens and other steroids, and generation of estrogens, by the breast cancer cells.

The downstream metabolite of DHT, 5α-androstane-3β,17β-diol (3βAdiol), is generated by the action of 3β-HSD. It has been known for some time that 3βAdiol can bind to both ERα and ERβ with approximately 30-fold and 14-fold lower affinity relative to that of E2, respectively, suggesting slight specificity for ERβ [156]. 3βAdiol has been extensively characterized as an ERβ ligand in *in vitro* ERβ-promoter driven luciferase assays [161, 162], gene expression assays [163, 164], and *in vivo* prostate and prostate cancer models [165, 166]. 3βAdiol has been shown to play a well defined role in prostate cancer etiology as an ERβ ligand. Weihua et al. demonstrated that 3βAdiol is anti-proliferative in prostate cancer via activation of ERβ [165, 166]. The cytochrome P450 CYP7B1 has been shown to be the primary enzyme responsible for the inactivation and elimination of 3βAdiol [51, 52]. Activation of ERβ by 3βAdiol and elimination of 3βAdiol by CYP7B1 have been shown to be critical regulators of prostate cancer growth as an anti-proliferative pathway [165, 167]. Recently, increased CYP7B1 levels were correlated with increased prostate cancer grade, suggesting that increased elimination of 3βAdiol removes tumor growth inhibition by ERβ [167]. Surprisingly, in spite of this work elucidating a role for 3βAdiol in prostate cancer, little is known about the importance of this steroid in breast cancer. Reporter studies have suggested that

androgen metabolites (largely undefined in these studies) can induce the expression of an estrogen-responsive luciferase construct, but little further analysis of the function of these metabolites has been reported [154, 168]. Interestingly, female knockout mice generated by Omoto et al that lack expression of CYP7B1 (the enzyme responsible for the elimination of 3βAdiol) showed increased proliferation of both mammary and other reproductive tissues, as well as early onset of puberty and early ovarian failure, suggesting that 3βAdiol is indeed estrogenic in the breast and reproductive tissues [169].

In this study, we report for the first time that 3βAdiol can induce the proliferation of breast cancer cells through direct activation of ERα. This growth-stimulation is antagonized by the anti-estrogens 4-hydroxytamoxifen and ICI 182,780. In addition to inducing growth, 3βAdiol also induces the expression of the ERα-specific downstream gene GREB1 which we have previously shown is a critical mediator of estrogen stimulated proliferation. These findings raise the possibility that in the absence of conventional estrogens, 3βAdiol may be an important mediator of estrogen dependent breast cancer growth. We hypothesize that the generation of 3βAdiol from testosterone via aromatase-independent pathways, represents a potential mechanism for resistance to AIs. The enzymes required for generation of 3βAdiol, 5α-reductase and 3β-HSD, are both expressed in a wide variety of tissues, primarily the adrenal glands and liver [170]. In addition, we have demonstrated that 3β- HSD is expressed in estrogen-deprived breast cancer cells. Thus, in the context of AI therapy, while circulating testosterone cannot be converted to 17β-estradiol due to inhibition of aromatase activity, it may readily be converted to 3βAdiol both systemically and, potentially, locally in the mammary tumor. In one study, plasma concentrations of 3βAdiol in humans were reported to be approximately 1.5nM [171]. These relatively low concentrations of circulating 3βAdiol may be sufficient to drive tumor growth in the absence of estrogen, particularly in women undergoing treatment with AIs. In addition, prior reports have demonstrated that breast cancer cells can become hypersensitive to extremely low concentrations of estrogens after long-term estrogen deprivation [101, 172]. These data suggest that tumors may be sensitive to very low concentrations of a weak ERα agonist such as 3βAdiol. Further, the

reported 3βAdiol plasma concentrations are greater than the calculated EC_{50} values for growth induction of breast cancer cells in culture (as shown in Figure 3).

In summary, these data demonstrate the important concept that the metabolism of testosterone by aromatase does not represent the only mechanism by which estrogen-like steroids may be generated in post-menopausal women. While inhibition of aromatase may be sufficient to block the production of canonical estrogens in the majority of patients treated with AIs, conditions causing an increase in activity of the enzymes responsible for 3βAdiol production, particularly locally within the tumor, may lead to production of estrogen-like steroids independent of aromatase. These pathways may represent an important mechanism for resistance to AI therapy and a more thorough understanding of the complexity of hormone metabolism may be extremely valuable in the refinement of optimal endocrine therapy for breast cancer. Other alternative pathways exist and may also contribute to AI resistance, as discussed in Chapter III. Long-term adaptation to metabolites produced by alternative pathways may represent important mechanisms of resistance to therapy (Chapter IV).

Chapter III.

Cytochrome P450 2B6 generates testosterone metabolites with unique steroidogenic properties in breast and prostate cancer cells

Introduction

In addition to the testosterone metabolism pathways responsible for the generation of E2 and 3βAdiol, testosterone may be instead metabolized by other enzymes, notably other cytochrome P450s. While most CYP450s are expressed primarily in the liver, many are expressed in peripheral tissues, including the breast and breast tumors [136-138]. We observed in gene expression array datasets (www.oncomine.org) that mRNA for Cytochrome P450 2B6 (CYP2B6) is over-expressed in ER-positive breast cancers. To confirm this, we examined CYP2B6 expression in our breast cancer cell lines, grown in normal *in vitro* culture conditions or *in vivo* as xenografts, by quantitative PCR (unpublished data, not shown). Our results confirmed that CYP2B6 is specifically expressed in ER-positive versus ER-negative breast cancer cells. Furthermore, CYP2B6 was only expressed in ER-positive cells when grown *in vivo* as xenografts. Though this was not entirely surprising since CYP450 expression is often lost when cells are grown in culture [173-176], it suggests that the role of CYP2B6 in breast cancer may have been overlooked due to the lack of expression in standard cell culture models. The role of CYP2B6 in hepatic drug metabolism of substrates including the antineoplastic agent cyclophosphamide, the antidepressant bupropion, and the antiviral efavirenz is well established [143]. However, the potential roles of CYP2B6 in metabolizing endogenous factors, e.g. steroid hormones, and in breast cancer etiology and response to therapy are not known.

Studies have shown that CYP2B1, the rat homolog of CYP2B6, exhibits minor estrogen metabolizing activity, but has a greater ability to metabolize androgens, producing a number of unique hydroxylated metabolites from both testosterone and androstenedione

[129]. CYP2B6 itself has been shown to hydroxylate testosterone at the 16-carbon, producing both 16α- and 16β-hydroxytestosterone (16αOH-TS and 16βOH-TS, respectively) (Figure 3.1) [134]. This hydroxylation is unique to CYP2B6, and has not been found for any other human CYP450 tested [128]. Additionally, Ekins et al. demonstrated that testosterone may also be unique as a CYP2B6 substrate in that its metabolism kinetics suggest that testosterone may induce auto-activation of CYP2B6 [133]. Taken together with the observations that CYP2B6 is expressed at high levels in ER-positive breast tumors, high levels of hydroxylated testosterone metabolites may be specifically generated in the breast. In addition to its potential role for metabolizing androgens in breast tumors, CYP2B6 activity may play a role in the etiology of prostate cancer. Analogous to breast cancer, prostate cancer is driven by androgens than activate the androgen receptor (AR) [177]. Androgens including TS and DHT are the primary AR ligands that bind and activate AR, similar to the role of E2 in the activation of ER. The abilities of 16α- and 16β-hydroxytestosterone to bind to and activate androgen or estrogen receptors have not been previously examined. Thus, it is unclear whether metabolism of testosterone by CYP2B6 represents a mechanism of steroid hormone clearance or generation of novel hormone receptor ligands. The contributions of these metabolites to breast and prostate cancer etiology and development, and response to endocrine therapy, have not previously been explored. In this chapter, we investigate the roles of CYP2B6-generated testosterone metabolites as ERα and AR ligands. Additionally, we describe efforts to characterize CYP2B6 activity in metabolizing testosterone in both recombinant and cell culture systems.

Methods

Cell Lines, Culture Conditions, and Growth Assays

16α-hydroxytestosterone and 16β-hydroxytestosterone were purchased from Steraloids. Other chemicals were obtained as described above. Anastrozole was obtained from Toronto Research Chemical (Toronto, Ontario, Canada). LNCaP cells were obtained from the laboratory of Ken Pienta at the University of Michigan and were routinely cultured as described in Chapter II. For assays in controlled hormone concentrations, LNCaP and MCF-7 cells were repeatedly washed as described in Chapter II. For growth

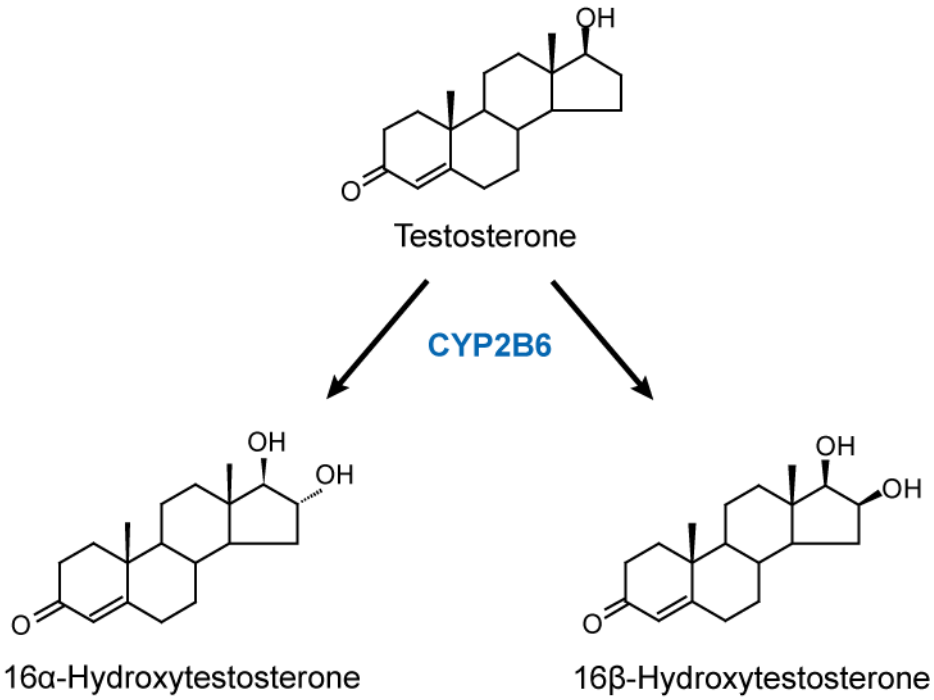

Figure 3.1. CYP2B6 metabolism of testosterone. TS is hydroxylated by CYP2B6 at the 16-carbon in either the alpha (back) or beta (forward) position.

assays, MCF-7 cells were processed as described in Chapter II. LNCaP cells were plated in steroid-depleted medium at 7.5 x 10^3 cells / well in 96-well plates (Falcon, Lincoln Park, NJ) coated with poly-D-lysine to improve cell adhesion. Cells were treated with drug or steroid as indicated within one hour of plating. Relative cell number for LNCaP cell assays was determined using the FluoReporter Blue Fluorometric dsDNA Quantitation Kit (F2962, Invitrogen) according to the manufacturer's instructions. Relative cell number for MCF-7 cell assays was determined using crystal violet staining as described in Chapter II.

Receptor binding assay

Fluorescence polarization-based competitive binding assays were performed to measure the relative binding affinity of 16-hydroxytestosterones for ERα using a commercially available kit (P2698, Invitrogen) as described in Chapter II.

CYP2B6 Expression Constructs

A wild-type CYP2B6 clone was obtained from the laboratory of Frank Gonzalez in a pUC9 entry plasmid for sub-cloning into mammalian expression vectors [178]. The CYP2B6 ORF was amplified by PCR with a consensus Kozak sequence and sub-cloned into a TOPO TA entry vector (Invitrogen). The clones were sequence verified prior to recombination into the pcDNA 6.2/V5-DEST vector using the Gateway LR Clonase recombination system (Invitrogen); the V5 tag contained in the vector was not attached to the CYP2B6 ORF. The final vector was sequence-verified prior to transfections (referred to as pcDNA/2B6 below). Additional CYP2B6 expression constructs were obtained from the laboratory of Ulrich Zanger; these pCMV4-based constructs had been demonstrated to generate functional CYP2B6 protein in COS-1 cells [179] (referred to as pCMV4/2B6 below). Of note, expression studies were performed with both the pcDNA/2B6 and pCMV4/2B6 plasmids due to the lack of a mammalian selection marker on the pCMV4/2B6 plasmid.

Expression plasmids were transfected into MCF-7, COS-7 and HEK293T cells using FuGene 6 (Roche Applied Science) according to the manufacturer's instructions. Cells

were also electroporated using an Amaxa Nucleofector II (Lonza-Walkersville, Walkersville, MD) according to the manufacturer's instructions. Co-transfection with pmaxGFP was used as visual confirmation of transfection and to assess transfection efficiency. Post-transfection, mRNA was harvested from cells using RNeasy Mini columns (Qiagen, Valencia, CA) according to the manufacturer's instructions. CYP2B6 mRNA expression was measured using reverse-transcription PCR with the following primers: forward – 5' AAT CGC CAT GGT CGA CCC ATT CTT 3'; reverse – 5' TGG CCG AAT ACA GAG CTG ATG AGT 3'. Protein was harvested according to methods obtained from the laboratory of Ulrich Zanger [179]. Cells were lysed in buffer containing 50mM Tris-HCl, 0.1% Triton X-100 and 5mM EDTA, supplemented with protease inhibitor cocktail (Complete mini, Roche) prior to western blotting as described above. Membranes were immunoblotted with WB-2B6-PEP antibody (BD Biosciences, San Jose, CA) at 1:2000 in 1% milk in 0.05% TBS-T with gentle shaking overnight at 4°C.

CYP7B1 Expression Construct

As additional efforts to express CYP450s in cell culture systems, CYP7B1 over-expression models were developed concurrently with the above CYP2B6 experiments. A pCMV6-based, expression-verified, DDK-tagged CYP7B1 plasmid was obtained from Origene (RC222647, Rockville, MD) (referred to as pCMV6/7B1 below). COS-7 and HEK293T cells were transfected as described above. Protein expression was measured after harvesting cell lysates (RIPA buffer, Thermo Pierce; supplemented with protease inhibitor cocktail) following western blotting as described above using HRP-conjugated anti-DDK antibody (ab49763, Abcam, Cambridge, MA).

Recombinant CYP2B6 testosterone metabolism

Recombinant wild-type CYP2B6 was prepared by the laboratory of Paul Hollenberg as previously described [134]. Additionally, plasmids encoding the CYP2B6 variants *4 (K262R), *9 (Q172H) and *6 (K262R and Q172H) were used to generate recombinant variant CYP2B6 protein. Testosterone oxidation reactions were also carried out as previously described [134]. Briefly, CYP2B6 protein was reconstituted with P450

reductase and lipid prior to incubation with 100μM TS for 40 minutes. Metabolites were extracted with ethyl acetate and reconstituted in methanol prior to separation by HPLC. Metabolites were compared to standards for identification and quantified by UV absorbance at 254nm. TS metabolism experiments were carried out in collaboration with Chitra Shidar of the Hollenberg laboratory.

Co-culture systems

To circumvent repeated difficulties with expression of CYP450s in MCF-7 cells, COS-7 cells transiently expressing CYP7B1 were co-cultured with MCF-7 cells. Co-culture was performed in 24-well plates (353504, BD Biosciences), with MCF-7 cells seeded in the lower primary well; COS-7 cells were seeded into the upper insert well (353495, BD Biosciences). Inserts contained 0.4μm high density pores, preventing cell migration between chambers but allowing fluid/solute transfer. COS-7 cells were transfected with pCMV4/2B6 or pCMV6/7B1 plasmid (or mock transfected) 24 hours prior to seeding. Upper wells (containing COS-7 cells) were treated with steroid hormones 24 hours after seeding as described in results. MCF-7 cells were assessed for growth 1-5 days after treatment and stained with crystal violet as described above, or harvested and counted using a Scepter cell counter (Millipore, Billerica, MA). COS-7 viability in insert wells was assessed via cell counting.

Results

16-hydroxylated testosterones are not estrogenic in breast cancer cells

MCF-7 cells under estrogen-free conditions were treated with increasing concentrations of 16αOH-TS or 16βOH-TS from 1pM to 10nM. Cell growth was measured following 5 days of growth post-treatment, and growth induced by hydroxytestosterones was compared to that induced by E2 and TS (Figure 3.2). E2 and TS induced growth are indicated by dashed and dotted lines, respectively. 16αOH-TS and 16βOH-TS did not induce growth at concentrations up to 10nM; growth was not significantly different than vehicle control.

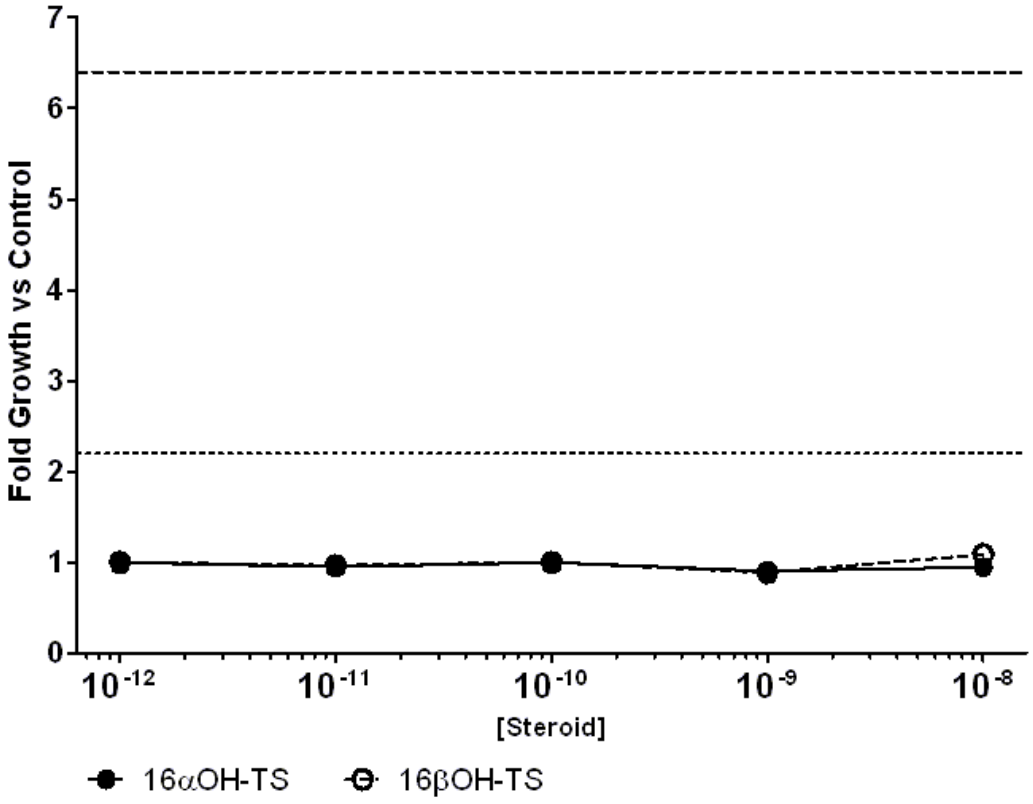

Figure 3.2. 16-hydroxytestosterones do not induce breast cancer cell growth. MCF-7 cells were treated as described above and assayed for growth 5 days after treatment. Points indicate average growth of 6 replicates versus vehicle control ± SEM. Small dashed line, growth induced by 10nM TS. Large dashed line, growth induced by 1nM E2.

Consistent with these results, when the binding of 16-hydroxytestosterones to ERα was assessed using competitive binding assays, we did not observe receptor binding. E2 bound recombinant ERα with an IC_{50} of ~10nM; neither 16α- nor 16βOH-TS exhibited any ERα binding at concentrations up to 10μM (data not shown).

16-hydroxylated testosterones are differentially androgenic in prostate cancer cells

LNCaP cells, following steroid washing as described above, were treated with increasing concentrations of DHT, 16αOH-TS or 16βOH-TS from 1pM to 10nM, in the presence or absence of the anti-androgen bicalutamide (Figure 3.3). DHT induced growth with an approximate EC_{50} of 180pM; maximal growth was induced by 1nM DHT (~4.1-fold vs. control). Since DHT induces growth via binding AR, growth could be inhibited using bicalutamide; 10μM bicalutamide increased the DHT EC_{50} >1 log. 16αOH-TS did not induce the growth of LNCaP cells at concentrations up to 10nM; the addition of bicalutamide had no effect. 16βOH-TS induced the growth of LNCaP cells at concentrations >100pM. 16βOH-TS was less potent than DHT (EC_{50} ~1.6nM), however, maximum growth induced by 16βOH-TS was greater than that by DHT (~5.5-fold vs. control at 3.5nM). Bicalutamide inhibited 16βOH-TS-induced growth similarly to inhibition of DHT-induced growth; the 16βOH-TS EC_{50} was increased beyond concentrations tested.

16-hydroxylated testosterones are not aromatase inhibitors

Though the above data suggest that 16-hydroxytestosterones are not directly estrogenic, 16α-hydroxytestosterone has been shown to be an estrogen precursor. E3 is the only steroid formed when 16αOH-TS is aromatized during incubation with human placental microsomes [180-182]. 16αOH-TS, however, is a relatively poor aromatase substrate, being metabolized ~100-fold slower than androstenedione [180]. These data, however, led us to hypothesize that 16-hydroxtestosterones may act as endogenous aromatase inhibitors by virtue of binding to aromatase and competing with other substrates due to their low rate of aromatization.

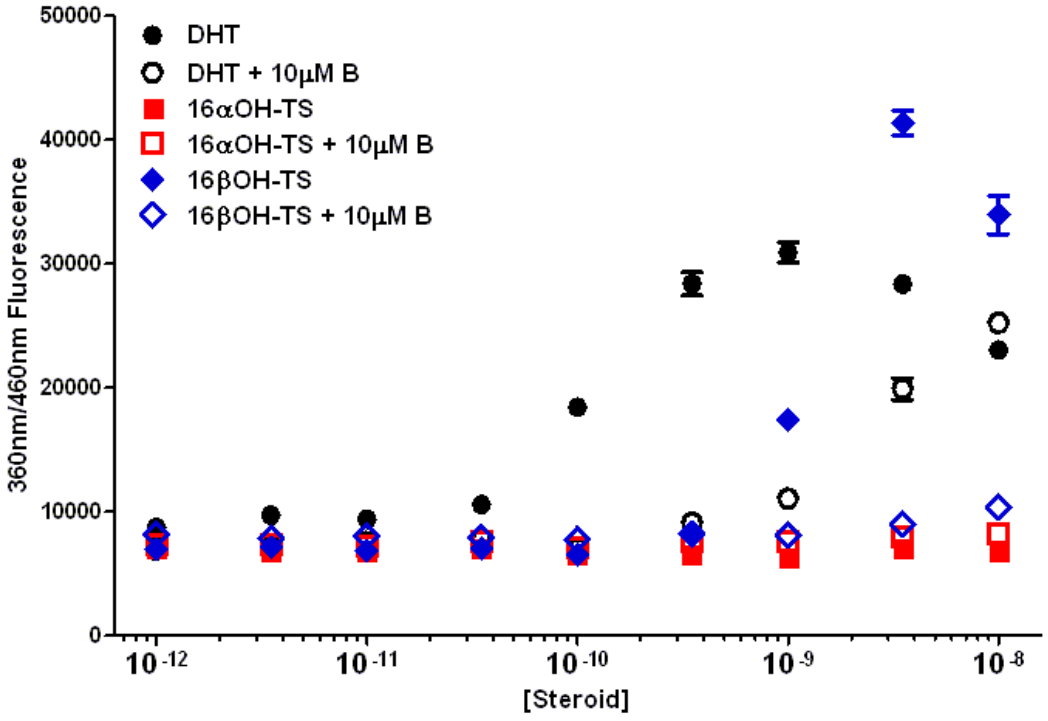

Figure 3.3. 16-hydroxytestosterones differentially induce LNCaP cell growth. LNCaP cells were treated as described above and assayed for growth 5 days following treatment. Points indicate average fluorescent readings of 6 replicates ± SEM.

To test this hypothesis, MCF-7 cells were treated with increasing concentrations of 16-hydroxytestosterones (up to 1μM) in the presence of 10nM TS. Growth induced by TS could be inhibited by 1μM anastrozole. However, neither 16-hydroxytestosterone inhibited TS-induced growth at any concentration tested (data not shown).

Recombinant CYP2B6 allelic variants differentially hydroxylate testosterone

Differential rates of TS metabolism by CYP2B6 may play a significant role in the effects of 16-hydroxytestosterones on breast cancer growth or in the availability of TS for other downstream metabolic pathways. CYP2B6 variants may metabolize TS at different rates versus the wild-type enzyme. To test this, TS was incubated with recombinant CYP2B6 wild-type (CYP2B6*1) and variant (CYP2B6*4, *6, *9) enzyme and the formation of 16-hydroxytestosterones was measured as described above.

Recombinant CYP2B1 was used as a positive control and HPLC standard for TS metabolism, and incubation of TS with CYP2B1 resulted in the formation of 16α- and 16βOH-TS in addition to androstenedione (data not shown). Shown in Figure 3.4, low amounts of 16αOH-TS and A were generated similarly by wild-type and variant enzymes whereas 16βOH-TS was the primary product; 16-hydroxytestosterones were generated by wild-type CYP2B6 at a >7:1 (β:α) ratio. CYP2B6*4 produced similar amounts of 16βOH-TS (~1.4-fold versus wild-type). However, both CYP2B6*6 and CYP2B6*9 produced decreased amounts of 16βOH-TS versus wild-type (15% and 33% of wild-type, respectively).

COS-7 and HEK293T but not MCF-7 will transiently express CYP450s

The function of CYP2B6 in breast cancer cells may be best elucidated by directly treating breast cancer cells expressing CYP2B6 with substrate, i.e. TS. As described above, however, we have observed that CYP2B6 expression is lost in breast cancer cells when grown in cell culture conditions. These observations suggest that an alternative system for expressing CYP2B6 may be required. CYP2B6 plasmids (described above) were transfected into HEK293T, COS-7 and MCF-7 cells; CYP2B6 mRNA expression and protein expression was measured as described above.

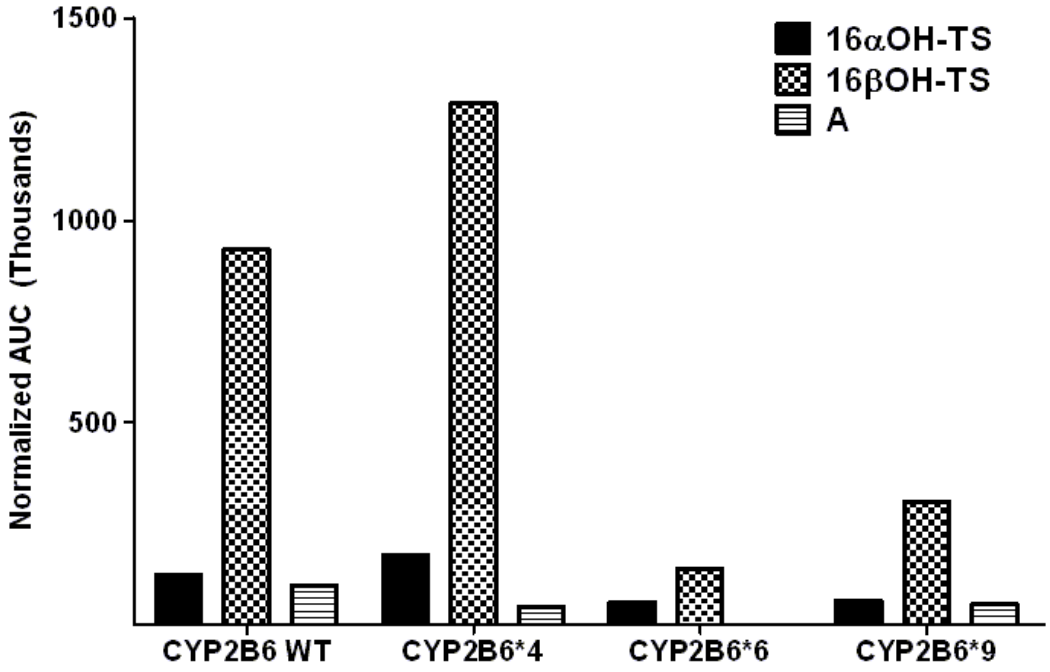

Figure 3.4. Testosterone metabolism by wild-type and variant recombinant CYP2B6. Recombinant CYP2B6 protein was incubated with 100μM TS for 40 minutes. Metabolites were extracted with ethyl acetate and reconstituted in methanol prior to separation by HPLC, with UV absorbance measured at 254 nm. Area under the curve (AUC) is normalized for extraction efficiency using an internal control (not shown). Data presented is representative of duplicate experiments.

CYP2B6 protein could not be detected in HEK293T or MCF-7 cells 24-72 hours after transfection or electroporation with pcDNA/2B6. RT-PCR following a similar time course indicated that CYP2B6 was highly expressed at the mRNA level despite the absence of detectable protein (data not shown). We hypothesized that selection of stable clones may select cells expressing protein. However, though blasticidin resistant clones for both cell lines were successfully selected within 2-3 weeks, no CYP2B6 protein could be detected despite an abundance of CYP2B6 mRNA (data not shown).

Ulrich Zanger and colleagues have utilized a CYP2B6 expression system using COS-1 cells and the pCMV4/2B6 plasmid described above to study the catalytic activity of wild-type CYP2B6 and allelic variants. Based on their observations, we tested pCMV4/2B6 in COS-7 cells, and compared protein expression generated by this plasmid versus pcDNA/2B6. COS-7 cells were transfected with either plasmid in two different transfection conditions and lysates were harvested after 48 hours. Shown in Figure 3.5A, only one transfection condition using pcDNA/2B6 induced the expression of low levels of CYP2B6 in COS-7 cells. The pCMV4/2B6 construct induced high levels of CYP2B6 protein. However, in the absence of a mammalian section marker, protein expression was lost 4-5 days following transfection (data not shown). Based on these results, it is unclear whether the loss of protein expression is due to a lack of plasmid incorporation into the genome or other loss of ORF expression. To test this, pcDNA/2B6 was transfected into COS-7 cells and blasticidin resistant clones were selected. Resistant clones were found to lack CYP2B6 expression at the protein level, but continued to express high levels of mRNA (J. Larios, Rae Laboratory; data not shown). Similar results were observed following transfection of pCMV6/7B1 into HEK293T and COS-7 cells. CYP7B1 protein was detected in both cell lines 48 hours after transient transfection (Figure 3.5B). Following 10 days of selection for G418 resistance in transfected COS-7 cells (maintained in medium supplemented with either FBS or CCS), CYP7B1 protein could no longer be detected (Figure 3.5C).

COS-7 co-cultures cannot confirm CYP450 activity after transient transfection

We hypothesized that co-culturing transiently transfected COS-7 with MCF-7 cells could circumvent problems with stable expression. Steroid hormones could be metabolized by COS-7-expressed CYP450s, and the effects of metabolites on MCF-7 cell growth could be monitored by standard assays. Specifically, we hypothesized that in the presence of mock-transfected COS-7 cells, 3βAdiol would induce MCF-7 cell proliferation. In the presence of CYP7B1-transfected COS-7 cells, 3βAdiol would be metabolized to inactive compounds and not induce MCF-7 cell proliferation. We also hypothesized that transient CYP2B6 expression may metabolize TS and reduce TS-induced growth of MCF-7 cells.

Proof-of-principle experiments with the co-culture system demonstrated that COS-7 cells grow as a viable monolayer on the co-culture insert membrane. Cells co-transfected with GFP can be visualized with fluorescence microscopy on the membranes, suggesting that protein expression will be maintained following seeding onto the insert membrane. E2 freely diffused through the insert membrane both with and without COS-7 cells to fully induce the growth of MCF-7 cells in the lower well (proof-of-principle data not shown). To examine CYP450 activity, insert wells seeded without COS-7 cells or with mock-, CYP7B1-, or CYP2B6-transfected COS-7 cells were treated with 1nM E2, 10nM TS, 10nM 3βAdiol or vehicle control and incubated with MCF-7 cells as described above for 5 days. MCF-7 growth was measured in independent experiments by both cell counting and crystal violet staining. However, MCF-7 growth was unchanged among treatment types for all insert well conditions (data not shown). Based on these results, it is unclear whether the transfected CYP450s are functional under these experimental conditions.

Discussion

Steroid hormone metabolism mediated by CYP450s plays a major role in the etiology of breast cancer. Metabolism of androgens, including androstenedione and testosterone to estrogens (estrone and estradiol, respectively), by CYP19A1 serves as the primary source of estrogens in postmenopausal women. As a result, aromatase is the primary target of current front line therapy for postmenopausal women with ER-positive breast cancer using aromatase inhibitors. CYP2B6 expressed in breast tumors may serve as another pathway of androgen metabolism which has not been explored in breast cancer.

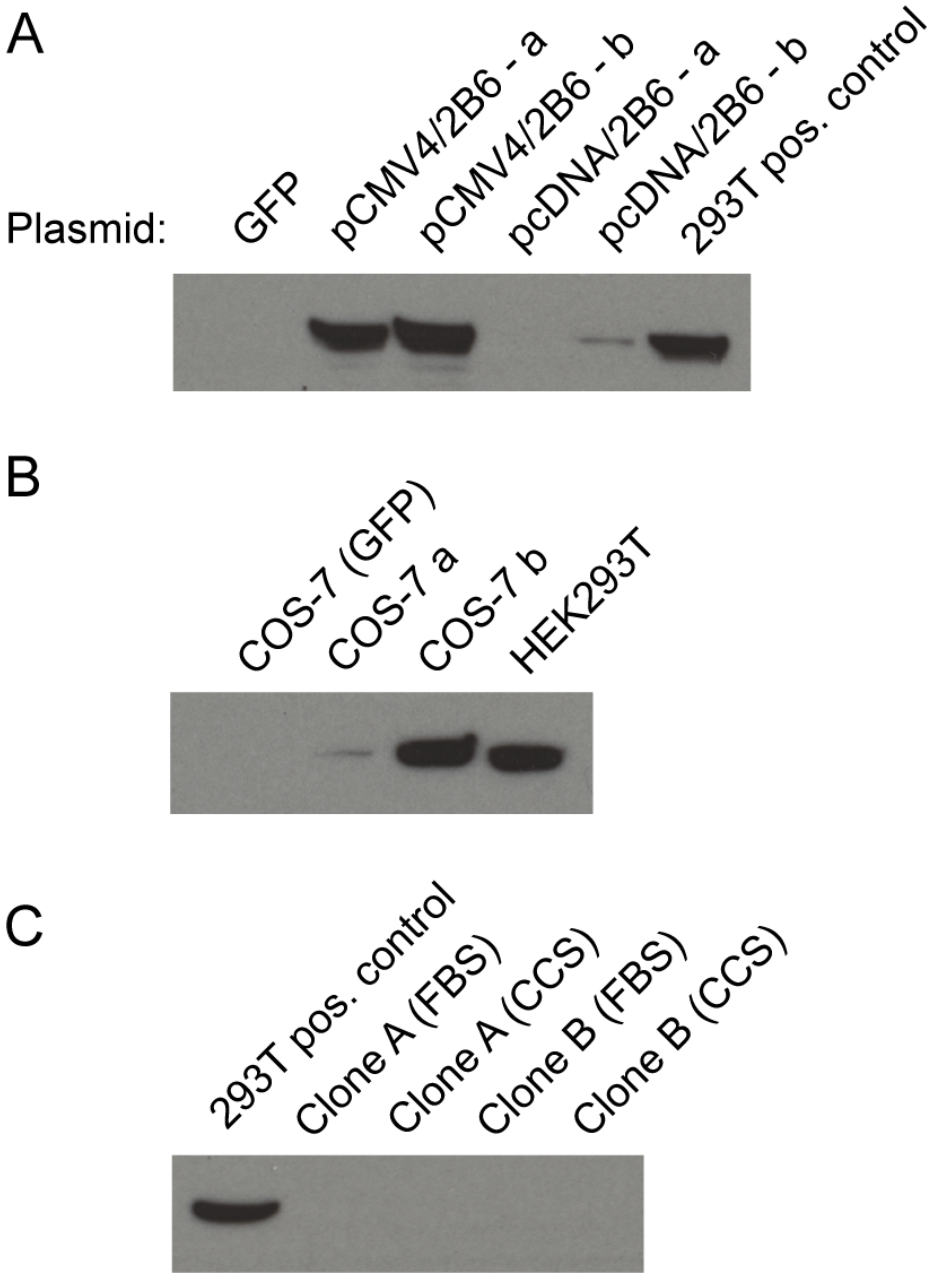

Figure 3.5. Transient expression of CYP450 protein in cell culture models. (A), COS-7 cells were transfected with the indicated plasmid and CYP2B6 expression was evaluated versus a positive control after 48 hours. 'a' and 'b' represent different transfection conditions, per the manufacturer's instructions. (B), the indicated cell line was transfected with either a GFP control plasmid or pCMV6/7B1. CYP7B1 expression was measured 48 hours after transfection. 'a' and 'b' represent different transfection conditions, per the manufacturer's instructions. (C), CYP7B1 expression in G418-resistant COS-7 clones maintained in FBS- or CCS-supplemented medium versus transiently transfected HEK293T cells.

The role of CYP2B6 in affecting therapeutic efficacy has been explored extensively from a pharmacogenomic approach due to its roles in the activation of cyclophosphamide and clearance of efavirenz. While other CYP450s have been extensively characterized for substrate/inhibitor specificity and the effects of polymorphisms, CYP2B6 remains less well characterized. However, 29 alleles have been defined to date, including well over 100 single nucleotide polymorphisms (SNPs) [143], making it one of the most polymorphic CYP450 genes in humans. Many of these SNPs are rare, but some range in frequency from 5% to as high as 50%, with marked interethnic differences [143]. The presence of variant alleles has been shown to correlate with enormous inter-patient variability in serum concentrations of drug substrates including cyclophosphamide and efavirenz [143, 183] among others. The clinical implications of these changes in CYP2B6 metabolism, including in breast cancer with cyclophosphamide therapy, are currently under investigation.

Increased CYP2B6 expression has also been shown to correlate with improved outcome in ER-positive breast cancer. Bieche et al., in a screen of drug metabolism enzymes, observed that elevated levels of CYP2B6 tended to correlate with increased survival in ER+ breast cancer [184]. In a small cohort of post-menopausal women with ER+ breast cancer treated with tamoxifen, CYP2B6 mRNA levels were significantly lower in patients who relapsed versus those that did not ($p = 0.011$). Patients with the strongest CYP2B6 expression tended to have the longest relapse-free survival time, the difference being nearly statistically significant ($p = 0.078$). Interactions between CYP2B6-mediated metabolism and aromatase inhibitors have recently been reported with exemestane and letrozole [185, 186]. In spite of these reports linking CYP2B6 to response to endocrine therapy, the role of CYP2B6 in metabolizing endogenous substrates, specifically steroid hormones, and altering therapeutic efficacy to AIs has not been explored.

We hypothesized that the unique ability of CYP2B6 to generate 16-hydroxylated metabolites from testosterone represented a novel, aromatase-independent pathway of the generation of estrogens from androgens. Importantly, our observation that CYP2B6 is expressed in breast cancer cells suggested that this may be an AI-resistant mechanism of

generating estrogens directly in tumor cells. To test this hypothesis, we treated MCF-7 cells in estrogen-free conditions with increasing concentrations of either 16αOH-TS or 16βOH-TS, and compared cell growth to cells treated with either E2 or TS. Neither 16αOH-TS nor 16βOH-TS induced MCF-7 cell growth at concentrations up to 10nM (Figure 3.1), and neither steroid bound ERα in recombinant receptor binding assays. These data suggest that neither metabolite is an ERα ligand or a substrate for aromatase at physiological concentrations. Based on these observations, metabolism of testosterone by CYP2B6 may serve as a clearance pathway of androgens to decrease total synthesis of estrogens. While this seems paradoxical given that estrogens are the primary driver of breast cancer growth, high concentrations of estrogen are toxic to ER-positive breast tumors, in both experimental and clinical scenarios (reviewed in [187]). Thus, CYP2B6 may be important in maintaining estrogen homeostasis in normal breast and/or breast tumors. The hypothesis that CYP2B6 decreases estrogen concentrations is consistent with the improved outcomes observed by Bieche et al discussed above, where tamoxifen may be more effective when less estrogen is present. These observations parallel the role of oxidative 17β-HSDs in improving outcomes on tamoxifen described in Chapter II. Additionally, these data do not rule out the potential that 16-hydroxylated testosterones may act as an ERβ ligand. There is evidence in the literature that ERβ represses estrogen-induced breast cancer cell growth [188, 189]. Conflicting evidence exist regarding ERβ expression in breast cancer cell lines; however ER-positivity in tumors often correlates with ERβ expression [190, 191]. The hypothesis that CYP2B6 negatively regulates breast cancer cell growth through androgen clearance or ERβ ligand generation may merit future investigation.

The pivotal role of androgens in prostate cancer suggests that CYP2B6-mediated testosterone metabolism may also play a role in prostate cancer etiology. Recently, the promising results of Phase I trials using the CYP17 inhibitor abiraterone acetate in patients with castration-resistant prostate cancer have revitalized interest in CYP450s in prostate cancer research [192-195]. However, minimal data exist regarding a role for CYP2B6 in prostate cancer. We examined the ability of 16αOH-TS and 16βOH-TS to induce the growth of the prostate cancer cell line LNCaP to explore a potential role of

CYP2B6 in prostate cancer, and as a marker for androgenic activity of the metabolites. We observed that while 16αOH-TS did not induce the growth of LNCaP cells, 16βOH-TS strongly induced the growth of LNCaP cells; 16βOH-TS was significantly more efficacious than DHT (5.5-fold vs. 4.1-fold maximum growth induction, respectively) but less potent (EC_{50} 1.6nM vs. 180pM, respectively). Though these data suggest that one of the metabolites is androgenic, LNCaP cells express the T877A AR mutant that is able to bind to and be activated by a broad range of steroids (including estrogens, progestins and anti-androgens). Receptor binding assays or growth assays using a wild-type AR expressing cell line would be necessary to confirm whether 16βOH-TS is in fact an AR ligand. However, the hypothesis that these metabolites are clearance products of TS, rather than AR ligands, is consistent with previously reported data. Kumagai et al reported that increased CYP2B6 expression in prostate tumors was inversely correlated with high Gleason score [196], suggesting that CYP2B6 expression decreases during prostate cancer progression. The authors also demonstrated that over-expression of CYP2B6 in LNCaP cells significantly decreased TS-induced proliferation. Based on these observations, prostate tumors may use CYP2B6 in a similar to role as postulated above in breast cancer, and that expression is decreased during prostate cancer progression to maintain androgen signaling, consistent with recent changes in the understanding of AR signaling in advanced prostate cancer (reviewed in [197]).

The above data suggest that CYP2B6 may be important in maintaining steroid hormone homeostasis through androgen clearance. Unfortunately, further experimentation in model systems is currently hindered due to difficulties in the expression of CYP450s in cell culture models. These difficulties are not unique to the cell line models described above (Figure 3.4). In human and rat hepatocytes and hepatocellular carcinoma cell lines (e.g. HepG2), the expression of CYP450s is rapidly decreased during growth in culture [173-176]. Recently, the development of perfused 'bioreactors' capable of maintaining primary human liver cells in 3-dimensional culture have been developed for use in hepatic pharmacological studies [198]. However, despite the advances of this model in mimicking an *in vivo* environment long-term, the expression and activity of CYP450s can only be maintained as long as 23 days [198]. The applicability of these bioreactor-based

conditions to cancer cell culture models has not been explored. The mechanisms causing the decrease in CYP450 expression in cell culture are unclear. As most CYP450s are localized to the endoplasmic reticulum, cells may be induced to degrade or eliminate CYP450 protein expression due to increased endoplasmic reticulum stress [199]. Two pathways have been identified as the major mechanisms of degrading CYP450 proteins, with individual isoforms being specifically degraded by either proteosomal or autophagic lysosomal pathways [200-202]. In some systems, the increased protein stability caused by proteosome inhibition can increase the amount of functional CYP450 [200]. Maintaining a low level of expression using tetracycline-inducible promoters (to prevent endoplasmic reticulum stress) or inhibiting the proteosomal/lysosomal degradation pathways may be useful future strategies for expressing CYP450 enzymes in model systems.

Given that CYP2B6 is highly polymorphic, better understanding of the substrate-specific activity of CYP2B6 variants may allow for significant data to be mined by retrospective genotyping of clinical trials. We have observed that the CYP2B6 variants *6 and *9 (both carrying a Q172H mutation) have diminished capacities for the generation of hydroxytestosterones (specifically 16βOH-TS) versus the wild-type or *4 variant. Differences in tumor biology or response to therapy in patients carrying *6 and/or *9 variant alleles versus other genotypes have not been explored. Many large clinical trials have collected formalin-fixed, paraffin-embedded (FFPE) tumor tissue; we have previously demonstrated that genotypes for drug metabolism enzymes are consistent between matched germline and tumor tissues [203]. CYP2B6 genotypes obtained from FFPE tissues can be associated with long-term outcomes data from these trials, which may also provide insight into the role of CYP2B6 in breast cancer. As genotyping from FFPE tissues is technically challenging, discussed in this dissertation are improved methods for genotyping from FFPE tissues [204] (discussed in Chapter V). Inhibitors of CYP2B6 (such as clopidogrel [205]) may be administered to cancer patients concurrently with anti-cancer agents, and may contribute to variability in CYP2B6 activity. The effects of CYP2B6 inhibitors on tumor biology may be evaluated in patients with and without co-administration of CYP2B6 inhibitors. Retrospective analysis of clinical trials based on

CYP2B6 genotype/activity using methods such as these may be critical for understanding the role of CYP2B6 in breast and prostate cancer.

Chapter IV.

Weak or partial agonism of ERα during long term estrogen deprivation drives novel mechanisms of estrogen-independent growth

Introduction

Endocrine therapy using aromatase inhibitors has significantly improved disease-free survival and overall survival in post-menopausal women with ER-positive breast cancer. However, recently published data demonstrates that ~20% of patients treated with AI therapy will experience disease relapse within 10 years of treatment initiation [83]. Mechanisms of resistance to AI therapy have been studied for over a decade, since the introduction of AIs as frontline endocrine therapy, and a number of pathways and mechanisms have been implicated in both acquired and *de novo* resistance. Mechanisms of acquired resistance to AI therapy have been studied largely through the use of long term estrogen deprivation (LTED) models, both in cell culture and xenograft settings. To mimic tumor conditions in patients on AI therapy, ER-positive breast cancer cells are maintained long term (generally 3-12 months) in the absence of steroid hormones, either in medium supplemented with charcoal-stripped calf serum (CCS) or in ovariectomized mice. Cells adapt to LTED and display an endocrine resistant phenotype, no longer requiring high concentrations of estrogen to maintain cell growth.

Though LTED models have implicated a number of mechanisms as drivers of estrogen-independent growth, these models are largely based on the hypothesis that AI therapy depletes nearly all circulating estrogens. Cells that are maintained in medium supplemented with charcoal stripped serum are almost totally deprived of any estrogenic stimulation. As described above in Chapter II, 3βAdiol can provide an estrogenic stimulus in breast cancer cells as an ERα ligand. Importantly, since 3βAdiol is generated independent of metabolism by aromatase, circulating 3βAdiol is unlikely to be decreased by AI therapy. In addition to the potential contribution of 3βAdiol as an ERα ligand, a

number of reports on the pharmacology of AIs have demonstrated that low levels of residual aromatization are maintained in patients on AI therapy. This low level of aromatization is sufficient to produce quantifiable, picomolar concentrations of circulating E2 in some patients [31, 206]. In MCF-7 cells in culture, E2 concentrations >100fM are sufficient to induce growth; half-maximal growth is induced with E2 concentratons of ~5pM (Appendix I). Based on these observations, we hypothesized that LTED may not accurately mimic estrogenic conditions for the subset of patients that maintain 3βAdiol or E2 concentrations sufficient to activate ERα. To model conditions in this subset of patients, MCF-7 cells were selected by long-term culture in medium supplemented with CCS and defined concentrations of either E2 or 3βAdiol (EC_{10} and EC_{90} concentrations of each steroid hormone). The development of estrogen-independence was assessed in these selected cell lines over time, and phenotypes were compared to LTED cells maintained concurrently and parental MCF-7 cells.

Following >7 months of selection, estrogen-independence developed in LTED cells, as well as cells maintained in low concentrations (EC_{10}) of E2 and 3βAdiol. However, the temporal nature of the development of estrogen-independence was unique to each selected line. Further, whereas estrogen-independent growth was maintained via an estrogen receptor-dependent mechanism in the low steroid selected cells, growth was estrogen receptor-independent in the LTED cells. Additionally, sensitivity to kinase inhibitors in selected cell lines was dependent on the presence/absence of the ERα ligand. These data offer a novel perspective on the development of resistance to AI therapy, and may yield novel approaches to treat AI-resistant tumors.

Methods

Cell Lines, Culture Conditions, and Growth Assays

MCF-7 cells were routinely maintained as described in Chapter II. For long term selections, MCF-7 cells were initially repeatedly washed (as described in Chapter II), and then maintained in phenol red-free Improved Minimum Essential Medium (IMEM) supplemented with 10% CCS and either vehicle (0.05% ethanol) or defined E2 concentrations (1pM or 50pM) or 3βAdiol concentrations (50pM or 1nM). Conditions

and naming conventions for the selected cell lines are listed in Table 4.1. For assays in estrogen-free conditions (or defined steroid hormone concentrations), cells were repeatedly washed as described above prior to plating; assays were performed in phenol red-free IMEM supplemented with 5% CCS. For kinase inhibitor growth assays in the presence of estrogens, cells were plated in selection conditions (as listed in Table 4.1) prior to treatment. Growth assays were performed in 96-well plates using the FluoReporter Blue fluorometric dsDNA quantitation kit (F2692, Invitrogen) according to the manufacturer's instructions. Briefly, cells were lysed in hypotonic conditions via freeze/thaw cycles, and lysates were stained with buffer containing Hoechst 33258. Fluorescence was read at 360nm excitation and 460nm emission wavelengths in a PolarStar Omega plate reader (BMG Labtech).

Western Blotting

Western blot analysis was performed on whole cell lysates from breast cancer cells. Cells were lysed using RIPA buffer (Thermo Pierce, Rockford, IL) supplemented with Protease Inhibitor Cocktail Tablets and Phosphatase Inhibitor Cocktail Tablets (Roche Applied Science). Total protein from cell lysates was quantified using the Bradford assay (Bradford Reagent; Bio-Rad, Hercules, CA). Thirty micrograms of protein per lane was resolved on 4-20% gradient polyacrylamide gels (Pierce, Rockford, IL), and transferred to a PVDF membrane. Antibodies used for immunoblotting were obtained from Cell Signaling (Boston, MA) and are listed in Appendix II; antibody dilutions were prepared according to the manufacturer's instructions.

Real-time PCR

mRNA was harvested from samples using RNeasy mini columns (Qiagen, Valencia, CA) according to the manufacturer's instructions. GREB1 mRNA expression were measured using a Taqman real-time PCR assay. Total RNA (1μg) was reverse transcribed using Reverse Transcription System (Promega, Madison, WI) and the resulting cDNA amplified in a 25μl reaction containing Gene Expression Master Mix (Applied Biosystems, Carlsbad, CA) and the following oligonucleotides: forward primer 5'AAT

Estrogen environment	Cell line name
10% FBS (Standard Cond.)	Parental
10% CCS + Vehicle (0.05% EtOH)	Veh
1pM E2	1pE
50pM E2	50pE
50pM 3 β Adiol	50p3β
1nM 3βAdiol	1n3β

Table 4.1. MCF-7 selection conditions and nomenclature.

CTG TAC CAC GCA ATG GA 3', reverse primer 5' TGC CAT CTC GTA TTC CTT GA 3', probe 5' FAM - CAA CCA GCA CGT GCA AAT GGC T - BHQ-1 3'. The primer/probe set is specific to GREB1 splice variant GREB1a and were designed by Genomic Health Inc. (Burbank, CA), and optimized for cycling conditions as previously described [207]. Reactions were performed using a CFX96 real-time thermocycler (Bio-Rad Laboratories, Inc., Hercules, CA). Target gene expression was normalized against GAPDH (Hs99999905_m1, Applied Biosystems) and relative expression was determined using the $\Delta\Delta C_T$ method [160].

Gene Expression Microarray Analysis

Whole genome expression analysis was performed using HumanHT-12 v4 Expression BeadChips (Illumina, San Diego, CA). For sample preparation, selected cell lines were plated in T75 flasks and washed as described above; cells were harvested, re-seeded in triplicate T75 flasks and allowed to grow for 3 days prior to sample harvest. Growth assays were performed in parallel to verify the estrogen-independent phenotypes. At harvest, each flask was separated into paired samples for gene expression and metabolomics analyses (results from metabolomics analyses performed at Georgetown University pending at time of publication). mRNA for gene expression analyses was harvested using RNeasy mini columns (Qiagen) according to the manufacturer's instructions. mRNA was prepared for the direct hybridization assay and scanned using a BeadArray reader (Illumina) by the University of Michigan DNA Sequencing Core Facility.

Array output data were quantile normalized using GenomeStudio software (Illumina) prior to analyses. The 47,313 probe sets on the array were filtered according to expression p-value; only probe sets with values significantly greater than background for at least one of the tested samples (any one of triplicate samples from any cell line) were used in further analyses. For the remaining 16,667 probe sets, differences in gene set expression between samples were analyzed using Gene Set Enrichment Analysis (GSEA; Broad Institute, Cambridge, MA) [208, 209]. Analyses used GSEA version 3.4 and Molecular Signatures Database (MSigDB) release 3.0. Default parameters were used in

analysis; triplicate samples were grouped as single phenotype groups. Analysis set-ups are described in the Results section below. 'Canonical pathways' refers to MSigDB gene set C2 CP, and 'Chemical and genetic perturbations' refers to MSigDB gene set C2 CGP (gene sets are annotated at http://www.broadinstitute.org/gsea/msigdb/genesets.jsp). Enrichment lists and associated figures were generated by the GSEA software; gene sets considered most enriched had the highest normalized enrichment score (NES) among all gene sets in that analysis (described in [208, 209]). Briefly, NES is the ratio of calculated gene set enrichment versus the mean enrichment of all permutations assessed, thus NES accounts for the overall size of the data set.

Results

Estrogen-independence develops in low-estrogen conditions

Throughout the selection process, cells were tested for their ability to grow in increasing concentrations of E2 or 3βAdiol, or in estrogen-free conditions in the presence or absence of ICI 182,780. Shown in Figure 4.1, selected cells in estrogen-free conditions (following repeated washing as described above) were treated with the indicated concentration of hormone or anti-estrogen. 50pE cells mimic parental MCF-7 cells' dependence on estrogen for growth following long-term selection; after washing and seeding in estrogen-free conditions, 50pE cell growth slows and stops (Figure 4.1C). The addition of ICI 182,780 does not further decrease growth (5-day control vs. 5-day ICI treatment, $p > 0.05$). Additionally, treatment of 50pE cells with 1nM E2 full induces growth, whereas 10nM 3βAdiol induces ~75% maximal growth, similar to parental MCF-7 cells. 1n3β cells also cease proliferating in estrogen-free conditions, after transient estrogen-independent growth within 3 days of seeding (Figure 4.1E). The addition of ICI 182,780 does not further decrease growth (5-day control vs. 5-day ICI treatment, $p > 0.05$). E2 treatment maximally induced the growth of 1n3β cells, as did 3βAdiol treatment. Veh cells demonstrated estrogen-independent growth (7.2-fold at day 5 versus pre-treatment); this growth was not inhibited by the addition of ICI 182,780 (Figure 4.1A) (5-day control vs. 5-day ICI treatment, $p > 0.05$). This phenotype developed 9-12 weeks after initiation of selection, consistent with previous reports [99, 100]. Veh cells also remained responsive to both E2 and 3βAdiol treatment. Both 1pE

cells and 50p3β cells demonstrated maintained growth in estrogen-free conditions (>10-fold day 5 growth versus pre-treatment control). Unlike Veh cells, however, this growth could be inhibited by the addition of ICI 182,780 (5-day control vs. 5-day ICI treatment; 1pE $p < 0.0001$, 50p3β $p = 0.0005$). The development of estrogen-independence was delayed, and only observed after 6-7mo and 4-5mo of selection for 1pE and 50p3β cells, respectively. Both 1pE cells and 50p3β cells remained responsive to the addition of E2 or 3βAdiol; however, 50p3β cells demonstrated the least growth induction of all selections following hormone treatment at the indicated concentrations.

Dose-response curves were generated for each cell line, to examine growth following increasing concentrations of E2 or 3βAdiol, to determine whether any of the selection lines had developed hypersensitivity to low concentrations of steroid hormone, as previously reported [99, 100]. Minor increases in sensitivity (<1-log decrease in EC_{50}) were observed versus parental MCF-7 cells in all selections except 50pE cells, consistent with their parallel phenotype to parental MCF-7 cells (Figure 4.2). Maximum E2-induced growth required $\geq 10^{-11}$M E2 for all cell lines, ~2-logs greater than previously reported for hypersensitive MCF-7 cells. No hypersensitivity was observed in growth induction by 3βAdiol in any selection cell line (data not shown).

Mechanisms of estrogen-independence are unique in low-estrogen conditions versus complete estrogen deprivation

To examine potential mechanisms of estrogen-independent growth, the expression and activation of the MAPK and PI_3K/Akt signaling pathways were examined via western blotting. Selected cell lines were assessed in estrogen-free conditions and compared to parental cells maintained in standard conditions (Figure 4.3). 50pE and 1n3β cells in estrogen-free conditions presented decreased levels of phosphorylated MAPK (pMAPK) versus parental MCF-7 cells, consistent with their lack of growth in these conditions. 1pE and 50p3β cells maintained pMAPK levels similar to those in parental MCF-7 cells while Veh cells had slightly lower levels of pMAPK. Activity of the PI_3K/Akt pathway was examined via phosphorylation of Akt on T308 and S473. pAkt-T308 was only observed in Veh, 1pE and 50p3β cells, suggesting that these cell lines have activated

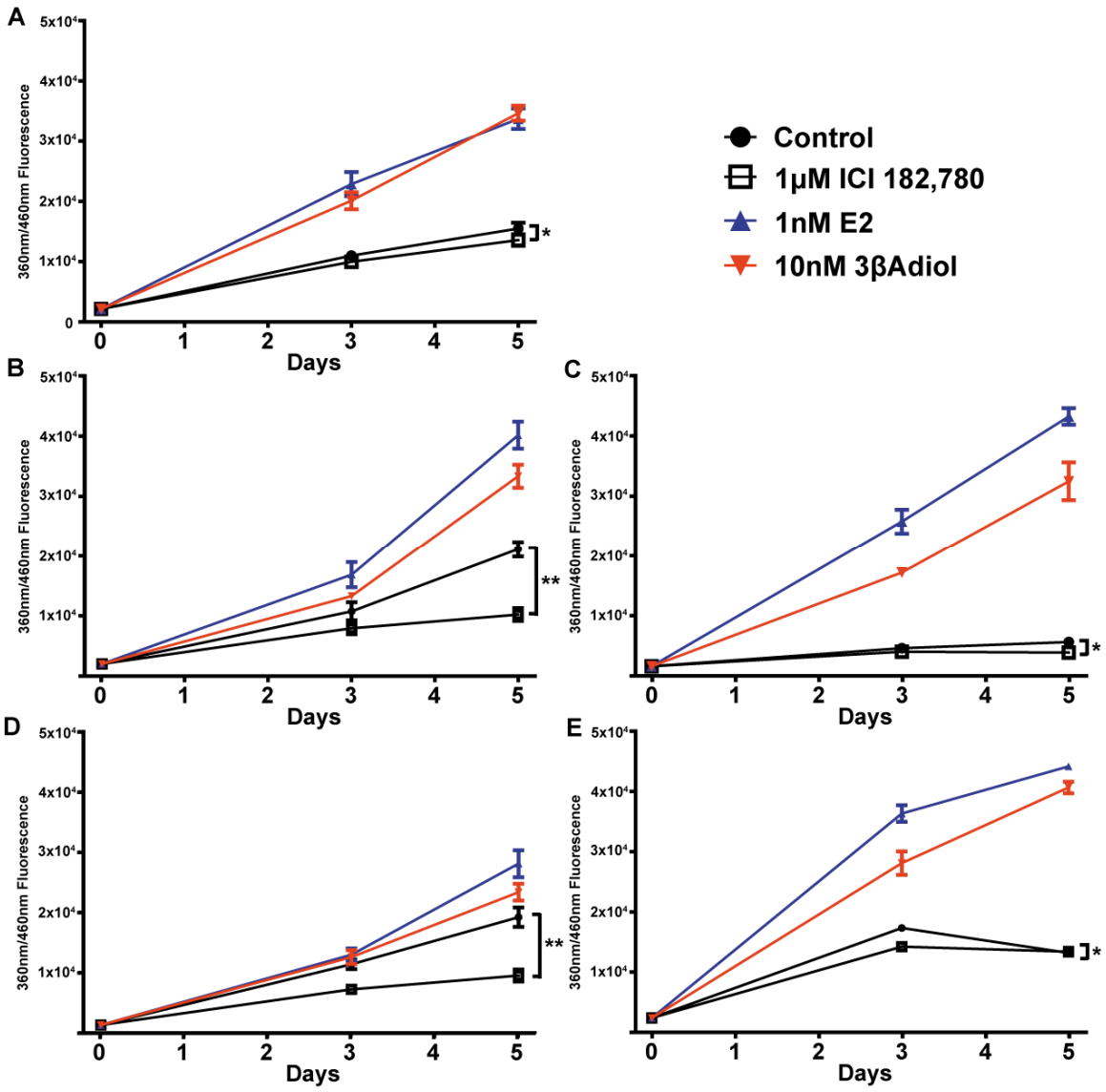

Figure 4.1. MCF-7 selected cell line growth in estrogen-free conditions. Cells were washed as described in Materials and Methods, and treated as indicated. (A), Veh cells; (B) 1pE cells; (C) 50pE cells; (D) 50p3β cells; (E) 1n3β cells. Growth was assessed at baseline, 3 days or 5 days after treatment. Points represent the average of 6 replicates ± SEM. Student's T-tests were used to compare growth after 5 days of treatment with ICI 182,780 versus control. *, $p > 0.05$. **, $p \leq 0.0005$.

A

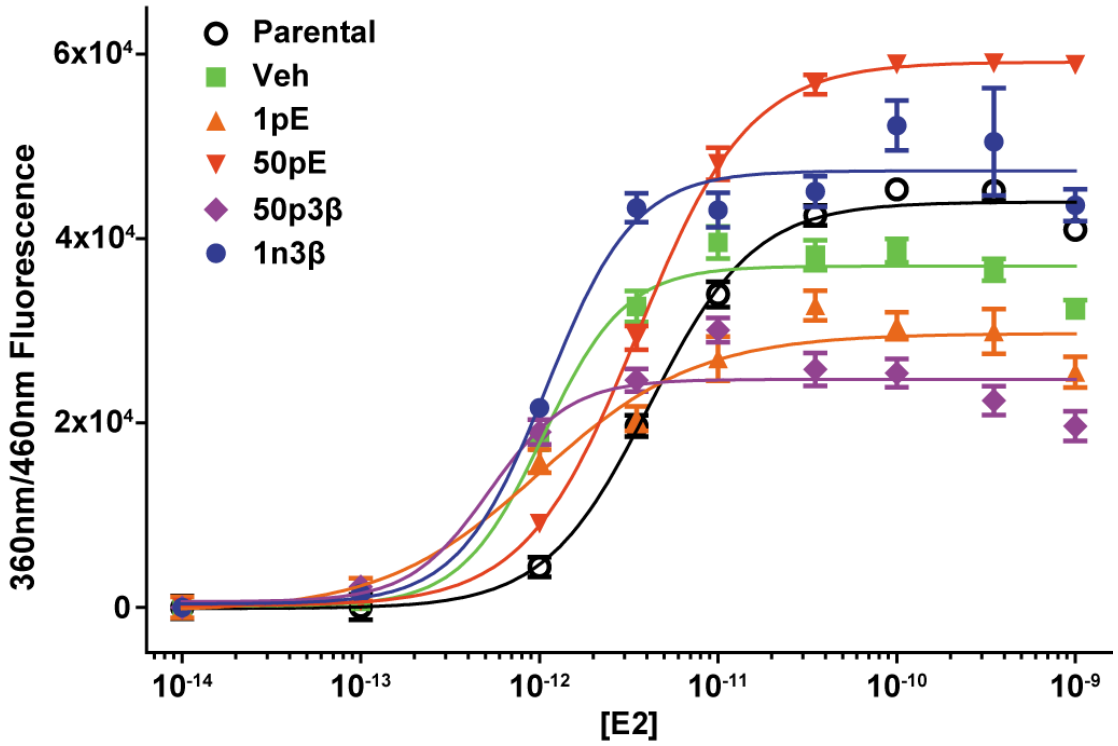

B

	EC_{50}	95% CI
Parental	4.13pM	3.17pM - 5.38pM
Veh	1.05pM	0.68pM - 1.63pM
1pE	1.01pM	0.32pM - 3.17pM
50pE	3.53pM	3.41pM - 3.66pM
50p3β	0.53pM	0.06pM - 4.86pM
1n3β	1.10pM	0.67pM - 1.79pM

Figure 4.2. MCF-7 selected cell line growth following E2 treatment. (A), MCF-7 selected cell lines were treated with increasing concentrations of E2 as indicated. Growth was assessed at 5 days after treatment. Data are normalized to baseline growth in estrogen-free conditions; Y-axis values represent growth above that baseline. Points represent the average of 6 replicates ± SEM. (B), estimated EC_{50} values for growth induction and 95% confidence intervals for the EC_{50}.

PI_3K signaling in the absence of estrogen. Similarly, pAkt-S473 was highest in 1pE and 50p3β cells, further suggesting the importance of Akt signaling in estrogen-independent growth in these cells. pAkt-S473 was also observed in Veh and 1n3β cells; Akt may play a role in Veh cell estrogen independent growth, as well as the transient estrogen independent growth in 1n3β cells. As both the Akt and MAPK pathways can activate ERα via phosphorylation, we examined ERα activation by phosphorylation on S167. All 5 selected lines express ERα when grown in estrogen-free conditions. However, pERα-S167 was only observed in 1pE and 50p3β cells. These data suggested that 1pE and 50p3β cells may maintain ERα in an active state in the absence of ligand, following steroid washing. ErbB2 expression was also examined; all selected cell lines up-regulated ErbB2 equivalently in estrogen-free conditions compared to parental cells.

To examine whether the observed phosphorylation of ERα was indicative of transcriptional activity of ERα in the absence of ligand, we examined the expression of GREB1 following steroid washing (Figure 4.4). GREB1 is an ERα-specific target critically involved in the estrogen induced growth of breast cancer cells [157]. Parental MCF-7 cells express very high levels of GREB1; this expression is completely blocked upon addition of ICI 182,780 (columns 1, 2). Following removal of estrogens from parental MCF-7 cells, GREB1 expression is effectively shut off; the addition of ICI 182,780 has no effect in the absence of estrogens (columns 3, 4). Veh, 50pE and 1n3β cells do not express GREB1 in estrogen-free conditions, consistent with ICI-insensitivity and lack of growth in estrogen-free conditions, respectively. However, both 1pE and 50p3β cells express GREB1 in estrogen-free conditions (columns 7, 11). Expression of GREB1 in these cells is likely ERα-dependent, as expression is completely blocked by the addition of ICI 182,780 (columns 8, 12). Taken together with above observations, these data suggest that 1pE and 50p3β cells may maintain ERα activation in the absence of ligand (potentially via MAPK and/or Akt signaling) to maintain estrogen-independent growth. Conversely, Veh cells do not appear to require ERα to maintain estrogen-independent growth.

Microarray analysis reveals potential drivers of estrogen-independent growth

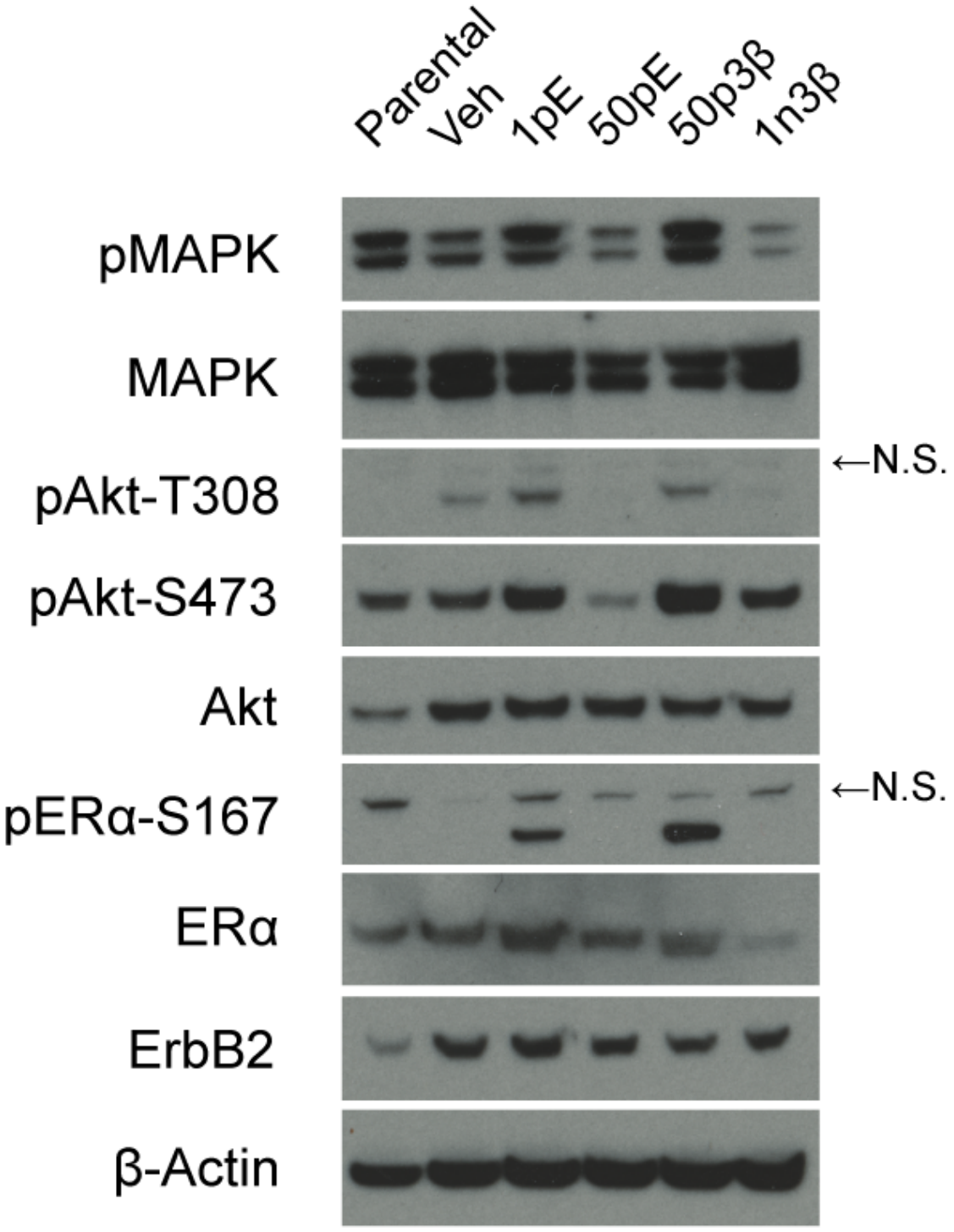

Figure 4.3. Kinase signaling pathways in selected cell lines in estrogen-free conditions. Parental cells were maintained in normal conditions with FBS; selected cells were washed and seeded in estrogen-free conditions prior to sample harvesting. N.S., non-specific band.

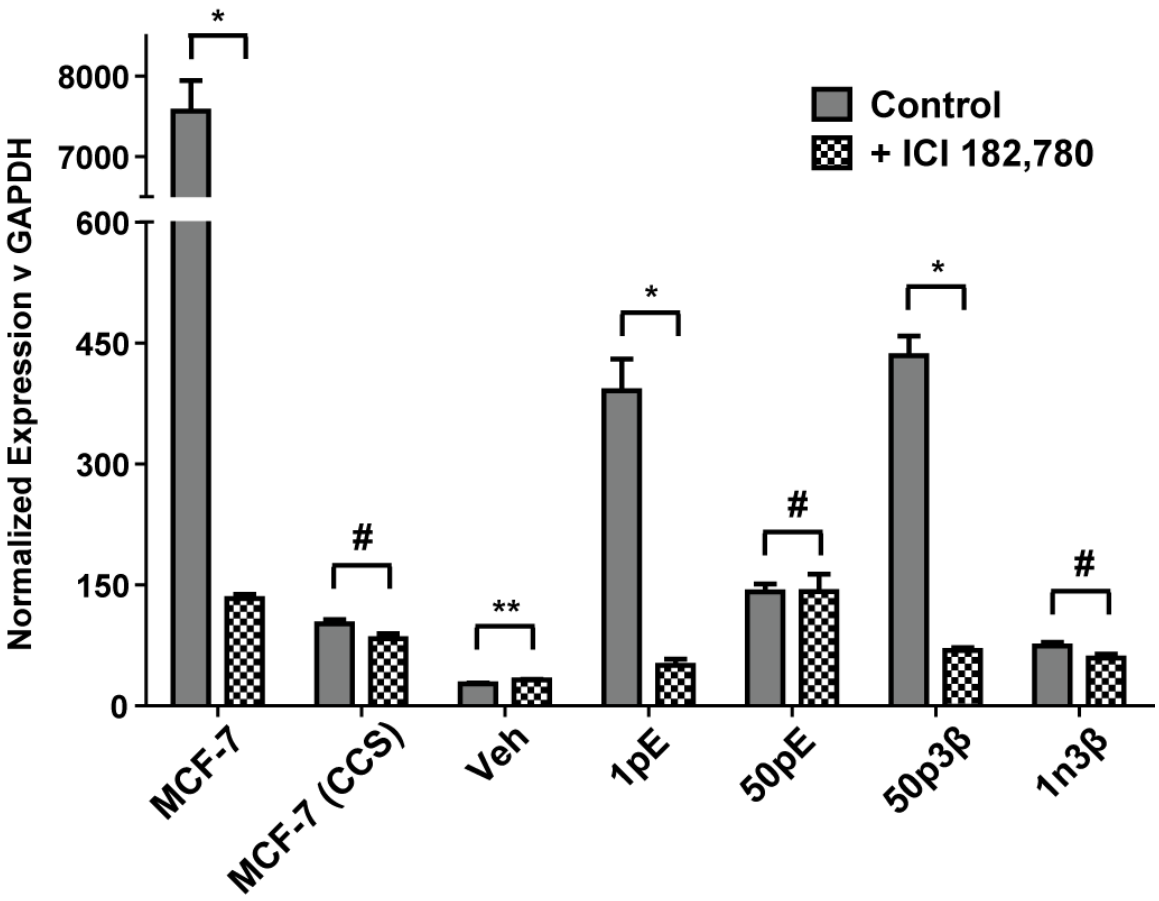

Figure 4.4. GREB1 expression in MCF-7 parental and selected cell lines. MCF-7 refers to the parental cell line; CCS indicates estrogen-free conditions. Veh, 1pE, 50pE, 50p3β and 1n3β cells were assayed in estrogen-free conditions. Cells were treated with either vehicle (0.1% EtOH) or 1μM ICI for 72hrs. Student's T-tests were used to compare expression in ICI 182,780-treated cells versus controls. *, $p < 0.001$. **, $p = 0.032$. #, $p > 0.05$.

We performed gene expression microarray analyses of selected cells in estrogen-free conditions to identify genes and pathways critical for estrogen independent growth. Gene expression data were analyzed using Gene Set Enrichment Analysis (GSEA; described above). As an initial validation of trends observed by GSEA, gene expression data from estrogen-independent proliferating cells (Veh, 1pE and 50p3β) were compared to the estrogen-dependent, non-proliferating cells (50pE, 1n3β). Listed in Table 4.2 are the GSEA canonical pathways most enriched in 'proliferating' vs. 'non-proliferating' cells, and consistent with these phenotypes, gene signatures associated with proliferation (i.e. mitotic progression, DNA replication, etc.) were strongly enriched in Veh, 1pE and 50p3β cells. Heat maps demonstrating signature enrichments are shown in Figure 4.5.

Gene expression data from Veh cells were compared to the other selected lines, and enrichment was evaluated against both the GSEA canonical pathways (CP) and chemical and genetic perturbations (CGP) database. Table 4.3 lists the most enriched signatures from these databases. 9 of the top 20 most enriched gene sets from the CGP datasets in Veh cells are related to hypoxia and/or HIF1α signaling. As none of the selected cells are in hypoxic conditions, these signatures may be the result of other activated signaling pathways in Veh cells. Accordingly, 7 of the top 20 most enriched signatures from the CP database are related to InsR/IGF1R signaling and/or carbohydrate metabolism. Heat maps demonstrating signature enrichments are shown in Figure 4.6. Both the hypoxia and carbohydrate metabolism signatures are potentially a result of increased InsR/IGF1R signaling, as these have been linked in a number of systems [210, 211]. Importantly, these data implicate InsR/IGF1R signaling in promoting estrogen-independent growth in Veh cells.

Initial growth data and western blot experiments suggest that a similar mechanism is responsible for driving estrogen-independent growth in 1pE and 50p3β cells. Based on these observations, GSEA was performed comparing these two cell lines together versus the other selected cell lines. Enrichment against the GSEA canonical pathways and GSEA CGP database initially provided primarily proliferation- and mitotic-associated gene signatures (data not shown); these were similar in ontology annotation to those

listed in Table 4.2. This is consistent with the increased estrogen-independent growth in these cell lines versus the other selected cell lines, including Veh cells (Figure 4.1). To enrich for signaling signatures relevant to driving growth in 1pE and 50p3β cells, a limited subset of the GSEA CGP database (2392 gene sets) was pared down to 332 gene sets relating specifically to breast cancer and/or cancer signaling pathways (i.e. receptor tyrosine kinases, MAPK pathway, etc.)(Appendix III). GSEA against this refined gene set list are shown in Table 4.4 and Figure 4.7. Consistent with the above data suggesting that canonical ERα signaling is maintained, 6 of the top 20 most enriched gene sets (from the refined CGP list) were associated with ERα signaling and specific ERα target genes. The most significantly enriched gene set in both 1pE and 50p3β is associated with response to the ErbB receptor family inhibitor CL-387785 (from Kobayashi et al., [212]). This implicates the ErbB receptor family (potentially EGFR and/or ErbB2) as responsible for activating ERα in estrogen-free conditions.

MAPK and Akt are upstream of ERα in 1pE and 50p3β cells

As demonstrated in Figure 4.3, 1pE and 50p3β cells maintain active MAPK and Akt in estrogen-free conditions. We hypothesized that activated MAPK and Akt may be responsible for phosphorylating ERα in the absence of ligand. Further, we hypothesized that 1pE and 50p3β cells would be growth-inhibited by the MEK inhibitor U0126 and the PI_3K inhibitor LY294002. Shown in Figure 4.8, selected cell lines in estrogen-free conditions were treated with increasing concentrations of ICI 182,780, U0126 or LY294002. ICI 182,780 inhibited cell growth of 1pE and 50p3β cells only, similar to observed above (Figure 4.8A). Both kinase inhibitors were selective for 1pE and 50p3β within the range of concentrations tested, reducing the estrogen-independent growth of 1pE and 50p3β cells by ~40% (Figure 4.8B-C). Selected cell lines were then treated with low concentrations of kinase inhibitors (selective for 1pE and 50p3β) as indicated; cells were treated in both estrogen-free conditions and in normal selection conditions, alone or in combination with ICI 182,780 (Figure 4.9). Veh cells were not growth inhibited by any combination of U0126, LY294002 or ICI 182,780 (data not shown). Under estrogen-free conditions, 50pE and 1n3β cells were not growth inhibited by any combination of U0126, LY294002 or ICI 182,780 at the indicated concentrations (data not shown).

Canonical pathways enriched in proliferating cells	NES
REACTOME_CELL_CYCLE_MITOTIC	2.827
REACTOME_MITOTIC_PROMETAPHASE	2.787
REACTOME_MITOTIC_M_M_G1_PHASES	2.688
REACTOME_DNA_REPLICATION_PRE_INITIATION	2.559
REACTOME_DNA_STRAND_ELONGATION	2.535
REACTOME_G1_S_TRANSITION	2.502
REACTOME_SYNTHESIS_OF_DNA	2.501
REACTOME_S_PHASE	2.490
REACTOME_EXTENSION_OF_TELOMERES	2.487
KEGG_DNA_REPLICATION	2.464
REACTOME_TRANSPORT_OF_RIBONUCLEOPROTEINS…	2.437
REACTOME_ACTIVATION_OF_THE_PRE_REPLICATIVE_COMPLEX	2.380
REACTOME_ACTIVATION_OF_ATR_IN_RESPONSE_TO_REPLICATION…	2.375
REACTOME_SNRNP_ASSEMBLY	2.361
REACTOME_PROCESSING_OF_CAPPED_INTRON_CONTAINING…	2.332
REACTOME_LAGGING_STRAND_SYNTHESIS	2.323
REACTOME_G2_M_CHECKPOINTS	2.322
REACTOME_METABOLISM_OF_RNA	2.317
REACTOME_E2F_TRANSCRIPTIONAL_TARGETS_AT_G1_S	2.316
REACTOME_CELL_CYCLE_CHECKPOINTS	2.305

Table 4.2. Canonical pathways enriched in proliferating cells.

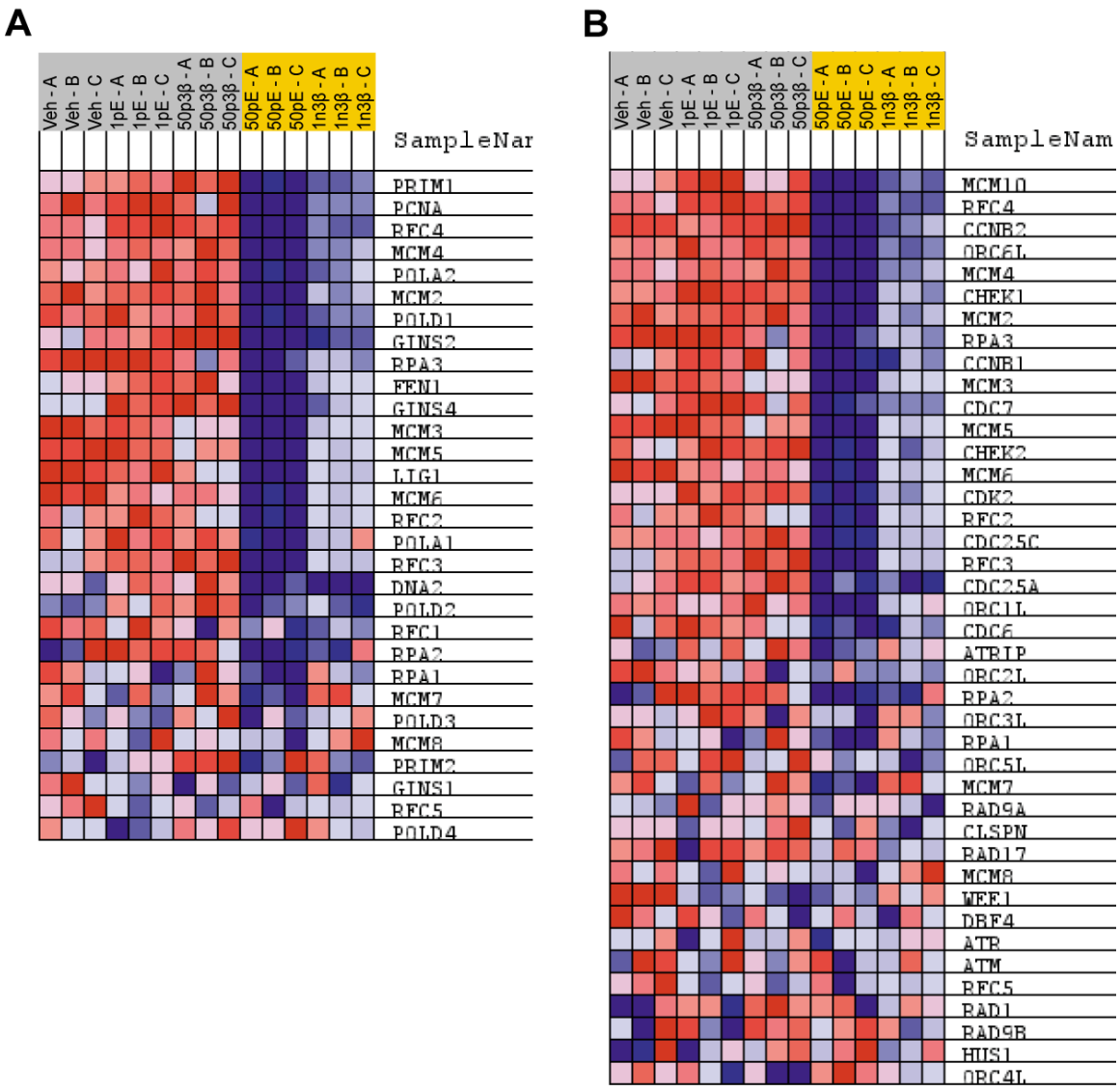

Figure 4.5. Heat maps of gene sets enriched in proliferating cells under estrogen-free conditions. (A), Reactome – DNA Strand Elongation; (B), Reactome – G2/M Checkpoints. Heat maps represent relative difference in expression (not raw expression) between phenotypes, Red = increased, blue = decreased. Each column represents one of the triplicate samples for each selected cell line. Headers shaded in gray vs. yellow represent phenotype comparison groups during anaylsis.

Chemical and genetic perturbation gene set enrichment	NES
ELVIDGE_HYPOXIA_UP	2.827
ELVIDGE_HYPOXIA_BY_DMOG_UP	2.802
ELVIDGE_HIF1A_AND_HIF2A_TARGETS_DN	2.728
ELVIDGE_HIF1A_TARGETS_DN	2.713
MENSE_HYPOXIA_UP	2.476
POTTI_CYTOXAN_SENSITIVITY	2.306
MANALO_HYPOXIA_UP	2.205
GRAHAM_NORMAL_QUIESCENT_VS_NORMAL_DIVIDING_DN	2.200
CROONQUIST_IL6_DEPRIVATION_DN	2.184
HARRIS_HYPOXIA	2.173
WINTER_HYPOXIA_METAGENE	2.121
CROONQUIST_STROMAL_STIMULATION_UP	2.120
MITSIADES_RESPONSE_TO_APLIDIN_DN	2.075
CROONQUIST_NRAS_VS_STROMAL_STIMULATION_DN	2.075
KAUFFMANN_MELANOMA_RELAPSE_UP	2.053
CROONQUIST_NRAS_SIGNALING_DN	2.050
VANTVEER_BREAST_CANCER_METASTASIS_DN	2.044
FINETTI_BREAST_CANCER_KINOME_RED	2.037
KANG_DOXORUBICIN_RESISTANCE_UP	2.036
JIANG_HYPOXIA_NORMAL	2.018

Canonical pathway database gene set enrichment	NES
REACTOME_GLYCOLYSIS	2.044
REACTOME_FANCONI_ANEMIA_PATHWAY	2.021
REACTOME_G2_M_CHECKPOINTS	2.010
REACTOME_DNA_STRAND_ELONGATION	2.006
REACTOME_HOMOLOGOUS_RECOMBINATION_REPAIR	1.997
REACTOME_GLUCOSE_TRANSPORT	1.979
REACTOME_ACTIVATION_OF_ATR_IN_RESPONSE_TO_REPLICATION…	1.963
BIOCARTA_CDMAC_PATHWAY	1.956
REACTOME_METABOLISM_OF_CARBOHYDRATES	1.947
BIOCARTA_CARDIACEGF_PATHWAY	1.923
REACTOME_ACTIVATION_OF_THE_PRE_REPLICATIVE_COMPLEX	1.887
BIOCARTA_IGF1_PATHWAY	1.873
BIOCARTA_SPPA_PATHWAY	1.858
KEGG_O_GLYCAN_BIOSYNTHESIS	1.841
BIOCARTA_INSULIN_PATHWAY	1.794
REACTOME_LAGGING_STRAND_SYNTHESIS	1.783
KEGG_FRUCTOSE_AND_MANNOSE_METABOLISM	1.775
REACTOME_DOUBLE_STRAND_BREAK_REPAIR	1.773
REACTOME_MAPK_TARGETS_NUCLEAR_EVENTS_MEDIATED…	1.752
KEGG_WNT_SIGNALING_PATHWAY	1.746

Table 4.3. Gene set enrichment from Veh cells.

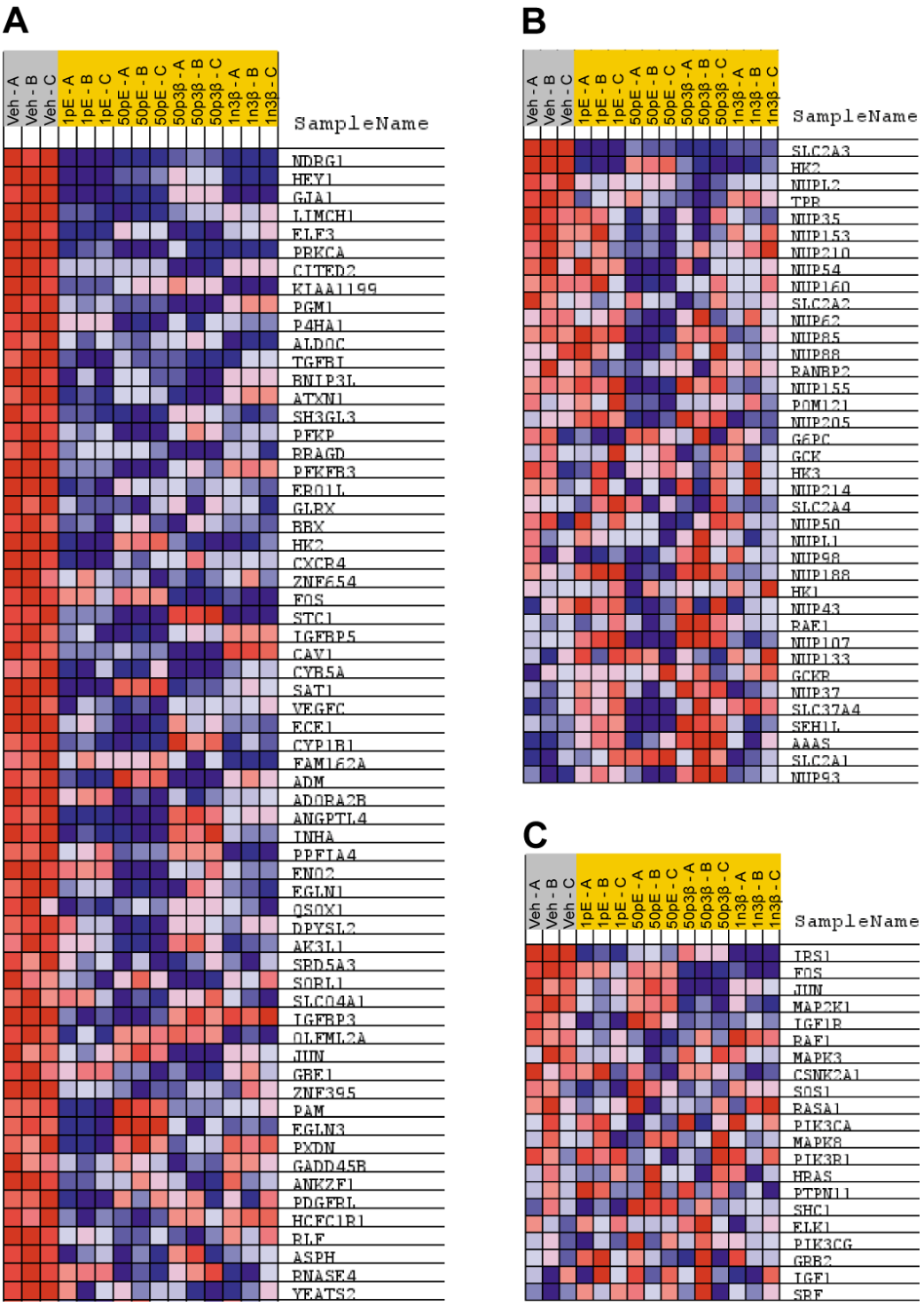

Figure 4.6. Heat maps of gene set enrichment in Veh cells. (A), Elvidge – Hypoxia Up (abridged); (B), Reactome – Glucose Transport; (C), Biocarta – IGF1R Pathway. Heat maps represent relative difference in expression (not raw expression) between phenotypes, Red = increased, blue = decreased. Each column represents one of the triplicate samples for each selected cell line. Headers shaded in gray vs. yellow represent phenotype comparison groups during anaylsis.

Gene set enrichment from limited subset of GSEA C2 CGP	NES
KOBAYASHI_EGFR_SIGNALING_24HR_DN	3.285
SOTIRIOU_BREAST_CANCER_GRADE_1_VS_3_UP	3.182
PUJANA_BREAST_CANCER_WITH_BRCA1_MUTATED_UP	2.628
FARMER_BREAST_CANCER_CLUSTER_2	2.581
ODONNELL_TARGETS_OF_MYC_AND_TFRC_DN	2.542
MASSARWEH_TAMOXIFEN_RESISTANCE_DN	2.526
WILLIAMS_ESR1_TARGETS_UP	2.435
FRASOR_RESPONSE_TO_SERM_OR_FULVESTRANT_DN	2.422
STEIN_ESRRA_TARGETS_RESPONSIVE_TO_ESTROGEN_DN	2.396
NADERI_BREAST_CANCER_PROGNOSIS_UP	2.380
STEIN_ESR1_TARGETS	2.361
VANTVEER_BREAST_CANCER_METASTASIS_DN	2.302
MASSARWEH_RESPONSE_TO_ESTRADIOL	2.289
FINETTI_BREAST_CANCER_BASAL_VS_LUMINAL	2.281
CREIGHTON_ENDOCRINE_THERAPY_RESISTANCE_1	2.280
FOURNIER_ACINAR_DEVELOPMENT_LATE_DN	2.262
POOLA_INVASIVE_BREAST_CANCER_UP	2.257
PUJANA_BREAST_CANCER_LIT_INT_NETWORK	2.236
CREIGHTON_ENDOCRINE_THERAPY_RESISTANCE_4	2.232
FRASOR_RESPONSE_TO_ESTRADIOL_UP	2.199

Table 4.4. Gene set enrichment from limited CGP database in low-steroid selected cells.

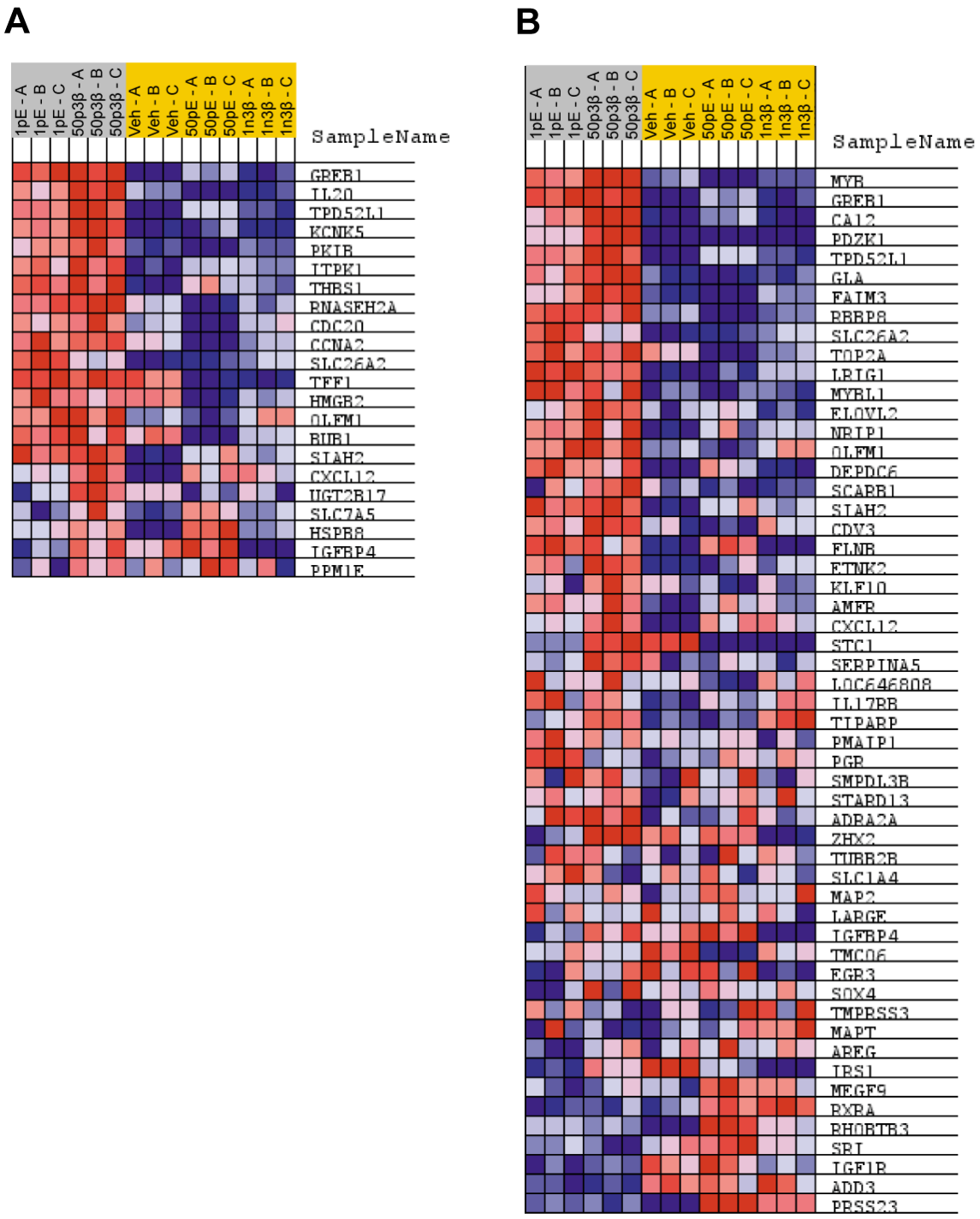

Figure 4.7. Heat maps of gene set enrichment from limited GSEA C2 CGP of 1pE and 50p3β cells. (A), Williams – ESR1 Targets Up; (B), Massarweh – Response to Estradiol. Heat maps represent relative difference in expression (not raw expression) between phenotypes, Red = increased, blue = decreased. Each column represents one of the triplicate samples for each selected cell line. Headers shaded in gray vs. yellow represent phenotype comparison groups during anaylsis.

U0126 and LY294002 partially inhibited the growth of 1pE and 50p3β cells in estrogen-free conditions; neither drug alone or in combination could inhibit cell growth to the extent of ICI 182,780 (Figure 4.9A-B). Under normal selection conditions (i.e. in the presence of E2 or 3βAdiol), neither U0126 nor LY294002 significantly inhibited cell growth in any selected cell line (Figure 4.9C-D) (50pE and 1n3β data not shown). Ligand-induced growth was inhibited by 100nM ICI 182,780. The observations that ICI 182,780 treatment is most effective in growth inhibition of 1pE and 50p3β cells in estrogen-free conditions and that U0126/LY294002 do not inhibit growth in the presence of ligand suggest that the MAPK and Akt pathways are upstream of ERα in 1pE and 50p3β cells.

EGFR/ErbB2 inhibitor lapatinib blocks estrogen-independent growth of 1pE and 50p3β cells

Based on the GSEA results above indicating enrichment of EGFR/ErbB2-driven gene expression patterns, we hypothesized that inhibition of EGFR and/or ErbB2 would block the estrogen-independent growth of 1pE and 50p3β cells. The small molecule inhibitor lapatinib is clinically used to inhibit the kinase activity of both EGFR and ErbB2 [213, 214]. Selected cells were treated with increasing concentrations of lapatinib in either estrogen-free conditions, or in normal selection conditions. Lapatinib did not inhibit the growth of 50pE or 1n3β cells under normal selection conditions (data not shown). The transient estrogen-independent growth of 1n3β cells was minimally inhibited by >100nM lapatinib (~20% reduction in growth) (data not shown). Additionally, lapatinib was not toxic to 50pE cells in estrogen-free conditions at the concentrations tested (data not shown). Veh cells were relatively resistant to lapatinib, as growth could not be completely inhibited with the concentrations tested (estimated IC_{50} > 1μM) (Figure 4.10). Lapatinib is a potent inhibitor of estrogen-independent growth of 1pE and 50p3β cells (IC_{50} = 8.6nM and 1.2nM, respectively); maximal growth inhibition by lapatinib was equivalent to maximal inhibition by ICI 182,780 under these conditions (data not shown). However, under normal selection conditions with estrogens present, lapatinib did not block the growth of 1pE or 50p3β cells (Figure 4.10). These data are consistent with the

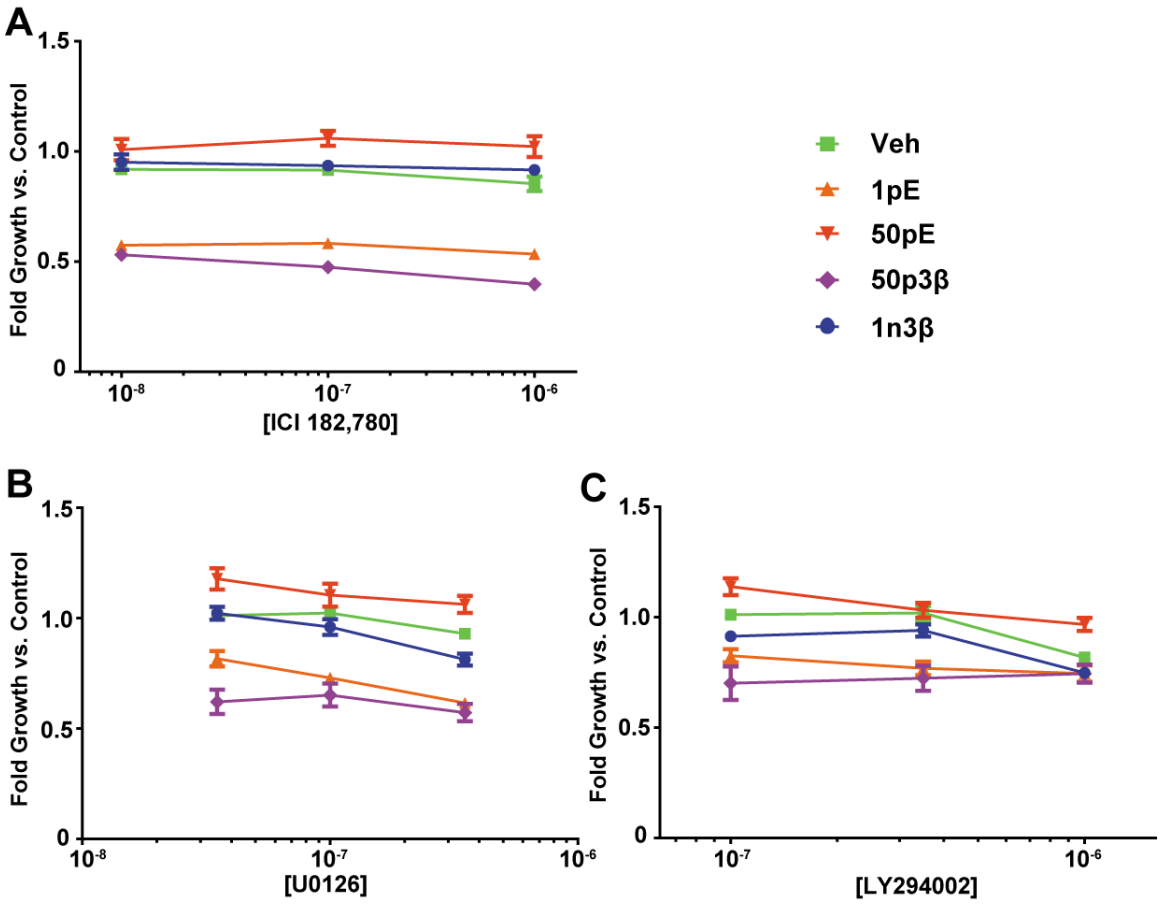

Figure 4.8. Inhibition of estrogen-independent growth with kinase inhibitors. Selected cell lines in estrogen-free conditions were treated with increasing concentration of (A) ICI, (B) U1026 or (C) LY294002. Growth was assessed 5 days after treatment. Fold versus control is relative to vehicle-treated cells of the same line. Points represent average of 6 replicates ± SEM.

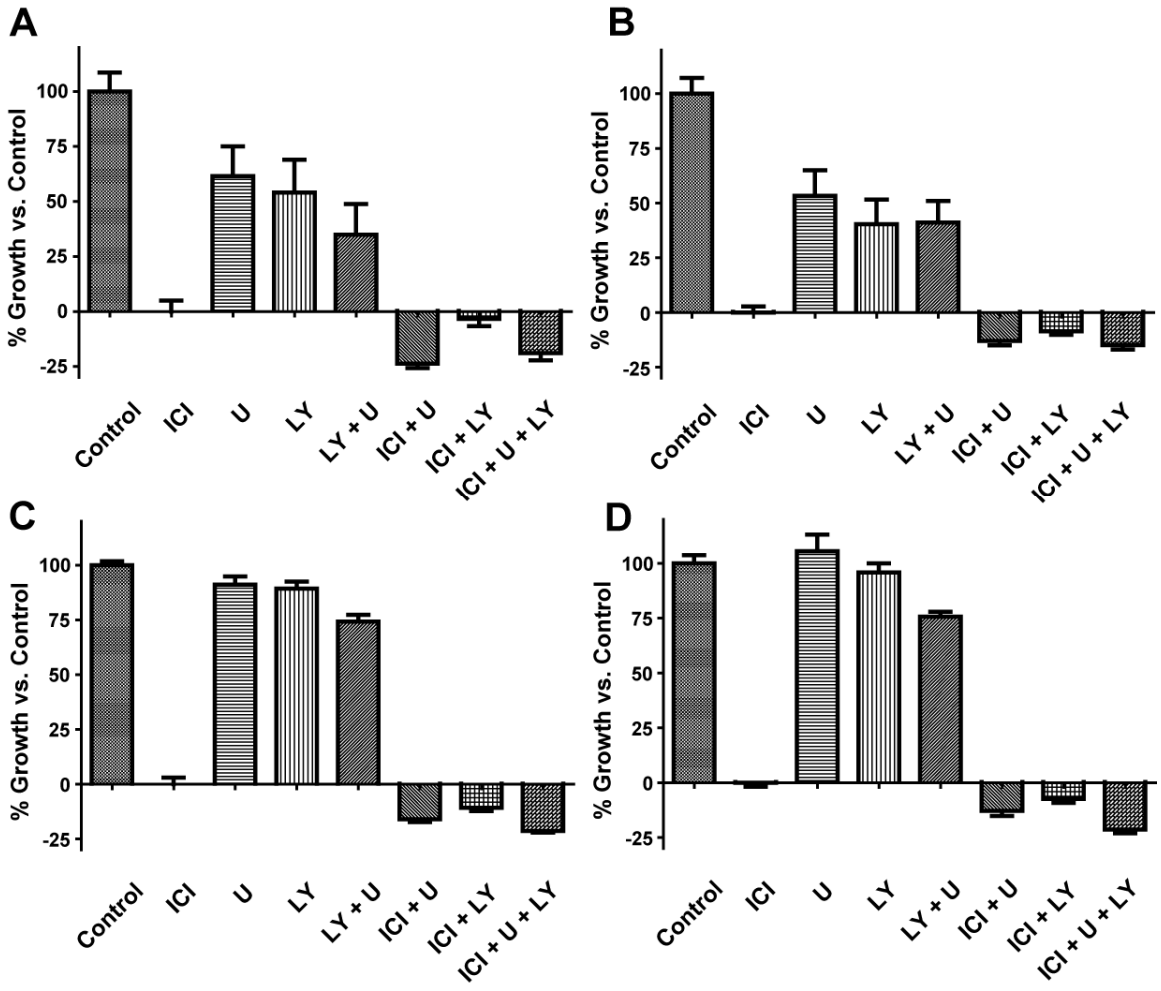

Figure 4.9. MAPK and PI3K inhibition block estrogen-independent growth. (A) 1pE and (B) 50p3β cells in estrogen-free conditions were treated with 100nM ICI, 100nM U0126 (U), 250nM LY294002 (LY) or combinations as indicated. Growth was assessed 4 days after treatment. Bars represent average of 6 replicates + SEM. (C) 1pE and (D) 50p3β cells in selection conditions (i.e. 1pM E2 and 50pM 3βAdiol, respectively) were treated as in A and B and assessed for growth 6 days after treatment. Bars represent average of 6 replicates + SEM.

previous observations that 1pE and 50p3β cells are only sensitive to kinase inhibitors in the absence of ligand. Further, these data are consistent with the hypothesis that an upstream receptor tyrosine kinase (i.e. a target of lapatinib, EGFR or ErbB2) signals through MAPK and/or Akt to maintain growth in estrogen-free conditions.

Kinase inhibitors decrease estrogen-independent phosphorylation and activity of ERα in 1pE and 50p3β cells

Estrogen receptor activation was examined via western blotting for phosphorylation of ERα at S167. 1pE and 50p3β cells were seeded in estrogen-free conditions, then treated with ICI 182,780 or kinase inhibitors as indicated (Figure 4.11). MAPK and Akt phosphorylation were examined by western blotting, in addition to ERα phosphorylation status. Levels of pMAPK or pAkt could be specifically decreased using U0126 or LY294002, respectively, in both cell lines. However, lapatinib completely eliminated all pMAPK and strongly decreased pAkt in both cell lines, suggesting that EGFR or ErbB2 is upstream of these signaling pathways in 1pE and 50p3β cells.

pER-S167 levels were strongly decreased by ICI 182,780 treatment, consistent with the concurrent decrease in total ER seen following ICI 182,780 treatment. U0126 did not decrease pER-S167 levels in either cell line, whereas LY294002 treatment did. This is consistent with previous reports that the PI_3K/Akt pathway is responsible for phosphorylating ERα at S167. Lapatinib strongly decreased pER-S167 levels in both 1pE and 50p3β cells, to a greater extent than LY294002 at the indicated concentrations. This differential ability to decrease pER-S167 parallels differential growth inhibition by each drug (as described above).

Selected cells developed differential resistance to tamoxifen and endoxifen

A number of previous reports using LTED models have demonstrated acquired resistance to the anti-estrogenic effect of tamoxifen following selection [215, 216]. We hypothesized that long term adaptation to 3βAdiol would present a unique environment for the development of tamoxifen resistance, as cells adapt long term to a structurally unique ligand. Selected cells in normal conditions were treated with increasing

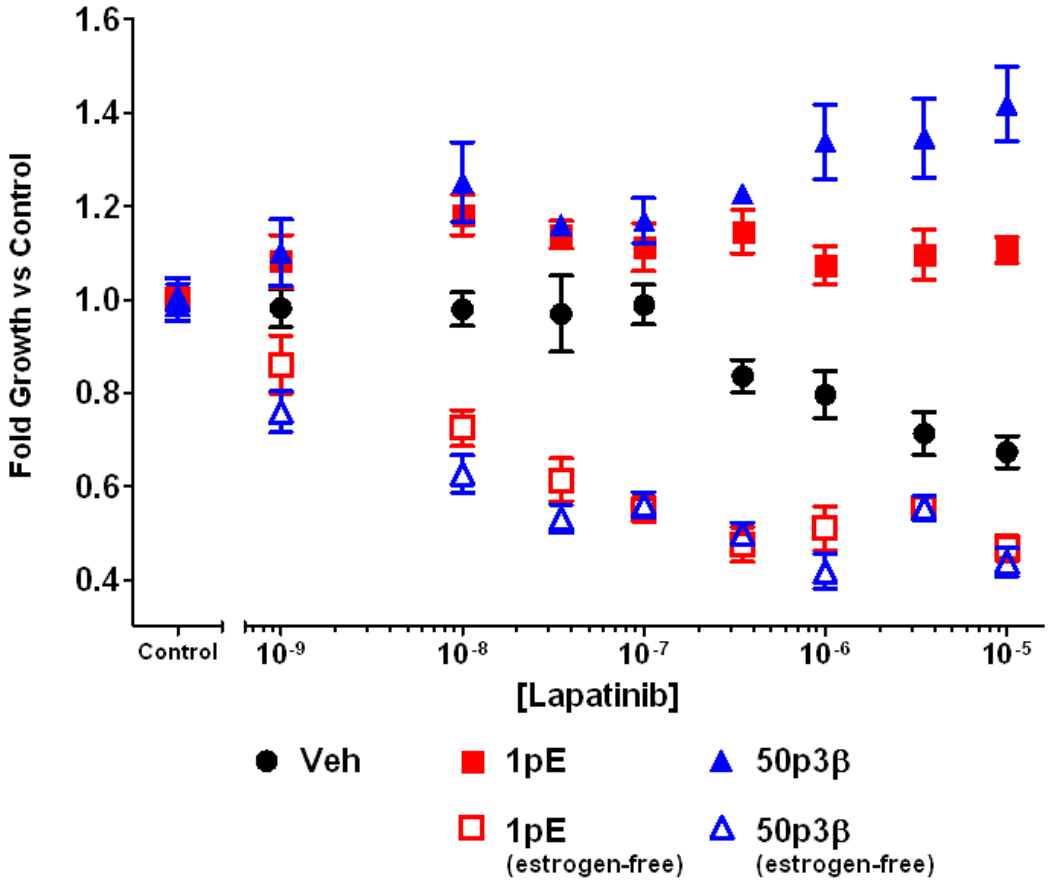

Figure 4.10. Lapatinib inhibits estrogen-independent growth. Selected cell lines were treated with vehicle (0.1% DMSO) or lapatinib as indicated. Growth was assessed 5 days after treatment. Points represent the average of 6 replicates ± SEM.

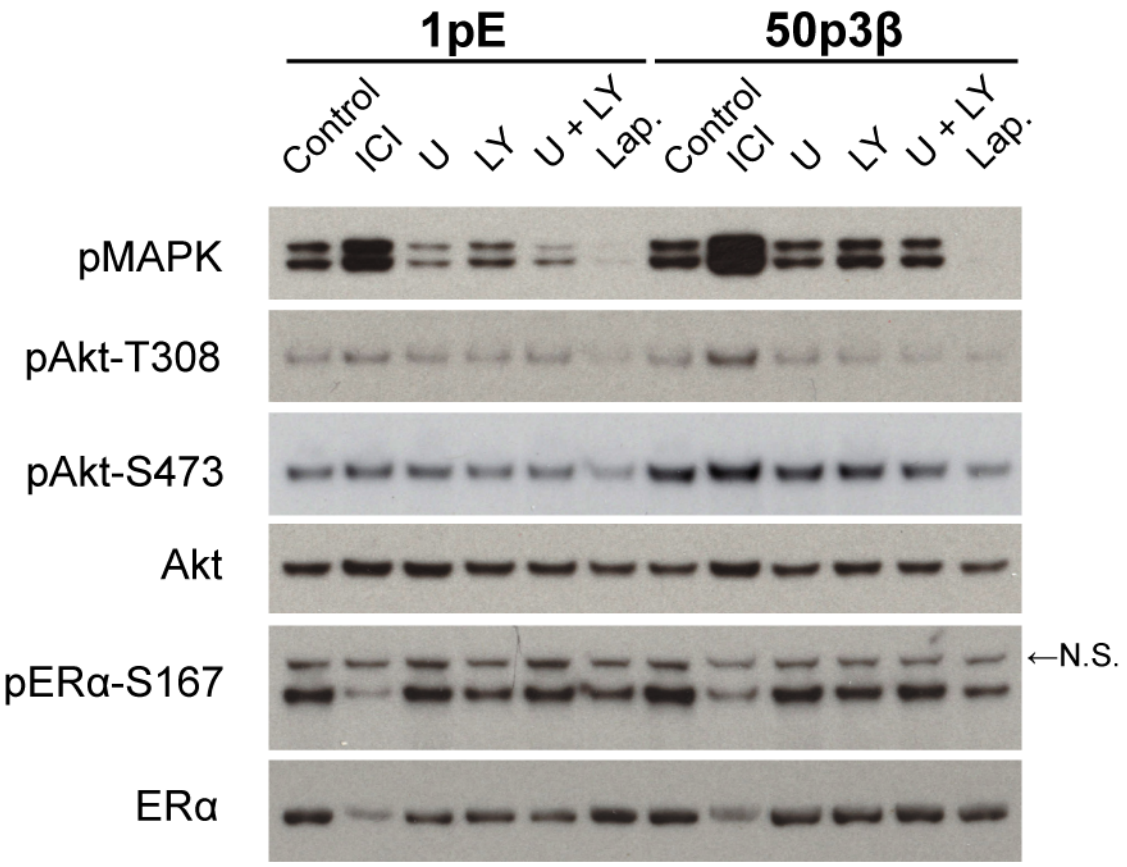

Figure 4.11. Kinase inhibitors decrease kinase and ERα activation in estrogen-free conditions. 1pE or 50p3β cells in estrogen-free conditions were treated with 100nM ICI, 100nM U0126 (U), 250nM LY294002 (LY), 1μM lapatinib (Lap) or combinations as indicated. Lysates were harvested 72 hours after treatment. N.S., non-specific band.

concentrations of tamoxifen or 4-hydroxy-N-desmethyl tamoxifen (endoxifen), an active anti-estrogenic metabolite of tamoxifen [159]. Tamoxifen was unable to significantly inhibit the growth of 1pE, 50pE, 50p3β or 1n3β cells at concentrations ≤100nM; 1μM tamoxifen reduced growth of those selected lines to 50-80% of maximum growth (Figure 4.12A). Despite the somewhat uniform effects of tamoxifen on the selected cell lines, response to endoxifen was variable. Endoxifen effectively reduced the growth of 50pE cells down to ~30% of maximum growth. However, endoxifen only reduced the growth of 1pE and 1n3β cells down to approximately 80% and 65% of maximum growth, respectively; 50p3β cells were not significantly growth inhibited by endoxifen (Figure 4.12B). Both tamoxifen and endoxifen induced the growth of Veh cells in a bell-shaped pattern. Tamoxifen induced growth at concentrations up to 10nM (~1.5-fold versus control), and growth was reduced to control levels at increased concentrations up to 1μM. Similarly, endoxifen induced growth at concentrations up to 100pM (~1.4-fold versus control), and growth was reduced to control levels at concentrations up to 1μM.

Discussion

Improved understanding of the molecular mechanisms used by breast tumors to adapt to estrogen deprivation during AI therapy is critical to implementing clinical interventions to either prevent the development of or treat recurrence. Additionally, insight into these mechanisms may provide useful biomarkers to predict resistance early on in the course of adjuvant therapy. Accurately modeling conditions in patients on AI therapy is likely critical in discovering clinically relevant mechanisms of resistance that will provide useful biomarkers and therapeutic targets.

Minimal clinical data exist regarding mechanisms of resistance to AI therapy. Recently, the use of the neoadjuvant treatment setting (2-12 week treatment prior to surgery) has proven useful in examining molecular changes in breast tumors in response to therapy [217-221]. Mitch Dowsett and colleagues have demonstrated that changes in the proliferation marker Ki67 before and after only 2 weeks of AI therapy are predictive of long-term outcome [221]. Patients with high Ki67 levels were found to recur significantly more rapidly, suggesting that tumor cells in these patients continue to proliferate in the

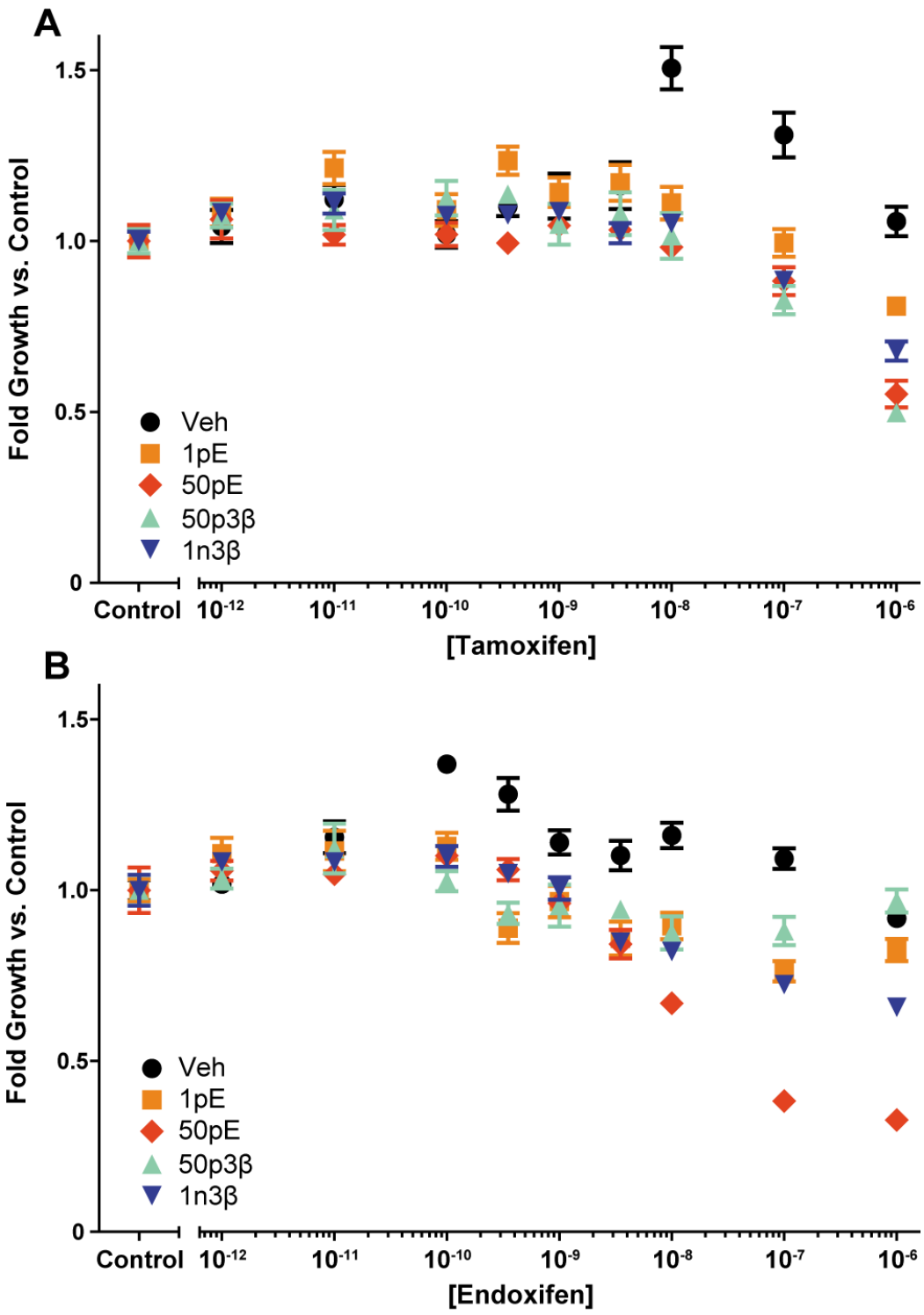

Figure 4.12. Anti-estrogen resistance in selected cell lines. Selected cell lines in normal selection conditions were treated with vehicle (0.1% EtOH) or increasing concentrations of tamoxifen (A) or endoxifen (B). Growth was assessed 5 days after treatment. Points represent the average of 6 replicates ± SEM.

presence of AIs. However, in spite of the usefulness of these biomarkers in predicting response to endocrine therapy, these studies do not provide insight into the mechanisms underlying resistance. William Miller and colleagues have begun to examine gene expression in tumors following neoadjuvant AI treatment to identify changes in gene expression between tumors responsive or resistant to AI therapy [222-224]. These studies have identified gene signatures that are associated with either response or resistance to therapy, however, many of these signatures are largely indicative of cellular proliferation or mitosis and the underlying mechanisms are unclear. More recent work by this group has examined changes in gene expression during extended neoadjuvant therapy; gene expression in tumors was measured at baseline and 14 days and 3 months after treatment initiation [225]. The number of genes with significantly different expression versus baseline was substantially higher after 3 months (340 probe sets) versus 14 days (117 probe sets). Gene ontology analysis also indicated that radically different classes of genes were altered at either timepoint. These observations suggest that whereas early changes in gene expression may be indicative of the removal of estrogens, late changes may be more representative of tumor adaptation to therapy. Changes in expression were also heterogeneous across tumors, with subgroups of samples exhibiting opposite changes in expression for specific genes versus the majority of the samples. Though these studies are ideal *in situ* models for assessing mechanisms of resistance, they illustrate the difficulties associated with understanding AI resistance. While assessing larger number of tumors may also be useful in identifying consensus changes in gene expression following AI therapy, mechanisms of resistance are heterogeneous and may be difficult to assess for individual tumors. Additional long-term studies of tumor adaptation to therapy *in situ* may prove difficult, as surgery must be timed to prevent tumor expansion. Thus the tumors where long-term gene expression data would prove most useful (i.e. tumors growing in the presence of AIs) must be excised.

Cell culture models may circumvent some of these issues and provide access to long-term changes to breast cancer cells following AI therapy. As discussed in Chapter I, long-term estrogen-deprived (LTED) cell culture models and aromatase over-expression models have been used to examine changes in breast cancer cells following long-term estrogen

withdrawal. Though these models have proven useful in generating endocrine-resistant variants of estrogen-dependent breast cancer cells, it is unclear whether the total absence of estrogenic stimuli as modeled with LTED accurately recapitulates conditions on AI therapy. As described above, 3βAdiol can activate ERα, and importantly, 3βAdiol is generated independent of aromatase and therefore is potentially present during AI therapy. Additionally, AIs are not successful in completely eliminating all serum estrogen, and residual aromatization remains. This low level of aromatization is sufficient to produce quantifiable, picomolar concentrations of circulating E2 in some patients [31, 206]. Dixon et al assessed serum E2 concentrations in patients receiving daily anastrozole or letrozole for 3 months (n = 54 for each arm) [206]. Though the majority of patients had serum E2 below the limit of quantification (3pmol/L), 19.4% of patients had E2 concentrations >3pmol/L. Importantly, 3pM E2 induces ~35% maximal growth in the MCF-7 cells (Appendix I). Based on these observations, we modified LTED to include defined concentrations of either E2 or 3βAdiol, and selected cells in these conditions for estrogen-independence, parallel with cells maintained in LTED. Importantly, cells maintained in LTED + high E2 (50pM) served as a control for changes in phenotype associated with long-term culture and growth in CCS, rather than specific to the changes in estrogenic stimuli.

Clear differences in the adaptation to the changes in levels of estrogens emerged across each selected cell line. In 50pE cells, the presence of near-saturating concentrations of E2 was sufficient to maintain the parental phenotype in these cells; 50pE cells remained wholly dependent on estrogen to maintain growth, and cease growth in estrogen-free conditions. 50pE cells also were growth induced by either E2 or 3βAdiol equivalently to parental MCF-7 cells. However, while ERα was also near-saturated in 1n3β cells, the partial agonist 3βAdiol was not equivalent to E2 in the maintenance of the parental phenotype. 1n3β cells recognized 3βAdiol as a full agonist, potentially suggesting changes in the co-factor cohort of the cells in recognizing activated ERα. Consistent with this observation, 1n3β cells were also resistant to the tamoxifen metabolite endoxifen and only weakly growth-inhibited by this anti-estrogen. 1n3β cells did however remain dependent on estrogens to maintain proliferation; in estrogen-free conditions, 1n3β cells

cease growth after 3-5 days. These data demonstrate that in the absence of E2 (following AI therapy), high concentrations of 3βAdiol are sufficient to promote tumor growth and the development of a novel, anti-estrogen resistant phenotype.

Though high concentrations of estrogens were sufficient to maintain an estrogen-dependent phenotype, low estrogen concentrations or absence of estrogens promoted the development of an estrogen-independent phenotype. Veh, 1pE and 50p3β cells all demonstrated cell growth in estrogen-free conditions following selection. However, unique mechanisms appear to drive growth in the LTED Veh cells versus those maintained in low estrogen concentrations (1pE and 50p3β). Growth in estrogen-free conditions both 1pE and 50p3β cells can be blocked by the addition of the pure anti-estrogen ICI 182,780, whereas Veh cells are ICI 182,780 resistant. This suggests that estrogen-independent growth in 1pE and 50p3β is ER-dependent, but ER-independent in Veh cells. Consistent with this, we observed that GREB1 is expressed in 1pE and 50p3β cells in estrogen-free conditions, and that GREB1 expression could be decreased by ICI 182,780; Veh cells did not express GREB1. Also, phosphorylated ERα was detected only in 1pE and 50p3β in estrogen-free conditions, further evidence of ERα activation in spite of the absence of ligand. These data suggest that following selection in low estrogen concentrations, breast cancer cells can maintain ERα activation in the absence of ligand, whereas LTED Veh cells no longer require ERα activity. Our data with inhibitors of kinase signaling pathways suggest that ERα activation is maintained by ErbB receptor tyrosine kinases that signal via the MAPK or PI_3K pathways.

The observations that ERα activation is maintained by a ligand-independent mechanism are consistent with those reported for LTED cells developed by the Dowsett and Santen laboratories (described in Chapter I). These previously developed LTED models also appear to require similar receptor tyrosine kinase signaling pathways to maintain estrogen-independent growth, and respond to inhibitors of these pathways. However, while 1pE and 50p3β cells are growth inhibited by lapatinib (in addition to MEK and PI_3K inhibitors), they are only sensitive to kinase inhibitors in the absence of estrogen. In their normal selection conditions (low estrogen concentrations) 1pE and 50p3β cells were

completely resistant to all kinase inhibitors tested, and were only growth inhibited by ICI 182,780. These observations may suggest that in patients with low serum estrogen concentrations on AI therapy, recurrent tumors will not respond to the addition of kinase inhibitors, as ligand will still be present to maintain ERα signaling. The removal of AIs from a treatment regimen in this scenario would allow estrogen concentrations to increase, which may also prevent sensitivity to other targeted therapies. Further, the specific sensitivity of 1pE and 50p3β cells to ICI 182,780 only suggests that in similar tumors, increased antagonism of estrogen signaling may be critical to blocking tumor growth.

A number of pre-clinical and clinical studies support a role for maximizing ERα blockade in recurrent tumors (reviewed in [119]). A number of Phase II clinical trials have demonstrated that ~28-44% of patients who have experienced disease progress after AI therapy receive clinical benefit from switching to ICI 182,780 [226-228]. Three large Phase III trials are currently underway to further examine the role of ICI 182,780 in advanced breast cancer. SWOG S0226 (NCT00075764) has completed accrual, and SOFEA (Study of Faslodex vs. Exemestane with/without Arimidex, NCT00253422) is currently still accruing patients. However, FACT (Fulvestrant and Anastrozole in Combination, NCT00256698) presented early results at the San Antonio Breast Cancer Symposium in 2009, and reported that adding ICI 182,780 to anastrozole provided no benefit to women with hormone-receptor-positive breast cancer (final results are expected in November 2011). While the early results from FACT may be at odds with the hypotheses generated by 1pE and 50p3β cells, it is clear that mechanisms of resistance are heterogeneous. Using only MCF-7 cells, we selected populations that were either sensitive or resistant to ICI 182,780 (1pE/50p3β cells and Veh cells respectively). The estrogen environment in which AI resistance develops is likely critical to the recurrent tumor phenotype. Biomarkers of ERα activation (such as phosphorylation at S167) may be necessary to identify patients that will benefit from ICI 182,780 or further AI treatment. Further, recent results of the CONFIRM trial (Comparison of Faslodex in Recurrent or Metastatic breast cancer, NCT00099437) demonstrated that increasing the dose of ICI 182,780 from 250mg to 500mg significantly reduced the risk of disease

progression in patients who had recurred on prior endocrine therapy [229]. Thus not only is it critical to identify recurrent tumors with ERα activity, but the relative concentrations of ICI 182,780 and competing estrogen concentrations at the site of action in recurrent tumors are likely determinants of whether ICI 182,780 can effectively antagonize ERα and block tumor growth. Initial AI treatment may also provide insight into mechanisms of resistance. Though most trials' inclusion criteria specifies steroidal vs. non-steroidal AIs, significant differences exist between the two non-steroidal AIs. Serum E2 concentrations reported by Dixon et al [206] demonstrated that letrozole more completely suppressed E2 versus anastrozole; 1/54 and 20/54 of letrozole and anastrozole treated patients, respectively has serum E2 concentrations >3pmol/L. Based on our observed phenotypes from LTED and low estrogen selected cells, patients who recur on letrozole may be predicted to have ER-independent, ICI-resistant tumors, whereas recurrences on anastrozole may be ER-dependent, ICI-sensitive tumors.

Our cell culture models suggest that the estrogen environment in which resistance to endocrine therapy develops promotes unique mechanisms of resistance that will display diverging sensitivity to targeted or endocrine therapies. The presence of residual E2 or alternative estrogens such as 3βAdiol may drive tumor growth in the presence of AIs and subsequently maintain the growth of recurrent tumors during additional therapies. These observations highlight the potential heterogeneity in mechanisms of endocrine resistance, and the need for specific biomarkers that will indicate which therapies may benefit individual patients. Additionally, the results of clinical trials using endocrine therapies in recurrent, metastatic breast cancer may be difficult to interpret due to the minimal patient pre-selection. Further understanding of the total estrogen environment in patients on AI therapy who experience recurrence is necessary to effectively treat these patients.

Chapter V.
High efficiency genotype analysis from formalin-fixed, paraffin-embedded tumor tissues

Introduction

Until recently, clinical trials in cancer did not routinely collect and store patient DNA samples, thus limiting the ability to conduct pharmacogenetic analysis of many large, landmark clinical trials. Another potential source of patient DNA does, however, exist in the form of formalin-fixed, paraffin-embedded (FFPE) tumor samples that were collected for the majority of clinical trials in oncology. Previously, we and others have demonstrated that DNA can be obtained from these tumor blocks, that SNP genotypes can be reliably determined from this DNA, and that the genotypes of SNPs in genes of pharmacogenetic interest (primarily involved in drug metabolism) derived from the tumor samples match those of the germline DNA [203, 230-232]. This technological advance demonstrated that FFPE samples could be used for pharmacogenetic analyses of historical prospective clinical trials, thereby allowing the existing wealth of large, carefully conducted clinical trials of chemotherapeutic agents to be mined for associations between inherited gene variants with drug toxicities and clinical outcomes.

Using DNA extracted from FFPE tumor samples for genotype analyses presents significant technical challenges due to the relatively low quantity and poor quality of the template DNA that is extracted from these samples. Standard DNA isolation methods used for FFPE samples typically produce severely sheared and fragmented DNA which is frequently not optimal for PCR-based genotyping [233-236]. All commonly used PCR-based genotyping assays have been designed to work using high quality DNA isolated from viable cells. Real-time PCR-based Taqman assays, for instance, involve the amplification of DNA segments 80-150 base pairs (bp) in length containing the SNP of interest[237]. In addition, 5-10μm FFPE tissue block sections typically only yield

sufficient DNA for 30-50 Taqman-based genotyping reactions (unpublished observations). Furthermore, Taqman PCR reactions using DNA extracted from FFPE samples are frequently inefficient, and yield irregular fluorescence output curves, making allelic determination difficult or ambiguous. Common practice when confronted with DNA samples that are difficult to genotype is to increase the amount of template DNA used per reaction. However, we have observed that doing this with FFPE-derived DNA often results in worsening rather than improvement of the PCR reaction. A simple method to determine the optimal amount of a given sample of FFPE-derived DNA for each assay would be valuable.

In this report, we describe methods to analyze DNA harvested from FFPE materials that allows the assessment of overall quality and quantification of 'amplification-quality DNA' or 'AQ-DNA' (DNA fragments large enough for efficient PCR-based analysis). Using materials evaluated in this manor, we describe how minimizing the amount of input DNA in Taqman-based genotyping reactions significantly improves PCR amplification efficiency, increases the accuracy of allelic determinations, and greatly increases the number of genotyping assays that can be performed per sample. We also demonstrate that FFPE tumor cores of the type used to generate tissue microarrays (TMAs) can be used as a source of DNA for Taqman-based genotyping. The methodological approaches described herein facilitate the improved application of Taqman-based SNP genotyping to FFPE-derived DNA, significantly increasing the number of assays that can be conducted using what is a valuable and limited tissue resource.

Methods

Sample Preparation

Samples were selected randomly from the routinely formalin-fixed, paraffin-processed breast tumour archive at the Royal Marsden Hospital, with the prerequisites that they (i) were pre-2006 in order to comply with HTA (Human Tissue Act) legislation regarding patient consent and (ii) were suitable to TMA (tissue microarray) core acquisition from both the tumor and intratumoral stromal compartments. In practice these were

predominantly invasive ductal carcinomas grade II/III. At the time of DNA extraction, tumor blocks ranged in age from 4-19 years, with a median age of 15 years. Specific FFPE samples used in each data figure are indicated in Table 5.1.

Tumour and stromal areas were marked on an H&E stained slide and then transposed onto the associated paraffin block. 0.6mm cores were punched in the marked areas using the Beecher tissue arrayer MTA1 and the extracted cores were transferred to RNAse, DNase free tubes. The needle punch was cleaned with ethanol and allowed to dry fully between each core acquisition to prevent cross contamination. Two 10μm paraffin embedded sections were cut from the same paraffin block prior to core acquisition. A new blade was used for each patient sample to eliminate the potential for cross-contamination. Gloves were worn at all times.

DNA Extraction from FFPE-Tissue Samples

Our previously described method for extracting DNA from FFPE samples[203] using the DNeasy Blood and Tissue Kit (Qiagen, Valencia, CA) was improved with minor modification to eliminate the use of solvents to de-paraffin samples. Briefly, samples (sections and cores, described above) were heated to 95ºC for 15 minutes in 180μL Buffer ATL and then allowed to cool to room temperature for a minimum of 5 minutes. Twenty microliters of Proteinase K solution (20mg/mL) was added to the samples, which were then incubated at 55ºC. After 8 hours, fresh Proteinase K solution (20μL) was added and the samples incubated for an additional 8 hours, then DNA extracted according to the manufacturer's instructions.

Quality Control Multiplex PCR

DNA quality was measured using a multiplex PCR-based method described by van Beers et al[238], with minor modifications. In addition to primer pairs for the 100, 200, 300, and 400bp fragments of GAPDH used by van Beers et al, additional primer pairs were added for 500, 600, and 700bp fragments. Primer sequences are available upon request. The 100 and 500-700bp primers were used at a final concentration of 266nM, and the 200-400bp primers at 133nM. Reactions were incubated at 94ºC for 1 minute, 56ºC for 1

Figure	# of FFPE Tissue Samples	Source
1	8	Royal Marsden; pilot study samples
2	0	High-quality lymphocyte DNA
3	0	High-quality lymphocyte DNA
4	60	Royal Marsden; 30 matched sample type set, 30 pilot study samples
5	117	Royal Marsden; 39 of each matched FFPE sample type
6	117	Royal Marsden; 39 of each matched FFPE sample type
7	117	Royal Marsden; 39 of each matched FFPE sample type
S1	6	Royal Marsden; 2 of each matched FFPE sample type

Table 5.1. FFPE samples used in study figures.

minute, and 72ºC for 3 minutes, for 35 cycles. PCR products were analyzed by capillary electrophoresis using an Agilent 2100 Bioanalyzer with DNA 1000 electrophoresis chips (Agilent Technologies, Santa Clara, CA).

Quantification of Amplification-Quality DNA (AQ-DNA)

In order to determine the amount of AQ-DNA in extracted FFPE samples we quantified the 100bp fragment of GAPDH using SYBR Green real-time PCR. Briefly, 25µL reactions containing: forward primer (GTT CCA ATA TGA TTC CAC CC) and reverse primer (CTC CTG GAA GAT GGT GAT GG) at final concentrations of 250nM, 12.5µL of Platinum SYBR Green Master Mix (Invitrogen, Carlsbad, CA) and template DNA were incubated for 40 cycles at 95ºC for 15 seconds and 56ºC for 45 seconds using an iCycler real-time thermocycler (BioRad, Madison, WI).

DNA was isolated from fresh human lymphocytes (Blood and Tissue Kit, Qiagen) and the concentration was measured using a NanoDrop ND-1000 spectrophotometer (Thermo Scientific, Waltham, MA). SYBR Green real-time PCR (described above) was performed using a dilution series of lymphocyte DNA (in Ultra-Pure H_2O, Invitrogen) from 1pg–1µg to generate standard curves. These standard curves were used to calculate the relative amount of AQ-DNA in FFPE-derived samples, compared to the high quality lymphocyte DNA. Standard curves were plotted as the cycle number at which SYBR Green fluorescence passed a software determined threshold (threshold cycle, Ct) versus DNA quantity (µg) using GraphPad Prism 4.03 (GraphPad Software, Inc., La Jolla, CA). AQ-DNA from FFPE samples was quantified by adding 1µL of each DNA sample per real-time PCR reaction. The threshold cycle for each FFPE sample was plotted on the standard curve to extrapolate the quantity of AQ-DNA, relative to the high quality lymphocyte DNA.

DNA Enzymatic Shearing

DNA was sheared enzymatically using an Enzyme Shearing Kit (Active Motif, Carlsbad, CA). Genomic DNA from lymphocytes at ~100ng/µL was diluted 1:10 with Digestion Buffer and 50µL aliquots made. Two and half microliters of Enzyme Cocktail (1:10,000

in 50% glycerol) was added to each aliquot, and incubated for times ranging from 10 to 180 minutes. The reactions were stopped by adding 1μL of ice-cold 0.5M EDTA and incubation on ice for 15 minutes. DNA was purified from shearing reactions for subsequent PCR using Nucleotide Clean-up kits (Qiagen, Valencia, CA) according to the manufacturer's instructions.

Genotyping

FFPE tissue-extracted DNA was genotyped for known single nucleotide polymorphisms (SNPs) in the cytochrome P450 2D6 (CYP2D6) gene. The following SNPs were genotyped: 1846G>A (rs3892097), T1707del (rs5030655), A2549del (rs35742686), 2988G>A (rs28371725), 100C>T (rs1065852), and 4180G>C (rs1135840). Genotyping for these SNPs allows the identification of the most common variant alleles of CYP2D6: CYP2D6*2, *3, *4, *6, *10, and *41. SNPs were determined using Taqman Allelic Discrimination Assays (Applied Biosystems, Foster City, CA) according to the manufacturer's instructions as previously described [239], with minor modification. Reactions were carried out to 60 cycles to allow amplification of sub-nanogram quantities of DNA. Reactions were conducted using Genotyping Master Mix (Applied Biosystems) in an iCycler real-time thermocycler (BioRad). Samples were also genotyped for UGT2B7 802T>C (rs7439366) using a Taqman Alleic Discrimination Assay with minor modification. Reactions were conducted, using 50 pg of DNA as determined by our methods described above, for 50 cycles on an iCycler real-time cycler.

In order to minimize the potential for DNA cross-contamination (a concern when amplifying sub-nanogram quantities of DNA), all genotyping reactions were prepared in a designated template-free zone in a vertical laminar flow hood (AirClean 600, AirClean Systems, Raleigh, NC), with HEPA filtration and UV light.

Results

Multiplex PCR Identifies Samples of Insufficient Quality to Genotype

To assess the quality of DNA from FFPE tissue samples, we adapted a method described by van Beers *et al*. in which 7 amplicons of increasing size, from 100-700 base pairs,

within the GAPDH gene are amplified by PCR.[238] The sizes of the amplicons produced using FFPE-derived template DNA correlates with the degree to which the DNA has been sheared or fragmented. We used this assay to screen a panel of DNA samples isolated from FFPE tissue. We selected samples that had previously been genotyped for a panel of SNPs in the Cytochrome P450 2D6 (CYP2D6) gene successfully (thus considered higher quality, HQ DNA) and unsuccessfully (thus considered lower quality, LQ DNA) (Figure 5.1). All 7 fragments are amplified from the high quality DNA control (lane 1). Samples that could not be genotyped (LQ) did not support amplification of any of the GAPDH fragments (lanes 2-5). We observed that FFPE DNA samples that performed well using Taqman genotyping assays (HQ) supported amplification of at least the 100bp fragment, and larger fragments up to 400bp (lanes 6-9).

Quantification of Amplification-Quality DNA by Real Time PCR

Standard methods for quantifying DNA, such as UV absorbance, do not provide information regarding the degree of DNA fragmentation; therefore, we set out to measure the amount of "amplification-quality DNA" or "AQ-DNA" in DNA samples from FFPE tissues. We developed a quantitative-PCR based assay that determines the amount of fragments of 100bp or greater relative to a high molecular weight DNA standard harvested from viable lymphocytes. This technique uses SYBR Green-based amplification and quantification of the 100bp fragment of GAPDH from the quality control PCR described above. To validate that amplification of this fragment has a linear relationship with DNA quantity, a dilution series of high quality DNA obtained from lymphocytes was generated as described in Materials and Methods.

The linear range of threshold cycle vs. quantity of DNA was found to be 1pg – 10ng (Figure 5.2A). Interestingly, adding greater than 10ng of DNA to the PCR reaction caused a loss in the linear relationship, and caused inefficiency in PCR amplification (Figure 5.2B). Furthermore, addition of 1μg of DNA completely quenched the PCR reaction and blocked any amplification (indicated by a threshold cycle of 39 cycles). The dashed line

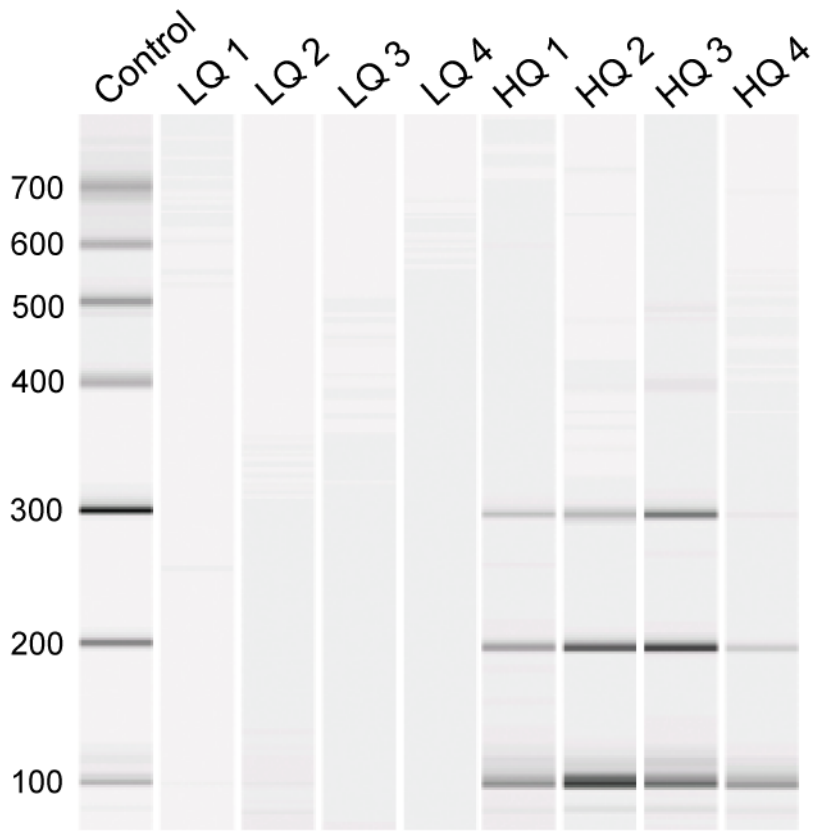

Figure 5.1. DNA quality assessment by multiplex PCR analysis. Samples shown are high quality lymphocyte DNA (control) and FFPE tissue DNA samples (LQ1-4, HQ1-4). All 7 amplicons were amplified in the control (lane 1). No amplicons were amplified in FFPE samples that could not successfully be genotyped (LQ, lanes 2-5). Amplicons of 100bp and greater were amplified from FFPE samples that were successfully genotyped (HQ, lanes 6-9).

in Figure 5.2B represents the linear regression from Figure 5.2A, to demonstrate the loss of linearity at >10ng of input DNA.

Sample Quality by Multiplex PCR Correlates with Quantification of AQ-DNA

To demonstrate that quantification of the 100bp fragment of GAPDH correlates with sample fragmentation as measured by the multiplex PCR described above, lymphocyte DNA was enzymatically sheared as described in Materials and Methods. The Enzymatic Shearing Kit was specifically designed so that increasing incubation time results in progressive fragmentation of the DNA. Overall quality and quantity of AQ-DNA was evaluated as described above.

As shown in Figure 5.3, increased digestion time caused a progressive loss of the larger PCR amplicons, with loss of the 500-700bp amplicons by 60 minutes, and loss of the 400bp amplicon by 120 minutes. Over-digestion with high concentration enzyme cocktail caused a loss of all bands (data not shown). Increased digestion time also correlated with a loss of AQ-DNA as determined by amplification of the 100bp GAPDH fragment, with a progressive decrease in quantity of AQ-DNA from 0-120 minutes of digestion. AQ-DNA decreased from 17.5ng/μL in the control digestion, to ~2ng/μL at >2hrs digestion. Further digestion up to 180 minutes with this dilution of enzyme cocktail appeared to have no further effect on fragment size or 100bp fragment quantification. Over-digestion with high concentration enzyme cocktail caused no 100bp amplicon signal to be seen with those samples, and decreased AQ-DNA to ~0ng/μL (data not shown).

Minimizing Input DNA Improves Genotyping Efficiency

Based on our quantification method described above, we attempted to establish the minimum amount of AQ-DNA required for assessment of genotypes using Taqman-based analyses. Ten FFPE-derived DNA samples were diluted from 1ng to 10pg of AQ-DNA per reaction, and genotyped for CYP2D6 1846G>A (CYP2D6*4). Results are shown in Table 5.2. Samples with wild-type genotypes for this SNP were successfully genotyped with only 10pg of input DNA. However, the mutant-specific probe in this assay required at least 50pg of input DNA to amplify successfully. Importantly, Sample J

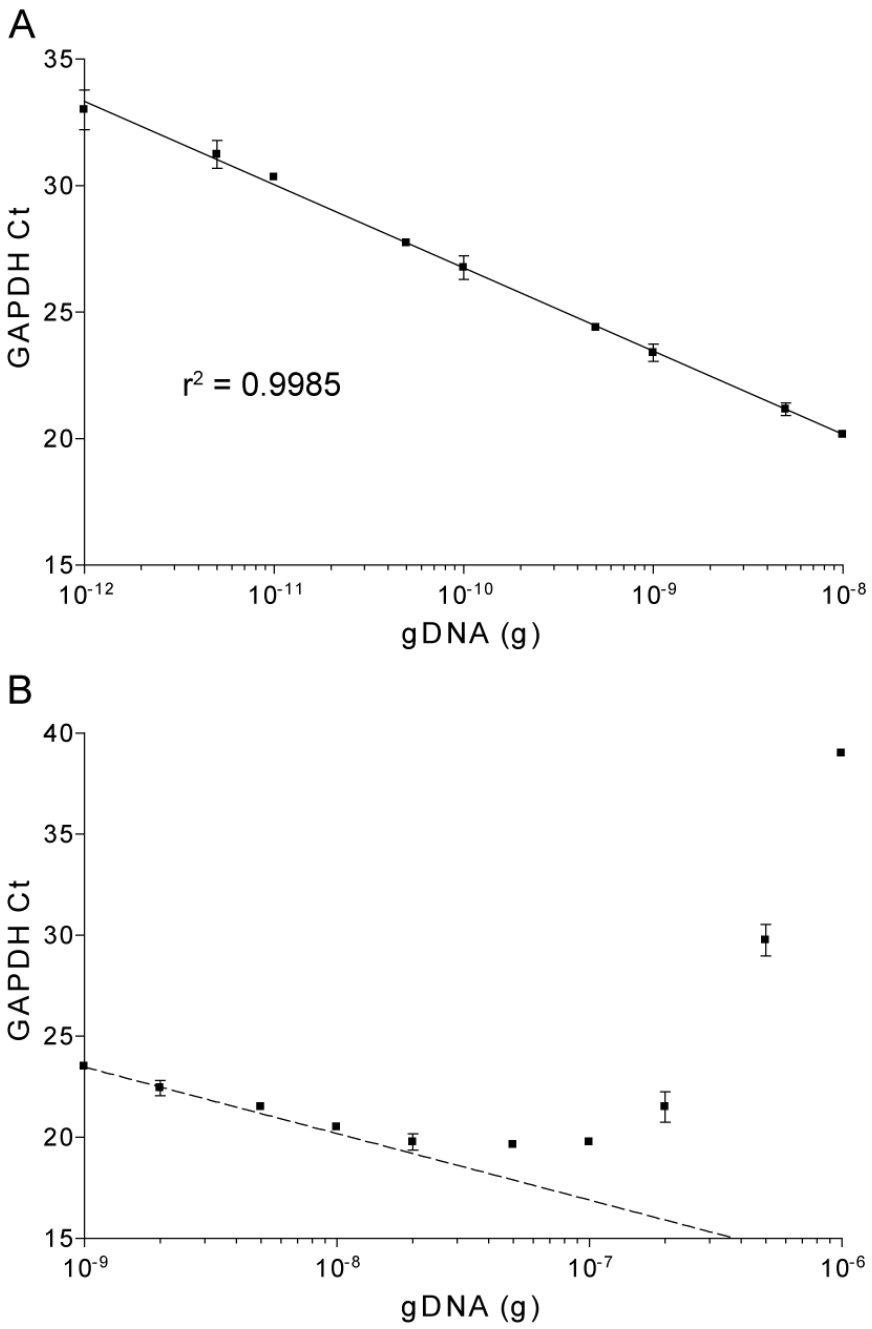

Figure 5.2. SYBR Green quantitative PCR amplification of the 100bp amplicon of GAPDH. A dilution series of high quality lymphocyte DNA was used to generate a standard curve as described in Materials and Methods. Reactions were performed in triplicate, error bars represent ± SD. GAPDH Ct represents the cycle at which reporter fluorescence crosses a software-defined threshold (described in text). **A,** The linear range of threshold cycle vs. DNA quantity was 1pg – 10ng. Solid line, linear regression of DNA quantity vs. threshold cycle. **B,** >10ng of DNA/reaction caused a loss in the linearity and inefficiency of PCR amplification. 1µg of DNA quenched the PCR reaction and blocked amplification. The dashed line in B represents the linear regression from A.

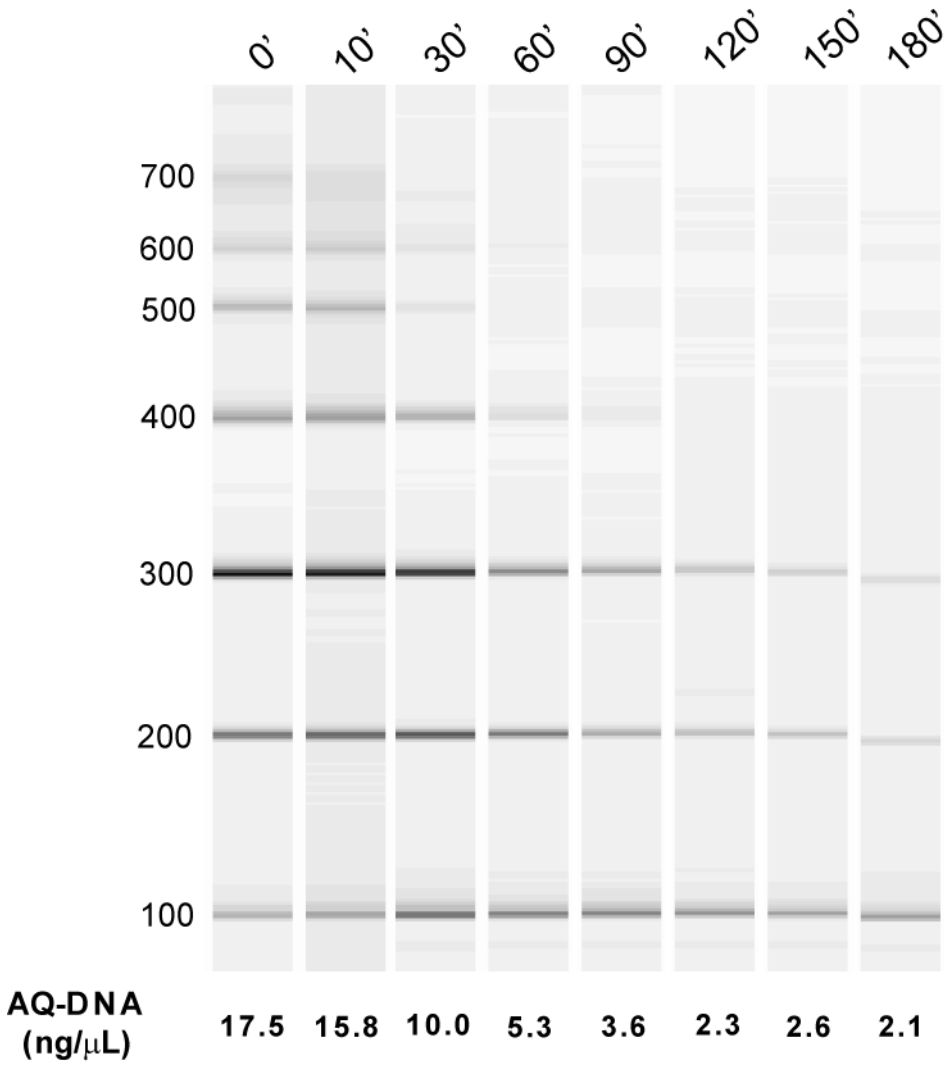

Figure 5.3. Multiplex PCR analysis and AQ-DNA quantification of high quality lymphocyte DNA subjected to enzymatic shearing. Samples were digested and processed as described in Materials and Methods. All seven amplicons are present in the non-digested control (0', lane 1), while larger amplicons are lost with increasing digestion time. Quantity of AQ-DNA also decreases with increasing digestion time.

was genotyped as a homozygous mutant with 50pg of input AQ-DNA, but a heterozygote with 100pg or more of AQ-DNA. Thus, the minimum quantity of AQ-DNA required for genotyping the CYP2D6*4 allele was set at 100pg. Additional optimization was performed using other Taqman assays. The UGT2B7 T848C (UGT2B7*2) assay required only 50pg of AQ-DNA to reliably genotype samples. Other assays, including CYP2D6 A2549del (CYP2D6*3), required 150pg or more of AQ-DNA to generate reliable genotype data (data not shown).

Importantly, optimizing Taqman reactions by minimizing the amount of input AQ-DNA improved Taqman reaction efficiency, and allowed for less ambiguous genotype determinations (Figure 5.4). To determine patient genotype, endpoint fluorescence from the Taqman-based PCR for each allele-specific probe is assigned to an axis on a scatter plot. A positive or negative signal from each probe is used to assign patient genotypes. However, the fluorescence output curves generated in real-time are representative of efficient vs. inefficient amplification, and can be used to evaluate potential false positives and negatives.

Figures 5.4A and 5.4B show representative real-time fluorescence outputs for the wild type probe of the CYP2D6 1846G>A (CYP2D6*4) Taqman assay, while Figures 5.4C and 5.4D show endpoint fluorescence as a scatter plot of wild-type probe vs. mutant probe (VIC vs. FAM fluorophores), with samples' assigned genotypes. In Figures 5.4A and 5.4C, 30 FFPE DNA samples were genotyped using only 100pg of input AQ-DNA. Efficient PCR amplification (shown by Figure 5.4A) allowed for clear threshold cut-offs, with no samples with endpoint fluorescence at or near the fluorescence threshold (Figure 5.4C), or the fluorescence value at which point an allele determination is made. Twenty nine of 30 samples genotyped by this method could be assigned a genotype, and only one sample could not be reliably genotyped (96.7% success rate). Shown in Figures 5.4B and 5.4D are an additional 30 samples genotyped for the same SNP using ~10ng of template DNA as determined by standard UV absorbance. Inefficient amplification caused clustering around the calculated threshold (Figure 5.4B, ~60 fluorescence units), making genotype determination difficult. Only 21 of 30 samples could be assigned a genotype for

	Tumor Section									
	A	B	C	D	E	F	G	H	I	J
10pg	WT	WT	WT	WT	WT	--	WT	WT	WT	--
50pg	WT	WT	WT	WT	WT	Mut	WT	WT	WT	Mut
100pg	WT	WT	WT	WT	WT	Mut	WT	WT	WT	Het
500pg	WT	WT	WT	WT	WT	Mut	WT	WT	WT	Het
1ng	WT	WT	WT	WT	WT	Mut	WT	WT	WT	Het

Table 5.2. CYP2D6*4 genotypes as determined with varying input AQ-DNA.

this SNP (70% success rate). However, as is evident in Figure 5.4C, many of these genotypes are likely un-reliable due to the lack of separation between samples deemed positive and negative for the wild-type allele (VIC fluorophore, y-axis).

Tumor Block Cores Yield Equivalent Amounts of AQ-DNA versus Sections

We next set out to determine whether tissue from tumor cores of the type generated for TMA construction, or cores from adjacent stromal tissue, could be used in pharmacogenomic analyses. To compare DNA yield from FFPE tumor block sections and core punches, we obtained 39 matched sets of sections, tumor cores, and cores of adjacent stromal tissue (described in Materials and Methods). Samples were processed and AQ-DNA was quantified as described above. As shown in Figure 5.5A, sections yielded 1.25±1.05ng/μL of AQ-DNA, and tumor cores yielded 1.20±0.91ng/μL of AQ-DNA, indicating no significant difference in AQ-DNA yield between tumor sections and cores ($p = 0.19$). These yields provide enough DNA for an average of ~1250 and ~1200 genotyping reactions, respectively, based on 100μL of eluent per sample and 100pg AQ-DNA per reaction. However, stromal cores yielded only 0.39±0.52ng/μL of AQ-DNA (~390 reactions on average), significantly less than both tumor cores and sections. Increased yield obtained from tumor sections correlated with increased yield from tumor cores (Figure 5.5B). Yield from neither sections nor tumor cores correlated with yield obtained from stroma cores (data not shown).

FFPE Tumor Block Age has Minimal Impact on AQ-DNA Yield

At the time of DNA extraction, 12 of 39 sample sets (30.8%) were from FFPE tumor blocks less than 10 years old; the remaining 27 (69.2%) were 10 years old or greater. We compared tumor block age to AQ-DNA yield for each sample type (Figure 5.6). For sections, there was a slight, but statistically significant ($p=0.0025$), decrease in AQ-DNA yield with increasing block age (Figure 5.6A; slope = -0.1ng/μL per year). The highest AQ-DNA yields from sections were obtained from blocks 4-6 years old. However, sections from blocks 14-19 years old routinely yielded AQ-DNA equivalent to blocks 6-13 years old. AQ-DNA yield from tumor cores (Figure 5.6B) and stroma cores (Figure

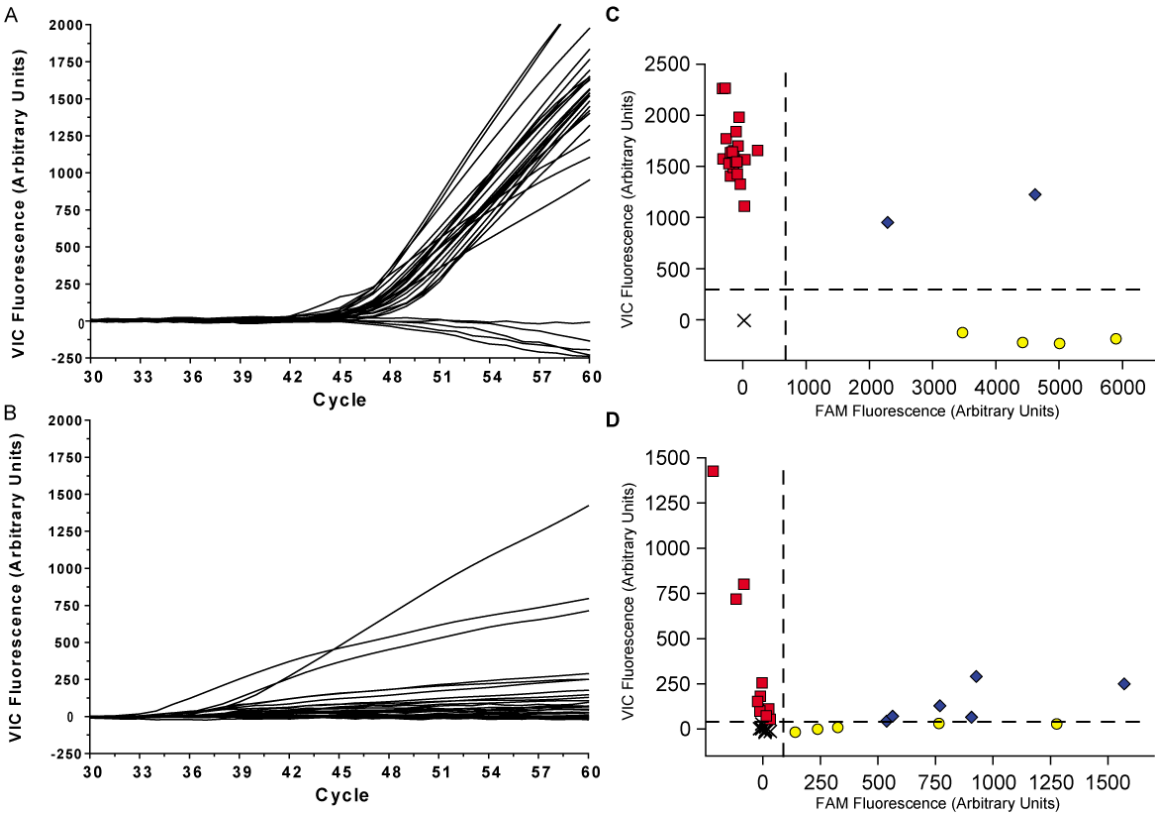

Figure 5.4. Improved genotype analysis with the CYP2D6*4 assay using AQ-DNA assessment. A,B, Real-time PCR fluorescence output curves for the wild-type allele probe of the CYP2D6*4 assay. **A,** 30 FFPE samples with reactions performed using optimal DNA quantities of AQ-DNA. Samples display efficient amplification and large separation between positive and negative results. **B,** 30 FFPE samples performed under standard conditions. Inefficient amplification results in minimal separation between positive and negative samples. **C,D,** Scatter plots of endpoint fluorescence for each allele-specific probe of the CYP2D6*4 assay. **C,** Optimized samples, and **D,** standard samples, were assigned genotypes as homozygous wild-type (red squares), heterozygous (blue diamonds), or homozygous mutant (yellow circles). Samples marked as a black 'X' could not be assigned a genotype.

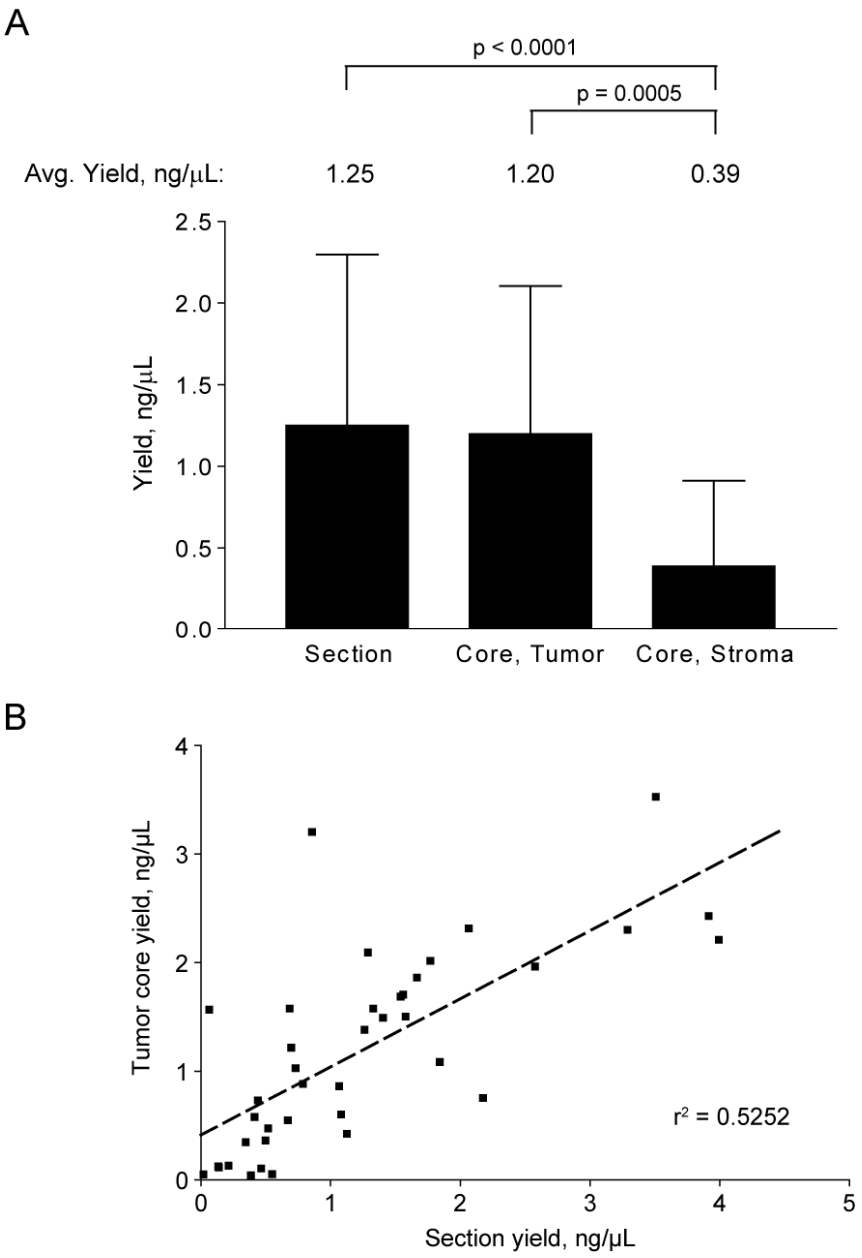

Figure 5.5. Quantification of AQ-DNA from 39 matched section, tumor core and stroma core samples. Quantification was performed by real-time PCR as described in Materials and Methods. **A,** Bars represent average sample yield (ng/μL) ± SD. P values were determined by Student's T-test. Sections and tumor cores yielded equivalent AQ-DNA on average ($p>0.05$). However, stroma cores yielded significantly less AQ-DNA than other sample types ($p < 0.0001$ and $p = 0.0005$ vs. sections and tumor cores, respectively). **B,** Scatterplot of yield from tumor cores (y-axis) vs. yield from matched sections (x-axis). The dashed line represents the linear regression between yield from sections and matched tumor cores ($p < 0.0001$).

5.6C) had slight trends toward decreased yield with block age, but neither of these trends were statistically significant ($p>0.05$).

Tumor DNA from Sections or Cores is Higher Quality than Stroma Core DNA

Six matched samples from each type were chosen at random to assess overall sample type quality by multiplex PCR as described above. On average, DNA from tumor block sections was of greater quality than that from tumor cores or stroma cores (Table 5.3). The maximum amplicon size obtained by multiplex PCR from each sample is shown in Table 5.2. Section-derived DNA had a maximum amplicon size of 400bp across all 6 samples, and an average maximum amplicon of 250bp. Tumor and stroma core-derived DNA both had maximum amplicons of 300bp, with average maximum amplicons of 200bp and 150bp respectively. Further, while all 6 sets of section and tumor core-derived DNA produced amplicons of at least 100bp, 3 of the 6 stroma core-derived DNA samples produced no amplicons. Examples of multiplex PCR results for each sample type are shown for samples B and F in Figure 5.7. In each sample, section DNA produces the greatest amplicon size, while tumor and stroma cores do not amplify the larger amplicons.

To assess the ability to determine SNP genotypes using DNA from each tumor block sample type, the matched sample sets were genotyped for the UGT2B7*2 allele (802T>C). Samples were quantified as described above before genotyping, and reactions were optimized at 50pg AQ-DNA per reaction (data not shown). Figures 5.8A, 5.8B, and 5.8C show initial real-time fluorescence outputs for the wild type probe of the UGT2B7 802T>C Taqman assay, for sections, tumor cores, and stroma cores, respectively. Thirty eight of 39 tumor section samples were successfully genotyped, with only 1 inefficient PCR amplification curve that requires re-genotyping (97.4% call rate). Thirty five of 39 tumor core samples were successfully genotyped (89.7% success rate). The endpoint fluorescence difference between samples above and below threshold fluorescence was decreased in tumor core-derived DNA versus section-derived DNA, and 4 amplification curves ended near the calculated threshold. This difference was decreased further in the stroma core-derived DNA, resulting in successful genotypes for only 30/39 samples

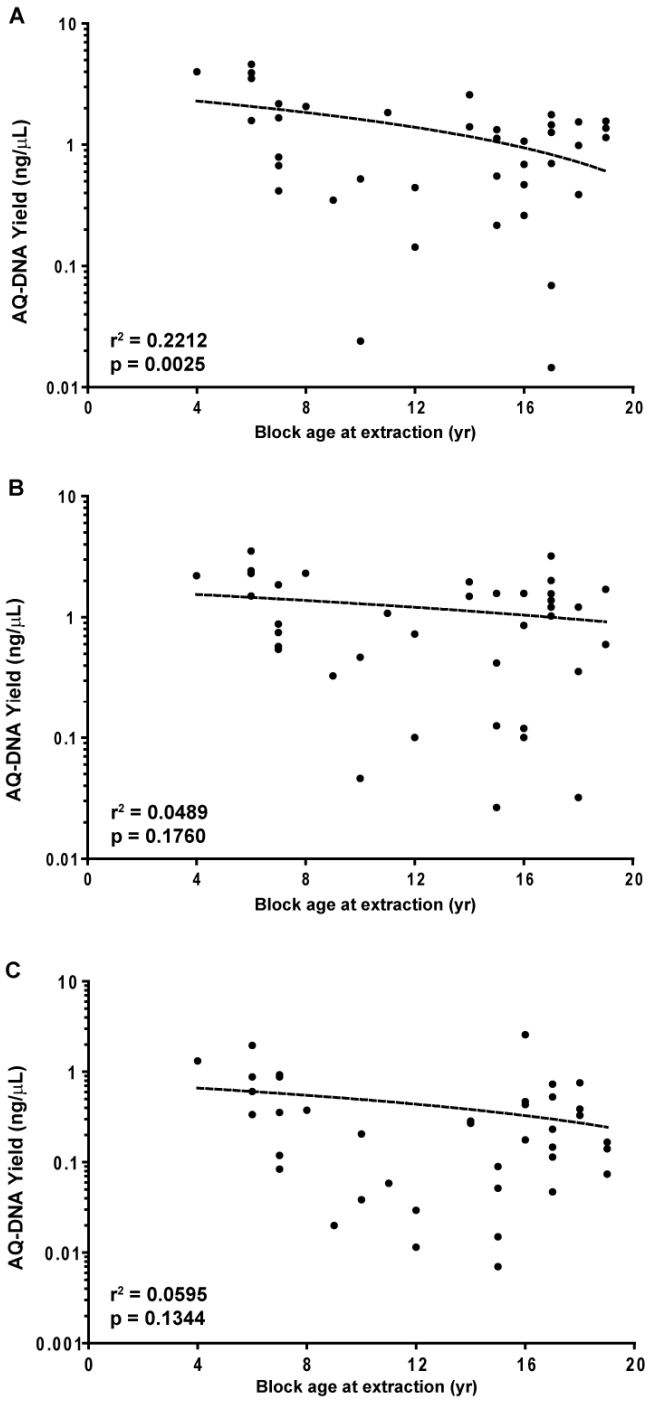

Figure 5.6. AQ-DNA yield versus FFPE tumor block age. AQ-DNA yield (ng/μL) for matched A, sections; B, tumor cores; and C, stroma cores; versus the age of the FFPE tumor block at the time of DNA extraction. AQ-DNA yield is shown on a log scale. P-value given is linear regression (dashed line) slope versus 0.

	Maximum Amplicon Size		
Sample	Section	Tumor Core	Stroma Core
A	300	300	300
B	400	300	300
C	200	200	300
D	100	100	0
E	200	100	0
F	300	200	0
Avg. Maximum Amplicon	250	200	150

Table 5.3. Maximum amplicons sizes from multiplex PCR of matched samples.

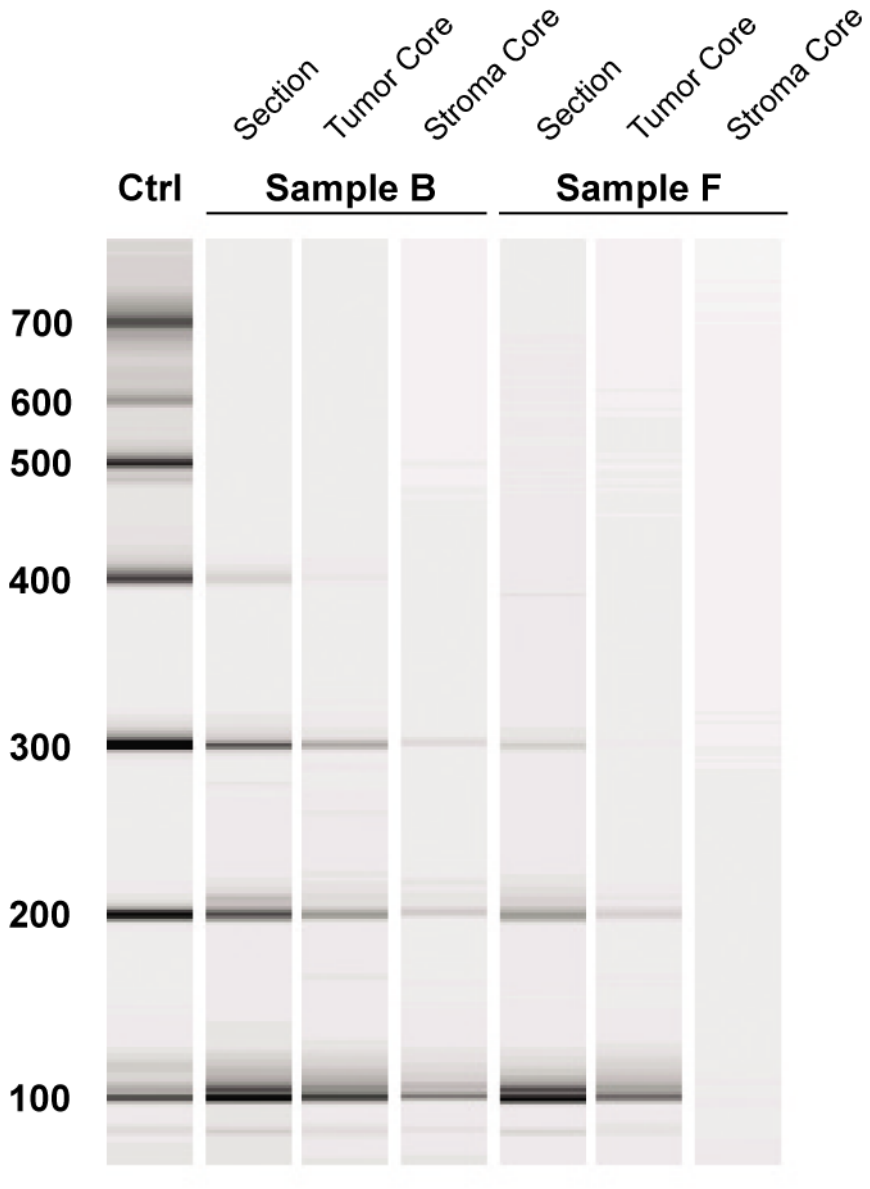

Figure 5.7. Multiplex PCR of two matched sample sets of FFPE sections, tumor cores, and stroma cores. Samples are from Table 5.3. Multiplex PCR was performed as described in Materials and Methods. All 7 amplicons were amplified in the high quality control (Ctrl, lane 1). Sections of both samples had the highest amplicon sizes, with other samples showing decreased maximum amplicon sizes.

(76.9% call rate). Samples that could not be assigned a genotype after this initial run were re-optimized and re-assessed.

Figures 5.8D, 5.8E, and 5.8F show endpoint fluorescence as a scatter plot of wild-type probe vs. mutant probe (VIC vs. FAM fluorophores), with samples' assigned genotypes, for sections, tumor cores, and stroma cores, respectively, following re-assessment. Thirty nine of 39 (100%) tumor section samples were successfully genotyped (Figure 5.8D), while 38 of 39 (97.4%) tumor cores (Figure 5.8E) and stroma cores (Figure 5.8F) were successfully genotyped. We have previously shown that genotypes from sections are 100% concordant with genotypes obtained from germ line DNA[203]. We assessed the agreement between genotypes (concordance) for the CYP2D6 gene (requiring identification of 6 SNP genotypes, listed in Materials and Methods) and the UGT2B7*2 allele (data not shown). Thirty two of 39 (82.1%) tumor core samples yielded identical CYP2D6 genotypes to section samples. However, 5 of 7 discordant genotypes were likely the results of poor AQ-DNA yields (< 0.1ng/μL) that were identified prior to genotype assessment. The two remaining samples differed in only a single SNP genotype (4180G>C; rs1135840). Only 27 of 39 stroma cores yielded identical CYP2D6 genotypes to the section samples, but half of the discordant samples (6 of 12) could be identified by low sample yield prior to genotyping. 3 of 12 differed in only a single SNP genotype. There was a higher degree of concordance between sections and the other sample types for the single SNP UGT2B7*2 allele. Thirty six of 39 (92.3%) tumor core genotypes or stroma core genotypes matched those obtained from section DNA, and 33 of 39 (84.6%) of samples had matching genotypes from all 3 sample types. The 3 tumor core samples that had discordant results versus their matched section for the UGT2B7*2 allele had the lowest AQ-DNA yields of all tumor cores (< 0.05ng/μL).

Discussion

Archival formalin-fixed, paraffin-embedded (FFPE) tumor tissue is an invaluable potential source of DNA for retrospective pharmacogenetic analyses from large clinical trials, and a number of groups have begun to use this approach for studies in breast cancer[231, 240, 241], colon cancer[230, 242], and leukemia[232]. Further, since our

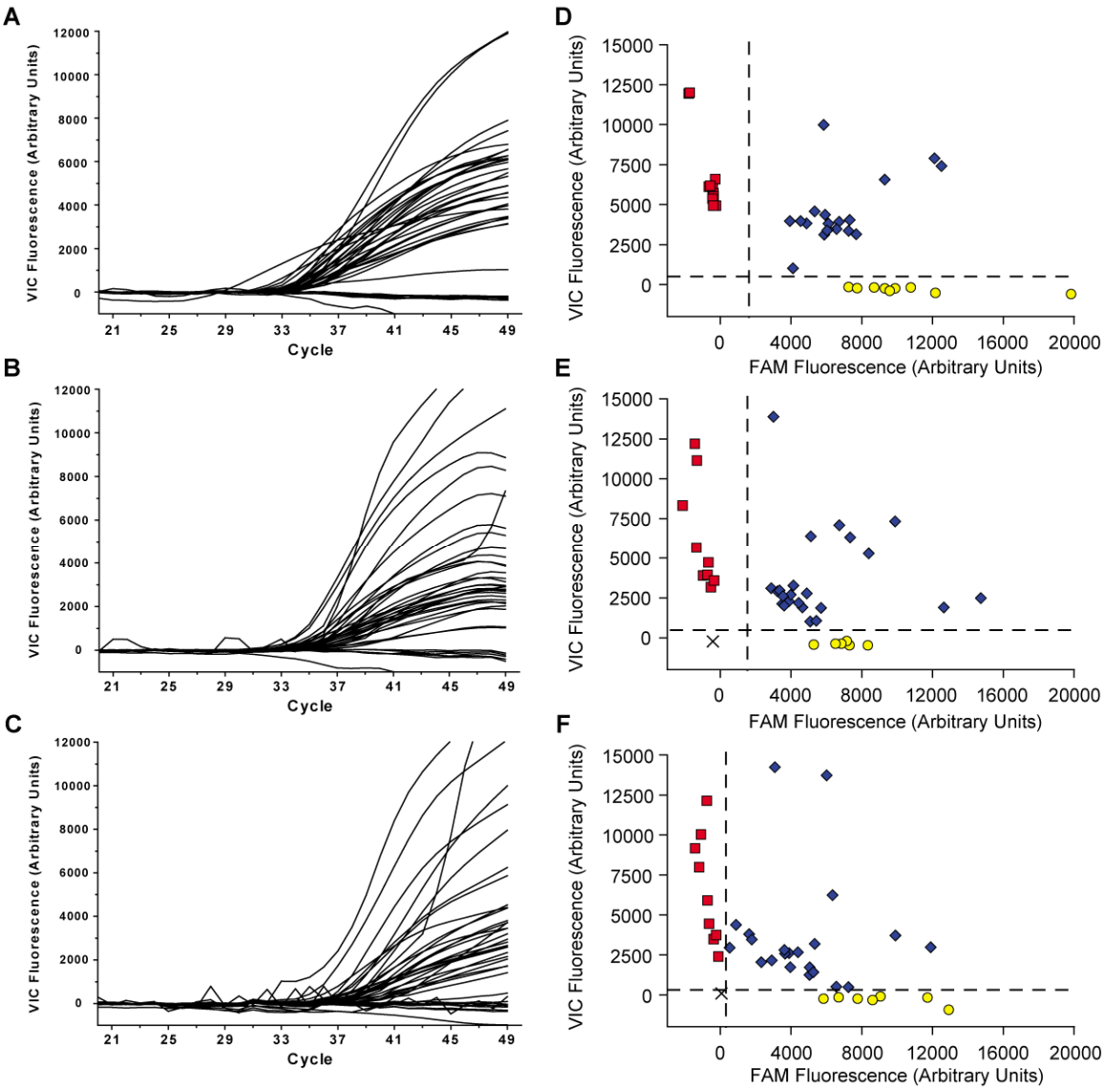

Figure 5.8. Genotype analysis between matched FFPE tumor block sample types. **A-C,** Real-time PCR fluorescence output curves of matched FFPE samples using the UGT2B7 802T>C Taqman assay (mutant allele probe shown). **A,** Section-derived DNA samples displayed efficient amplification, with clear separation between positive and negative results. **B,** Tumor core-derived DNA samples and **C,** stroma core-derived DNA samples did not all clearly pass fluorescence thresholds. **D-F,** Scatter plots of endpoint fluorescence for each allele-specific probe of the UGT2B7 802T>C assay. **D,** Section-derived, **E,** Tumor core-derived, and **F,** Stroma core derived samples were assigned genotypes as homozygous wild-type (red squares), heterozygous (blue diamonds), or homozygous mutant (yellow circles). Samples marked as a black 'X' could not be assigned a genotype.

initial report[203], advances in genotyping using Taqman-based assays and MALDI-TOF mass spectrometry[243] have been reported, and recently, high quality genomic copy number analysis using DNA from FFPE tissue[244] has been described. Despite the increasing use of FFPE samples for genotype analysis and improved methods, several key issues still significantly inhibit the wider application of this approach. The blocks from historical trials with long follow up are a finite and valuable resource and, quite appropriately, access to these materials is tightly controlled. It is very important, therefore, that sample preparation and assay methods be rigorously optimized in order to maximize the amount of information that can be obtained from the minimum amount of tissue. Access to sections of blocks from important clinical trials is being further complicated by the increasing application of tissue microarray (TMA) technology. IHC-based methods can be applied very efficiently to TMA sections providing high quality data regarding the presence of tumor antigens within all the cases of entire clinical trials with a minimum expenditure of reagents and tumor tissues. As a result, there is an increasing trend toward the preparation of TMAs from the blocks from clinical trials, with the result that access to entire sections of each block is even more limited.

In this study we, therefore, set out to achieve two goals: 1) to develop an approach to maximizing the genotyping assay yield that can be achieved from a given amount of DNA prepared from FFPE materials, and 2) to evaluate the practicality and utility of isolating DNA suitable for genotyping studies from cores of the type used to prepare TMAs. Our hope was that by demonstrating the tremendous potential value of DNA harvested from TMA cores, we would encourage investigators contemplating the production of TMAs to harvest additional tumor cores at the time of TMA manufacture for the preparation of DNA for future genetic analysis.

DNA isolated from FFPE tissues is notoriously challenging to work with due to degradation, shearing, and chemical modification which can cause significant difficulty with downstream applications [233-236]. This includes PCR-RFLP or Taqman-based assays, since both assays require minimum fragment lengths to be amplified efficiently for analysis [203, 233, 245-247]. Simple UV absorbance based assessment of DNA

quality and quantity does not adequately predict performance in PCR-based applications [248]. This is likely the result of small DNA fragments that inflate UV absorbance readings, in spite of being too small for efficient PCR. Ideally, genotyping reactions should be set up with just sufficient sample to provide enough DNA template of adequate fragment length to allow efficient amplification. This would minimize the amount of sample used and ensure optimal efficiency of the genotyping assay, thereby maximizing the number of genotyping reactions that can be conducted with a given sample. In this report we describe the strategy we have employed to optimize genotyping assays by: 1) determining the amount of "amplification quality DNA" or "AQ-DNA" in FFPE-derived samples relative to a high-quality DNA calibrator, and 2) establishing the optimum amount of AQ-DNA required for individual assays. Previous reports have proposed or described various strategies for assessing the quality of DNA extracted from FFPE materials for subsequent assay [238, 248-251]. In fact, a similar approach of quantifying amplifiable DNA was used successfully by Farrand and colleagues to identify samples amenable to loss-of-heterozygosity analyses [250]. However, this is the first time that the systematic quantification of amplification competent DNA has been applied to the optimization of Taqman-based genotyping assays.

In this report, we demonstrate that a multiplex PCR using 100-700bp amplicons from the GAPDH gene can identify FFPE tissue-derived DNA samples that are too fragmented to genotype. Since the majority of samples amenable to genotype analysis demonstrated amplification of at least the 100bp amplicon in this multiplex analysis, the 100bp amplicon was chosen as a marker of AQ-DNA. Additionally, assessing AQ-DNA based on a minimum fragment size of 100bp is in line with previous reports regarding optimal amplicon size in genotype assessment and other PCR-based analyses from archival tissue [233, 234, 243, 250, 252, 253]. We show that the amount of AQ-DNA in FFPE-derived samples, relative to a high quality DNA control, can be quantified based on real-time quantitative PCR-based amplification of this amplicon (Figure 5.2). Optimization of Taqman-based genotyping assays using this quantification showed that using minimal quantities of AQ-DNA (as little as 50pg per reaction) actually improves genotyping efficiency (Figure 5.4). Based on this optimization and quantification, sample yield

increased to an average of ~1250 assays (at 100pg/assay) from a single 10μm section (Figure 5.5). However, it is important to note that the minimal amount of AQ-DNA required for reliable genotyping varied for each individual Taqman-based assay, ranging from 50-150pg in the Taqman assays tested in this report. Importantly, as our measurements of AQ-DNA are based on the use of high-quality DNA as a calibrator, individual assessment of AQ-DNA necessary per reaction will be likely be laboratory-dependent, based on the calibrator used. However, the end results of increased efficiency and increased sample yield will still apply. Individual genotyping assays will also require specific optimization for ideal amplification of both the mutant and wild-type probe sets in each assay. Our optimization of the CYP2D6 1846G>A assay (Table 5.2) shows that while some genotypes can be assessed using as low as 10pg of input AQ-DNA, some allele-specific Taqman reagents may not amplify efficiently until more AQ-DNA is added to the reaction. This may be most important in the case of heterozygote genotypes. As seen in Table 5.2, Sample J would have been assessed as a homozygous mutant if only 50pg of DNA were used. Since only one copy of the mutant gene was present per genome, additional DNA was required to achieve optimal amplification of this gene. Taqman-based assays must be optimized to allow for the amplification of both the mutant or wild-type allele for heterozygotes, and should ideally be performed with known controls of each potential genotype.

We also evaluated the usefulness of FFPE block tumor cores and stroma cores, of the type used to generate tissue microarrays (TMAs), in performing genotype analysis. We observed that tumor tissue cores yield a comparable amount of AQ-DNA to a matched section, however, matched stroma cores yielded considerably less AQ-DNA versus both sections and tumor cores (Figure 5.5). DNA from tumor cores have slightly decreased but comparable quality versus sections as determined by multiplex PCR, however, stroma core-derived samples showed significantly decreased quality (Table 5.3, Figure 5.7). These initial observations with DNA obtained from tumor cores suggested that such samples may serve as a useful source of DNA for SNP genotype analysis. We then evaluated real-time PCR amplification efficiency and genotyping success rates for each sample type (Figure 5.8). To determine genotype accuracy, we compared genotypes

across sample types, since we and others have reported that genotypes obtained from tissue sections were 100% concordant with matched germline samples [203, 231, 232, 240, 241]. In spite of decreased success in initial genotype assessment in both tumor and stroma cores, it was possible to determine a genotype from the majority of all sample types with repeated optimization and assessment. However, in this study we did observe a decreased concordance between section and tumor core genotypes for the six CYP2D6 SNPs (82.1%) and the UGT2B7*2 allele (92.3%). It is important to note, however, that for all of the UGT2B7*2 discordances, and 5 of the 7 CYP2D6 discordances, the samples had been identified prior to genotyping as having very low AQ-DNA yields and thus unlikely amenable to genotyping. Further, the remaining two discordances in CYP2D6 genotype were due to a single SNP genotype. This SNP is used by our laboratory as a secondary confirmation of other SNP assays, and an inaccurate genotype from this SNP would not alter the predicted CYP2D6 phenotype of the patient as determined by CYP2D6 activity score (data not shown)[92, 140]. Genotype discordance is likely due to both low AQ-DNA yields and decreased DNA quality as observed in Figure 5.7 and Table 5.3. Assay optimization (input AQ-DNA per assay, cycling conditions, etc.) specifically for tumor core-derived samples is likely necessary and will potentially overcome these discordances. Further, whereas standard operating procedure for genotyping from sections has been to include repeat assays for 10-20% of samples to verify genotypes, increasing validation assays may be necessary for genotyping from tumor cores. This would likely reduce genotyping errors caused by decreased DNA quality. We have been unable to address the decrease in DNA quality, but not total AQ-DNA yield, from tumor cores versus sections. These differences potentially arise from sample processing from the original FFPE block; the shearing generated by either microtome slicing or core punching likely alters how nuclei are exposed and the efficiency of cross-linking removal. Further studies will be necessary to optimize DNA extraction specifically from tumor cores to obtain high AQ-DNA yield and high overall quality. Though tumor cores will potentially serve as a useful source of DNA with increased optimization, stroma cores appear to be unsuitable for reliable SNP genotype analysis by Taqman-based methods, due largely to poor quantity and quality DNA yielded and subsequent assay failure. The unsuitability of stroma cores as a source of

DNA may be unique to FFPE samples from breast tumors, as these cores likely contain a high proportion of adipose tissue and therefore have a relatively lower cellular density compared to the nearby tumor tissue. The usefulness of FFPE stroma cores as a source of genomic DNA for pharmacogenomic analyses will most likely need to be individually evaluated for specific tumor types.

As our AQ-DNA measurements were all performed on freshly extracted DNA, we were unable to evaluate changes in AQ-DNA values following long term storage of extracted DNA. However, we have observed that when measuring AQ-DNA from a series of FFPE tissue derived DNA that had been in storage at -20ºC for ~2 years that these samples did not appear to contain lower amounts of AQ-DNA than other freshly extracted samples (data not shown). Based on these data, and the comparison of AQ-DNA yields from FFPE blocks of varying ages (Figure 5.6), we do not anticipate that increased storage time or sample age will have a major impact on AQ-DNA yields.

These data show that through the technical advances presented, yield and genotyping efficiency of DNA from FFPE tissues can be improved. These advances should greatly increase the number of genotype analyses that can be performed using minimal amounts of valuable archival tissue from clinical trials, reducing tissue waste and increasing cost-effectiveness. Our observation that cores of tumor tissue are a potentially useful source of DNA for pharmacogenomic analyses may also make tissue procurement from clinical trials much easier. With the construction of TMAs becoming more widespread, pathologists now have the option of simply reserving an additional punch for DNA extraction. We expect that these advances will dramatically increase the usefulness of FFPE tissue for genotyping, and further provide an additional source of samples, in TMA cores. This will allow for much simpler sample procurement, and greatly reduce the amount of tissue required for any pharmacogenomic analyses.

Chapter VI.
Implications for resistance to aromatase inhibitor therapy – conclusions and future directions

Discussion

Endocrine therapies that block the action or production of estrogens are effective in blocking the growth of ER-positive breast tumors. In post-menopausal women, adjuvant aromatase inhibitors, which block the peripheral conversion of androgens to estrogens, reduce serum E2 concentrations. AIs have improved breast cancer outcomes compared to treatment with the SERM tamoxifen for post-menopausal patients [33-35]. However, recent long-term follow-up data shows that almost 20% of women treated with AIs will experience disease recurrence within 10 years of treatment initiation [83]. Currently there are no effective strategies for identifying women who will benefit from AI therapy. Minimal data exist for identifying AI-resistant tumors, mechanisms of resistance and effective treatments for recurrent tumors.

We hypothesize that in patients receiving AI therapy, androgens may be metabolized by aromatase-independent pathways. These alternative pathways of hormone metabolism produce estrogen-like compounds that may confer resistance to AIs and activate ERα in the absence of estrogen. The production of alternative estrogenic steroids may represent novel mechanisms of resistance to therapy. Understanding these pathways may provide insight into useful biomarkers and therapeutic targets. This dissertation investigated the potential role of alternative androgen metabolism in maintaining tumor growth in spite of the estrogen depletion achieved during AI therapy. The role of cytochrome P450 enzymes in these alternative pathways was also examined.

In Chapter II, we hypothesized that 3βAdiol, a downstream metabolite of the androgens TS and DHT, would act as an estrogen in breast cancer cells and induce growth in the

absence of E2. 3βAdiol represents an attractive candidate as an alternative estrogen due to its unique structure (Figure 1.1). While 3βAdiol has a fully saturated 'A' ring as opposed to the planar aromatic 'A' ring of E1 and E2, 3βAdiol has a 3β-carbon hydroxyl group, versus the 3-carbon keto group of other androgens. This 3β-carbon hydroxyl group appears to be critical for steroid binding to estrogen receptors [254]. Though significant evidence existed implicating 3βAdiol as an ERα-ligand (discussed in Chapter II), the ability of 3βAdiol to induce breast cancer cell growth had not been directly investigated. We demonstrated that 3βAdiol induces the growth of ER-positive breast cancer cells in culture, and that growth induction is independent of metabolism by aromatase. Further, growth induction is due to direct binding and activation of ERα by 3βAdiol.

These data suggest that since 3βAdiol is generated independent of aromatase, it may maintain breast tumor growth in the absence of estrogen during AI therapy. Similarly to E2, the enzymes necessary to generate 3βAdiol are expressed in breast tumors (discussed in Chapter I), thus this androgen metabolite may be generated directly at the site of action in breast tumors. Further characterization of this metabolic pathway may yield biomarkers and therapeutic targets. Serum or tumor concentrations of 3βAdiol may also prove useful in identifying patients likely to recur on AI therapy. Patients with enzyme variants limiting 3βAdiol concentrations may be predicted to be more likely to benefit from AI therapy, whereas inhibition of 3βAdiol production may represent a potential target for preventing resistance (discussed further below).

Chapter III examines the potential role of a second alternative androgen metabolism pathway in generating hormone receptor ligands. CYP2B6 is unique among CYP450 enzymes in the ability to 16-hydroxylate TS, forming 16αOH-TS and 16βOH-TS. Though early studies with placental microsomes demonstrated that 16αOH-TS can be aromatized to the estrogen E3, neither TS metabolite had been evaluated for their ability to bind ERα or AR. We demonstrated that neither metabolite was estrogenic in breast cancer cells, and did not bind to recombinant ERα. Though only 16βOH-TS could induce the growth of LNCaP prostate cancer cells, taken together with previous reports it is unlikely that either 16-hydroxytestosterone binds the wild-type AR. These data suggest

that metabolism of TS by CYP2B6 represents a mechanism to clear TS and limit the available TS for downstream generation of androgens or estrogens. This hypothesis could be best evaluated in a cell culture model that expresses CYP2B6. However, extensive efforts to express CYP450s in cell culture were unsuccessful in breast cancer cells, and only successful transiently in other cell lines. Using recombinant CYP2B6 protein, the ability of wild-type and variant CYP2B6 to 16-hydroxylate TS was evaluated; the common CYP2B6*6 and *9 variants were found to have a decreased capacity for metabolizing TS. Based on this observation, future directions for evaluating the contribution of CYP2B6-mediated TS metabolism to breast cancer etiology, leveraging retrospective analyses of clinical trials, are discussed in Chapter III.

Efforts to more accurately recapitulate the estrogen environment in patients on AI therapy in a cell culture model are detailed in Chapter IV. These studies modified complete LTED to account for estrogenic signaling that may be present during AI therapy due to generation of 3βAdiol or residual aromatization. Long-term selection in a high concentration of 3βAdiol (1n3β cells) demonstrated that breast cancer cells can grow long-term in an alternative estrogen and that the cells remained estrogen-dependent during selection. 1n3β cells also generated anti-estrogen resistance, potentially caused by adaptation to the unique structure of 3βAdiol versus E2. MCF-7 cells were also able to maintain long-term growth in low concentrations of estrogens (1pE and 50p3β cells). Unlike 50pE and 1n3β cells, 1pE and 50p3β cells also developed the ability to grow in estrogen-free conditions, as did cells maintained in complete LTED (Veh cells). However, unique mechanisms were responsible for the estrogen-independent phenotype in Veh cells versus those maintained in low estrogen concentrations. Growth assays and gene expression data suggested that estrogen-independent growth in 1pE and 50p3β cells is ER-dependent and ICI-sensitive, whereas Veh cell growth is ER-independent and ICI-insensitive. Further, following selection in low estrogen concentrations, 1pE and 50p3β cells maintained ERα activation in the absence of ligand, whereas LTED Veh cells no longer require ERα activity. ERα activation is likely maintained by ErbB receptor tyrosine kinases that signal via the MAPK or PI_3K pathways. However, a key finding of this chapter is that 1pE and 50p3β cells were only sensitive to kinase inhibitors in the

absence of ligand, when cells were grown in estrogen-free conditions. If 1pE or 50p3β cells were treated with kinase inhibitors in their selection conditions (with E2 or 3βAdiol), they were resistant to all kinase inhibitors tested.

These models suggest that the estrogen environment in which AI resistance develops changes the mechanism responsible for resistance. With even very low amounts of estrogen present, cells remained ER-dependent, though ligand-independent; in total estrogen-free conditions, cells become ER-independent. These data also suggest that after tumor progression on AIs, continued ablation of estrogen signaling may be necessary for targeted therapeutics to be effective, particularly in patients with measurable levels of circulating estrogens. Cessation of AI therapy after tumor progression, continued residual aromatization or production of 3βAdiol represent sources of estrogens that may prevent kinase inhibitors including lapatinib from blocking tumor growth. These observations lead to the hypothesis that estrogens must be maintained at low levels (or more likely further decreased) and ERα signaling must be ablated to effectively treat this subset of AI resistant tumors. Evidence supporting this hypothesis can be taken from the xenograft models developed in the Brodie laboratory. Reviewed in [111] are treatment strategies for AI resistant xenograft tumors. In one model, letrozole-resistant tumors were treated with trastuzumab with or without continued letrozole. Trastuzumab alone only delayed tumor progression ~4-6 weeks, whereas trastuzumab with continued letrozole led to prolonged blockade of tumor growth. In a model of anastrozole-resistant tumors, switching to ICI 182,780 also only delayed tumor progression (likely due in part to increased E2 concentrations and competition with the anti-estrogen), whereas the addition of ICI 182,780 to anastrozole produced prolonged blockade of tumor growth. These models demonstrate that continued aromatase inhibition was necessary for optimal response to a second-line targeted therapy. Based on this, the subset of patients represented by the above hypotheses may benefit from additional therapies targeted at reducing circulating estrogens in addition to other targeted therapies (discussed further below).

Changes in the catalytic activity of enzymes involved in steroidogenesis may have significant impact on the presence of alternative estrogens during AI therapy. In particular, 3β-HSD and CYP7B1 are responsible for the generation and elimination of 3βAdiol, respectively. Both HSD3B1 and HSD3B2 are polymorphic, and each isoform was recently demonstrated to have at least 17 and 9 unique SNPs, respectively [255]. Several of the SNPs for each isoform were demonstrated to cause a significant decrease in the amount of protein expressed from transfected COS-1 cells. If decreased expression in the cell culture model correlates with decreased enzymatic activity of 3β-HSD *in vivo*, patients with these SNPs would convert less DHT to 3βAdiol. AKR1C enzymes, which can catalyze the 3β-HSD reaction, are also polymorphic. At least 9 non-synonymous SNPs have been reported for each of AKR1C1, 1C2, 1C3 and 1C4 in NCBI dbSNP. Minimal frequency data exist for the majority of these SNPs, however, some are present at high frequency (AKR1C1 rs11474 and AKR1C4 rs111784931 have reported heterozygote rates of 35% and 50%, respectively). A number of studies have linked SNPs in AKR1C family members to changes in DHT metabolism, breast/prostate cancer risk and breast phenotypes [256-260]. Patients with SNPs decreasing overall 3β-HSD activity may produce lower levels of alternative estrogens (i.e. 3βAdiol) from androgens, and may be more likely to respond to AI therapy.

While polymorphisms in many CYP450s have been well studied (described in Chapters I and III), minimal data exist on polymorphisms in CYP7B1. Only one functional SNP has been reported in the literature to date [261], correlating a promoter SNP to increases in CYP7B1 gene expression. To address this, we resequenced the CYP7B1 gene from 48 Caucasian and 48 African-American normal controls (samples from HD50CAU and HD50AA, Coriell Institute, Camden, NJ). Resequencing revealed a total of 10 novel SNPs: 2 in the promoter region, 2 in the 5' UTR, one intronic SNP, 2 in the 3' UTR, and 3 exonic SNPs (L19P, R324H and L488L) (Appendix IV). For each cohort, these SNPs ranged in frequency from 1.0 – 52.1% with broad interethnic differences. For example, the L19P SNP was found exclusively in the African-American cohort, whereas the intron 1 SNP was 4 times as frequent in Caucasians as African-Americans. SNPs discovered from this resequencing, as well as other coding SNPs, have since been annotated in NCBI

dbSNP through the 1000Genomes project; a total of 12 coding SNPs have been cataloged. Mutations causing complete loss-of-function for CYP7B1 have been linked to several hereditary disorders [135]; however, no data exist linking SNPs in CYP7B1 to changes in enzymatic activity. Conversely to the above hypothesis regarding 3β-HSD activity, patients with CYP7B1 SNPs correlating with decreased activity would clear less 3βAdiol, and thus these SNPs would be potential markers for AI resistance.

As discussed in Chapters III and V, retrospective analysis of clinical trials with long-term follow-up may provide a wealth of insight into the effects of SNPs in steroidogenic enzymes on breast cancer etiology. Until recently, most large clinical trials did not collect patients' blood samples for future pharmacogenomic analyses, making high quality DNA samples from these trials rare. However, many trials created banks of formalin-fixed paraffin-embedded (FFPE) tumor tissue, which we previously demonstrated to be a useful source of DNA for genotyping SNPs [203]. Chapter V outlines technical advances in DNA extraction and genotype assessment from FFPE tumor tissues [204]. DNA isolated from FFPE tissues is challenging to work with due to degradation which causes difficulty with downstream applications, in particular PCR-based analyses. The advances described are based on the quantification of DNA that is of sufficient quality for PCR, or AQ-DNA. By quantifying AQ-DNA, yield and genotyping efficiency of DNA from FFPE tissues are improved. These advances will increase the usefulness of FFPE tissue for genotyping. The first report of the value of DNA extracted from cores, of the type used to construct TMAs, for genotype analyses is also described. This additional source of DNA, coupled with the improved methods described, will make large-scale pharmacogenomic analyses of clinical trials using FFPE tissues more feasible. The roles of steroidogenic enzymes in breast cancer etiology can be directly assessed through associations between SNPs and patient outcomes.

The data presented in this dissertation suggest that in a subset of patients, aromatase inhibitors may not be sufficient to inhibit the production of estrogenic steroids that can promote tumor growth. Additional therapeutic approaches may be required to prevent alternative androgen metabolism or residual aromatization from producing estrogens that

can confer resistance to AI therapy. Therapeutics targeting additional points along the steroid hormone biosynthesis pathway (Figure 1.1) are currently in clinical trials or are in development. As discussed in Chapter I, STS inhibitors are hypothesized to prevent circulating steroid-sulfate conjugates (DHEA-S and E1-S) from being hydrolyzed into active steroids. A number of STS inhibitors, including those with anti-estrogen or anti-aromatase activity, have been developed in pre-clinical models [73]. However, only STX 64 (BN83495) has been entered into Phase I trials. 14 patients with metastatic, ER-positive breast cancer were treated with STX 64 and a 99% inhibition of STS activity in breast tumor tissue was achieved within 5 days. STX 64 decreased serum E2 concentrations by ~45%. Four patients who had advanced on previous AI therapy achieved stable disease for 3-7 months [76]. Several additional Phase I and II trials using STX 64 have finished accrual or continue accrual, including a Phase II neoadjuvant trial using STX 64 as front-line therapy prior to surgery (NCT01230970). Combinations of STS inhibitors and AIs have not been tested to date, but dual STS/aromatase inhibitors have been tested in pre-clinical models [73]; dual blockade of steroidogenesis may prove a successful strategy for preventing estrogen synthesis. 3β-HSD inhibitors, in particular trilostane, were tested in the early 1990s in metastatic breast cancer patients with some efficacy in producing clinical benefit [262, 263]. However, non-selective inhibition of 3β-HSD isoforms causes significant toxicity due to inhibition of mineralocorticoid and glucocorticoid synthesis (see Figure 1.1). Specific inhibition of the non-adrenal isoform, HSD3B1, may effectively block the synthesis of A and 3βAdiol in tumor tissue while minimizing other toxicity. It is unclear whether current inhibitors also target AKR1C enzymes, or whether these enzymes can act in a compensatory manner during HSD3B inhibition.

Recent work in prostate cancer has hypothesized that targeting enzymes further upstream can ablate the synthesis of all sex steroid hormones. This resulted in the development of inhibitors of CYP17A1. CYP17A1 is the only enzyme capable of converting pregnenolone to DHEA and therefore CYP17A1 inhibition would block the synthesis of all downstream androgens and estrogens, including E2 and 3βAdiol (see Figure 1.1). The CYP17A1 inhibitor abiraterone acetate was initially developed to treat castrate-resistant

prostate cancer [197], with promising Phase I/II trial results [192-195]. The accrual of Phase III trials in prostate cancer is currently ongoing. Evaluation of abiraterone acetate is currently underway in advanced and metastatic breast cancer by Cancer Research UK (NCT00755885), with accrual expected to be completed by the time of publication of this dissertation. The relative success of this agent in treating advanced, AI-resistant breast cancer will provide significant insight into the role of alternative androgen metabolism in breast cancer.

Inhibition of the generation of DHEA from pregnenolone should effectively prevent the generation of alternative androgen metabolites, and circumvent this AI resistance pathway. However, in the advanced or recurrent setting, the cell culture models described in Chapter IV suggest that tumors that progress in the presence of low estrogen concentrations (on AI therapy) may be resistant to complete estrogen deprivation. Tumors similar to 1pE and 50p3β cells would be predicted to be resistant to second-line abiraterone acetate, due to their ligand-independent activation of ERα. Treatment of these tumors with abiraterone acetate would likely render the cells sensitive to inhibition of kinase pathways using agents including lapatinib. Identification of these tumors may be critical to the clinical success of steroidogenesis inhibitors including abiraterone acetate. The advances developed in this dissertation may ultimately be useful in identifying and understanding biomarkers for this resistance pathway, such as phosphorylation of ERα (S167). These biomarkers could be used to identify patients that will resist abiraterone acetate monotherapy, but will respond to dual treatment with steroidogenesis- and growth factor receptor-inhibition. Identification of the complete pathways responsible for ligand-independent ERα activity will provide useful targets for therapy in conjunction with estrogen depletion. A significant proportion of tumors may also mimic LTED Veh cells; the same biomarkers that establish sensitivity to further estrogen depletion could identify those that are both estrogen- and ER-independent. These tumors are very unlikely to respond to further steroid hormone depletion, and patients could instead be treated with other targeted therapies.

The studies detailed above provide a basis for further clinical investigation into the tumor estrogen environment. A better understanding of the tumor estrogen environment *in vivo*, including primary and alternative estrogens, is necessary to correctly evaluate the mechanisms conferring resistance to AI therapy. The production of alternative estrogens such as 3βAdiol represents a potential mechanism of AI resistance that can be targeted with novel therapeutic strategies. The advances made in this dissertation strongly suggest that the presence of low estrogen concentrations promotes unique mechanisms of resistance versus complete estrogen deprivation. Further, low estrogen concentrations may confer resistance to targeted therapies. Correctly identifying mechanisms of resistance, based in part on biomarkers that can be developed using the models described herein, will allow patients to be treated using therapies specifically targeted to their tumor, sparing ineffective therapies and improving clinical outcomes.

Appendices

Appendix I. Concentration-effect curves for MCF-7 cell growth induced by steroid hormones.

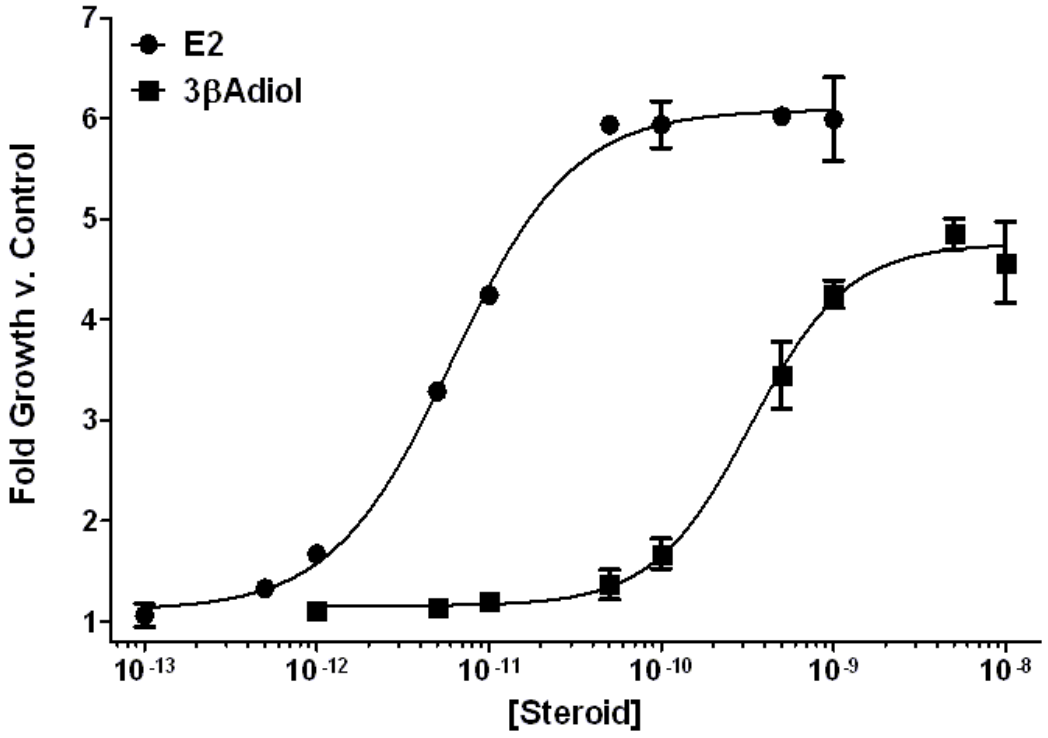

Appendix I. MCF-7 cells in estrogen-free conditions were treated with steroid hormone as indicated. Cell growth was measured 5 days after treatment using crystal violet as described in Chapter II.

Appendix II. Antibodies used in Chapter IV.

Target	Isotype	Cell Signal Catalog #
MAPK (Erk1/2)	Rabbit	4695
p-MAPK	Rabbit	4370
ERα	Mouse	2512
p-ERα (S118)	Mouse	2511
p-ERα (S167)	Rabbit	5587
ErbB2 (HER2)	Rabbit	4290
Akt	Rabbit	4691
p-Akt (T308)	Rabbit	2965
p-Akt (S473)	Rabbit	4060
β -Actin	HRP-conj.	5125
anti-Mouse 2'	N/A	7076
anti-Rabbit 2'	N/A	7074

Appendix III. Limited subset of GSEA C2 CGP.

PARENT_MTOR_SIGNALING_UP
PARENT_MTOR_SIGNALING_DN
BERTUCCI_MEDULLARY_VS_DUCTAL_BREAST_CANCER_UP
BERTUCCI_MEDULLARY_VS_DUCTAL_BREAST_CANCER_DN
SCHUETZ_BREAST_CANCER_DUCTAL_INVASIVE_UP
SCHUETZ_BREAST_CANCER_DUCTAL_INVASIVE_DN
FOURNIER_ACINAR_DEVELOPMENT_EARLY_UP
FOURNIER_ACINAR_DEVELOPMENT_EARLY_DN
FOURNIER_ACINAR_DEVELOPMENT_LATE_UP
FOURNIER_ACINAR_DEVELOPMENT_LATE_DN
FRASOR_TAMOXIFEN_RESPONSE_UP
FRASOR_TAMOXIFEN_RESPONSE_DN
KOBAYASHI_EGFR_SIGNALING_6HR_UP
KOBAYASHI_EGFR_SIGNALING_6HR_DN
SOTIRIOU_BREAST_CANCER_GRADE_1_VS_3_UP
SOTIRIOU_BREAST_CANCER_GRADE_1_VS_3_DN
TURASHVILI_BREAST_NORMAL_DUCTAL_VS_LOBULAR_UP
TURASHVILI_BREAST_NORMAL_DUCTAL_VS_LOBULAR_DN
TURASHVILI_BREAST_DUCTAL_CARCINOMA_VS_DUCTAL_NORMAL_UP
TURASHVILI_BREAST_DUCTAL_CARCINOMA_VS_DUCTAL_NORMAL_DN
TURASHVILI_BREAST_DUCTAL_CARCINOMA_VS_LOBULAR_NORMAL_UP
TURASHVILI_BREAST_DUCTAL_CARCINOMA_VS_LOBULAR_NORMAL_DN
TURASHVILI_BREAST_CARCINOMA_DUCTAL_VS_LOBULAR_UP
TURASHVILI_BREAST_CARCINOMA_DUCTAL_VS_LOBULAR_DN
TURASHVILI_BREAST_LOBULAR_CARCINOMA_VS_DUCTAL_NORMAL_UP
TURASHVILI_BREAST_LOBULAR_CARCINOMA_VS_DUCTAL_NORMAL_DN
TURASHVILI_BREAST_LOBULAR_CARCINOMA_VS_LOBULAR_NORMAL_UP
TURASHVILI_BREAST_LOBULAR_CARCINOMA_VS_LOBULAR_NORMAL_DN
CHANDRAN_METASTASIS_TOP50_UP
CHANDRAN_METASTASIS_TOP50_DN
LIU_CMYB_TARGETS_UP
LIU_CMYB_TARGETS_DN
LIU_VMYB_TARGETS_UP
LIU_TARGETS_OF_VMYB_VS_CMYB_UP
LIU_TARGETS_OF_VMYB_VS_CMYB_DN
CHARAFE_BREAST_CANCER_LUMINAL_VS_BASAL_UP
CHARAFE_BREAST_CANCER_LUMINAL_VS_BASAL_DN
CHARAFE_BREAST_CANCER_LUMINAL_VS_MESENCHYMAL_UP
CHARAFE_BREAST_CANCER_LUMINAL_VS_MESENCHYMAL_DN
CHARAFE_BREAST_CANCER_BASAL_VS_MESENCHYMAL_UP
CHARAFE_BREAST_CANCER_BASAL_VS_MESENCHYMAL_DN
DOANE_BREAST_CANCER_CLASSES_UP
DOANE_BREAST_CANCER_CLASSES_DN
DOANE_RESPONSE_TO_ANDROGEN_UP
DOANE_RESPONSE_TO_ANDROGEN_DN
DOANE_BREAST_CANCER_ESR1_UP
DOANE_BREAST_CANCER_ESR1_DN
WANG_RESPONSE_TO_ANDROGEN_UP
GINESTIER_BREAST_CANCER_ZNF217_AMPLIFIED_UP
GINESTIER_BREAST_CANCER_ZNF217_AMPLIFIED_DN
GINESTIER_BREAST_CANCER_20Q13_AMPLIFICATION_UP
GINESTIER_BREAST_CANCER_20Q13_AMPLIFICATION_DN
ODONNELL_TARGETS_OF_MYC_AND_TFRC_UP
ODONNELL_TARGETS_OF_MYC_AND_TFRC_DN
NAGASHIMA_EGF_SIGNALING_UP
ELVIDGE_HIF1A_TARGETS_UP
ELVIDGE_HIF1A_TARGETS_DN
ELVIDGE_HIF2A_TARGETS_UP
ELVIDGE_HIF1A_AND_HIF2A_TARGETS_UP
ELVIDGE_HIF1A_AND_HIF2A_TARGETS_DN
GOZGIT_ESR1_TARGETS_UP
GOZGIT_ESR1_TARGETS_DN
PACHER_TARGETS_OF_IGF1_AND_IGF2_UP
LANDIS_BREAST_CANCER_PROGRESSION_UP
LANDIS_BREAST_CANCER_PROGRESSION_DN
CREIGHTON_AKT1_SIGNALING_VIA_MTOR_UP
CREIGHTON_AKT1_SIGNALING_VIA_MTOR_DN
NADERI_BREAST_CANCER_PROGNOSIS_UP
NADERI_BREAST_CANCER_PROGNOSIS_DN
CHIN_BREAST_CANCER_COPY_NUMBER_UP
CHIN_BREAST_CANCER_COPY_NUMBER_DN
LANDIS_ERBB2_BREAST_TUMORS_65_UP
LANDIS_ERBB2_BREAST_TUMORS_65_DN
LANDIS_ERBB2_BREAST_PRENEOPLASTIC_UP
LANDIS_ERBB2_BREAST_PRENEOPLASTIC_DN
LANDIS_ERBB2_BREAST_TUMORS_324_UP
LANDIS_ERBB2_BREAST_TUMORS_324_DN
ROYLANCE_BREAST_CANCER_16Q_COPY_NUMBER_UP
ROYLANCE_BREAST_CANCER_16Q_COPY_NUMBER_DN
VETTER_TARGETS_OF_PRKCA_AND_ETS1_UP
VETTER_TARGETS_OF_PRKCA_AND_ETS1_DN
MARKS_HDAC_TARGETS_UP
MARKS_HDAC_TARGETS_DN
TAKAYAMA_BOUND_BY_AR
TURJANSKI_MAPK1_AND_MAPK2_TARGETS
TURJANSKI_MAPK8_AND_MAPK9_TARGETS
TURJANSKI_MAPK7_TARGETS

TURJANSKI_MAPK11_TARGETS
TURJANSKI_MAPK14_TARGETS
MARTIN_INTERACT_WITH_HDAC
FARMER_BREAST_CANCER_APOCRINE VS LUMINAL
FARMER_BREAST_CANCER_APOCRINE_VS_BASAL
FARMER_BREAST_CANCER_BASAL_VS_LULMINAL
FARMER_BREAST_CANCER_CLUSTER_1
FARMER_BREAST_CANCER_CLUSTER_8
FARMER_BREAST_CANCER_CLUSTER_7
FARMER_BREAST_CANCER_CLUSTER_6
FARMER_BREAST_CANCER_CLUSTER_5
FARMER_BREAST_CANCER_CLUSTER_4
FARMER_BREAST_CANCER_CLUSTER_2
HONRADO_BREAST_CANCER_BRCA1_VS_BRCA2
BOWIE_RESPONSE_TO_EXTRACELLULAR_MATRIX
BOWIE_RESPONSE_TO_TAMOXIFEN
WANG_METHYLATED_IN_BREAST_CANCER
JAZAG_TGFB1_SIGNALING_UP
JAZAG_TGFB1_SIGNALING_DN
JAZAG_TGFB1_SIGNALING_VIA_SMAD4_UP
JAZAG_TGFB1_SIGNALING_VIA_SMAD4_DN
FARMER_BREAST_CANCER_CLUSTER_3
YANG_BREAST_CANCER_ESR1_UP
YANG_BREAST_CANCER_ESR1_DN
YANG_BREAST_CANCER_ESR1_LASER_UP
YANG_BREAST_CANCER_ESR1_LASER_DN
YANG_BREAST_CANCER_ESR1_BULK_UP
YANG_BREAST_CANCER_ESR1_BULK_DN
PUJANA_BREAST_CANCER_LIT_INT_NETWORK
WILLIAMS_ESR1_TARGETS_UP
WILLIAMS_ESR1_TARGETS_DN
WILLIAMS_ESR2_TARGETS_UP
WILLIAMS_ESR2_TARGETS_DN
NUYTTEN_EZH2_TARGETS_UP
NUYTTEN_EZH2_TARGETS_DN
LIU_BREAST_CANCER
AMIT_EGF_RESPONSE_20_HELA
AMIT_EGF_RESPONSE_40_HELA
AMIT_EGF_RESPONSE_60_HELA
AMIT_EGF_RESPONSE_120_HELA
AMIT_EGF_RESPONSE_240_HELA
AMIT_EGF_RESPONSE_480_HELA
AMIT_EGF_RESPONSE_20_MCF10A
AMIT_EGF_RESPONSE_40_MCF10A
AMIT_EGF_RESPONSE_60_MCF10A
AMIT_EGF_RESPONSE_120_MCF10A
AMIT_EGF_RESPONSE_240_MCF10A
AMIT_EGF_RESPONSE_480_MCF10A
NIKOLSKY_BREAST_CANCER_1Q21_AMPLICON
NIKOLSKY_BREAST_CANCER_1Q32_AMPLICON
NIKOLSKY_BREAST_CANCER_5P15_AMPLICON
NIKOLSKY_BREAST_CANCER_6P24_P22_AMPLICON
NIKOLSKY_BREAST_CANCER_7P22_AMPLICON
NIKOLSKY_BREAST_CANCER_7P15_AMPLICON
NIKOLSKY_BREAST_CANCER_7Q21_Q22_AMPLICON
NIKOLSKY_BREAST_CANCER_8P12_P11_AMPLICON
NIKOLSKY_BREAST_CANCER_8Q12_Q22_AMPLICON
NIKOLSKY_BREAST_CANCER_8Q23_Q24_AMPLICON
NIKOLSKY_BREAST_CANCER_10Q22_AMPLICON
NIKOLSKY_BREAST_CANCER_11Q12_Q14_AMPLICON
NIKOLSKY_BREAST_CANCER_12Q13_Q21_AMPLICON
NIKOLSKY_BREAST_CANCER_12Q24_AMPLICON
NIKOLSKY_BREAST_CANCER_14Q22_AMPLICON
NIKOLSKY_BREAST_CANCER_15Q26_AMPLICON
NIKOLSKY_BREAST_CANCER_16P13_AMPLICON
NIKOLSKY_BREAST_CANCER_16Q24_AMPLICON
NIKOLSKY_BREAST_CANCER_17P11_AMPLICON
NIKOLSKY_BREAST_CANCER_17Q11_Q21_AMPLICON
NIKOLSKY_BREAST_CANCER_17Q21_Q25_AMPLICON
NIKOLSKY_BREAST_CANCER_19P13_AMPLICON
NIKOLSKY_BREAST_CANCER_19Q13.1_AMPLICON
NIKOLSKY_BREAST_CANCER_19Q13.4_AMPLICON
NIKOLSKY_BREAST_CANCER_20P13_AMPLICON
NIKOLSKY_BREAST_CANCER_20Q11_AMPLICON
NIKOLSKY_BREAST_CANCER_20Q12_Q13_AMPLICON
NIKOLSKY_BREAST_CANCER_21Q22_AMPLICON
NIKOLSKY_BREAST_CANCER_22Q13_AMPLICON
NIKOLSKY_MUTATED_AND_AMPLIFIED_IN_BREAST_CANCER
MENSSEN_MYC_TARGETS
FRASOR_RESPONSE_TO_ESTRADIOL_UP
WILLERT_WNT_SIGNALING
BECKER_TAMOXIFEN_RESISTANCE_UP
NELSON_RESPONSE_TO_ANDROGEN_UP
VANTVEER_BREAST_CANCER_METASTASIS_DN
VANTVEER_BREAST_CANCER_METASTASIS_UP
COLLER_MYC_TARGETS_UP
BECKER_TAMOXIFEN_RESISTANCE_DN
COLLER_MYC_TARGETS_DN
PENG_RAPAMYCIN_RESPONSE_UP
STOSSI_RESPONSE_TO_ESTRADIOL
LEI_MYB_TARGETS
BILD_MYC_ONCOGENIC_SIGNATURE
BILD_E2F3_ONCOGENIC_SIGNATURE
BILD_HRAS_ONCOGENIC_SIGNATURE
BILD_SRC_ONCOGENIC_SIGNATURE
CREIGHTON_ENDOCRINE_THERAPY_RESISTANCE_1
CREIGHTON_ENDOCRINE_THERAPY_RESISTANCE_2
CREIGHTON_ENDOCRINE_THERAPY_RESISTANCE_3
CREIGHTON_ENDOCRINE_THERAPY_RESISTANCE_4
CREIGHTON_ENDOCRINE_THERAPY_RESISTANCE_5
RIGGINS_TAMOXIFEN_RESISTANCE_UP

RIGGINS_TAMOXIFEN_RESISTANCE_DN
STEIN_ESRRA_TARGETS_RESPONSIVE_TO_ESTROGEN_UP
STEIN_ESRRA_TARGETS_RESPONSIVE_TO_ESTROGEN_DN
STEIN_ESRRA_TARGETS_UP
STEIN_ESRRA_TARGETS_DN
KONDO_EZH2_TARGETS
HELLER_HDAC_TARGETS_UP
HELLER_HDAC_TARGETS_DN
HELLER_HDAC_TARGETS_SILENCED_BY_METHYLATION_UP
HELLER_HDAC_TARGETS_SILENCED_BY_METHYLATION_DN
FINETTI_BREAST_CANCER_KINOME_RED
FINETTI_BREAST_CANCER_KINOME_GREEN
FINETTI_BREAST_CANCERS_KINOME_BLUE
FINETTI_BREAST_CANCERS_KINOME_GRAY
FINETTI_BREAST_CANCER_BASAL_VS_LUMINAL
MASSARWEH_TAMOXIFEN_RESISTANCE_UP
MASSARWEH_TAMOXIFEN_RESISTANCE_DN
MASSARWEH_RESPONSE_TO_ESTRADIOL
CHENG_IMPRINTED_BY_ESTRADIOL
MCCABE_HOXC6_TARGETS_CANCER_UP
MCCABE_HOXC6_TARGETS_CANCER_DN
SMID_BREAST_CANCER_RELAPSE_IN_BRAIN_UP
SMID_BREAST_CANCER_RELAPSE_IN_BRAIN_DN
SMID_BREAST_CANCER_RELAPSE_IN_BONE_UP
SMID_BREAST_CANCER_RELAPSE_IN_BONE_DN
SMID_BREAST_CANCER_RELAPSE_IN_LUNG_UP
SMID_BREAST_CANCER_RELAPSE_IN_LUNG_DN
SMID_BREAST_CANCER_RELAPSE_IN_LIVER_UP
SMID_BREAST_CANCER_RELAPSE_IN_LIVER_DN
SMID_BREAST_CANCER_RELAPSE_IN_PLEURA_UP
SMID_BREAST_CANCER_RELAPSE_IN_PLEURA_DN
SMID_BREAST_CANCER_LUMINAL_B_UP
SMID_BREAST_CANCER_LUMINAL_B_DN
SMID_BREAST_CANCER_LUMINAL_A_UP
SMID_BREAST_CANCER_LUMINAL_A_DN
SMID_BREAST_CANCER_ERBB2_UP
SMID_BREAST_CANCER_ERBB2_DN
SMID_BREAST_CANCER_NORMAL_LIKE_UP
SMID_BREAST_CANCER_NORMAL_LIKE_DN
SMID_BREAST_CANCER_BASAL_UP
SMID_BREAST_CANCER_BASAL_DN
CLIMENT_BREAST_CANCER_COPY_NUMBER_UP
CLIMENT_BREAST_CANCER_COPY_NUMBER_DN
HUPER_BREAST_BASAL_VS_LUMINAL_UP
HUPER_BREAST_BASAL_VS_LUMINAL_DN
FRASOR_RESPONSE_TO_SERM_OR_FULVESTRANT_UP
FRASOR_RESPONSE_TO_SERM_OR_FULVESTRANT_DN
VANTVEER_BREAST_CANCER_ESR1_UP
VANTVEER_BREAST_CANCER_ESR1_DN
VANTVEER_BREAST_CANCER_BRCA1_UP
VANTVEER_BREAST_CANCER_BRCA1_DN
FINAK_BREAST_CANCER_SDPP_SIGNATURE
POOLA_INVASIVE_BREAST_CANCER_UP
POOLA_INVASIVE_BREAST_CANCER_DN
PUJANA_BREAST_CANCER_WITH_BRCA1_MUTATED_UP
PUJANA_BREAST_CANCER_WITH_BRCA1_MUTATED_DN
SYED_ESTRADIOL_RESPONSE
STEIN_ESR1_TARGETS
STEIN_ESRRA_TARGETS
STEIN_ESTROGEN_RESPONSE_NOT_VIA_ESRRA
KOBAYASHI_EGFR_SIGNALING_24HR_UP
KOBAYASHI_EGFR_SIGNALING_24HR_DN
VANTVEER_BREAST_CANCER_POOR_PROGNOSIS
DANG_REGULATED_BY_MYC_UP
DANG_REGULATED_BY_MYC_DN
DANG_MYC_TARGETS_UP
DANG_MYC_TARGETS_DN
DANG_BOUND_BY_MYC
HEDENFALK_BREAST_CANCER_BRACX_DN
HEDENFALK_BREAST_CANCER_BRACX_UP
JAZAERI_BREAST_CANCER_BRCA1_VS_BRCA2_DN
JAZAERI_BREAST_CANCER_BRCA1_VS_BRCA2_UP
HEDENFALK_BREAST_CANCER_HEREDITARY_VS_SPORADIC
HEDENFALK_BREAST_CANCER_BRCA1_VS_BRCA2
XU_GH1_AUTOCRINE_TARGETS_DN
XU_GH1_AUTOCRINE_TARGETS_UP
XU_GH1_EXOGENOUS_TARGETS_DN
XU_GH1_EXOGENOUS_TARGETS_UP
KEGG_STEROID_BIOSYNTHESIS
KEGG_STEROID_HORMONE_BIOSYNTHESIS
KEGG_MAPK_SIGNALING_PATHWAY
KEGG_ERBB_SIGNALING_PATHWAY
KEGG_PHOSPHATIDYLINOSITOL_SIGNALING_SYSTEM
KEGG_MTOR_SIGNALING_PATHWAY
KEGG_WNT_SIGNALING_PATHWAY
KEGG_TGF_BETA_SIGNALING_PATHWAY
KEGG_VEGF_SIGNALING_PATHWAY
KEGG_JAK_STAT_SIGNALING_PATHWAY
KEGG_PATHWAYS_IN_CANCER
BIOCARTA_CXCR4_PATHWAY
BIOCARTA_EGF_PATHWAY
BIOCARTA_EPHA4_PATHWAY
BIOCARTA_ERK_PATHWAY
BIOCARTA_FAS_PATHWAY
BIOCARTA_GH_PATHWAY
BIOCARTA_HIF_PATHWAY
BIOCARTA_IGF1_PATHWAY
BIOCARTA_RACCYCD_PATHWAY
BIOCARTA_INSULIN_PATHWAY
BIOCARTA_NFKB_PATHWAY
BIOCARTA_P38MAPK_PATHWAY
BIOCARTA_PDGF_PATHWAY
BIOCARTA_PTDINS_PATHWAY
BIOCARTA_PLCE_PATHWAY
BIOCARTA_MYOSIN_PATHWAY
BIOCARTA_RAS_PATHWAY

BIOCARTA_CARDIACEGF_PATHWAY
BIOCARTA_HER2_PATHWAY
BIOCARTA_SHH_PATHWAY
BIOCARTA_PTC1_PATHWAY
BIOCARTA_TGFB_PATHWAY
BIOCARTA_LONGEVITY_PATHWAY
BIOCARTA_WNT_PATHWAY
REACTOME_CYTOCHROME_P450_ARRANGED_BY_SUBSTRATE_TYPE
REACTOME_ERK_MAPK_TARGETS
REACTOME_HORMONE_BIOSYNTHESIS
REACTOME_HORMONE_LIGAND_BINDING_RECEPTORS
REACTOME_INSULIN_SYNTHESIS_AND_SECRETION
REACTOME_IRS_RELATED_EVENTS
REACTOME_MTOR_SIGNALLING
REACTOME_MTORC1_MEDIATED_SIGNALLING
REACTOME_PI3K_AKT_SIGNALLING
REACTOME_PLC_BETA_MEDIATED_EVENTS
REACTOME_PLC_GAMMA1_SIGNALLING
REACTOME_SHC_MEDIATED_SIGNALLING
REACTOME_SHC_RELATED_EVENTS
REACTOME_SIGNALING_BY_EGFR
REACTOME_SIGNALING_BY_PDGF
REACTOME_SIGNALING_BY_TGF_BETA
REACTOME_SIGNALING_BY_VEGF
REACTOME_SIGNALING_BY_WNT
REACTOME_SIGNALLING_TO_ERKS
REACTOME_SIGNALLING_TO_RAS
REACTOME_STEROID_HORMONE_BIOSYNTHESIS
REACTOME_STEROID_HORMONES
REACTOME_STEROID_METABOLISM
REACTOME_PI3K_CASCADE
REACTOME_PHOSPHOLIPASE_CMEDIATED_CASCADE
ST_ERK1_ERK2_MAPK_PATHWAY
ST_P38_MAPK_PATHWAY
WNT_SIGNALING
ST_JAK_STAT_PATHWAY
ST_WNT_BETA_CATENIN_PATHWAY
ST_PHOSPHOINOSITIDE_3_KINASE_PATHWAY

Appendix IV. Single nucleotide polymorphisms in the CYP7B1 gene.

A

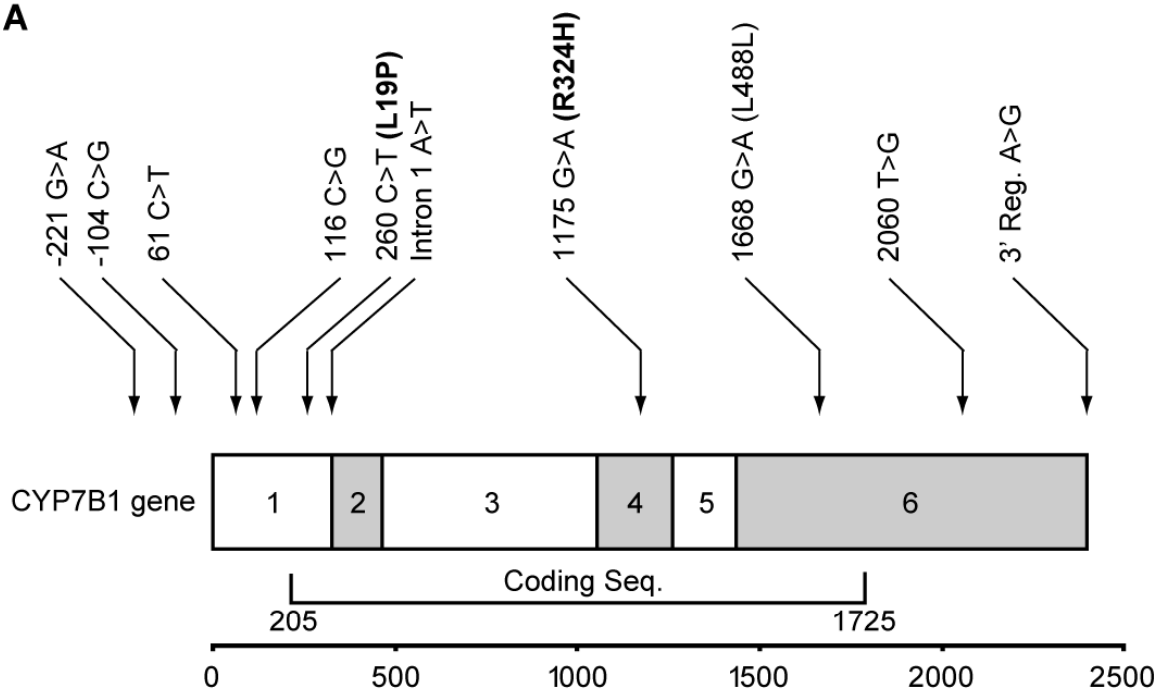

B

SNP	Mutation	Allele Frequency	
		Afr. Amer.	Cauc.
-221G>A	--	1	0
-104C>G	--	2.1	3.1
61C>T	--	1	0
116C>G	--	4.2	1
260C>T	L19P	16.7	0
Intron 1 A>T	--	13.5	52.1
1175G>A	R324H	0	4.2
1668G>A	L488L	0	3.1
2060G>T	--	0	3.1
3' Region	--	8.3	1

Appendix V. Efavirenz Directly Modulates Estrogen Receptor and Induces Breast Cancer Cell Growth.

Introduction

The introduction of highly active antiretroviral therapy (HAART) multi-drug combination regimens has considerably improved the prognosis of patients infected with human immunodeficiency virus (HIV) by reducing AIDS-related morbidity and mortality [264]. However, chronic treatment with these regimens is associated with multiple adverse effects, non-adherence and eventually therapy failure [265]. Treatment regimens containing the non-nucleoside reverse transcriptase inhibitor (NNRTI) efavirenz are preferred in treatment-naive patients and are widely used in other settings [266]. While efavirenz is generally well tolerated, concentration-dependent side effects that impact drug adherence and promote resistance have been documented [267]. Common adverse effects of efavirenz include central nervous system symptoms, occurring in up to 50% of patients [268], but other less common adverse effects have also been reported. An increasing number of reports suggest that the use of HAART, in particular efavirenz-based therapy, is associated with breast hypertrophy or gynecomastia [269-274]. While mechanisms underlying efavirenz-induced gynecomastia are not well understood, a number of hypotheses exist, including a direct estrogenic effect, induction of immune response, or altered steroid hormone metabolism by cytochrome P450 enzymes. To our knowledge, none of these hypotheses have been tested directly. In this study, we tested whether efavirenz can induce breast cancer cell growth by binding and modulating estrogen receptor activity. We examined the ability of efavirenz to (a) induce the growth of the estrogen-dependent, ER-positive breast cancer cell lines MCF-7, T47D and ZR-75-1, in the presence or absence of the pure anti-estrogen ICI 182,780; and (b) directly bind ER using an *in vitro* fluorescence polarization-based receptor binding assay.

Materials and Methods

Cell lines and culture conditions

Cell lines and culture conditions used are as described in the Methods section of Chapter II. Efavirenz was obtained from Toronto Research Chemical.

Receptor binding assay

Fluorescence polarization based competitive binding assays were performed as described in the Methods section of Chapter II.

Statistical analyses and curve fitting

Student's t tests were used to compare treatments to respective controls (SigmaStat Version 3.5, Systat Software Inc, San Jose, CA). Curve fitting and effect concentration for half-maximal growth (EC_{50}) or binding (IC_{50}) were determined using GraphPad Prism Version 4.03 (GraphPad Software, San Diego, CA).

Results

Efavirenz induces breast cancer cell growth

Efavirenz (10μM) stimulated the growth of MCF-7 cells ~1.2-fold greater than vehicle treatment (Figure A.1A; right, solid bar). This effect was blocked by the anti-estrogen ICI 182,780 (Figure A.1A; right, checkered bar). As expected, E2 (10nM) maximally stimulates growth (~3.2-fold) versus vehicle treatment (Figure A.1A; left, solid bar). ICI 182,780 completely blocked E2-induced growth (Figure A.1A; left, checkered bar). Efavirenz induced a similar amount of growth in ZR-75-1 cells following 4 days of treatment (Figure A.1B), and this growth was blocked by ICI 182,780 (data not shown). However, efavirenz did not stimulate the growth of T47D cells following 6 days of treatment (Figure A.1B).

The concentration-effect curve for efavirenz-induced growth in MCF-7 cells is shown in Figure A.1C. Efavirenz induced cellular growth was concentration-dependent up to 10μM. Growth induced at any concentration was completely blocked by 1μM ICI 182,780 (data not shown). Higher efavirenz concentrations (50 or 100μM) were growth inhibitory to MCF-7, T47D, and ZR-75-1 cells; this effect could not be blocked by ICI 182,780 (data not shown). Although this growth inhibition at high concentrations prevented full characterization of the concentration-effect relationship, we estimated an

EC_{50} of approximately 15.7μM using the data obtained from lower concentrations (1-10μM).

Efavirenz directly binds estrogen receptor alpha

The relative affinity of efavirenz binding to the ER relative to that of E2 was determined using a competitive binding assay as described in the Materials and Methods section. Efavirenz bound ER-alpha at a >1000-fold higher concentration (IC_{50} of ~52μM) than E2 (IC_{50} of ~16nM) under these experimental conditions (Figure A.2).

Discussion

Reports show that 1.8 – 8.4% of male patients develop gynecomastia with efavirenz treatment.[269-274] However, the precise mechanism of this adverse effect remains unknown. Our data suggest that efavirenz-induced gynecomastia may be due to direct estrogenic effects in breast tissues. We demonstrate that efavirenz induces the growth of the estrogen-dependent, ER-positive breast cancer cell lines MCF-7 and ZR-75-1 and that this effect is completely reversed by the anti-estrogen ICI 182,780. We have also provided evidence that efavirenz binds directly to ER-alpha. These data provide the first evidence that efavirenz-induced breast hypertrophy and gynecomastia may be due in part to the ability of the drug to directly activate ER.

Our data is the first to directly demonstrate that efavirenz indeed binds to ER-alpha and that it induces cell growth in an E2-dependent breast cancer model. While efavirenz induced growth at ~10^5-fold greater concentrations than E2, it bound ER-alpha *in vitro* at relatively much lower concentrations (only 10^3-fold greater concentration than E2), consistent with the hypothesis that efavirenz acts as a weak agonist of ER. Further, although efavirenz was much less potent than E2 in inducing growth (EC_{50}'s of 15.7μM vs. 5pM [63]), our findings may be clinically important, because efavirenz concentrations that induce growth in our cell model are within the therapeutic plasma concentration range achieved after daily oral administration of 600mg daily (mean steady state C_{min} and C_{max} of 5.6μM and 12.9μM respectively, with inter-patient variability ranging from

A

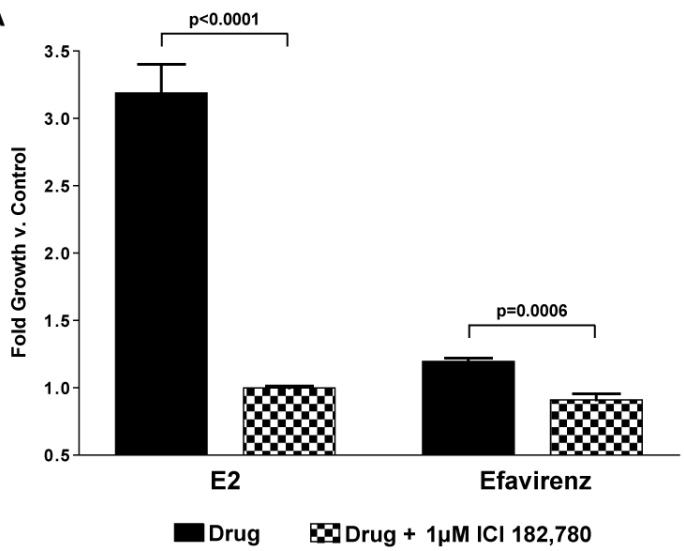

B

	MCF-7	T47D	ZR-75-1
Treatment Time	4 days	6 days	4 days
Fold v. Control ± SD	1.20 ± 0.02	1.06 ± 0.03	1.15 ± 0.07
p-value	0.0006	0.16	0.0068

C

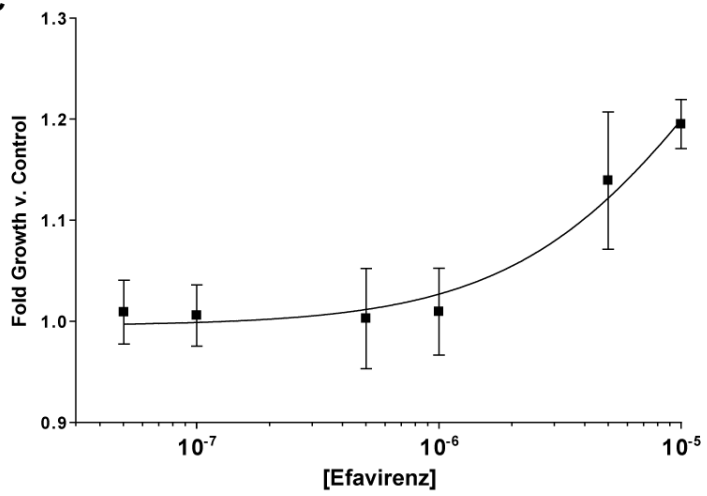

Figure A.1. MCF-7 cells were grown in estrogen-free conditions as described in Materials and Methods. (A) E2 was added to a final concentration of 10nM, and efavirenz was added to a final concentration of 10μM. Cells were treated in the absence (solid bars) or presence (checkered bars) of ICI 182,780 at a final concentration of 1μM. Bars represent 4-day growth vs. vehicle-treated control ± SD of experiments in triplicate. (B) Growth induced by 10μM efavirenz in breast cancer cell lines. SD, Standard Deviation. P-values were determined for efavirenz-treated cells versus vehicle control. (C) Efavirenz was added at increasing concentrations from 50nM – 10μM. Points represent 4-day growth vs. vehicle-treated control ± SD of experiments in triplicate.

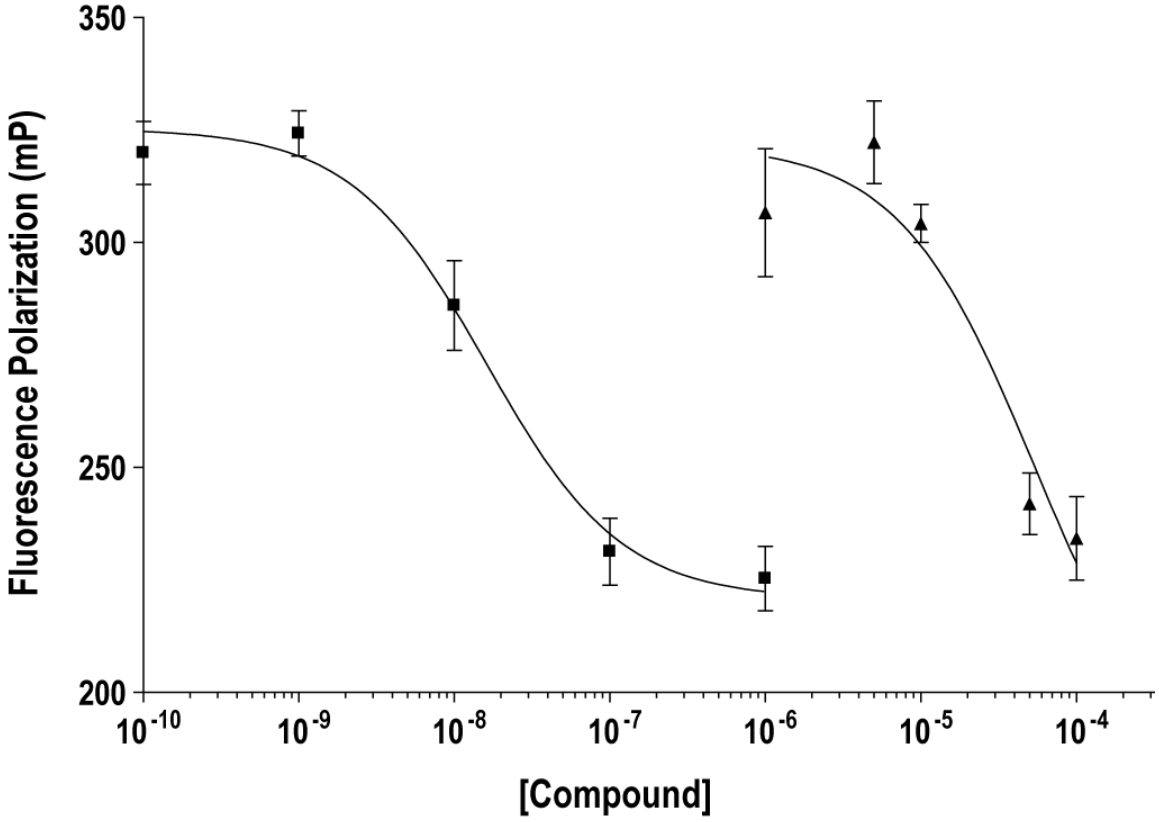

Figure A.2. Fluorescence polarization based ER-alpha binding assays were performed as described in Materials and Methods. Decreasing polarization (Y-axis) represents increased receptor occupancy by the test compound, 17β-estradiol (■) or efavirenz (▲). Points represent polarization ± SD of experiments in triplicate.

0.4μM to 48μM)[267, 275]. In addition, given the lipophilicity of efavirenz and thus very large volume of distribution, it is likely that the concentration in breast tissues is much higher than in plasma. Efavirenz steady state plasma concentrations in HIV patients exhibit wide intersubject variability due to the effects of genetic polymorphisms and drug interactions [267, 275]. Given the concentration-dependent ER-alpha binding and MCF-7 growth induction observed in our study, and that patients with higher efavirenz exposure are at increased risk for adverse effects [267, 275], it is possible that patients achieving higher plasma concentrations of efavirenz are more likely to experience breast hypertrophy and gynecomastia.

The fact that efavirenz induces growth in MCF-7 and ZR-75-1 cells, but not T47D cells, suggests that the efavirenz-induced growth may be dependent on the expression of specific ER transcription co-factors. Unique nuclear receptor co-factor expression is known to play a role in the transcriptional activity of other clinically used agents, particularly the selective estrogen receptor modulator (SERM) tamoxifen, which has differing estrogenic and anti-estrogenic activity in varying target tissues[276].

We were unable to study the effect of efavirenz at high concentrations (>10μM), due to non-specific cytotoxicity or cytostatic effects. However, the fact that high-dose efavirenz-induced growth inhibition was not blocked by the ICI 182,780 suggests that this is unrelated to its estrogenic activity. Interestingly, we found that high concentrations of efavirenz (1-10μM) could antagonize growth induced by 5pM E2, providing additional evidence that efavirenz indeed acts as a weak or partial agonist of ER-alpha (data not shown). However, we could not confirm that this growth antagonism was specifically due to competition for binding to ER-alpha with E2.

Our data may have implications beyond efavirenz's potential role in gynecomastia. Evidence exists for an increased incidence of AIDS-defining and certain non-AIDS-defining cancers, including breast cancer, in HIV-infected patients. Generally, HAART use has been shown to be protective for AIDS-defining cancers, although the extent of this protection for non-AIDS-defining cancers seems limited. A recent meta-analysis of

the incidence of non-AIDS-defining cancers in HIV patients suggests that the incidence of breast cancer in these patients has significantly increased since the implementation of HAART as standard therapy [277]. Further epidemiological studies comparing efavirenz-based and non-efavirenz-based therapies will be needed to rule out the possibility that the estrogenic activity of efavirenz may promote breast cancer. It also remains to be seen whether efavirenz interferes with endocrine treatment of breast cancer and contributes to drug resistance.

This study demonstrates that efavirenz directly binds and activates ER, providing a plausible mechanistic explanation for efavirenz-induced gynecomastia in HIV patients. Additional indirect support to this suggestion has been provided by Kegg and Lau, who reported a case of efavirenz-induced gynecomastia that was successfully reversed using 20mg daily tamoxifen [278]. Tamoxifen has been widely used for the treatment and prophylaxis of anti-androgen induced gynecomastia in prostate cancer patients with high efficacy and low toxicity [279, 280] in addition to its widespread use as a front line therapy for the treatment and prevention of breast cancer. As multiple anti-retroviral drugs are currently available to treat HIV infection, switching from efavirenz to alternative anti-retroviral drugs may be one potential strategy to alleviate this adverse effect. However, multiple factors need to be considered before switching to an alternate therapy. Based on our *in vitro* data and evidence from the literature, tamoxifen and other anti-estrogens may be useful in the treatment of efavirenz-induced gynecomastia. Importantly, before considering the addition of an anti-estrogen to a patient's treatment regimen, other potential causes of gynecomastia should be assessed. A randomized control trial would be necessary to fully evaluate the utility, and more importantly tolerability, of anti-estrogens as a treatment for efavirenz-induced gynecomastia.

Appendix VI. Reprint permission licenses.

Text and figures from [63] are reprinted with permission:

SPRINGER LICENSE
TERMS AND CONDITIONS
Oct 07, 2010

This is a License Agreement between Matthew J Sikora ("You") and Springer ("Springer") provided by Copyright Clearance Center ("CCC"). The license consists of your order details, the terms and conditions provided by Springer, and the payment terms and conditions.

License Number	2523780030070
License date	Oct 07, 2010
Licensed content publisher	Springer
Licensed content publication	Breast Cancer Research and Treatment
Licensed content title	The androgen metabolite 5α-androstane-3β,17β-diol (3βAdiol) induces breast cancer growth via estrogen receptor: implications for aromatase inhibitor resistance
Licensed content author	Matthew J. Sikora
Licensed content date	Jan 1, 2008
Volume number	115
Issue number	2
Type of Use	Thesis/Dissertation
Portion	Full text
Number of copies	1
Author of this Springer article	Yes and you are a contributor of the new work
Order reference number	
Title of your thesis / dissertation	CYP450s in Breast Cancer: Androgen Metabolites in Resistance to Endocrine Therapy
Expected completion date	Apr 2011
Estimated size(pages)	120
Total	0.00 USD

Terms and Conditions

Introduction

The publisher for this copyrighted material is Springer Science + Business Media. By clicking "accept" in connection with completing this licensing transaction, you agree that the following terms and conditions apply to this transaction (along with the Billing and Payment terms and conditions established by Copyright Clearance Center, Inc. ("CCC"), at the time that you opened your Rightslink account and that are available at any time at http://myaccount.copyright.com).

Limited License

With reference to your request to reprint in your thesis material on which Springer Science and Business Media control the copyright, permission is granted, free of charge, for the use indicated in your enquiry. Licenses are for one-time use only with a maximum distribution equal to the number that you identified in

the licensing process.

This License includes use in an electronic form, provided it is password protected or on the university's intranet, destined to microfilming by UMI and University repository. For any other electronic use, please contact Springer at (permissions.dordrecht@springer.com or permissions.heidelberg@springer.com)

The material can only be used for the purpose of defending your thesis, and with a maximum of 100 extra copies in paper.

Although Springer holds copyright to the material and is entitled to negotiate on rights, this license is only valid, provided permission is also obtained from the (co) author (address is given with the article/chapter) and provided it concerns original material which does not carry references to other sources (if material in question appears with credit to another source, authorization from that source is required as well). Permission free of charge on this occasion does not prejudice any rights we might have to charge for reproduction of our copyrighted material in the future.

Altering/Modifying Material: Not Permitted
However figures and illustrations may be altered minimally to serve your work. Any other abbreviations, additions, deletions and/or any other alterations shall be made only with prior written authorization of the author(s) and/or Springer Science + Business Media. (Please contact Springer at permissions.dordrecht@springer.com or permissions.heidelberg@springer.com)

Reservation of Rights
Springer Science + Business Media reserves all rights not specifically granted in the combination of (i) the license details provided by you and accepted in the course of this licensing transaction, (ii) these terms and conditions and (iii) CCC's Billing and Payment terms and conditions.

Copyright Notice:
Please include the following copyright citation referencing the publication in which the material was originally published. Where wording is within brackets, please include verbatim.
"With kind permission from Springer Science+Business Media: <book/journal title, chapter/article title, volume, year of publication, page, name(s) of author(s), figure number(s), and any original (first) copyright notice displayed with material>."

Warranties: Springer Science + Business Media makes no representations or warranties with respect to the licensed material.

Indemnity
You hereby indemnify and agree to hold harmless Springer Science + Business Media and CCC, and their respective officers, directors, employees and agents, from and against any and all claims arising out of your use of the licensed material other than as specifically authorized pursuant to this license.

No Transfer of License
This license is personal to you and may not be sublicensed, assigned, or transferred by you to any other person without Springer Science + Business Media's written permission.

No Amendment Except in Writing
This license may not be amended except in a writing signed by both parties (or, in the case of Springer Science + Business Media, by CCC on Springer Science + Business Media's behalf).

Objection to Contrary Terms
Springer Science + Business Media hereby objects to any terms contained in any purchase order, acknowledgment, check endorsement or other writing prepared by you, which terms are inconsistent with

these terms and conditions or CCC's Billing and Payment terms and conditions. These terms and conditions, together with CCC's Billing and Payment terms and conditions (which are incorporated herein), comprise the entire agreement between you and Springer Science + Business Media (and CCC) concerning this licensing transaction. In the event of any conflict between your obligations established by these terms and conditions and those established by CCC's Billing and Payment terms and conditions, these terms and conditions shall control.

Jurisdiction
All disputes that may arise in connection with this present License, or the breach thereof, shall be settled exclusively by the country's law in which the work was originally published.

Text and figures from [204] are reprinted with permission:

Title:	High-efficiency genotype analysis from formalin-fixed, paraffin-embedded tumor tissues
Author:	M J Sikora, J N Thibert, J Salter, M Dowsett, M D Johnson et al.
Publication:	The Pharmacogenomics Journal
Publisher:	Nature Publishing Group
Date:	Jun 15, 2010

If you are the author of this content (or his/her designated agent) please read the following. If you are not the author of this content, please click the Back button and select an alternative Requestor Type to obtain a quick price or to place an order.

Ownership of copyright in the article remains with the Authors, and provided that, when reproducing the Contribution or extracts from it, the Authors acknowledge first and reference publication in the Journal, the Authors retain the following non-exclusive rights:

a) To reproduce the Contribution in whole or in part in any printed volume (book or thesis) of which they are the author(s).

b) They and any academic institution where they work at the time may reproduce the Contribution for the purpose of course teaching.

c) To reuse figures or tables created by them and contained in the Contribution in other works created by them.

d) To post a copy of the Contribution as accepted for publication after peer review (in Word or Tex format) on the Author's own web site, or the Author's institutional repository, or the Author's funding body's archive, six months after publication of the printed or online edition of the Journal, provided that they also link to the Journal article on NPG's web site (eg through the DOI).

NPG encourages the self-archiving of the accepted version of your manuscript in your funding agency's or institution's repository, six months after publication. This policy complements the recently announced policies of the US National Instutes of Health, Wellcome Trust and other research funding bodies around the world. NPG recognises the efforts of funding bodies to increase access to the research they fund, and we strongly encourage authors to participate in such efforts.

Text and figures from [281] are reprinted with permission:

JOHN WILEY AND SONS LICENSE TERMS AND CONDITIONS

Oct 07, 2010

This is a License Agreement between Matthew J Sikora ("You") and John Wiley and Sons ("John Wiley and Sons") provided by Copyright Clearance Center ("CCC"). The license consists of your order details, the terms and conditions provided by John Wiley and Sons, and the payment terms and conditions.

License Number	2523780189209
License date	Oct 07, 2010
Licensed content publisher	John Wiley and Sons
Licensed content publication	HIV Medicine
Licensed content title	Efavirenz directly modulates the oestrogen receptor and induces breast cancer cell growth
Licensed content author	MJ Sikora,JM Rae,MD Johnson,Z Desta
Licensed content date	Oct 1, 2010
Start page	603
End page	607
Type of use	Dissertation/Thesis
Requestor type	Author of this Wiley article
Format	Print and electronic
Portion	Full article
Will you be translating?	No
Order reference number	
Total	0.00 USD
Terms and Conditions	

TERMS AND CONDITIONS

This copyrighted material is owned by or exclusively licensed to John Wiley & Sons, Inc. or one if its group companies (each a “Wiley Company”) or a society for whom a Wiley Company has exclusive publishing rights in relation to a particular journal (collectively “WILEY”). By clicking “accept” in connection with completing this licensing transaction, you agree that the following terms and conditions apply to this transaction (along with the billing and payment terms and conditions established by the Copyright Clearance Center Inc., (“CCC’s Billing and Payment terms and conditions”), at the time that you opened your Rightslink account (these are available at any time at http://myaccount.copyright.com).

Terms and Conditions

1. The materials you have requested permission to reproduce (the "Materials") are protected by copyright.
2. You are hereby granted a personal, non-exclusive, non-sublicensable, non-transferable, worldwide, limited license to reproduce the Materials for the purpose specified in the licensing process. This license is for a one-time use only with a maximum distribution equal to the number that you identified in the licensing process. Any form of republication granted by this licence must be completed within two years of the date of the grant of this licence (although copies prepared before may be distributed thereafter). Any electronic posting of the Materials is limited to one year from the date permission is granted and is on the condition that a link is placed to the journal homepage on Wiley’s online journals publication platform at www.interscience.wiley.com. The Materials shall not be used in any other manner or for any other

purpose. Permission is granted subject to an appropriate acknowledgement given to the author, title of the material/book/journal and the publisher and on the understanding that nowhere in the text is a previously published source acknowledged for all or part of this Material. Any third party material is expressly excluded from this permission.

3. With respect to the Materials, all rights are reserved. No part of the Materials may be copied, modified, adapted, translated, reproduced, transferred or distributed, in any form or by any means, and no derivative works may be made based on the Materials without the prior permission of the respective copyright owner. You may not alter, remove or suppress in any manner any copyright, trademark or other notices displayed by the Materials. You may not license, rent, sell, loan, lease, pledge, offer as security, transfer or assign the Materials, or any of the rights granted to you hereunder to any other person.

4. The Materials and all of the intellectual property rights therein shall at all times remain the exclusive property of John Wiley & Sons Inc or one of its related companies (WILEY) or their respective licensors, and your interest therein is only that of having possession of and the right to reproduce the Materials pursuant to Section 2 herein during the continuance of this Agreement. You agree that you own no right, title or interest in or to the Materials or any of the intellectual property rights therein. You shall have no rights hereunder other than the license as provided for above in Section 2. No right, license or interest to any trademark, trade name, service mark or other branding ("Marks") of WILEY or its licensors is granted hereunder, and you agree that you shall not assert any such right, license or interest with respect thereto.

5. WILEY DOES NOT MAKE ANY WARRANTY OR REPRESENTATION OF ANY KIND TO YOU OR ANY THIRD PARTY, EXPRESS, IMPLIED OR STATUTORY, WITH RESPECT TO THE MATERIALS OR THE ACCURACY OF ANY INFORMATION CONTAINED IN THE MATERIALS, INCLUDING, WITHOUT LIMITATION, ANY IMPLIED WARRANTY OF MERCHANTABILITY, ACCURACY, SATISFACTORY QUALITY, FITNESS FOR A PARTICULAR PURPOSE, USABILITY, INTEGRATION OR NON-INFRINGEMENT AND ALL SUCH WARRANTIES ARE HEREBY EXCLUDED BY WILEY AND WAIVED BY YOU.

6. WILEY shall have the right to terminate this Agreement immediately upon breach of this Agreement by you.

7. You shall indemnify, defend and hold harmless WILEY, its directors, officers, agents and employees, from and against any actual or threatened claims, demands, causes of action or proceedings arising from any breach of this Agreement by you.

8. IN NO EVENT SHALL WILEY BE LIABLE TO YOU OR ANY OTHER PARTY OR ANY OTHER PERSON OR ENTITY FOR ANY SPECIAL, CONSEQUENTIAL, INCIDENTAL, INDIRECT, EXEMPLARY OR PUNITIVE DAMAGES, HOWEVER CAUSED, ARISING OUT OF OR IN CONNECTION WITH THE DOWNLOADING, PROVISIONING, VIEWING OR USE OF THE MATERIALS REGARDLESS OF THE FORM OF ACTION, WHETHER FOR BREACH OF CONTRACT, BREACH OF WARRANTY, TORT, NEGLIGENCE, INFRINGEMENT OR OTHERWISE (INCLUDING, WITHOUT LIMITATION, DAMAGES BASED ON LOSS OF PROFITS, DATA, FILES, USE, BUSINESS OPPORTUNITY OR CLAIMS OF THIRD PARTIES), AND WHETHER OR NOT THE PARTY HAS BEEN ADVISED OF THE POSSIBILITY OF SUCH DAMAGES. THIS LIMITATION SHALL APPLY NOTWITHSTANDING ANY FAILURE OF ESSENTIAL PURPOSE OF ANY LIMITED REMEDY PROVIDED HEREIN.

9. Should any provision of this Agreement be held by a court of competent jurisdiction to be illegal, invalid, or unenforceable, that provision shall be deemed amended to achieve as nearly as possible the same economic effect as the original provision, and the legality, validity and enforceability of the remaining provisions of this Agreement shall not be affected or impaired thereby.

10. The failure of either party to enforce any term or condition of this Agreement shall not constitute a waiver of either party's right to enforce each and every term and condition of this Agreement. No breach under this agreement shall be deemed waived or excused by either party unless such waiver or consent is in writing signed by the party granting such waiver or consent. The waiver by or consent of a party to a breach of any provision of this Agreement shall not operate or be construed as a waiver of or consent to any other or subsequent breach by such other party.

11. This Agreement may not be assigned (including by operation of law or otherwise) by you without WILEY's prior written consent.

12. These terms and conditions together with CCC’s Billing and Payment terms and conditions (which are incorporated herein) form the entire agreement between you and WILEY concerning this licensing

transaction and (in the absence of fraud) supersedes all prior agreements and representations of the parties, oral or written. This Agreement may not be amended except in a writing signed by both parties. This Agreement shall be binding upon and inure to the benefit of the parties' successors, legal representatives, and authorized assigns.

13. In the event of any conflict between your obligations established by these terms and conditions and those established by CCC's Billing and Payment terms and conditions, these terms and conditions shall prevail.

14. WILEY expressly reserves all rights not specifically granted in the combination of (i) the license details provided by you and accepted in the course of this licensing transaction, (ii) these terms and conditions and (iii) CCC's Billing and Payment terms and conditions.

15. This Agreement shall be governed by and construed in accordance with the laws of England and you agree to submit to the exclusive jurisdiction of the English courts.

16. Other Terms and Conditions:

References

1. NCI: **SEER Breast Cancer Statistics**. *Surveillance, Epidemiology, and End Results (SEER) Program* 2010.
2. Harris JR: **Diseases of the breast**, 3rd edn. Philadelphia: Lippincott Williams & Wilkins; 2004.
3. McGuire WL, Carbone PP, Vollmer EP, National Cancer Institute (U.S.) Breast Cancer Treatment Committee.: **Estrogen receptors in human breast cancer**. New York: Raven Press; 1975.
4. Osborne CK: **Tamoxifen in the treatment of breast cancer**. *N Engl J Med* 1998, **339**(22):1609-1618.
5. Powles T, Eeles R, Ashley S, Easton D, Chang J, Dowsett M, Tidy A, Viggers J, Davey J: **Interim analysis of the incidence of breast cancer in the Royal Marsden Hospital tamoxifen randomised chemoprevention trial**. *Lancet* 1998, **352**(9122):98-101.
6. Powles TJ, Ashley S, Tidy A, Smith IE, Dowsett M: **Twenty-year follow-up of the Royal Marsden randomized, double-blinded tamoxifen breast cancer prevention trial**. *J Natl Cancer Inst* 2007, **99**(4):283-290.
7. Fisher B, Costantino JP, Wickerham DL, Redmond CK, Kavanah M, Cronin WM, Vogel V, Robidoux A, Dimitrov N, Atkins J *et al*: **Tamoxifen for prevention of breast cancer: report of the National Surgical Adjuvant Breast and Bowel Project P-1 Study**. *J Natl Cancer Inst* 1998, **90**(18):1371-1388.
8. Jordan VC: **Tamoxifen: catalyst for the change to targeted therapy**. *Eur J Cancer* 2008, **44**(1):30-38.
9. Jordan VC, Koerner S: **Tamoxifen (ICI 46,474) and the human carcinoma 8S oestrogen receptor**. *Eur J Cancer* 1975, **11**(3):205-206.
10. Lippman ME, Bolan G: **Oestrogen-responsive human breast cancer in long term tissue culture**. *Nature* 1975, **256**(5518):592-593.
11. Jordan VC: **Effect of tamoxifen (ICI 46,474) on initiation and growth of DMBA-induced rat mammary carcinomata**. *Eur J Cancer* 1976, **12**(6):419-424.
12. Jordan VC, Allen KE: **Evaluation of the antitumour activity of the non-steroidal antioestrogen monohydroxytamoxifen in the DMBA-induced rat mammary carcinoma model**. *Eur J Cancer* 1980, **16**(2):239-251.
13. Gottardis MM, Robinson SP, Jordan VC: **Estradiol-stimulated growth of MCF-7 tumors implanted in athymic mice: a model to study the tumoristatic action of tamoxifen**. *J Steroid Biochem* 1988, **30**(1-6):311-314.
14. **Tamoxifen for early breast cancer: an overview of the randomised trials. Early Breast Cancer Trialists' Collaborative Group**. *Lancet* 1998, **351**(9114):1451-1467.

15. Santen RJ, Brodie H, Simpson ER, Siiteri PK, Brodie A: **History of aromatase: saga of an important biological mediator and therapeutic target**. *Endocr Rev* 2009, **30**(4):343-375.
16. Ackerman GE, Smith ME, Mendelson CR, MacDonald PC, Simpson ER: **Aromatization of androstenedione by human adipose tissue stromal cells in monolayer culture**. *J Clin Endocrinol Metab* 1981, **53**(2):412-417.
17. Edman CD, Aiman EJ, Porter JC, MacDonald PC: **Identification of the estrogen product of extraglandular aromatization of plasma androstenedione**. *Am J Obstet Gynecol* 1978, **130**(4):439-447.
18. Forney JP, Milewich L, Chen GT, Garlock JL, Schwarz BE, Edman CD, MacDonald PC: **Aromatization of androstenedione to estrone by human adipose tissue in vitro. Correlation with adipose tissue mass, age, and endometrial neoplasia**. *J Clin Endocrinol Metab* 1981, **53**(1):192-199.
19. Hemsell DL, Edman CD, Marks JF, Siiteri PK, MacDonald PC: **Massive extranglandular aromatization of plasma androstenedione resulting in feminization of a prepubertal boy**. *J Clin Invest* 1977, **60**(2):455-464.
20. Grodin JM, Siiteri PK, MacDonald PC: **Source of estrogen production in postmenopausal women**. *J Clin Endocrinol Metab* 1973, **36**(2):207-214.
21. Lipton A, Santen RJ, Santner SJ, Harvey HA, Sanders SI, Matthews YL: **Prognostic value of breast cancer aromatase**. *Cancer* 1992, **70**(7):1951-1955.
22. Lu Q, Nakmura J, Savinov A, Yue W, Weisz J, Dabbs DJ, Wolz G, Brodie A: **Expression of aromatase protein and messenger ribonucleic acid in tumor epithelial cells and evidence of functional significance of locally produced estrogen in human breast cancers**. *Endocrinology* 1996, **137**(7):3061-3068.
23. Tilson-Mallett N, Santner SJ, Feil PD, Santen RJ: **Biological significance of aromatase activity in human breast tumors**. *J Clin Endocrinol Metab* 1983, **57**(6):1125-1128.
24. Chakraborty J, Hopkins R, Parke DV: **Inhibition studies on the aromatization of androst-4-ene-3,17-dione by human placental microsomal preparations**. *Biochem J* 1972, **130**(1):19P-20P.
25. Siiteri PK, Thompson EA: **Studies of human placental aromatase**. *J Steroid Biochem* 1975, **6**(3-4):317-322.
26. Coombes RC, Goss P, Dowsett M, Gazet JC, Brodie A: **4-Hydroxyandrostenedione in treatment of postmenopausal patients with advanced breast cancer**. *Lancet* 1984, **2**(8414):1237-1239.
27. Goss PE, Powles TJ, Dowsett M, Hutchison G, Brodie AM, Gazet JC, Coombes RC: **Treatment of advanced postmenopausal breast cancer with an aromatase inhibitor, 4-hydroxyandrostenedione: phase II report**. *Cancer Res* 1986, **46**(9):4823-4826.
28. Santen RJ, Worgul TJ, Samojlik E, Interrante A, Boucher AE, Lipton A, Harvey HA, White DS, Smart E, Cox C *et al*: **A randomized trial comparing surgical adrenalectomy with aminoglutethimide plus hydrocortisone in women with advanced breast cancer**. *N Engl J Med* 1981, **305**(10):545-551.
29. Santen RJ, Samojlik E, Wells SA: **Resistance of the ovary to blockade of aromatization with aminoglutethimide**. *J Clin Endocrinol Metab* 1980, **51**(3):473-477.

30. Goss PE, Strasser K: **Aromatase inhibitors in the treatment and prevention of breast cancer**. *J Clin Oncol* 2001, **19**(3):881-894.
31. Haynes BP, Dowsett M, Miller WR, Dixon JM, Bhatnagar AS: **The pharmacology of letrozole**. *J Steroid Biochem Mol Biol* 2003, **87**(1):35-45.
32. Lonning PE, Geisler J: **Evaluation of plasma and tissue estrogen suppression with third-generation aromatase inhibitors: of relevance to clinical understanding?** *J Steroid Biochem Mol Biol*, **118**(4-5):288-293.
33. Coates AS, Keshaviah A, Thurlimann B, Mouridsen H, Mauriac L, Forbes JF, Paridaens R, Castiglione-Gertsch M, Gelber RD, Colleoni M *et al*: **Five years of letrozole compared with tamoxifen as initial adjuvant therapy for postmenopausal women with endocrine-responsive early breast cancer: update of study BIG 1-98**. *J Clin Oncol* 2007, **25**(5):486-492.
34. Coombes RC, Kilburn LS, Snowdon CF, Paridaens R, Coleman RE, Jones SE, Jassem J, Van de Velde CJ, Delozier T, Alvarez I *et al*: **Survival and safety of exemestane versus tamoxifen after 2-3 years' tamoxifen treatment (Intergroup Exemestane Study): a randomised controlled trial**. *Lancet* 2007, **369**(9561):559-570.
35. Howell A, Cuzick J, Baum M, Buzdar A, Dowsett M, Forbes JF, Hoctin-Boes G, Houghton J, Locker GY, Tobias JS: **Results of the ATAC (Arimidex, Tamoxifen, Alone or in Combination) trial after completion of 5 years' adjuvant treatment for breast cancer**. *Lancet* 2005, **365**(9453):60-62.
36. Burstein HJ, Prestrud AA, Seidenfeld J, Anderson H, Buchholz TA, Davidson NE, Gelmon KE, Giordano SH, Hudis CA, Malin J *et al*: **American Society of Clinical Oncology clinical practice guideline: update on adjuvant endocrine therapy for women with hormone receptor-positive breast cancer**. *J Clin Oncol*, **28**(23):3784-3796.
37. Auchus RJ: **Overview of dehydroepiandrosterone biosynthesis**. *Semin Reprod Med* 2004, **22**(4):281-288.
38. Thomas JL, Myers RP, Strickler RC: **Human placental 3 beta-hydroxy-5-ene-steroid dehydrogenase and steroid 5----4-ene-isomerase: purification from mitochondria and kinetic profiles, biophysical characterization of the purified mitochondrial and microsomal enzymes**. *J Steroid Biochem* 1989, **33**(2):209-217.
39. Zuber MX, Simpson ER, Waterman MR: **Expression of bovine 17 alpha-hydroxylase cytochrome P-450 cDNA in nonsteroidogenic (COS 1) cells**. *Science* 1986, **234**(4781):1258-1261.
40. Luu-The V, Labrie F: **The intracrine sex steroid biosynthesis pathways**. *Prog Brain Res*, **181**:177-192.
41. Day JM, Tutill HJ, Purohit A, Reed MJ: **Design and validation of specific inhibitors of 17beta-hydroxysteroid dehydrogenases for therapeutic application in breast and prostate cancer, and in endometriosis**. *Endocr Relat Cancer* 2008, **15**(3):665-692.
42. Penning TM, Byrns MC: **Steroid hormone transforming aldo-keto reductases and cancer**. *Ann N Y Acad Sci* 2009, **1155**:33-42.

43. Simard J, Ricketts ML, Gingras S, Soucy P, Feltus FA, Melner MH: **Molecular biology of the 3beta-hydroxysteroid dehydrogenase/delta5-delta4 isomerase gene family**. *Endocr Rev* 2005, **26**(4):525-582.
44. Andersson S, Russell DW: **Structural and biochemical properties of cloned and expressed human and rat steroid 5 alpha-reductases**. *Proc Natl Acad Sci U S A* 1990, **87**(10):3640-3644.
45. Uemura M, Tamura K, Chung S, Honma S, Okuyama A, Nakamura Y, Nakagawa H: **Novel 5 alpha-steroid reductase (SRD5A3, type-3) is overexpressed in hormone-refractory prostate cancer**. *Cancer Sci* 2008, **99**(1):81-86.
46. Mizrachi D, Auchus RJ: **Androgens, estrogens, and hydroxysteroid dehydrogenases**. *Mol Cell Endocrinol* 2009, **301**(1-2):37-42.
47. Kellis JT, Jr., Vickery LE: **Purification and characterization of human placental aromatase cytochrome P-450**. *J Biol Chem* 1987, **262**(9):4413-4420.
48. Reed KC, Ohno S: **Kinetic properties of human placental aromatase. Application of an assay measuring 3H2O release from 1beta,2beta-3H-androgens**. *J Biol Chem* 1976, **251**(6):1625-1631.
49. Lippman M, Monaco ME, Bolan G: **Effects of estrone, estradiol, and estriol on hormone-responsive human breast cancer in long-term tissue culture**. *Cancer Res* 1977, **37**(6):1901-1907.
50. Nguyen BL, Chetrite G, Pasqualini JR: **Transformation of estrone and estradiol in hormone-dependent and hormone-independent human breast cancer cells. Effects of the antiestrogen ICI 164,384, danazol, and promegestone (R-5020)**. *Breast Cancer Res Treat* 1995, **34**(2):139-146.
51. Isaacs JT, McDermott IR, Coffey DS: **Characterization of two new enzymatic activities of the rat ventral prostate: 5 alpha-androstane-3 beta, 17 beta-diol 6 alpha-hydroxylase and 5 alpha-androstane-3 beta, 17 beta-diol 7 alpha-hydroxylase**. *Steroids* 1979, **33**(6):675-692.
52. Sundin M, Warner M, Haaparanta T, Gustafsson JA: **Isolation and catalytic activity of cytochrome P-450 from ventral prostate of control rats**. *J Biol Chem* 1987, **262**(25):12293-12297.
53. Hawkins RA, Thomson ML, Killen E: **Oestrone sulphate, adipose tissue, and breast cancer**. *Breast Cancer Res Treat* 1985, **6**(1):75-87.
54. Lonning PE, Helle H, Duong NK, Ekse D, Aas T, Geisler J: **Tissue estradiol is selectively elevated in receptor positive breast cancers while tumour estrone is reduced independent of receptor status**. *J Steroid Biochem Mol Biol* 2009, **117**(1-3):31-41.
55. Miller WR, Anderson TJ, Jack WJ: **Relationship between tumour aromatase activity, tumour characteristics and response to therapy**. *J Steroid Biochem Mol Biol* 1990, **37**(6):1055-1059.
56. van Landeghem AA, Poortman J, Nabuurs M, Thijssen JH: **Endogenous concentration and subcellular distribution of estrogens in normal and malignant human breast tissue**. *Cancer Res* 1985, **45**(6):2900-2906.
57. Haynes BP, Straume AH, Geisler J, A'Hern R, Helle H, Smith IE, Lonning PE, Dowsett M: **Intratumoral estrogen disposition in breast cancer**. *Clin Cancer Res*, **16**(6):1790-1801.

58. Sasano H, Miki Y, Nagasaki S, Suzuki T: **In situ estrogen production and its regulation in human breast carcinoma: from endocrinology to intracrinology**. *Pathol Int* 2009, **59**(11):777-789.
59. Suzuki T, Miki Y, Nakamura Y, Moriya T, Ito K, Ohuchi N, Sasano H: **Sex steroid-producing enzymes in human breast cancer**. *Endocr Relat Cancer* 2005, **12**(4):701-720.
60. Miki Y, Suzuki T, Tazawa C, Yamaguchi Y, Kitada K, Honma S, Moriya T, Hirakawa H, Evans DB, Hayashi S *et al*: **Aromatase localization in human breast cancer tissues: possible interactions between intratumoral stromal and parenchymal cells**. *Cancer Res* 2007, **67**(8):3945-3954.
61. MacIndoe JH: **Estradiol formation from testosterone by continuously cultured human breast cancer cells**. *J Clin Endocrinol Metab* 1979, **49**(2):272-277.
62. Sonne-Hansen K, Lykkesfeldt AE: **Endogenous aromatization of testosterone results in growth stimulation of the human MCF-7 breast cancer cell line**. *J Steroid Biochem Mol Biol* 2005, **93**(1):25-34.
63. Sikora MJ, Cordero KE, Larios JM, Johnson MD, Lippman ME, Rae JM: **The androgen metabolite 5alpha-androstane-3beta,17beta-diol (3betaAdiol) induces breast cancer growth via estrogen receptor: implications for aromatase inhibitor resistance**. *Breast Cancer Res Treat* 2009, **115**(2):289-296.
64. Rheaume E, Lachance Y, Zhao HF, Breton N, Dumont M, de Launoit Y, Trudel C, Luu-The V, Simard J, Labrie F: **Structure and expression of a new complementary DNA encoding the almost exclusive 3 beta-hydroxysteroid dehydrogenase/delta 5-delta 4-isomerase in human adrenals and gonads**. *Mol Endocrinol* 1991, **5**(8):1147-1157.
65. Li Z, Luu-The V, Poisson-Pare D, Ouellet J, Li S, Labrie F, Pelletier G: **Expression of enzymes involved in synthesis and metabolism of estradiol in human breast as studied by immunocytochemistry and in situ hybridization**. *Histol Histopathol* 2009, **24**(3):273-282.
66. Thomas JL, Bucholtz KM, Sun J, Mack VL, Kacsoh B: **Structural basis for the selective inhibition of human 3beta-hydroxysteroid dehydrogenase 1 in human breast tumor MCF-7 cells**. *Mol Cell Endocrinol* 2009, **301**(1-2):174-182.
67. Gunasegaram R, Peh KL, Loganath A, Ratnam SS: **Expression of 3beta-hydroxysteroid dehydrogenase-5,4-en isomerase activity by infiltrating ductal human breast carcinoma in vitro**. *Breast Cancer Res Treat* 1998, **50**(2):117-123.
68. Suzuki T, Miki Y, Takagi K, Hirakawa H, Moriya T, Ohuchi N, Sasano H: **Androgens in human breast carcinoma**. *Med Mol Morphol*, **43**(2):75-81.
69. Gunnarsson C, Hellqvist E, Stal O: **17beta-Hydroxysteroid dehydrogenases involved in local oestrogen synthesis have prognostic significance in breast cancer**. *Br J Cancer* 2005, **92**(3):547-552.
70. Jansson A: **17Beta-hydroxysteroid dehydrogenase enzymes and breast cancer**. *J Steroid Biochem Mol Biol* 2009, **114**(1-2):64-67.
71. Miettinen M, Mustonen M, Poutanen M, Isomaa V, Wickman M, Soderqvist G, Vihko R, Vihko P: **17Beta-hydroxysteroid dehydrogenases in normal human**

mammary epithelial cells and breast tissue. *Breast Cancer Res Treat* 1999, **57**(2):175-182.
72. McNeill JM, Reed MJ, Beranek PA, Bonney RC, Ghilchik MW, Robinson DJ, James VH: **A comparison of the in vivo uptake and metabolism of 3H-oestrone and 3H-oestradiol by normal breast and breast tumour tissues in post-menopausal women**. *Int J Cancer* 1986, **38**(2):193-196.
73. Geisler J, Sasano H, Chen S, Purohit A: **Steroid Sulfatase Inhibitors: Promising New Tools for Breast Cancer Therapy?** *J Steroid Biochem Mol Biol*.
74. Al Sarakbi W, Mokbel R, Salhab M, Jiang WG, Reed MJ, Mokbel K: **The role of STS and OATP-B mRNA expression in predicting the clinical outcome in human breast cancer**. *Anticancer Res* 2006, **26**(6C):4985-4990.
75. Evans TR, Rowlands MG, Law M, Coombes RC: **Intratumoral oestrone sulphatase activity as a prognostic marker in human breast carcinoma**. *Br J Cancer* 1994, **69**(3):555-561.
76. Stanway SJ, Purohit A, Woo LW, Sufi S, Vigushin D, Ward R, Wilson RH, Stanczyk FZ, Dobbs N, Kulinskaya E *et al*: **Phase I study of STX 64 (667 Coumate) in breast cancer patients: the first study of a steroid sulfatase inhibitor**. *Clin Cancer Res* 2006, **12**(5):1585-1592.
77. Poirier D: **17beta-Hydroxysteroid dehydrogenase inhibitors: a patent review**. *Expert Opin Ther Pat*, **20**(9):1123-1145.
78. Gunnarsson C, Olsson BM, Stal O: **Abnormal expression of 17beta-hydroxysteroid dehydrogenases in breast cancer predicts late recurrence**. *Cancer Res* 2001, **61**(23):8448-8451.
79. Oduwole OO, Li Y, Isomaa VV, Mantyniemi A, Pulkka AE, Soini Y, Vihko PT: **17beta-hydroxysteroid dehydrogenase type 1 is an independent prognostic marker in breast cancer**. *Cancer Res* 2004, **64**(20):7604-7609.
80. Jansson A, Delander L, Gunnarsson C, Fornander T, Skoog L, Nordenskjold B, Stal O: **Ratio of 17HSD1 to 17HSD2 protein expression predicts the outcome of tamoxifen treatment in postmenopausal breast cancer patients**. *Clin Cancer Res* 2009, **15**(10):3610-3616.
81. Kallstrom AC, Salme R, Ryden L, Nordenskjold B, Jonsson PE, Stal O: **17ss-Hydroxysteroid dehydrogenase type 1 as predictor of tamoxifen response in premenopausal breast cancer**. *Eur J Cancer*, **46**(5):892-900.
82. Suzuki T, Moriya T, Ariga N, Kaneko C, Kanazawa M, Sasano H: **17Beta-hydroxysteroid dehydrogenase type 1 and type 2 in human breast carcinoma: a correlation to clinicopathological parameters**. *Br J Cancer* 2000, **82**(3):518-523.
83. Cuzick J, Sestak I, Baum M, Buzdar A, Howell A, Dowsett M, Forbes JF: **Effect of anastrozole and tamoxifen as adjuvant treatment for early-stage breast cancer: 10-year analysis of the ATAC trial**. *Lancet Oncol*, **11**(12):1135-1141.
84. Partridge AH, Avorn J, Wang PS, Winer EP: **Adherence to therapy with oral antineoplastic agents**. *J Natl Cancer Inst* 2002, **94**(9):652-661.
85. Demissie S, Silliman RA, Lash TL: **Adjuvant tamoxifen: predictors of use, side effects, and discontinuation in older women**. *J Clin Oncol* 2001, **19**(2):322-328.
86. Fisher B, Dignam J, Bryant J, Wolmark N: **Five versus more than five years of tamoxifen for lymph node-negative breast cancer: updated findings from the**

National Surgical Adjuvant Breast and Bowel Project B-14 randomized trial. *J Natl Cancer Inst* 2001, **93**(9):684-690.

87. Grunfeld EA, Hunter MS, Sikka P, Mittal S: **Adherence beliefs among breast cancer patients taking tamoxifen**. *Patient Educ Couns* 2005, **59**(1):97-102.
88. Lash TL, Fox MP, Westrup JL, Fink AK, Silliman RA: **Adherence to tamoxifen over the five-year course**. *Breast Cancer Res Treat* 2006, **99**(2):215-220.
89. Maurice A, Howell A, Evans DG, O'Neil AC, Scobie S: **Predicting compliance in a breast cancer prevention trial**. *Breast J* 2006, **12**(5):446-450.
90. Partridge AH: **Non-adherence to endocrine therapy for breast cancer**. *Ann Oncol* 2006, **17**(2):183-184.
91. Partridge AH, LaFountain A, Mayer E, Taylor BS, Winer E, Asnis-Alibozek A: **Adherence to initial adjuvant anastrozole therapy among women with early-stage breast cancer**. *J Clin Oncol* 2008, **26**(4):556-562.
92. Rae JM, Sikora MJ, Henry NL, Li L, Kim S, Oesterreich S, Skaar TC, Nguyen AT, Desta Z, Storniolo AM *et al*: **Cytochrome P450 2D6 activity predicts discontinuation of tamoxifen therapy in breast cancer patients**. *Pharmacogenomics J* 2009.
93. Ma CX, Adjei AA, Salavaggione OE, Coronel J, Pelleymounter L, Wang L, Eckloff BW, Schaid D, Wieben ED, Weinshilboum RM: **Human aromatase: gene resequencing and functional genomics**. *Cancer Res* 2005, **65**(23):11071-11082.
94. Colomer R, Monzo M, Tusquets I, Rifa J, Baena JM, Barnadas A, Calvo L, Carabantes F, Crespo C, Munoz M *et al*: **A single-nucleotide polymorphism in the aromatase gene is associated with the efficacy of the aromatase inhibitor letrozole in advanced breast carcinoma**. *Clin Cancer Res* 2008, **14**(3):811-816.
95. Lazarus P, Sun D: **Potential role of UGT pharmacogenetics in cancer treatment and prevention: focus on tamoxifen and aromatase inhibitors**. *Drug Metab Rev*, **42**(1):182-194.
96. Sun D, Chen G, Dellinger RW, Sharma AK, Lazarus P: **Characterization of 17-dihydroexemestane glucuronidation: potential role of the UGT2B17 deletion in exemestane pharmacogenetics**. *Pharmacogenet Genomics*, **20**(10):575-585.
97. Henry NL, Giles JT, Ang D, Mohan M, Dadabhoy D, Robarge J, Hayden J, Lemler S, Shahverdi K, Powers P *et al*: **Prospective characterization of musculoskeletal symptoms in early stage breast cancer patients treated with aromatase inhibitors**. *Breast Cancer Res Treat* 2008, **111**(2):365-372.
98. Henry NL, Giles JT, Stearns V: **Aromatase inhibitor-associated musculoskeletal symptoms: etiology and strategies for management**. *Oncology (Williston Park)* 2008, **22**(12):1401-1408.
99. Santen RJ, Song RX, Masamura S, Yue W, Fan P, Sogon T, Hayashi S, Nakachi K, Eguchi H: **Adaptation to estradiol deprivation causes up-regulation of growth factor pathways and hypersensitivity to estradiol in breast cancer cells**. *Adv Exp Med Biol* 2008, **630**:19-34.
100. Dunbier AK, Martin LA, Dowsett M: **New and translational perspectives of oestrogen deprivation in breast cancer**. *Mol Cell Endocrinol*.

101. Masamura S, Santner SJ, Heitjan DF, Santen RJ: **Estrogen deprivation causes estradiol hypersensitivity in human breast cancer cells**. *J Clin Endocrinol Metab* 1995, **80**(10):2918-2925.
102. Chan CM, Martin LA, Johnston SR, Ali S, Dowsett M: **Molecular changes associated with the acquisition of oestrogen hypersensitivity in MCF-7 breast cancer cells on long-term oestrogen deprivation**. *J Steroid Biochem Mol Biol* 2002, **81**(4-5):333-341.
103. Dowsett M, Stein RC, Coombes RC: **Aromatization inhibition alone or in combination with GnRH agonists for the treatment of premenopausal breast cancer patients**. *J Steroid Biochem Mol Biol* 1992, **43**(1-3):155-159.
104. Martin LA, Farmer I, Johnston SR, Ali S, Marshall C, Dowsett M: **Enhanced estrogen receptor (ER) alpha, ERBB2, and MAPK signal transduction pathways operate during the adaptation of MCF-7 cells to long term estrogen deprivation**. *J Biol Chem* 2003, **278**(33):30458-30468.
105. Martin LA, Farmer I, Johnston SR, Ali S, Dowsett M: **Elevated ERK1/ERK2/estrogen receptor cross-talk enhances estrogen-mediated signaling during long-term estrogen deprivation**. *Endocr Relat Cancer* 2005, **12 Suppl 1**:S75-84.
106. Song RX, McPherson RA, Adam L, Bao Y, Shupnik M, Kumar R, Santen RJ: **Linkage of rapid estrogen action to MAPK activation by ERalpha-Shc association and Shc pathway activation**. *Mol Endocrinol* 2002, **16**(1):116-127.
107. Yue W, Wang J, Li Y, Fan P, Santen RJ: **Farnesylthiosalicylic acid blocks mammalian target of rapamycin signaling in breast cancer cells**. *Int J Cancer* 2005, **117**(5):746-754.
108. Song RX, Barnes CJ, Zhang Z, Bao Y, Kumar R, Santen RJ: **The role of Shc and insulin-like growth factor 1 receptor in mediating the translocation of estrogen receptor alpha to the plasma membrane**. *Proc Natl Acad Sci U S A* 2004, **101**(7):2076-2081.
109. Zhou DJ, Pompon D, Chen SA: **Stable expression of human aromatase complementary DNA in mammalian cells: a useful system for aromatase inhibitor screening**. *Cancer Res* 1990, **50**(21):6949-6954.
110. Brodie A, Macedo L, Sabnis G: **Aromatase resistance mechanisms in model systems in vivo**. *J Steroid Biochem Mol Biol*, **118**(4-5):283-287.
111. Sabnis G, Brodie A: **Adaptive changes results in activation of alternate signaling pathways and resistance to aromatase inhibitor resistance**. *Mol Cell Endocrinol*.
112. Long BJ, Jelovac D, Handratta V, Thiantanawat A, MacPherson N, Ragaz J, Goloubeva OG, Brodie AM: **Therapeutic strategies using the aromatase inhibitor letrozole and tamoxifen in a breast cancer model**. *J Natl Cancer Inst* 2004, **96**(6):456-465.
113. Long BJ, Jelovac D, Thiantanawat A, Brodie AM: **The effect of second-line antiestrogen therapy on breast tumor growth after first-line treatment with the aromatase inhibitor letrozole: long-term studies using the intratumoral aromatase postmenopausal breast cancer model**. *Clin Cancer Res* 2002, **8**(7):2378-2388.

114. Sabnis G, Schayowitz A, Goloubeva O, Macedo L, Brodie A: **Trastuzumab reverses letrozole resistance and amplifies the sensitivity of breast cancer cells to estrogen**. *Cancer Res* 2009, **69**(4):1416-1428.
115. Miller TW, Hennessy BT, Gonzalez-Angulo AM, Fox EM, Mills GB, Chen H, Higham C, Garcia-Echeverria C, Shyr Y, Arteaga CL: **Hyperactivation of phosphatidylinositol-3 kinase promotes escape from hormone dependence in estrogen receptor-positive human breast cancer**. *J Clin Invest*, **120**(7):2406-2413.
116. Miller TW, Balko JM, Ghazoui Z, Dunbier AK, Anderson H, Dowsett M, Gonzalez-Angulo AM, Mills GB, Miller WR, Wu H *et al*: **A gene expression signature from human breast cancer cells with acquired hormone independence identifies MYC as a mediator of antiestrogen resistance**. *Clin Cancer Res*.
117. Aguilar H, Sole X, Bonifaci N, Serra-Musach J, Islam A, Lopez-Bigas N, Mendez-Pertuz M, Beijersbergen RL, Lazaro C, Urruticoechea A *et al*: **Biological reprogramming in acquired resistance to endocrine therapy of breast cancer**. *Oncogene*, **29**(45):6071-6083.
118. Chen S: **An "Omics" Approach to Determine the Mechanisms of Acquired Aromatase Inhibitor Resistance**. *OMICS*.
119. Johnston SR: **Enhancing the efficacy of hormonal agents with selected targeted agents**. *Clin Breast Cancer* 2009, **9 Suppl 1**:S28-36.
120. Montgomery RB, Mostaghel EA, Vessella R, Hess DL, Kalhorn TF, Higano CS, True LD, Nelson PS: **Maintenance of intratumoral androgens in metastatic prostate cancer: a mechanism for castration-resistant tumor growth**. *Cancer Res* 2008, **68**(11):4447-4454.
121. Stanbrough M, Bubley GJ, Ross K, Golub TR, Rubin MA, Penning TM, Febbo PG, Balk SP: **Increased expression of genes converting adrenal androgens to testosterone in androgen-independent prostate cancer**. *Cancer Res* 2006, **66**(5):2815-2825.
122. Guengerich FP: **Cytochrome P450: what have we learned and what are the future issues?** *Drug Metab Rev* 2004, **36**(2):159-197.
123. Lee AJ, Cai MX, Thomas PE, Conney AH, Zhu BT: **Characterization of the oxidative metabolites of 17beta-estradiol and estrone formed by 15 selectively expressed human cytochrome p450 isoforms**. *Endocrinology* 2003, **144**(8):3382-3398.
124. Zhu BT, Lee AJ: **NADPH-dependent metabolism of 17beta-estradiol and estrone to polar and nonpolar metabolites by human tissues and cytochrome P450 isoforms**. *Steroids* 2005, **70**(4):225-244.
125. Ohe T, Hirobe M, Mashino T: **Novel metabolic pathway of estrone and 17beta-estradiol catalyzed by cytochrome P-450**. *Drug Metab Dispos* 2000, **28**(2):110-112.
126. Bolton JL, Thatcher GR: **Potential mechanisms of estrogen quinone carcinogenesis**. *Chem Res Toxicol* 2008, **21**(1):93-101.
127. Pasqualini JR, Chetrite GS: **Recent insight on the control of enzymes involved in estrogen formation and transformation in human breast cancer**. *J Steroid Biochem Mol Biol* 2005, **93**(2-5):221-236.

128. Imaoka S, Yamada T, Hiroi T, Hayashi K, Sakaki T, Yabusaki Y, Funae Y: **Multiple forms of human P450 expressed in Saccharomyces cerevisiae. Systematic characterization and comparison with those of the rat**. *Biochem Pharmacol* 1996, **51**(8):1041-1050.
129. Waxman DJ: **Interactions of hepatic cytochromes P-450 with steroid hormones. Regioselectivity and stereospecificity of steroid metabolism and hormonal regulation of rat P-450 enzyme expression**. *Biochem Pharmacol* 1988, **37**(1):71-84.
130. Wood AW, Ryan DE, Thomas PE, Levin W: **Regio- and stereoselective metabolism of two C19 steroids by five highly purified and reconstituted rat hepatic cytochrome P-450 isozymes**. *J Biol Chem* 1983, **258**(14):8839-8847.
131. Waxman DJ, Attisano C, Guengerich FP, Lapenson DP: **Human liver microsomal steroid metabolism: identification of the major microsomal steroid hormone 6 beta-hydroxylase cytochrome P-450 enzyme**. *Arch Biochem Biophys* 1988, **263**(2):424-436.
132. Waxman DJ, Lapenson DP, Aoyama T, Gelboin HV, Gonzalez FJ, Korzekwa K: **Steroid hormone hydroxylase specificities of eleven cDNA-expressed human cytochrome P450s**. *Arch Biochem Biophys* 1991, **290**(1):160-166.
133. Ekins S, Vandenbranden M, Ring BJ, Gillespie JS, Yang TJ, Gelboin HV, Wrighton SA: **Further characterization of the expression in liver and catalytic activity of CYP2B6**. *J Pharmacol Exp Ther* 1998, **286**(3):1253-1259.
134. Hanna IH, Reed JR, Guengerich FP, Hollenberg PF: **Expression of human cytochrome P450 2B6 in Escherichia coli: characterization of catalytic activity and expression levels in human liver**. *Arch Biochem Biophys* 2000, **376**(1):206-216.
135. Stiles AR, McDonald JG, Bauman DR, Russell DW: **CYP7B1: one cytochrome P450, two human genetic diseases, and multiple physiological functions**. *J Biol Chem* 2009, **284**(42):28485-28489.
136. El-Rayes BF, Ali S, Heilbrun LK, Lababidi S, Bouwman D, Visscher D, Philip PA: **Cytochrome p450 and glutathione transferase expression in human breast cancer**. *Clin Cancer Res* 2003, **9**(5):1705-1709.
137. Hellmold H, Rylander T, Magnusson M, Reihner E, Warner M, Gustafsson JA: **Characterization of cytochrome P450 enzymes in human breast tissue from reduction mammaplasties**. *J Clin Endocrinol Metab* 1998, **83**(3):886-895.
138. Iscan M, Klaavuniemi T, Coban T, Kapucuoglu N, Pelkonen O, Raunio H: **The expression of cytochrome P450 enzymes in human breast tumours and normal breast tissue**. *Breast Cancer Res Treat* 2001, **70**(1):47-54.
139. Ingelman-Sundberg M, Sim SC, Gomez A, Rodriguez-Antona C: **Influence of cytochrome P450 polymorphisms on drug therapies: pharmacogenetic, pharmacoepigenetic and clinical aspects**. *Pharmacol Ther* 2007, **116**(3):496-526.
140. Gaedigk A, Simon SD, Pearce RE, Bradford LD, Kennedy MJ, Leeder JS: **The CYP2D6 activity score: translating genotype information into a qualitative measure of phenotype**. *Clin Pharmacol Ther* 2008, **83**(2):234-242.

141. Dorado P, Penas-Lledo EM, Llerena A: **CYP2D6 polymorphism: implications for antipsychotic drug response, schizophrenia and personality traits**. *Pharmacogenomics* 2007, **8**(11):1597-1608.
142. Stearns V, Rae JM: **Pharmacogenetics and breast cancer endocrine therapy: CYP2D6 as a predictive factor for tamoxifen metabolism and drug response?** *Expert Rev Mol Med* 2008, **10**:e34.
143. Zanger UM, Klein K, Saussele T, Blievernicht J, M HH, Schwab M: **Polymorphic CYP2B6: molecular mechanisms and emerging clinical significance**. *Pharmacogenomics* 2007, **8**(7):743-759.
144. Domanski TL, He YQ, Scott EE, Wang Q, Halpert JR: **The role of cytochrome 2B1 substrate recognition site residues 115, 294, 297, 298, and 362 in the oxidation of steroids and 7-alkoxycoumarins**. *Arch Biochem Biophys* 2001, **394**(1):21-28.
145. Macedo LF, Guo Z, Tilghman SL, Sabnis GJ, Qiu Y, Brodie A: **Role of androgens on MCF-7 breast cancer cell growth and on the inhibitory effect of letrozole**. *Cancer Res* 2006, **66**(15):7775-7782.
146. Iveson TJ, Smith IE, Ahern J, Smithers DA, Trunet PF, Dowsett M: **Phase I study of the oral nonsteroidal aromatase inhibitor CGS 20267 in postmenopausal patients with advanced breast cancer**. *Cancer Res* 1993, **53**(2):266-270.
147. Santen RJ, Demers L, Ohorodnik S, Settlage J, Langecker P, Blanchett D, Goss PE, Wang S: **Superiority of gas chromatography/tandem mass spectrometry assay (GC/MS/MS) for estradiol for monitoring of aromatase inhibitor therapy**. *Steroids* 2007, **72**(8):666-671.
148. Winer EP, Hudis C, Burstein HJ, Wolff AC, Pritchard KI, Ingle JN, Chlebowski RT, Gelber R, Edge SB, Gralow J *et al*: **American Society of Clinical Oncology technology assessment on the use of aromatase inhibitors as adjuvant therapy for postmenopausal women with hormone receptor-positive breast cancer: status report 2004**. *J Clin Oncol* 2005, **23**(3):619-629.
149. Iveson TJ, Smith IE, Ahern J, Smithers DA, Trunet PF, Dowsett M: **Phase I study of the oral nonsteroidal aromatase inhibitor CGS 20267 in healthy postmenopausal women**. *J Clin Endocrinol Metab* 1993, **77**(2):324-331.
150. Lipton A, Demers LM, Harvey HA, Kambic KB, Grossberg H, Brady C, Adlercruetz H, Trunet PF, Santen RJ: **Letrozole (CGS 20267). A phase I study of a new potent oral aromatase inhibitor of breast cancer**. *Cancer* 1995, **75**(8):2132-2138.
151. Birrell SN, Bentel JM, Hickey TE, Ricciardelli C, Weger MA, Horsfall DJ, Tilley WD: **Androgens induce divergent proliferative responses in human breast cancer cell lines**. *J Steroid Biochem Mol Biol* 1995, **52**(5):459-467.
152. Lippman M, Bolan G, Huff K: **The effects of androgens and antiandrogens on hormone-responsive human breast cancer in long-term tissue culture**. *Cancer Res* 1976, **36**(12):4610-4618.
153. Burak WE, Jr., Quinn AL, Farrar WB, Brueggemeier RW: **Androgens influence estrogen-induced responses in human breast carcinoma cells through cytochrome P450 aromatase**. *Breast Cancer Res Treat* 1997, **44**(1):57-64.

154. Maggiolini M, Donze O, Jeannin E, Ando S, Picard D: **Adrenal androgens stimulate the proliferation of breast cancer cells as direct activators of estrogen receptor alpha**. *Cancer Res* 1999, **59**(19):4864-4869.
155. Lippman ME, Bolan G, Huff K: **Human breast cancer responsive to androgen in long term tissue culture**. *Nature* 1975, **258**(5533):339-341.
156. Kuiper GG, Carlsson B, Grandien K, Enmark E, Haggblad J, Nilsson S, Gustafsson JA: **Comparison of the ligand binding specificity and transcript tissue distribution of estrogen receptors alpha and beta**. *Endocrinology* 1997, **138**(3):863-870.
157. Rae JM, Johnson MD, Scheys JO, Cordero KE, Larios JM, Lippman ME: **GREB 1 is a critical regulator of hormone dependent breast cancer growth**. *Breast Cancer Res Treat* 2005, **92**(2):141-149.
158. Rae JM, Lippman ME: **Evaluation of novel epidermal growth factor receptor tyrosine kinase inhibitors**. *Breast Cancer Res Treat* 2004, **83**(2):99-107.
159. Johnson MD, Zuo H, Lee KH, Trebley JP, Rae JM, Weatherman RV, Desta Z, Flockhart DA, Skaar TC: **Pharmacological characterization of 4-hydroxy-N-desmethyl tamoxifen, a novel active metabolite of tamoxifen**. *Breast Cancer Res Treat* 2004, **85**(2):151-159.
160. Livak KJ, Schmittgen TD: **Analysis of relative gene expression data using real-time quantitative PCR and the 2(-Delta Delta C(T)) Method**. *Methods* 2001, **25**(4):402-408.
161. Pettersson H, Holmberg L, Axelson M, Norlin M: **CYP7B1-mediated metabolism of dehydroepiandrosterone and 5alpha-androstane-3beta,17beta-diol - potential role(s) for estrogen signaling**. *FEBS J* 2008, **275**(8):1778-1789.
162. Pak TR, Chung WC, Lund TD, Hinds LR, Clay CM, Handa RJ: **The androgen metabolite, 5alpha-androstane-3beta, 17beta-diol, is a potent modulator of estrogen receptor-beta1-mediated gene transcription in neuronal cells**. *Endocrinology* 2005, **146**(1):147-155.
163. Oliveira AG, Coelho PH, Guedes FD, Mahecha GA, Hess RA, Oliveira CA: **5alpha-Androstane-3beta,17beta-diol (3beta-diol), an estrogenic metabolite of 5alpha-dihydrotestosterone, is a potent modulator of estrogen receptor ERbeta expression in the ventral prostrate of adult rats**. *Steroids* 2007, **72**(14):914-922.
164. Guerini V, Sau D, Scaccianoce E, Rusmini P, Ciana P, Maggi A, Martini PG, Katzenellenbogen BS, Martini L, Motta M *et al*: **The androgen derivative 5alpha-androstane-3beta,17beta-diol inhibits prostate cancer cell migration through activation of the estrogen receptor beta subtype**. *Cancer Res* 2005, **65**(12):5445-5453.
165. Weihua Z, Lathe R, Warner M, Gustafsson JA: **An endocrine pathway in the prostate, ERbeta, AR, 5alpha-androstane-3beta,17beta-diol, and CYP7B1, regulates prostate growth**. *Proc Natl Acad Sci U S A* 2002, **99**(21):13589-13594.
166. Weihua Z, Makela S, Andersson LC, Salmi S, Saji S, Webster JI, Jensen EV, Nilsson S, Warner M, Gustafsson JA: **A role for estrogen receptor beta in the regulation of growth of the ventral prostate**. *Proc Natl Acad Sci U S A* 2001, **98**(11):6330-6335.

167. Olsson M, Gustafsson O, Skogastierna C, Tolf A, Rietz BD, Morfin R, Rane A, Ekstrom L: **Regulation and expression of human CYP7B1 in prostate: overexpression of CYP7B1 during progression of prostatic adenocarcinoma**. *Prostate* 2007, **67**(13):1439-1446.
168. Ishikawa T, Glidewell-Kenney C, Jameson JL: **Aromatase-independent testosterone conversion into estrogenic steroids is inhibited by a 5 alpha-reductase inhibitor**. *J Steroid Biochem Mol Biol* 2006, **98**(2-3):133-138.
169. Omoto Y, Lathe R, Warner M, Gustafsson JA: **Early onset of puberty and early ovarian failure in CYP7B1 knockout mice**. *Proc Natl Acad Sci U S A* 2005, **102**(8):2814-2819.
170. Martel C, Melner MH, Gagne D, Simard J, Labrie F: **Widespread tissue distribution of steroid sulfatase, 3 beta-hydroxysteroid dehydrogenase/delta 5-delta 4 isomerase (3 beta-HSD), 17 beta-HSD 5 alpha-reductase and aromatase activities in the rhesus monkey**. *Mol Cell Endocrinol* 1994, **104**(1):103-111.
171. Voigt KD, Bartsch W: **Intratissular androgens in benign prostatic hyperplasia and prostatic cancer**. *J Steroid Biochem* 1986, **25**(5B):749-757.
172. Jeng MH, Shupnik MA, Bender TP, Westin EH, Bandyopadhyay D, Kumar R, Masamura S, Santen RJ: **Estrogen receptor expression and function in long-term estrogen-deprived human breast cancer cells**. *Endocrinology* 1998, **139**(10):4164-4174.
173. Donato MT, Lahoz A, Castell JV, Gomez-Lechon MJ: **Cell lines: a tool for in vitro drug metabolism studies**. *Curr Drug Metab* 2008, **9**(1):1-11.
174. Gomez-Lechon MJ, Lopez P, Donato T, Montoya A, Larrauri A, Gimenez P, Trullenque R, Fabra R, Castell JV: **Culture of human hepatocytes from small surgical liver biopsies. Biochemical characterization and comparison with in vivo**. *In Vitro Cell Dev Biol* 1990, **26**(1):67-74.
175. Kocarek TA, Schuetz EG, Guzelian PS: **Expression of multiple forms of cytochrome P450 mRNAs in primary cultures of rat hepatocytes maintained on matrigel**. *Mol Pharmacol* 1993, **43**(3):328-334.
176. Sassa S, Sugita O, Galbraith RA, Kappas A: **Drug metabolism by the human hepatoma cell, Hep G2**. *Biochem Biophys Res Commun* 1987, **143**(1):52-57.
177. Risbridger GP, Davis ID, Birrell SN, Tilley WD: **Breast and prostate cancer: more similar than different**. *Nat Rev Cancer*, **10**(3):205-212.
178. Yamano S, Nhamburo PT, Aoyama T, Meyer UA, Inaba T, Kalow W, Gelboin HV, McBride OW, Gonzalez FJ: **cDNA cloning and sequence and cDNA-directed expression of human P450 IIB1: identification of a normal and two variant cDNAs derived from the CYP2B locus on chromosome 19 and differential expression of the IIB mRNAs in human liver**. *Biochemistry* 1989, **28**(18):7340-7348.
179. Lang T, Klein K, Richter T, Zibat A, Kerb R, Eichelbaum M, Schwab M, Zanger UM: **Multiple novel nonsynonymous CYP2B6 gene polymorphisms in Caucasians: demonstration of phenotypic null alleles**. *J Pharmacol Exp Ther* 2004, **311**(1):34-43.

180. Canick JA, Ryan KJ: **Cytochrome P-450 and the aromatization of 16alpha-hydroxytestosterone and androstenedione by human placental microsomes**. *Mol Cell Endocrinol* 1976, **6**(2):105-115.
181. Numazawa M, Osada R, Tsuji M, Osawa Y: **High-performance liquid chromatographic determination of aromatization of 16 alpha-hydroxylated androgens with human placental microsomes**. *Anal Biochem* 1985, **146**(1):75-81.
182. Ryan KJ: **Metabolism of C-16-oxygenated steroids by human placenta: the formation of estriol**. *J Biol Chem* 1959, **234**(8):2006-2008.
183. Desta Z, Saussele T, Ward B, Blievernicht J, Li L, Klein K, Flockhart DA, Zanger UM: **Impact of CYP2B6 polymorphism on hepatic efavirenz metabolism in vitro**. *Pharmacogenomics* 2007, **8**(6):547-558.
184. Bieche I, Girault I, Urbain E, Tozlu S, Lidereau R: **Relationship between intratumoral expression of genes coding for xenobiotic-metabolizing enzymes and benefit from adjuvant tamoxifen in estrogen receptor alpha-positive postmenopausal breast carcinoma**. *Breast Cancer Res* 2004, **6**(3):R252-263.
185. Jeong S, Woo MM, Flockhart DA, Desta Z: **Inhibition of drug metabolizing cytochrome P450s by the aromatase inhibitor drug letrozole and its major oxidative metabolite 4,4'-methanol-bisbenzonitrile in vitro**. *Cancer Chemother Pharmacol* 2009, **64**(5):867-875.
186. Kamdem LK, Flockhart DA, Desta Z: **In vitro cytochrome P450-mediated metabolism of exemestane**. *Drug Metab Dispos*, **39**(1):98-105.
187. Lewis-Wambi JS, Jordan VC: **Estrogen regulation of apoptosis: how can one hormone stimulate and inhibit?** *Breast Cancer Res* 2009, **11**(3):206.
188. Paruthiyil S, Parmar H, Kerekatte V, Cunha GR, Firestone GL, Leitman DC: **Estrogen receptor beta inhibits human breast cancer cell proliferation and tumor formation by causing a G2 cell cycle arrest**. *Cancer Res* 2004, **64**(1):423-428.
189. Strom A, Hartman J, Foster JS, Kietz S, Wimalasena J, Gustafsson JA: **Estrogen receptor beta inhibits 17beta-estradiol-stimulated proliferation of the breast cancer cell line T47D**. *Proc Natl Acad Sci U S A* 2004, **101**(6):1566-1571.
190. Fox EM, Davis RJ, Shupnik MA: **ERbeta in breast cancer--onlooker, passive player, or active protector?** *Steroids* 2008, **73**(11):1039-1051.
191. Mann S, Laucirica R, Carlson N, Younes PS, Ali N, Younes A, Li Y, Younes M: **Estrogen receptor beta expression in invasive breast cancer**. *Hum Pathol* 2001, **32**(1):113-118.
192. Attard G, Reid AH, A'Hern R, Parker C, Oommen NB, Folkerd E, Messiou C, Molife LR, Maier G, Thompson E *et al*: **Selective inhibition of CYP17 with abiraterone acetate is highly active in the treatment of castration-resistant prostate cancer**. *J Clin Oncol* 2009, **27**(23):3742-3748.
193. Danila DC, Morris MJ, de Bono JS, Ryan CJ, Denmeade SR, Smith MR, Taplin ME, Bubley GJ, Kheoh T, Haqq C *et al*: **Phase II multicenter study of abiraterone acetate plus prednisone therapy in patients with docetaxel-treated castration-resistant prostate cancer**. *J Clin Oncol*, **28**(9):1496-1501.
194. Reid AH, Attard G, Danila DC, Oommen NB, Olmos D, Fong PC, Molife LR, Hunt J, Messiou C, Parker C *et al*: **Significant and sustained antitumor activity**

in post-docetaxel, castration-resistant prostate cancer with the CYP17 inhibitor abiraterone acetate. *J Clin Oncol*, **28**(9):1489-1495.
195. Ryan CJ, Smith MR, Fong L, Rosenberg JE, Kantoff P, Raynaud F, Martins V, Lee G, Kheoh T, Kim J *et al*: **Phase I clinical trial of the CYP17 inhibitor abiraterone acetate demonstrating clinical activity in patients with castration-resistant prostate cancer who received prior ketoconazole therapy**. *J Clin Oncol*, **28**(9):1481-1488.
196. Kumagai J, Fujimura T, Takahashi S, Urano T, Ogushi T, Horie-Inoue K, Ouchi Y, Kitamura T, Muramatsu M, Blumberg B *et al*: **Cytochrome P450 2B6 is a growth-inhibitory and prognostic factor for prostate cancer**. *Prostate* 2007, **67**(10):1029-1037.
197. Ang JE, Olmos D, de Bono JS: **CYP17 blockade by abiraterone: further evidence for frequent continued hormone-dependence in castration-resistant prostate cancer**. *Br J Cancer* 2009, **100**(5):671-675.
198. Zeilinger K, Schreiter T, Darnell M, Soderdahl T, Lubberstedt M, Dillner B, Knobeloch D, Nussler AK, Gerlach JC, Andersson TB: **Scaling Down of a Clinical Three-Dimensional Perfusion Multicompartment Hollow Fiber Liver Bioreactor Developed for Extracorporeal Liver Support to an Analytical Scale Device Useful for Hepatic Pharmacological In Vitro Studies**. *Tissue Eng Part C Methods*.
199. Narjoz C, Marisa L, Imbeaud S, Paris A, Delacroix H, Beaune P, De Waziers I: **Genomic consequences of cytochrome P450 2C9 overexpression in human hepatoma cells**. *Chem Res Toxicol* 2009, **22**(5):779-787.
200. Kim SM, Acharya P, Engel JC, Correia MA: **Liver cytochrome P450 3A ubiquitination in vivo by gp78/autocrine motility factor receptor and C terminus of Hsp70-interacting protein (CHIP) E3 ubiquitin ligases: physiological and pharmacological relevance**. *J Biol Chem*, **285**(46):35866-35877.
201. Liao M, Zgoda VG, Murray BP, Correia MA: **Vacuolar degradation of rat liver CYP2B1 in Saccharomyces cerevisiae: further validation of the yeast model and structural implications for the degradation of mammalian endoplasmic reticulum P450 proteins**. *Mol Pharmacol* 2005, **67**(5):1460-1469.
202. Morishima Y, Peng HM, Lin HL, Hollenberg PF, Sunahara RK, Osawa Y, Pratt WB: **Regulation of cytochrome P450 2E1 by heat shock protein 90-dependent stabilization and CHIP-dependent proteasomal degradation**. *Biochemistry* 2005, **44**(49):16333-16340.
203. Rae JM, Cordero KE, Scheys JO, Lippman ME, Flockhart DA, Johnson MD: **Genotyping for polymorphic drug metabolizing enzymes from paraffin-embedded and immunohistochemically stained tumor samples**. *Pharmacogenetics* 2003, **13**(8):501-507.
204. Sikora MJ, Thibert JN, Salter J, Dowsett M, Johnson MD, Rae JM: **High-efficiency genotype analysis from formalin-fixed, paraffin-embedded tumor tissues**. *Pharmacogenomics J*.
205. Walsky RL, Obach RS: **A comparison of 2-phenyl-2-(1-piperidinyl)propane (ppp), 1,1',1''-phosphinothioylidynetrisaziridine (thioTEPA), clopidogrel,**

and ticlopidine as selective inactivators of human cytochrome P450 2B6. *Drug Metab Dispos* 2007, **35**(11):2053-2059.

206. Dixon JM, Renshaw L, Young O, Murray J, Macaskill EJ, McHugh M, Folkerd E, Cameron DA, A'Hern RP, Dowsett M: **Letrozole suppresses plasma estradiol and estrone sulphate more completely than anastrozole in postmenopausal women with breast cancer**. *J Clin Oncol* 2008, **26**(10):1671-1676.
207. Cronin M, Pho M, Dutta D, Stephans JC, Shak S, Kiefer MC, Esteban JM, Baker JB: **Measurement of gene expression in archival paraffin-embedded tissues: development and performance of a 92-gene reverse transcriptase-polymerase chain reaction assay**. *Am J Pathol* 2004, **164**(1):35-42.
208. Mootha VK, Lindgren CM, Eriksson KF, Subramanian A, Sihag S, Lehar J, Puigserver P, Carlsson E, Ridderstrale M, Laurila E *et al*: **PGC-1alpha-responsive genes involved in oxidative phosphorylation are coordinately downregulated in human diabetes**. *Nat Genet* 2003, **34**(3):267-273.
209. Subramanian A, Tamayo P, Mootha VK, Mukherjee S, Ebert BL, Gillette MA, Paulovich A, Pomeroy SL, Golub TR, Lander ES *et al*: **Gene set enrichment analysis: a knowledge-based approach for interpreting genome-wide expression profiles**. *Proc Natl Acad Sci U S A* 2005, **102**(43):15545-15550.
210. Clemmons DR: **Modifying IGF1 activity: an approach to treat endocrine disorders, atherosclerosis and cancer**. *Nat Rev Drug Discov* 2007, **6**(10):821-833.
211. Riedemann J, Macaulay VM: **IGF1R signalling and its inhibition**. *Endocr Relat Cancer* 2006, **13 Suppl 1**:S33-43.
212. Kobayashi S, Shimamura T, Monti S, Steidl U, Hetherington CJ, Lowell AM, Golub T, Meyerson M, Tenen DG, Shapiro GI *et al*: **Transcriptional profiling identifies cyclin D1 as a critical downstream effector of mutant epidermal growth factor receptor signaling**. *Cancer Res* 2006, **66**(23):11389-11398.
213. Burris HA, 3rd: **Dual kinase inhibition in the treatment of breast cancer: initial experience with the EGFR/ErbB-2 inhibitor lapatinib**. *Oncologist* 2004, **9 Suppl 3**:10-15.
214. Moy B, Goss PE: **Lapatinib: current status and future directions in breast cancer**. *Oncologist* 2006, **11**(10):1047-1057.
215. Fan P, Wang J, Santen RJ, Yue W: **Long-term treatment with tamoxifen facilitates translocation of estrogen receptor alpha out of the nucleus and enhances its interaction with EGFR in MCF-7 breast cancer cells**. *Cancer Res* 2007, **67**(3):1352-1360.
216. Pancholi S, Lykkesfeldt AE, Hilmi C, Banerjee S, Leary A, Drury S, Johnston S, Dowsett M, Martin LA: **ERBB2 influences the subcellular localization of the estrogen receptor in tamoxifen-resistant MCF-7 cells leading to the activation of AKT and RPS6KA2**. *Endocr Relat Cancer* 2008, **15**(4):985-1002.
217. Dowsett M, Dunbier A, Anderson H, Salter J, Detre S, Jones R, Skene A, Dixon M, Smith I: **Biomarkers and predictive factors of response to neoadjuvant treatment**. *Breast Cancer Res* 2009, **11 Suppl 1**:S11.
218. Dunbier AK, Anderson H, Ghazoui Z, Folkerd EJ, A'Hern R, Crowder RJ, Hoog J, Smith IE, Osin P, Nerurkar A *et al*: **Relationship between plasma estradiol**

levels and estrogen-responsive gene expression in estrogen receptor-positive breast cancer in postmenopausal women. *J Clin Oncol*, **28**(7):1161-1167.

219. Ellis MJ, Tao Y, Luo J, A'Hern R, Evans DB, Bhatnagar AS, Chaudri Ross HA, von Kameke A, Miller WR, Smith I *et al*: **Outcome prediction for estrogen receptor-positive breast cancer based on postneoadjuvant endocrine therapy tumor characteristics**. *J Natl Cancer Inst* 2008, **100**(19):1380-1388.
220. Jones RL, Salter J, A'Hern R, Nerurkar A, Parton M, Reis-Filho JS, Smith IE, Dowsett M: **Relationship between oestrogen receptor status and proliferation in predicting response and long-term outcome to neoadjuvant chemotherapy for breast cancer**. *Breast Cancer Res Treat*, **119**(2):315-323.
221. Dowsett M, Smith IE, Ebbs SR, Dixon JM, Skene A, Griffith C, Boeddinghaus I, Salter J, Detre S, Hills M *et al*: **Short-term changes in Ki-67 during neoadjuvant treatment of primary breast cancer with anastrozole or tamoxifen alone or combined correlate with recurrence-free survival**. *Clin Cancer Res* 2005, **11**(2 Pt 2):951s-958s.
222. Mello-Grand M, Singh V, Ghimenti C, Scatolini M, Regolo L, Grosso E, Zambelli A, Da Prada GA, Villani L, Fregoni V *et al*: **Gene expression profiling and prediction of response to hormonal neoadjuvant treatment with anastrozole in surgically resectable breast cancer**. *Breast Cancer Res Treat*, **121**(2):399-411.
223. Miller WR: **Clinical, pathological, proliferative and molecular responses associated with neoadjuvant aromatase inhibitor treatment in breast cancer**. *J Steroid Biochem Mol Biol*, **118**(4-5):273-276.
224. Miller WR, Larionov A, Renshaw L, Anderson TJ, Walker JR, Krause A, Sing T, Evans DB, Dixon JM: **Gene expression profiles differentiating between breast cancers clinically responsive or resistant to letrozole**. *J Clin Oncol* 2009, **27**(9):1382-1387.
225. Miller WR, Larionov A, Anderson TJ, Evans DB, Dixon JM: **Sequential changes in gene expression profiles in breast cancers during treatment with the aromatase inhibitor, letrozole**. *Pharmacogenomics J*.
226. Ingle JN, Suman VJ, Rowland KM, Mirchandani D, Bernath AM, Camoriano JK, Fishkin PA, Nikcevich DA, Perez EA: **Fulvestrant in women with advanced breast cancer after progression on prior aromatase inhibitor therapy: North Central Cancer Treatment Group Trial N0032**. *J Clin Oncol* 2006, **24**(7):1052-1056.
227. Perey L, Paridaens R, Hawle H, Zaman K, Nole F, Wildiers H, Fiche M, Dietrich D, Clement P, Koberle D *et al*: **Clinical benefit of fulvestrant in postmenopausal women with advanced breast cancer and primary or acquired resistance to aromatase inhibitors: final results of phase II Swiss Group for Clinical Cancer Research Trial (SAKK 21/00)**. *Ann Oncol* 2007, **18**(1):64-69.
228. Steger GG, Bartsch R, Wenzel C, Pluschnig U, Hussian D, Sevelda U, Locker GJ, Gnant MF, Jakesz R, Zielinski CC: **Fulvestrant ('Faslodex') in pre-treated patients with advanced breast cancer: a single-centre experience**. *Eur J Cancer* 2005, **41**(17):2655-2661.

229. Di Leo A, Jerusalem G, Petruzelka L, Torres R, Bondarenko IN, Khasanov R, Verhoeven D, Pedrini JL, Smirnova I, Lichinitser MR *et al*: **Results of the CONFIRM phase III trial comparing fulvestrant 250 mg with fulvestrant 500 mg in postmenopausal women with estrogen receptor-positive advanced breast cancer**. *J Clin Oncol*, **28**(30):4594-4600.
230. Marsh S, Mallon MA, Goodfellow P, McLeod HL: **Concordance of pharmacogenetic markers in germline and colorectal tumor DNA**. *Pharmacogenomics* 2005, **6**(8):873-877.
231. Schneider BP, Skaar TC, Sledge GW, Badve S, Li L, Flockhart DA: **Analysis of angiogenesis genes from paraffin-embedded breast tumor and lymph nodes**. *Breast Cancer Res Treat* 2006, **96**(3):209-215.
232. Weiss JR, Baer MR, Ambrosone CB, Blanco JG, Hutson A, Ford LA, Moysich KB: **Concordance of pharmacogenetic polymorphisms in tumor and germ line DNA in adult patients with acute myeloid leukemia**. *Cancer Epidemiol Biomarkers Prev* 2007, **16**(5):1038-1041.
233. Farragher SM, Tanney A, Kennedy RD, Paul Harkin D: **RNA expression analysis from formalin fixed paraffin embedded tissues**. *Histochem Cell Biol* 2008, **130**(3):435-445.
234. Greer CE, Peterson SL, Kiviat NB, Manos MM: **PCR amplification from paraffin-embedded tissues. Effects of fixative and fixation time**. *Am J Clin Pathol* 1991, **95**(2):117-124.
235. Iwamoto KS, Mizuno T, Ito T, Akiyama M, Takeichi N, Mabuchi K, Seyama T: **Feasibility of using decades-old archival tissues in molecular oncology/epidemiology**. *Am J Pathol* 1996, **149**(2):399-406.
236. Romero RL, Juston AC, Ballantyne J, Henry BE: **The applicability of formalin-fixed and formalin fixed paraffin embedded tissues in forensic DNA analysis**. *J Forensic Sci* 1997, **42**(4):708-714.
237. Hui L, DelMonte T, Ranade K: **Genotyping using the TaqMan assay**. *Curr Protoc Hum Genet* 2008, **Chapter 2**:Unit 2 10.
238. van Beers EH, Joosse SA, Ligtenberg MJ, Fles R, Hogervorst FB, Verhoef S, Nederlof PM: **A multiplex PCR predictor for aCGH success of FFPE samples**. *Br J Cancer* 2006, **94**(2):333-337.
239. Jin Y, Desta Z, Stearns V, Ward B, Ho H, Lee KH, Skaar T, Storniolo AM, Li L, Araba A *et al*: **CYP2D6 genotype, antidepressant use, and tamoxifen metabolism during adjuvant breast cancer treatment**. *J Natl Cancer Inst* 2005, **97**(1):30-39.
240. Goetz MP, Rae JM, Suman VJ, Safgren SL, Ames MM, Visscher DW, Reynolds C, Couch FJ, Lingle WL, Flockhart DA *et al*: **Pharmacogenetics of tamoxifen biotransformation is associated with clinical outcomes of efficacy and hot flashes**. *J Clin Oncol* 2005, **23**(36):9312-9318.
241. Xie B, Freudenheim JL, Cummings SS, Singh B, He H, McCann SE, Moysich KB, Shields PG: **Accurate genotyping from paraffin-embedded normal tissue adjacent to breast cancer**. *Carcinogenesis* 2006, **27**(2):307-310.
242. Mort R, Mo L, McEwan C, Melton DW: **Lack of involvement of nucleotide excision repair gene polymorphisms in colorectal cancer**. *Br J Cancer* 2003, **89**(2):333-337.

243. Jaremko M, Justenhoven C, Abraham BK, Schroth W, Fritz P, Brod S, Vollmert C, Illig T, Brauch H: **MALDI-TOF MS and TaqMan assisted SNP genotyping of DNA isolated from formalin-fixed and paraffin-embedded tissues (FFPET)**. *Hum Mutat* 2005, **25**(3):232-238.
244. Wang Y, Carlton VE, Karlin-Neumann G, Sapolsky R, Zhang L, Moorhead M, Wang ZC, Richardson AL, Warren R, Walther A *et al*: **High quality copy number and genotype data from FFPE samples using Molecular Inversion Probe (MIP) microarrays**. *BMC Med Genomics* 2009, **2**:8.
245. Johnson NA, Hamoudi RA, Ichimura K, Liu L, Pearson DM, Collins VP, Du MQ: **Application of array CGH on archival formalin-fixed paraffin-embedded tissues including small numbers of microdissected cells**. *Lab Invest* 2006, **86**(9):968-978.
246. Koch I, Slotta-Huspenina J, Hollweck R, Anastasov N, Hofler H, Quintanilla-Martinez L, Fend F: **Real-time quantitative RT-PCR shows variable, assay-dependent sensitivity to formalin fixation: implications for direct comparison of transcript levels in paraffin-embedded tissues**. *Diagn Mol Pathol* 2006, **15**(3):149-156.
247. Andreassen CN, Sorensen FB, Overgaard J, Alsner J: **Optimisation and validation of methods to assess single nucleotide polymorphisms (SNPs) in archival histological material**. *Radiother Oncol* 2004, **72**(3):351-356.
248. Lehmann U, Kreipe H: **Real-time PCR analysis of DNA and RNA extracted from formalin-fixed and paraffin-embedded biopsies**. *Methods* 2001, **25**(4):409-418.
249. Siwoski A, Ishkanian A, Garnis C, Zhang L, Rosin M, Lam WL: **An efficient method for the assessment of DNA quality of archival microdissected specimens**. *Mod Pathol* 2002, **15**(8):889-892.
250. Farrand K, Jovanovic L, Delahunt B, McIver B, Hay ID, Eberhardt NL, Grebe SK: **Loss of heterozygosity studies revisited: prior quantification of the amplifiable DNA content of archival samples improves efficiency and reliability**. *J Mol Diagn* 2002, **4**(3):150-158.
251. Gilbert MT, Sanchez JJ, Haselkorn T, Jewell LD, Lucas SB, Van Marck E, Borsting C, Morling N, Worobey M: **Multiplex PCR with minisequencing as an effective high-throughput SNP typing method for formalin-fixed tissue**. *Electrophoresis* 2007, **28**(14):2361-2367.
252. Godfrey TE, Kim SH, Chavira M, Ruff DW, Warren RS, Gray JW, Jensen RH: **Quantitative mRNA expression analysis from formalin-fixed, paraffin-embedded tissues using 5' nuclease quantitative reverse transcription-polymerase chain reaction**. *J Mol Diagn* 2000, **2**(2):84-91.
253. Abrahamsen HN, Steiniche T, Nexo E, Hamilton-Dutoit SJ, Sorensen BS: **Towards quantitative mRNA analysis in paraffin-embedded tissues using real-time reverse transcriptase-polymerase chain reaction: a methodological study on lymph nodes from melanoma patients**. *J Mol Diagn* 2003, **5**(1):34-41.
254. Anstead GM, Carlson KE, Katzenellenbogen JA: **The estradiol pharmacophore: ligand structure-estrogen receptor binding affinity relationships and a model for the receptor binding site**. *Steroids* 1997, **62**(3):268-303.

255. Wang L, Salavaggione E, Pelleymounter L, Eckloff B, Wieben E, Weinshilboum R: **Human 3beta-hydroxysteroid dehydrogenase types 1 and 2: Gene sequence variation and functional genomics**. *J Steroid Biochem Mol Biol* 2007, **107**(1-2):88-99.
256. Reding KW, Li CI, Weiss NS, Chen C, Carlson CS, Duggan D, Thummel KE, Daling JR, Malone KE: **Genetic variation in the progesterone receptor and metabolism pathways and hormone therapy in relation to breast cancer risk**. *Am J Epidemiol* 2009, **170**(10):1241-1249.
257. Takahashi RH, Grigliatti TA, Reid RE, Riggs KW: **The effect of allelic variation in aldo-keto reductase 1C2 on the in vitro metabolism of dihydrotestosterone**. *J Pharmacol Exp Ther* 2009, **329**(3):1032-1039.
258. Beckmann L, Husing A, Setiawan VW, Amiano P, Clavel-Chapelon F, Chanock SJ, Cox DG, Diver R, Dossus L, Feigelson HS *et al*: **Comprehensive analysis of hormone and genetic variation in 36 genes related to steroid hormone metabolism in pre- and postmenopausal women from the breast and prostate cancer cohort consortium (BPC3)**. *J Clin Endocrinol Metab*, **96**(2):E360-367.
259. Jakobsson J, Palonek E, Lorentzon M, Ohlsson C, Rane A, Ekstrom L: **A novel polymorphism in the 17beta-hydroxysteroid dehydrogenase type 5 (aldo-keto reductase 1C3) gene is associated with lower serum testosterone levels in caucasian men**. *Pharmacogenomics J* 2007, **7**(4):282-289.
260. Lord SJ, Mack WJ, Van Den Berg D, Pike MC, Ingles SA, Haiman CA, Wang W, Parisky YR, Hodis HN, Ursin G: **Polymorphisms in genes involved in estrogen and progesterone metabolism and mammographic density changes in women randomized to postmenopausal hormone therapy: results from a pilot study**. *Breast Cancer Res* 2005, **7**(3):R336-344.
261. Jakobsson J, Karypidis H, Johansson JE, Roh HK, Rane A, Ekstrom L: **A functional C-G polymorphism in the CYP7B1 promoter region and its different distribution in Orientals and Caucasians**. *Pharmacogenomics J* 2004, **4**(4):245-250.
262. Ingle JN, Krook JE, Schaid DJ, Everson LK, Mailliard JA, Long HJ, McCormack GW: **Evaluation of trilostane plus hydrocortisone in women with metastatic breast cancer and prior hormonal therapy exposure**. *Am J Clin Oncol* 1990, **13**(2):93-97.
263. Williams CJ, Barley VL, Blackledge GR, Rowland CG, Tyrrell CJ: **Multicentre cross over study of aminoglutethimide and trilostane in advanced postmenopausal breast cancer**. *Br J Cancer* 1993, **68**(6):1210-1215.
264. Palella FJ, Jr., Delaney KM, Moorman AC, Loveless MO, Fuhrer J, Satten GA, Aschman DJ, Holmberg SD: **Declining morbidity and mortality among patients with advanced human immunodeficiency virus infection. HIV Outpatient Study Investigators**. *N Engl J Med* 1998, **338**(13):853-860.
265. Carr A, Cooper DA: **Adverse effects of antiretroviral therapy**. *Lancet* 2000, **356**(9239):1423-1430.
266. Hammer SM, Eron JJ, Jr., Reiss P, Schooley RT, Thompson MA, Walmsley S, Cahn P, Fischl MA, Gatell JM, Hirsch MS *et al*: **Antiretroviral treatment of adult HIV infection: 2008 recommendations of the International AIDS Society-USA panel**. *JAMA* 2008, **300**(5):555-570.

267. Marzolini C, Telenti A, Decosterd LA, Greub G, Biollaz J, Buclin T: **Efavirenz plasma levels can predict treatment failure and central nervous system side effects in HIV-1-infected patients**. *AIDS* 2001, **15**(1):71-75.
268. Cespedes MS, Aberg JA: **Neuropsychiatric complications of antiretroviral therapy**. *Drug Saf* 2006, **29**(10):865-874.
269. Caso JA, Prieto Jde M, Casas E, Sanz J: **Gynecomastia without lipodystrophy syndrome in HIV-infected men treated with efavirenz**. *AIDS* 2001, **15**(11):1447-1448.
270. Mercie P, Viallard JF, Thiebaut R, Faure I, Rispal P, Leng B, Pellegrin JL: **Efavirenz-associated breast hypertrophy in HIV-infection patients**. *AIDS* 2001, **15**(1):126-129.
271. Rahim S, Ortiz O, Maslow M, Holzman R: **A case-control study of gynecomastia in HIV-1-infected patients receiving HAART**. *AIDS Read* 2004, **14**(1):23-24, 29-32, 35-40.
272. Manfredi R, Calza L, Chiodo F: **Efavirenz versus nevirapine in current clinical practice: a prospective, open-label observational study**. *J Acquir Immune Defic Syndr* 2004, **35**(5):492-502.
273. Jover F, Cuadrado JM, Roig P, Rodriguez M, Andreu L, Merino J: **Efavirenz-associated gynecomastia: report of five cases and review of the literature**. *Breast J* 2004, **10**(3):244-246.
274. Mira JA, Lozano F, Santos J, Ramayo E, Terron A, Palacios R, Leon EM, Marquez M, Macias J, Fernandez-Palacin A *et al*: **Gynaecomastia in HIV-infected men on highly active antiretroviral therapy: association with efavirenz and didanosine treatment**. *Antivir Ther* 2004, **9**(4):511-517.
275. Stahle L, Moberg L, Svensson JO, Sonnerborg A: **Efavirenz plasma concentrations in HIV-infected patients: inter- and intraindividual variability and clinical effects**. *Ther Drug Monit* 2004, **26**(3):267-270.
276. Dobrzycka KM, Townson SM, Jiang S, Oesterreich S: **Estrogen receptor corepressors -- a role in human breast cancer?** *Endocr Relat Cancer* 2003, **10**(4):517-536.
277. Shiels MS, Cole SR, Kirk GD, Poole C: **A meta-analysis of the incidence of non-AIDS cancers in HIV-infected individuals**. *J Acquir Immune Defic Syndr* 2009, **52**(5):611-622.
278. Kegg S, Lau R: **Tamoxifen in antiretroviral-associated gynaecomastia**. *Int J STD AIDS* 2002, **13**(8):582-583.
279. Perdona S, Autorino R, De Placido S, D'Armiento M, Gallo A, Damiano R, Pingitore D, Gallo L, De Sio M, Bianco AR *et al*: **Efficacy of tamoxifen and radiotherapy for prevention and treatment of gynaecomastia and breast pain caused by bicalutamide in prostate cancer: a randomised controlled trial**. *Lancet Oncol* 2005, **6**(5):295-300.
280. Fradet Y, Egerdie B, Andersen M, Tammela TL, Nachabe M, Armstrong J, Morris T, Navani S: **Tamoxifen as prophylaxis for prevention of gynaecomastia and breast pain associated with bicalutamide 150 mg monotherapy in patients with prostate cancer: a randomised, placebo-controlled, dose-response study**. *Eur Urol* 2007, **52**(1):106-114.

281. Sikora MJ, Rae JM, Johnson MD, Desta Z: **Efavirenz directly modulates the oestrogen receptor and induces breast cancer cell growth**. *HIV Med*, **11**(9):603-607.